

**DEVULCANISATION OF TRUCK TYRE TREAD
VULCANISATES IN SUPERCRITICAL CARBON
DIOXIDE USING DIPHENYL DISULPHIDE AND 2,2-
DITHIOBIS(BENZOTHAZOLE)**

B. Mabuto

2019

**DEVULCANISATION OF TRUCK TYRE TREAD VULCANISATES IN
SUPERCRITICAL CARBON DIOXIDE USING DIPHENYL
DISULPHIDE AND 2,2-DITHIOBIS(BENZOTHAZOLE)**

By

Briswell Mabuto

**Submitted in fulfilment of the requirements for the degree of *Magister Scientiae* in the
Faculty of Science, at the Nelson Mandela University.**

April 2019

Supervisor: Dr S. P. Hlangothi

Co-supervisor: Dr A. Ogunlanja

Co-supervisor: Mr R. M. Bosch

Co-supervisor: Dr K. Garde

DECLARATION

I, Briswell Mabuto (210154799), hereby declare that the research in this dissertation for the award of Magister Scientiae is my original work, and has not been submitted for assessment or completion of any postgraduate qualification in another University.



Briswell Mabuto (Mr)

DEDICATION

This thesis is dedicated to my grandmother, Mrs Julia Masunda, who after, over eleven years of courageously battling cancer in the throat, gave in on the 9th of January 2019. A lot of hearts are pained by her passing but solace is in the peace she's now at, a better place. Love forever...

ACKNOWLEDGEMENTS

I would like to express my sincere appreciation and acknowledgements to the following individuals, departments and institutions for their contribution towards the completion of this research study;

- Dr S. P. Hlangothi; for his un-withheld support, since my BSc Honours right through to my MSc studies. He gave me the opportunity to pursue my studies when I was despondent and beat down by life challenges. Had he not empathised and given me a helping hand when I needed it the most, I do not know where I would be in life. Besides that, he has been a supportive, optimistic and instrumental supervisor throughout the whole research project.
- Dr A. Ogunlanja; for his time, availing himself at short notice to assist with any challenges faced; for challenging me to think out of the box, “more chemistry” he would say. Also, for his guidance, illuminating ideas and support whenever I needed it.
- Mr C. Bosma; for squeezing me into his schedule without an appointment for statistical analysis consultation. For assisting with different statistical methods of approach whenever I hit a stumbling block.
- Dr K. Garde; for her un-withheld support and supervision. Identifying key challenges and aspects in need of tweaking in the thesis.
- Dr R. Bosch; for his insightful suggestions and remedies to certain challenges faced during the study. For the use of his facilities in conducting parts of the experiments.
- Mr S. Grewar; for the reactor design and construction, going the extra mile and turning a blind eye to the proposed budget. For his anytime assistance and support whenever I encountered challenges with the reactor.
- Mr H. Schalekamp; for borrowing me his dry ice making nozzle and support with equipment I needed for experiments.
- Dr J. Carson, Dr R. Neglur, Dr D. Grooff, Dr B. Hlangothi, Mr C. Marius, Mr L. Compton, Mr L. Bolo, Ms P. Sobekwa, Mr J. Gumede, Dr M. Phiri, Mr M. Mngoma, Mr F. Mathe, Mr E. Bashman, Dr E. Horsten, Mr V. C. Akbagoba and Ms Z. Dyan; for their support when I needed it.
- Chemistry department, Centre of Rubber Science and Technology, Physics department, ENSTA, University of Stellenbosch for their assistance.

ABSTRACT

A lot of work has been done in the recycling industry in an effort to increase the amount of reclaimed rubber used in new tyre formulations. The major drawback has been inferior physical and mechanical properties of reclaimed/virgin rubber blends in comparison to the virgin rubber material. Deterioration in these properties has been identified to be a result of chain degradation during reclamation processes as well as presence of crosslinks in the final reclaim product. Devulcanisation techniques have gained precedence due to the relatively improved properties of devulcanised/virgin rubber blends. The concept of devulcanisation is to reverse vulcanisation, resulting in total or partial cleavage of crosslinks. In this way, chain degradation is minimised while crosslink scission is maximised, thereby resulting in good quality devulcanised rubber. However, due to the persistence of chain degradation and crosslinks during devulcanisation processes, a very limited number of reports have claimed success in achieving this goal. Therefore there is still the need to develop a devulcanisation method that ensures improved quality and productivity of devulcanised rubber. Typical truck tyre tread vulcanisates were used for optimisation of time, temperature, heating rate, pressure and amount of devulcanising agent while monitoring percentage devulcanisation in supercritical carbon dioxide medium. Optimisation of the devulcanisation conditions was done by employing a two-level central composite design in the isothermal and non-isothermal heating stages. This was followed by a single factor analysis of devulcanisation conditions in the non-isothermal stage. The effect of the presence of carbon black was investigated by comparing the percentage devulcanisation of carbon black filled and unfilled samples. The results show that supercritical carbon dioxide is an effective medium of devulcanisation using diphenyl disulphide (DD) and 2,2-dithiobis(benzothiazole) (MBTS). The relatively higher degree of devulcanisation observed during the non-isothermal stage compared to the isothermal stage, led to a shift of focus to non-isothermal devulcanisation. Temperature and time were found to have a significant antagonistic effect on the percentage devulcanisation, while changes in pressure above critical point and mass of devulcanising agent showed no effect on percentage devulcanisation. The heating rate was determined by the set-point, of which 180 °C set-point temperature resulted in desirable degree of devulcanisation for both DD and MBTS. 76.18 ± 5.50 % devulcanisation in 5 minutes at 102 °C was observed for DD whilst 70.92 ± 4.10 % devulcanisation in 4 minutes at 97 °C was observed for MBTS. Changes in pressure above critical point and mass of devulcanising agent used in devulcanisation showed no significant effect in the percentage devulcanisation and so they were kept constant at 80 bars and 1.00 %

(of weight of rubber sample) devulcanisation agent, respectively. The presence of carbon black was found to have an effect on the degree of devulcanisation; 87.95 % and 81.33 % devulcanisation was observed for unfilled samples devulcanised using DD and MBTS respectively. Thermogravimetric analysis of the natural rubber/styrene butadiene rubber (NR/SBR respectively) relative composition of devulcanisates indicated uneven devulcanisation when using DD, whereas MBTS did not show any form of preference. DD showed preference for NR devulcanisation over SBR. Further analysis of the sol and gel fractions were performed using; Differential Scanning Calorimetry, Fourier Transform Infrared Spectroscopy, Gel Permeation Chromatography and Gas Chromatography coupled with Mass Spectroscopy. Application of the optimised conditions to devulcanise ground tyre rubber (GTR) resulted in relatively lower degrees of devulcanisation for both DD and MBTS; 41.22 ± 4.22 and 22.41 ± 1.97 respectively. The differences in the degree of devulcanisation of the laboratory prepared vulcanisates and the GTR was determined to be due to sample differences; *i.e.* sample constituents, particle dimensions and crosslink network (crosslink distribution in particular).

Keywords: vulcanisation, reclamation, devulcanisation, supercritical carbon dioxide, diphenyl disulphide, dithiobis(benzothiazole), central composite design and percentage devulcanisation.

TABLE OF CONTENTS

DECLARATION	i
DEDICATION	ii
ACKNOWLEDGEMENTS	iii
ABSTRACT	iv
LIST OF FIGURES	xiii
LIST OF TABLES	xvii
CHAPTER ONE: INTRODUCTION	1
1.1 MOTIVATION	1
1.2 RESEARCH ASPECTS	2
1.2.1 RESEARCH QUESTIONS	2
1.2.2 RESEARCH STATEMENT	2
1.2.3 HYPOTHESIS	3
1.2.4 RESEARCH AIMS	3
1.2.5 RESEARCH OBJECTIVES	3
1.3 BACKGROUND	4
1.3.1 Vulcanisation	4
1.3.2 Network structure	4
1.3.2.1 Crosslink distribution	5
1.3.2.2 Crosslink density	7
1.3.3 Crosslinking in blends and co-vulcanisation	12
1.3.4 Rubber waste management	14
1.3.4.1 Landfilling	14
1.3.4.2 Energy recovery	14
1.3.4.3 Recycling	15
1.3.4.4 Re-use	15
1.3.4.5 Prevention	15

1.3.5	Rubber recycling processes	16
1.3.5.1	<i>GTR production</i>	16
1.3.5.2	<i>Compression moulding</i>	18
1.3.5.3	<i>Reclamation processes</i>	18
1.3.6	Techniques used in reclamation	22
1.3.6.1	<i>Physical techniques</i>	22
1.3.6.2	<i>Chemical techniques</i>	25
1.3.6.3	<i>Physico-chemical techniques</i>	25
1.3.6.4	<i>Thermal techniques</i>	26
1.3.6.5	<i>Biotechnological techniques</i>	28
1.4	REVIEW OF LITERATURE	29
1.4.1	Thermo-chemical devulcanisation	29
1.4.2	Possible devulcanisation mechanism	30
1.4.3	Choice of solvent.....	33
1.5	SIGNIFICANCE OF THE RESEARCH	34
1.6	SCOPE AND LIMITATIONS	35
1.7	OVERVIEW OF CHAPTERS	37
1.8	GLOSSARY.....	39
1.9	REFERENCES.....	40
	CHAPTER 2: REACTOR CALIBRATION AND INSTRUMENTATION USED	45
2.1	SUPERCRITICAL REACTOR	45
2.1.1	Features of PID temperature controller	47
2.1.2	Reactor calibration	48
2.1.2.1	<i>Pressure-temperature relation</i>	48
2.1.2.2	<i>Reactor heating profile</i>	52
2.1.2.3	<i>Effect of thermal mass on the heating rate</i>	53
2.2	OTHER INSTRUMENTATION USED.....	54

2.2.1	Weight determination	54
2.2.2	Rubber compounding	55
2.2.2.1	<i>Banbury internal mixer</i>	55
2.2.2.2	<i>Two roll mill</i>	56
2.2.2.3	<i>Rubber process analyser (RPA)</i>	57
2.2.2.4	<i>Cure press</i>	59
2.2.3	Accelerated ageing	60
2.2.3.1	<i>Water bath</i>	60
2.2.4	Soxhlet extraction.....	60
2.2.5	Refractometer	60
2.2.6	Drying equipment.....	61
2.2.6.1	<i>Vacuum desiccator</i>	61
2.2.6.2	<i>Forced air ventilation oven</i>	61
2.2.6.3	<i>Rotary evaporator</i>	62
2.2.7	Characterisation and analysis equipment	63
2.2.7.1	<i>Muffle furnace</i>	63
2.2.7.2	<i>Fourier transform-infrared spectroscopy, FTIR</i>	64
2.2.7.3	<i>Gas chromatograph-mass spectrometer (GCMS)</i>	64
2.2.7.4	<i>Differential scanning calorimetry, DSC</i>	66
2.2.7.5	<i>Thermogravimetric analyser, TGA</i>	67
2.2.7.6	<i>Gel permeation chromatography, GPC</i>	68
2.2.8	GTR preparation.....	70
2.3	SUMMARY OF FINDINGS	72
2.4	REFERENCES.....	73
	CHAPTER 3: ISOTHERMAL PROCESS OPTIMISATION	74
3.1	INTRODUCTION	74
3.2	EXPERIMENTAL.....	77

3.2.1	Materials.....	77
	3.2.1.1 <i>Compounding materials</i>	77
	3.2.1.2 <i>Devulcanisation materials</i>	77
3.2.2	General procedure	78
	3.2.2.1 <i>Compounding</i>	79
	3.2.2.2 <i>Ageing</i>	82
	3.2.2.3 <i>Soxhlet extraction</i>	82
	3.2.2.4 <i>Sol and gel fractionation</i>	85
3.2.3	Statistical methods.....	86
	3.2.3.1 <i>Characterisation</i>	86
	3.2.3.2 <i>Isothermal devulcanisation</i>	87
3.2.4	Analysis.....	90
	3.2.4.1 <i>Cure characterisation</i>	90
	3.2.4.2 <i>Thermal decomposition of DD and MBTS</i>	90
	3.2.4.3 <i>TGA analysis of vulcanisates and gel</i>	90
	3.2.4.4 <i>Crosslink density</i>	91
3.3	RESULTS AND DISCUSSION	92
	3.3.2 Characterisation of uncured rubber, cured rubber and devulcanising agents	92
	3.3.2.1 <i>Cure characteristics of uncured rubber samples</i>	92
	3.3.2.2 <i>Analysis of cured rubber composition.</i>	93
	3.3.2.3 <i>Thermal analysis of devulcanising agents</i>	96
	3.3.3 Optimisation of isothermal devulcanisation.....	98
	3.3.3.1 <i>Possible reasons why no model could be found</i>	101
	3.3.3.2 <i>Isothermal vs. non-isothermal devulcanisation</i>	102
3.4	SUMMARY OF FINDINGS	103
3.5	REFERENCES.....	104
3.6	APPENDIX.....	106

CHAPTER 4: OPTIMISATION OF NON-ISOTHERMAL DEVULCANISATION	112
4.1 INTRODUCTION	112
4.2 EXPERIMENTAL	113
4.2.1 Materials and general procedure	113
4.2.1.1 <i>Non-isothermal devulcanisation</i>	113
4.2.1.2 <i>Single factor analysis</i>	113
4.2.2 Statistical Methods	114
4.2.2.1 <i>Empirical model formulation</i>	114
4.2.2.2 <i>Statistical analysis</i>	115
4.2.2.3 <i>Instantaneous heating rate determination</i>	117
4.2.3 Analysis	119
4.2.3.1 <i>Molecular weight determination</i>	119
4.2.3.2 <i>Structural analysis of sol</i>	120
4.2.3.3 <i>GCMS analysis</i>	120
4.3 RESULTS AND DISCUSSIONS	121
4.3.1 Optimisation of non-isothermal devulcanisation	121
4.3.1.1 <i>% Devulcanisation obtained using DD</i>	121
4.3.1.2 <i>% Devulcanisation obtained using MBTS</i>	122
4.3.1.3 <i>Thermal contribution towards % devulcanisation</i>	124
4.3.1.4 <i>Effect of heating rate on % devulcanisation</i>	125
4.3.1.5 <i>Empirical model formulation</i>	126
4.3.1.6 <i>Possible reasons why the models were not able to predict feasible optimum</i>	132
4.3.1.7 <i>Chosen optimum conditions: time & temperature</i>	133
4.3.2 Single factor analysis: amount of dA and pressure	134
4.3.2.1 <i>Effect of amount of dA on % devulcanisation</i>	134
4.3.2.2 <i>Effect of pressure on % devulcanisation</i>	137

4.3.3	Final optimum conditions.....	139
4.3.4	Effect of CB filler on % devulcanisation	140
4.3.5	Processes involved during devulcanisation.....	141
4.3.5.1	<i>% Devulcanisation vs. % sol</i>	141
4.3.5.1	<i>Devulcanisation vs. competing processes</i>	144
4.3.6	Product analysis.....	148
4.3.6.1	<i>GPC analyses</i>	148
4.3.6.2	<i>FTIR analyses</i>	150
4.4	SUMMARY OF FINDINGS	153
4.5	REFERENCES.....	154
4.6	APPENDIX.....	156
	DEVULCANISATION OF GTR USING OPTIMISED CONDITIONS.....	169
5.1	INTRODUCTION	169
5.2	METHODS AND MATERIALS	170
5.2.1	Materials and reagents.....	170
5.2.2	GTR preparation.....	170
5.2.3	Characterisation.....	171
5.2.3.1	<i>Size determination</i>	171
5.2.3.2	<i>Surface features</i>	171
5.2.3.3	<i>GTR composition</i>	171
5.2.4	GTR devulcanisation.....	173
5.2.5	Analysis of GTR and dGTR.....	173
5.2.6	Determination of crosslink distribution.....	173
5.2.6.1	<i>Polysulphidic crosslink determination</i>	173
5.2.6.2	<i>Mono & di-sulphidic crosslink determination</i>	174
5.3	RESULTS AND DISCUSSION	175
5.3.1	Characterisation of GTR	175

5.3.1.1	<i>GTR surface morphology</i>	175
5.3.1.2	<i>Determination of GTR composition using TGA</i>	176
5.3.2	Devulcanisation of GTR under optimised conditions.....	178
5.3.4	Analysis of devulcanisation products.....	184
5.3.4.1	<i>Determination of molecular weights and distribution.</i>	184
5.3.4.2	<i>FTIR analysis of the GTR and sol components</i>	185
5.3.4.3	<i>Glass transition determination, Tg.</i>	189
5.4	SUMMARY OF FINDINGS	192
5.5	REFERENCES.....	193
5.6	APPENDIX.....	194
	CHAPTER 6: CONCLUSIONS AND RECOMMENDATIONS FOR FUTURE WORK	198
6.1	CONCLUSIONS.....	198
6.2	RECOMMENDATIONS FOR FUTURE WORK	200

LIST OF FIGURES

Figure 1.1: Typical network structure of a sulphur cured vulcanisate ^[15]	5
Figure 1.2: Influence of crosslink density on vulcanisate properties ^[15]	7
Figure 2.1: Supercritical reactor top view. Labelled in the picture are the major components; (a) pressure gauge, (b) reaction chamber, (c) PID temperature controller and (d) thermocouple connection.	45
Figure 2.2: Design of supercritical reactor / autoclave.	46
Figure 2.3: Temperature controller control panel.	47
Figure 2.4: Tuning temperature controller; a) set-point not reached, b) closer to set-point c) large deviations at set-point steady state.....	48
Figure 2.5: Ideal gas behaviour vs. real gas (CO ₂) behaviour at 180 °C set-point and 80 bars pressure.	50
Figure 2.6: CO ₂ phase diagram (<i>adapted from Wikipedia</i> ^[126]).....	51
Figure 2.7: Reactor heating profile at 140 °C and 180 °C set-points.....	52
Figure 2.8: Heating profiles showing the effect of thermal mass on the heating rate at 140 and 180 °C set-point.	53
Figure 2.9a: Mettler Toledo weighing balance (AB204-S.....	54
Figure 2.9b: Mettler Toledo microbalance (MX5 UMT2)	55
Figure 2.10a: Banbury internal mixer a) chamber b) open chamber c) tangential mixing blades.	55
Figure 2.11: Two roll mill used for sheeting. Indicated are the 1) two rolls, 2) temperature and rotor speed regulator and 3) safety mechanism (trip switch).....	57
Figure 2.12: 1) Dynamic moving die rheometer 2) shows upper and lower die systems.....	58

Figure 2.13: Cure press used for compression moulding. Indicated is the 1) motor for the hydraulic system, 2) mould plates, and 3) temperature control unit.....	59
Figure 2.14: Water bath used for accelerated ageing.....	60
Figure 2.15: Refractometer for checking consistency in acetone/chloroform composition. ...	61
Figure 2.16: Vacuum dessicator.	61
Figure 2.17: Forced air ventilation oven.....	62
Figure 2.18: Rotary evaporator, RE300.....	63
Figure 2.19: Muffle furnace used for GTR ash content determination.....	63
Figure 2.20: FTIR spectrophotometer, Tensor 27.	64
Figure 2.21: Agilent GCMS for qualitative analysis of devulcanisation extracts.	66
Figure 2.22: a) Scheme for a typical cell of a heat flux DSC ^[135] , b) Discovery DSC instrument.	67
Figure 2.23: Scheme of TGA setup ^[135]	68
Figure 2.24: General layout of a typical GPC system setup (<i>adapted from Malvern et al</i> ^[11]).	69
Figure 2.25: Taurus coffee grinder used to make GTR	70
Figure 3.1: Chemical structures of DD and MBTS	77
Figure 3.2: Standard curve showing refractive indices of a range of acetone/chloroform mixtures.....	83
Figure 3.3: Soxhlet extraction setup	84
Figure 3.4: (a) Autoclave lid mounted with silicone O-ring (b) comparison between two O-rings after a successful run (intact) and unsuccessful run (torn).	88
Figure 3.5: Cure curves obtained for carbon black (CB) filled vulcanisates.....	92

Figure 3.6: Reciprocal of swell ratios of vulcanisates before (B) and after (A) aging of unfilled and filled rubber samples.	94
Figure 3.7a: Overlay of TGA curves of three randomly picked samples from cured compound.	94
Figure 3.7b: TGA curve quantification of sample composition (sample C).....	95
Figure 3.8: Thermal decomposition of DD and MBTS using high resolution TGA at 50 °C min ⁻¹ in an inert N ₂ (g) atmosphere	97
Figure 3.9: Surface plots for (a) dA vs. time (b) dA vs. temperature and (c) time vs. temperature against % devulcanisation.....	99
Figure 3.9: % Devulcanisation during temperature ramp (non-isothermal) vs. overall time period (isothermal) for (a) DD and (b) MBTS.....	102
Figure 4.1a: Overlay of heating profile and instantaneous heating rate for DD devulcanisation at 180 °C set-point.....	118
Figure 4.1b: Overlay of heating profile and instantaneous heating rate for MBTS devulcanisation at 180 °C set-point.	118
Figure 4.2: % Devulcanisation using DD at 140 °C and 180 °C set-points.....	121
Figure 4.3: % Devulcanisation using MBTS at 140 °C and 180 °C set-points.....	123
Figure 4.5a: Overlay of % Devulcanisation and heating rate for DD.....	125
Figure 4.5b: Overlay of % Devulcanisation and heating rate for MBTS.	126
Figure 4.6: Model validation plot for DD non-isothermal devulcanisation at 180 °C set-point.	128
Figure 4.7: Model validation plot for MBTS non-isothermal devulcanisation at 180 °C set-point.	131
Figure 4.8: Summary of changes in the crosslink densities of vulcanisates during analysis.	134
Figure 4.9: Effect of amount of (a) DD and (b) MBTS used on % devulcanisation.	135

Figure 4.10: Effect of pressure on % devulcanisation using DD and MBTS at optimum conditions.....	138
Figure 4.11: Effect of filler on degree of devulcanisation using DD and MBTS.....	140
Figure 4.12: Relation between the (a) degree of devulcanisation and (b) amount of sol produced with changes in the crosslink density over time using DD.....	142
Figure 4.13: Relation between the (a) degree of devulcanisation and (b) amount of sol produced with changes in the crosslink density over time using MBTS.....	143
Figure: 4.14: Change in NR/SBR relative composition due to preferential devulcanisation by (a) DD and (b) MBTS	146
Figure 4.15: Shore-A hardness of gels taken at 5, 15 and 30 minutes.....	147
Figure 4.16: FTIR analyses of DD and MBTS devulcanisates. The spectra shows; a) standard SBR, <i>i.e.</i> uncured starting material, b) neat vulcanisate c) MBTS devulcanisate and d) DD devulcanisate.....	151
Figure 5.1: Size reduction to achieve coarse grade crumb; $1 < x \leq 2.36$ mm (<i>i.e.</i> 8 – 18 mesh) size range.	171
Figure 5.2: Cryogenically ground truck tyre tread produced (a, b and c).....	175
Figure 5.3: Determination of GTR composition using high resolution TGA.....	177
Figure 5.4: Degree of devulcanisation of GTR obtained at optimised conditions.....	179
Figure 5.5: Crosslink distribution of LPV and GTR.	181
Figure 5.6: FTIR analysis of d) neat GTR and sol components obtained from devulcanisation using (e) DD and (f) MBTS. (a), (b) and (c) represent raw NR, SBR and BR respectively.	187
Figure 5.7: FTIR spectra of GTR devulcanisates showing (a) raw NR, (b) raw SBR, (c) raw BR, and GTR devulcanisates obtained from using (d) DD and (e) MBTS.	189
Figure 5.8: Tg of GTR gel samples for neat GTR, devulcanisates of DD and MBTS.....	190

LIST OF TABLES

Table 1.1: Influence of cure system on vulcanisate network structure ^[27]	6
Table 1.2: Bond energies of chemical bonds involved in the sulphur crosslink network	20
Table 1.3: Elastic constants of chemical bonds in the sulphur crosslink network ^[84, 85]	21
Table 2.1a: Reactor parameters.....	49
Table 2.1b: Calculated vs. Observed values	49
Table 3.1: Compound formulation used (<i>adapted from Nocil Limited</i>).	81
Table 3.2: Experimental domain for multiple linear regression of isothermal devulcanisation.	87
Table 3.3: Cure characteristics for CB-filled and unfilled vulcanisates.	92
Table 3.4: TGA percentage weight changes for identified sample composition.	95
Table 3.5a: Accepted final regression outputs for DD using logistic model ($H_0: b_i = 0$).	99
Table 3.5b: Rejected regression outputs for DD using logistic model ($H_0: b_i = 0$).	100
Table 3.6a: Accepted regression outputs for MBTS using logistic model ($H_0: b_i = 0$).	100
Table 3.6b: Rejected regression outputs for MBTS using logistic model ($H_0: b_i = 0$).	101
Table 4.1: Experimental domain for multiple linear regression of non-isothermal region ...	115
Table 4.2: t-Test: Two-sample assuming equal variances for DD devulcanisation at 140 °C and 180 °C set-points	122
Table 4.3: t-Test: Two-sample assuming equal variances for MBTS devulcanisation at 140 and 180 °C set-points	123
Table 4.4a: Accepted regression outputs for DD devulcanisation; ($H_0: b_i = 0$).....	127
Table 4.4b: Rejected regression outputs for DD devulcanisation ($H_0: b_i = 0$).....	127

Table 4.5: Optimum conditions predicted by solver tool for DD devulcanisation.....	128
Table 4.6a: Accepted regression outputs for MBTS non-isothermal devulcanisation ($H_0: b_i = 0$).....	129
Table 4.6b: Rejected regression outputs for MBTS non-isothermal devulcanisation; ($H_0: b_i = 0$).....	130
Table 4.7: Optimum conditions as predicted by the solver tool in Microsoft excel.....	131
Table 4.8 a) Correlation factors for DD devulcanisation process variables at 180 °C set-point.....	132
Table 4.8 b) Correlation factors for MBTS devulcanisation process variables at 180 °C set-point.....	132
Table 4.9: Summary of optimum conditions obtained for DD and MBTS.	133
Table 4.10a: Single factor ANOVA outputs for DD % devulcanisation ($H_0: \mu_{1\%} = \mu_{5\%} = \mu_{10\%}$).	135
SUMMARY.....	135
Table 4.10b: Single factor ANOVA outputs for MBTS % devulcanisation ($H_0 : \mu_{1\%} = \mu_{5\%} = \mu_{10\%}$).	136
SUMMARY.....	136
Table 4.11: GCMS analysed of acetone extract for DD and MBTS devulcanisates.	137
Table 4.12a: t-Test: two sample assuming equal variance for DD devulcanisation ($H_0: \mu_{80} = \mu_{100}$).....	138
Table 4.12b: t-Test: two sample assuming equal variance for MBTS devulcanisation ($H_0: \mu_{80} = \mu_{100}$).....	138
Table 4.13: Final optimum conditions obtained for DD and MBTS.	139
Table 4.14a: t-Test: Two-sample assuming equal variations for DD devulcanisation.	140

Table 4.14b: t-Test: Two-sample assuming equal variations for MBTS devulcanisation.....	141
Table 4.15a: Sol component molecular weights from DD devulcanisation	148
Table 4.15b: Sol component molecular weights from MBTS devulcanisation.....	149
Table 4.16: Summary outputs of optimum conditions.....	152
Table 5.1: Summary of GTR composition.....	178
Table 5.2: Final optimum conditions obtained for DD and MBTS.	178
Table 5.3: Single factor ANOVA for DD devulcanisation of GTR	182
Table 5.4: Single factor ANOVA for MBTS devulcanisation of GTR	183
Table 5.5: Molecular weights as determined by GPC	184
Table 5.6: Summary of GTR devulcanisation outputs.....	190

CHAPTER ONE: INTRODUCTION

1.1 MOTIVATION

The discovery of the process of vulcanisation in 1839 by Charles Goodyear and Thomas Hancock resulted in a huge demand for rubber, especially after the invention of automobiles. Vulcanisation confers improved mechanical properties of the rubber product as explained in the vulcanisation section. However, inasmuch as this is beneficial for the rubber industry, crosslinks render the rubber insoluble and infusible thereby presenting problems of recycling when rubber products *e.g.* tyres, reach their end life. The global production of elastomers reached 26 million tons in the year 2012, 40 % of this being NR and the remainder being the various synthetic rubbers ^[2]. The bulk of elastomers produced in industries is used in tyre manufacture. Due to their abundance and short life cycles, tyres present a huge waste management challenge. Around 800 million tyres are discarded per annum, and this value is increasing by about 2 % per year ^[2]. In view of this, recycling of waste tyres has gained a lot of attention. Therefore it is necessary and industrially relevant to find efficient means of recycling and reprocessing elastomers. A lot of research has been done on recycling of waste rubber using various techniques. However, none of these recycling processes have been able to establish a balance between quality and productivity of good quality reclaimed rubber ^[3].

Regeneration of good quality reclaim rubber needs that the Mw of the reclaim rubber be comparable to that of original rubber ^[4]. However, a lot of reclamation processes result in a high degree of polymer chain (*i.e.* C – C bond) breakdown due to intense working conditions. For example, mechanical reclamation processes involve massive shear forces and high temperatures that degrade polymer chains ^[4]. Also, most reclaiming processes are performed in the presence of oxygen which causes more chain scissions *via* thermo-oxidative degradation ^[5, 6]. Organic solvents (or reclaim oils) are usually used to swell the elastomer matrix so as to facilitate diffusion of reclaiming agents into the crosslink network. It is assumed that the reclaim oil aids oxidation of rubber chains since they easily form radicals due to their unsaturation ^[6]. As a result, the quality of reclaimed rubber is compromised. The reclaim rubber produced usually has properties that are inferior to the virgin polymer properties chiefly due to;

- Reduced molecular weight (Mw) of polymer chains due to C–C chain scission [3, 4, 7]
- Presence of oils or solvents used for reclamation, since they are not easily removable [4, 8]
- Presence of crosslinks in reclaimed rubber [3, 9, 10]
- Compromised structural integrity of polymer chains through shear forces, additives used and high temperatures *e.g.* cis-trans ratio, vinyl content, and formation of pendant groups [6, 11, 12].

For regeneration of rubber material with properties similar to original rubber, a method that ensures selective scission of crosslinks without main chain scission is needed.

1.2 RESEARCH ASPECTS

1.2.1 RESEARCH QUESTIONS

Is there a method of reclamation or devulcanisation that can establish a balance in the quality and productivity of reclaim or devulcanised rubber?

Can optimisation of devulcanisation processes result in an increased efficiency of rubber recycling?

In ensuring good quality devulcanised rubber, can use of environmentally friendly solvents as well as accelerators for vulcanisation be employed successfully in recycling processes without lowering the efficiency of devulcanisation?

1.2.2 RESEARCH STATEMENT

Currently available devulcanisation methods can be improved by means of optimisation using the degree of devulcanisation as the response variable to achieve maximum efficiency of devulcanisation. This would ensure good quality devulcanised rubber by maximising the degree of crosslink scission while minimising rubber main-chain scission.

1.2.3 HYPOTHESIS

Optimisation of devulcanisation processes using the degree of devulcanisation as the response variable would result in a high degree of crosslink scission with a corresponding minimum chain degradation.

1.2.4 RESEARCH AIMS

The research is aimed at improving the quality of devulcanised rubber by optimisation of devulcanisation conditions.

1.2.5 RESEARCH OBJECTIVES

- To employ a 2-level central composite design in the optimisation of isothermal devulcanisation conditions. Hence establish factors that influence devulcanisation processes.
- To make use of the degree of devulcanisation as the response variable for optimisation, thereby improve efficiency of devulcanisation.
- To compare the degree of devulcanisation between isothermal and non-isothermal devulcanisation, thereafter work on maximising the degree of devulcanisation.
- To show how the degree of devulcanisation and the amount of sol are correlated to the reduction of crosslinks during devulcanisation processes. Hence establish the best response variable for optimisation of devulcanisation processes.
- To optimise and determine the highest achievable degree of devulcanisation occurring during the non-isothermal stage within reaction parameters.
- To apply the optimised devulcanisation conditions on a commercial waste truck tyre tread.

1.3 BACKGROUND

Originally, the term rubber referred to natural rubber (NR), obtained in the form of latex from the *Hevea Braziliensis* tree ^[13]. The term was derived from the ability of the material to erase pencil marks on paper. Current usage of the term rubber is not limited only to NR, but is used arbitrarily to refer to any material with mechanical properties similar to that of NR regardless of chemical composition ^[13]. Nowadays use of the term elastomer has gained precedence. The term elastomer is used in relation to synthetic materials with rubber like properties. Most rubber materials exhibit poor properties when unvulcanised. For most applications, the rubber is vulcanised prior use, resulting in improved rubber properties.

1.3.1 Vulcanisation

In its original context, vulcanisation refers to the formation of a three dimensional network of sulphur crosslinks interconnecting polymer chains ^[14]. This phenomenon results in the modification of physico-mechanical properties of polymers. These changes include improvements in tensile strength, elastic modulus, compression set, heat evolution, swelling stability, insolubility in organic solvents, permeability to gases and resistance to low temperatures ^[15]. Owing mostly to technological advancement, different crosslinking agents such as metal oxides, sulphur monochloride, tellurium, selenium, thiuram accelerators, polysulphide polymers, p-quinone dioximes, organic peroxides, di-isocyanates peroxides and sulphur donors have since been discovered ^[15]. The term vulcanisation is used synonymously with crosslinking, curing and interlinking reactions; which in a way makes sense because all these terms refer to crosslink formation. However, to avoid ambiguity in reference to sulphur and non-sulphur curing systems, here the term vulcanisation is used specifically to refer to sulphur vulcanisation.

1.3.2 Network structure

The subject of vulcanisation is a broad and complex study on its own. For this reason, this research work only hints at the concept and relevant basics of the same. The effect of vulcanisation on rubber properties can be explained by the introduced crosslink network, and as such, knowledge of the crosslink network structure is important in understanding rubber properties. The chemistry of vulcanisation has been studied largely by use of low-molecular

weight analogues of polymers and extrapolating the results to the polymeric systems. Network structures of sulphur-vulcanised rubbers have been determined by spectroscopic analyses such as; Infrared (IR), Ultra Violet (UV), Electron-Spin Resonance (ESR), and Raman [16-18]. Use of solid state ^{13}C -Nuclear Magnetic Resonance Spectroscopy (^{13}C NMR) gained popularity in network structure analysis [19-22]. Figure 1.1 shows the proposed network structure for a typical sulphur-vulcanisate [15, 23-25].

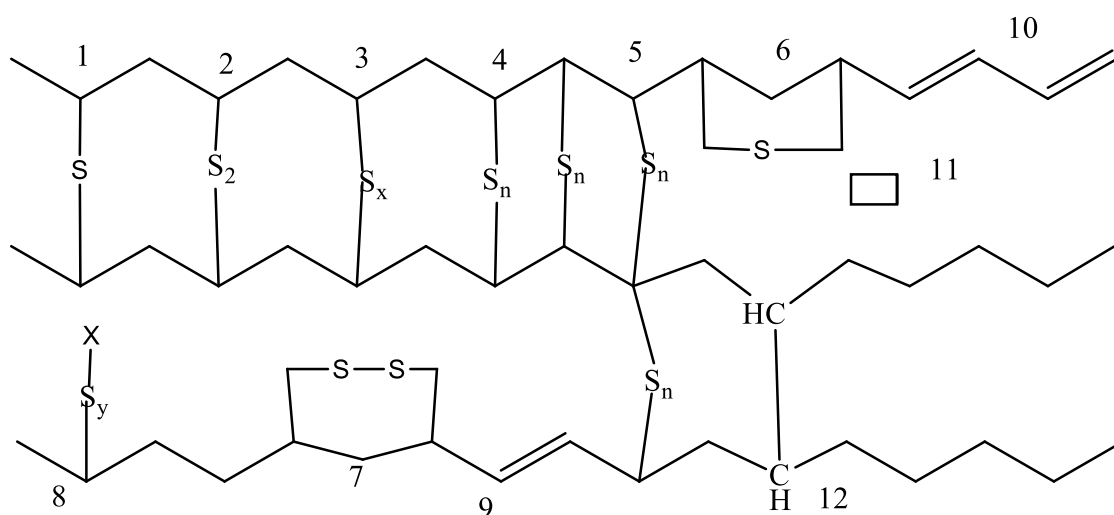


Figure 1.1: Typical network structure of a sulphur cured vulcanisate [15]

Where; (1) monosulphidic cross links, (2) disulphidic cross links, (3) polysulphidic cross links, (4) parallel vicinal cross links ($n=1$ to 6) attached to adjacent main chain atoms and act as a one cross link, (5) cross links that are attached to common or adjacent carbon atom, (6) intra-chain cyclic monosulphides, (7) intra-chain cyclic disulphides, (8) pendent sulphidic group terminated by moiety X derived from accelerator, (9) conjugated diene, (10) conjugated triene, (11) extra network material and (12) carbon-carbon cross links (probably absent) [23].

Of all the possible structures shown in Figure 1.1, crosslink distribution and density have been reported to be responsible for the modifications in rubber properties.

1.3.2.1 Crosslink distribution

The proposed network structure shows that there are three types of crosslinks; mono-, di- and poly-sulphide crosslinks. The relative composition of mono-, di- and poly-sulphidic crosslinks is known as the crosslink distribution. The distribution and density of crosslinks is affected by

factors such as accelerator type, sulphur dosage, accelerator to sulphur ratio, cure time and temperature ^[15]. Typical properties that distinguish the types of sulphur crosslinks are shown in Table 1.1. These give information about the ability of the crosslink system to produce the desired types and proportions of crosslinks as well as the degree of crosslinking. These systems are classified as efficient vulcanisation (EV), conventional vulcanisation (CV) and semi-efficient vulcanisation (SEV) ^[15]. The accelerator/sulphur ratio is the only difference among these systems. Generally, high accelerator to sulphur ratio and longer cure times increase the number of mono and di-sulphide crosslink formation at the expense of polysulphide crosslinks ^[15, 26]. Such networks, rich in mono and di-sulphide crosslinks, show better heat stability, lower compression set and longer reversion time as compared to polysulphide predominant network due to better stability of C-S bonds compared to S-S bonds. Conversely, vulcanisates containing a relatively higher degree of polysulphide crosslinks offer greater tensile strength, tear strength and flex-fatigue resistance due to the ability of S-S bonds to break reversibly, thereby releasing local stresses which could initiate failure ^[26].

Table 1.1: Influence of cure system on vulcanisate network structure ^[27]

	Conventional	Semi-EV	EV
Poly & disulphidic crosslinks (%)	95	50	20
Monosulphidic crosslinks (%)	5	50	80
Cyclic sulphide concentration	High	Medium	Low
Low temperature crystallisation resistance	High	Medium	Low
Heat ageing resistance	Low	Medium	High
Reversion resistance	Low	Medium	High
Compression set, 22 hours at 70 °C	30	20	10

1.3.2.2 Crosslink density

Crosslink density (ν) refers to the molar concentration of sulphur crosslinks per unit volume [26]. ν studies are important in understanding ν influence on physical and dynamic mechanical properties of cured rubber articles. Changes in the ν have been reported [13, 15, 23, 28] to have a direct influence on rubber properties such as tensile strength, shore-A hardness, elongation, resilience and other mechanical properties. So by simply changing the ν desired rubber properties can be attained. The effect that different ν has on various physical properties of vulcanisates is shown on Figure 1.2;

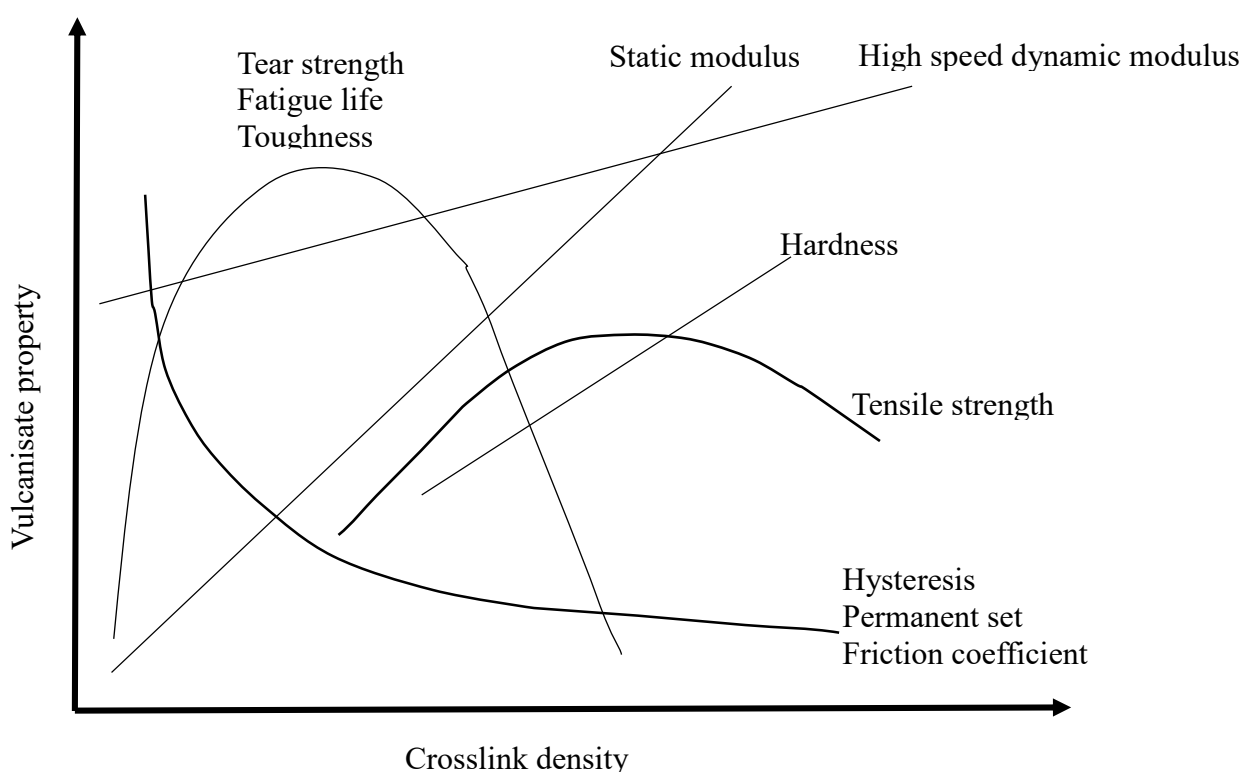


Figure 1.2: Influence of crosslink density on vulcanisate properties [15].

Tear strength, fatigue and toughness initially increase as ν is increased, and then decline as ν is increased further. Hysteresis, permanent set and friction coefficient decrease with an increase in ν [15, 23, 26]. Hardness, static (or elastic) and dynamic modulus increase with ν . The dynamic

modulus is dependent on the visco-elastic property of the vulcanisate [15]. Viscoelasticity implies behaviour that is similar to that of viscous liquids and pure elastic solids. In viscous systems, all the energy applied to the system is dissipated as heat (*i.e.* hysteresis) whereas in elastic systems the energy is stored as potential energy such as in a spring [29]. When deforming energy is applied onto a vulcanisate, part of the energy is stored as elastic energy while the rest is dissipated as heat due to molecular motion. Both of these components contribute towards preventing chain breaking. As the vulcanisate is further crosslinked, chain mobility becomes highly restricted and the chains cannot effectively dissipate heat generated by deformation via molecular motion, resulting in easy and brittle rupture at low elongation [26]. Consequently, tensile strength increases to a maximum and then starts decreasing as crosslink density is increased.

i **Determination of Crosslink density**

The strong correlation of ν and vulcanisate properties only drives to the question of how one can determine the ν of a rubber vulcanisate. The most common techniques used to determine ν are equilibrium swelling [30-34], stress-strain measurements [35] and solid state NMR [19, 22, 36-40]. However, a lot of techniques have been reported to give an indication of crosslinking; *e.g.* dynamic mechanical thermal analysis (DMTA) [41, 42], differential scanning calorimetry (DSC) [43], and atomic force microscopy (AFM) [44]. In this study equilibrium swelling method is used to determine ν of rubber vulcanisates. This method also allows determination of the average molecular weight between crosslinks (M_c), according to the equation; $\nu = \rho_R/2M_c$ (defined per volume of rubber of density ρ_R) [26].

a) Thermodynamics of solvent swelling of vulcanisates

The Flory – Rehner model is usually used to explain the thermodynamics of rubber swelling. During solvent swelling, the suitable solvent penetrates the rubber matrix causing the rubber vulcanisate to swell. This occurs until the retractive forces of the rubber network balance the solvent force, at this state the system has reached equilibrium swelling and Gibb's free energy is at zero ($\Delta G = 0$).

The total Gibb's energy is a function of the elastic and mixing components. For a swollen vulcanisate, the mixing and elastic components of the free energy are additive and separable [45], this leads to;

$$\Delta G_{total} = \Delta G_{mix} + \Delta G_{elastic} \quad (1)$$

Then at equilibrium;

$$\Delta G_{mix} = -\Delta G_{elastic}$$

This can be expressed in terms of change in the chemical potential of the solvent ($\Delta\mu_s$) [45];

$$\frac{\Delta\mu_s^{mix}}{RT} = \frac{\Delta\mu_s^{elastic}}{RT} \quad (2)$$

Where, R is the ideal gas constant and T is the temperature. The Flory – Huggins expression is usually used in defining the mixing term, and as such;

$$\frac{\Delta\mu_s^{mix}}{RT} = \ln(1 - \phi_R) + \phi_R + \chi\phi_R^2 \quad (3)$$

Where ϕ_R is the volume fraction of the rubber and χ is the Flory - Huggins polymer – solvent interaction parameter. In the Flory – Rehner equation, the elastic contribution is expressed in terms of the Affine deformation model [45];

$$\Delta G_{elastic} = \frac{RT}{2M_c} (\lambda_x^2 + \lambda_y^2 + \lambda_z^2 - 3) - \frac{2RT \ln \frac{V}{V_0}}{fM_c} \quad (4)$$

Where λ_i is the expansion in three dimensions (where i = x, y or z), V is the swollen polymer volume, V_0 is the pure polymer volume and f is the functionality of the crosslinks. Derivation of the Affine model and equating to the mixing term according to equation 3 gives the Flory – Rehner equation;

$$\ln(1 - \phi_R) + \phi_R + \chi\phi_R^2 = -\frac{\rho_R}{M_c} V_s \left(\phi_R^{\frac{1}{3}} - \frac{2\phi_R}{f} \right) \quad (5)$$

Where V_s is the molar volume of solvent (in cm^3/mol .) For unfilled rubber vulcanisates, equation 5 is usually expressed as ^[26];

$$v = -\frac{1}{2V_s} \frac{\ln(1 - \phi_R) + \phi_R + \chi\phi_R^2}{\phi_R^{1/3} - \frac{\phi_R}{2}} \quad (6)$$

Where, v is the crosslink density in $\text{mol}\cdot\text{cm}^{-3}$. Equation 6 assumes tetra-functional crosslinks.

For vulcanisates with filler, equation 6 has to be corrected for filler interactions otherwise this would result in overestimation of crosslink density. So the ϕ_R is obtained from ^[26];

$$\frac{\phi_R}{\phi_{fR}} = 1 - [3c(1 - \phi_R^{1/3}) + \phi_R - 1] \frac{\phi_f}{1 - \phi_f} \quad (7)$$

Where ϕ_{fR} is the volume fraction of the filled rubber in swollen gel, C is the filler rubber interaction parameter and ϕ_f is the filler volume fraction in unswollen vulcanisate.

b) Uncertainties in equilibrium swelling method

Valentin *et al* ^[45] reported on several uncertainties involved in the equilibrium swelling method that result in significant deviations from the true value of crosslink density. They identified uncertainties in determination of χ , ϕ_R and the model used to explain the elastic term on the commonly used Flory – Rehner equation. Bills *et al* ^[46] also pointed on uncertainties that may result from sol and filler – rubber interactions upon determination of ϕ_R .

The Flory – Huggins solvent interaction parameter (χ) has been used as the key descriptor of polymer properties in solution or swelling for a polymer network ^[45]. It gives an indication of the relation or interaction of solvent with polymer molecules. It is influenced by entropic and heat of mixing terms ^[45]. It was defined as inversely related to temperature, and not related to polymer fraction. However, experiments have shown that the parameter is also dependent on the volume fraction of polymer. McKenna *et al* ^[18, 47-50] and Horkay *et al* ^[51-56] showed *via* extensive research on the parameter, that it is different for crosslinked and uncrosslinked

polymers at similar polymer volume fractions. In all systems investigated it was found that χ for crosslinked polymer is greater than for the uncrosslinked polymer. Flory later on made changes in the description of χ due to the new developments^[45]. Thus upon use of the parameter for a polymer-solvent pair, one has to be aware of these factors in order to minimise deviations from true crosslink density determination.

Valentin *et al*^[45] and Ellis *et al*^[57, 58] point out to missing components in the determination of the polymer volume fraction (ϕ_R). ϕ_R is determined by a simple expression; $\phi_R = \frac{V_R}{V_R + V_S}$. This definition of ϕ_R is however not representative of the true volume fraction as it does not factor in effects of insoluble components in the vulcanisate, such as ZnO and some curatives. It was shown that the presence of insoluble components in the swollen vulcanisates, distorts the value of ϕ_R via additional volume (of insoluble components) plus excess solvent uptake due to trapping of solvent in vacuoles formed at ZnO – rubber interface. Therefore corrections for these factors were suggested by Valentin *et al*^[45] and Ellis *et al*^[57, 58]. According to Martin *et al*, the amount of sol (linear polymers not involved in the network) in a vulcanisate may be quite significant to affect ν determinations. Bills *et al*^[46] showed corrections that can be made to nullify the effect of sol. Nonetheless, ASTM D6814 suggests treating the vulcanisate with solvents prior to crosslink density determinations. This should in the least, get rid of or reduce the amount of sol in the vulcanisate. Another source of error in the determination of ϕ_R using the gravimetric method is the choice of density of polymer used. It is common practice to use the original polymer density, which is incorrect since the polymer in the vulcanisate is in a totally different system as in the original unvulcanised polymer state. Therefore the polymer density is bound to change. Fortunately, ASTM D6814 provides a method to account for the changes in the density of polymer, thereby enabling determination of the actual polymer density in the test sample.

According to Valentin *et al*^[45], the elastic term on the Flory-Rehner equation is questionable by some works, and it is thought that the real behaviour of swollen vulcanisates should be between the two suggested behaviours of the Affine and Phantom models. The Affine model suggests that deformation at macro scale is the same as at micro scale, implying that the crosslinks are in a fixed state. On the other hand the Phantom model suggests free crosslink movement about a mean position^[45]. These two ideas were factored into the Flory-Erman model, which by means of a K-parameter, attempts to reconcile the aforementioned two extremes, thereby giving a more realistic representation of the process^[59].

For quantitative determinations of the crosslink density, the above mentioned corrections should be considered. Otherwise values of ν determined without careful consideration of factors at play would only be a good qualitative measure as they would likely contain the underlined uncertainties. The reciprocal of the swelling factor has been used ^[31, 32, 34] to indicate degree of crosslinking according to the expression; $\nu \propto \frac{1}{Q}$, where Q is the equilibrium swelling factor of vulcanisate given by; $Q = \frac{W_s - W_d}{W_d}$, where W_s and W_d are the weights of swollen and unswollen (dried) rubber samples. So from this expression, increasing crosslink density results in low degree of swelling. Which makes sense since an increase in crosslink density would cause an increase in the retractive forces of vulcanisate, therefore restraining swelling. This relationship between Q and ν should be free of uncertainties from effects of insolubles, polymer – solvent parameters, polymer volume fractions and effects of fillers given these factors remain constant in the test samples, so that any variations in swelling are solely due to differences in degree of crosslinking. This relationship was employed in this study to give a qualitative indication of changes in the crosslink densities.

1.3.3 Crosslinking in blends and co-vulcanisation

Industries usually blend polymers in an attempt to produce products of improved physio-mechanical properties, *i.e.* properties better than those of the individual polymers. This probably makes sense in that if one wants to achieve certain desired qualities that cannot be supplied by one type of polymer, combining polymers with different properties should yield a product of desired properties. One of the challenges in this approach is the incompatibility of polymers upon blending, which results in multi-phase systems ^[41]. For mutual solution of two materials to happen, the free energy of mixing has to be negative ^[60, 61]. Usually, mixing of polymers is an endothermic process with a very low entropy contribution due to the large sizes of polymers ^[62]. A study by Corish *et al* ^[60] revealed the presence of discrete zones of each elastomer upon blending. Microphotometer measurements indicated areas of zones to be approximately the same proportion as the volume composition of the blends. However, zone sizes decreased with mixing time ^[62], but reached a minimum value at long mixing times with a particular blender. Many blend properties depend on the blend composition whereas mixing procedure and shear control the domain size and have a more pronounced influence on morphology than blend composition.

It has been reported that elastomer blends do not co-vulcanise, and resultant blend properties are usually inferior to those predicted from the component elastomers^[63]. Co-vulcanisation is the ability of two elastomers to form a single network structure in which both elastomers, and their interphases, have become crosslinked to similar extents^[64]. Failure to co-vulcanise has been reported to be due to migration of vulcanisation ingredients from one phase to the other^[61, 63], resulting in differences in crosslink densities of the different phases. The major driving force for migration of ingredients is differences in solubility of curatives in component elastomers^[63]. Curatives would readily migrate from an elastomer in which they are least soluble to one they are most soluble in. As a result there is improper distribution of curatives between the different phases, which subsequently affects the degree of curing in different phases. Reaction kinetics also play a part in the migration of ingredients, i.e. relative rates of vulcanisation in the different phases^[60, 65]. Huson *et al*^[43] found that in a particular polybutadiene/natural rubber blend (BR/NR) containing tetramethyl thiuram disulphide (TMTD), the ν ratio was 2:1. This was attributed to the higher concentration of curatives (TMTD and sulphur) in the BR phase, owing to their higher solubility in that phase. In a similar polybutadiene/isoprene blend (BR/IR) the crosslink ratio was 4.1:1. The increased crosslink density in the BR in this case was attributed to the relatively slower curing rate of the IR phase, therefore allowing more time for migration to the BR phase. McGill *et al*^[62] concluded that the solubility of curatives in a phase, at the cure temperature, played the major role in determining the cure characteristics of a blend, while the rates of reaction of the elastomers played a secondary role. In other words, cure characteristics should give a hint on the degree of migration and homogeneity in a blend; homogeneity here referring to distribution of the different phases throughout the sample. If there is poor or uneven phase distribution in the sample, it would show by a marked variation in cure characteristics of different regions of the sample. Conversely, if different regions of the sample show slight differences in cure characteristics, this should translate to low levels of migration occurring and or good phase distribution. In this work, a blend of NR and SBR (styrene butadiene rubber) was used in a typical truck tyre tread formulation. The author is aware of existence of multiphase systems upon blending, as a result random sampling of the compound was done to determine variations in cure characteristics. In addition, thermogravimetric analysis (TGA) was done on the randomly chosen samples to establish consistency of NR/SBR composition throughout the blend. This should give an indication of how well mixed the blend is, and should help explain properties of the cured compound.

1.3.4 Rubber waste management

Various methods of waste tyre management have been implemented. These methods are classified according to the hierarchy proposed in the European Union (EU) guidelines ^[66]. In the order; least to most preferred, these methods include; landfilling, energy recovery, recycle, re-use and prevention.

1.3.4.1 Landfilling

Landfilling involves dumping waste tires and is the easiest means of disposing waste tires. This practice is highly discouraged and has been banned in some countries since it poses a great danger to the environment ^[67]. In South Africa, according to the Environment Conservation Act, (ECA, Act No. 73 of 1989) ^[68] on waste tyre management, it is illegal for any individual to dispose of a tyre anyhow without authorization. Landfilling has been banned by the European Commission since 1999 ^[69].

1.3.4.2 Energy recovery

Energy recovery involves burning of tyres for the purposes of harnessing energy. Waste rubber has a high calorific content (*ca.* 32.6 mega-J/kg), compared with that of coal (18.6–27.9 mega-J/kg) ^[4]. Thus waste rubber has the potential of relieving pressure on the use of fossils for energy production. A lot of kilns make use of waste tyre combustion in cement production. However, waste rubber combustion has to be controlled otherwise it creates a problem of air pollution via production of acrid black smokes and high levels of sulphur dioxide ^[8]. According to the ECA, a tyre producer, tyre dealer, or any other person involved in the tyre industry must first investigate the options of reusing or recycling waste tyres before recovering the energy potential of waste tyres or disposing of a waste tyre at a waste disposal facility ^[67]. Besides combustion of waste rubber, pyrolysis can be employed. Pyrolysis is a thermo-chemical process where organic solids are decomposed or volatilised *via* heating in the absence of oxygen at temperatures ranging between 400-800 °C ^[4]. This process results in the production of hydrocarbons, char and steel when waste tyres are treated. A more recent possibility of using waste rubber for energy production exists in the field of microbial fuel cells, whose applications are limited by the high cost of electrode material ^[8].

1.3.4.3 Recycling

High demand for rubber especially during the World War II implied tremendous strains in the supplies of rubber from natural resources. And as such, production of synthetic rubbers on its own was not enough to supplement the huge demands for rubber. Therefore rubber recycling was an inevitable necessity. These processes will be touched on later in the chapter.

1.3.4.4 Re-use

Most of the discarded rubber products are usually re-used for various purposes which they were not originally intended to serve. For example waste tyres turned to shoes or chairs. According to European Union (EU), re-use is defined as repeating the original use of an object, *e.g.* re-treading of end of life tires for re-use ^[66]. Re-use thus presents an easy way of waste management.

1.3.4.5 Prevention

The highest level of the waste management method is prevention of waste production. Prevention is at its infancy in waste management especially for rubber waste. Eco-design is part of the EU guidelines on waste management ^[8]. Tackling the environmental issues at an early stage, during the conception and design phase of a product, can indeed permit to create eco-friendlier products. For example in the rubber industry; rubber products with self-healing properties have been made by incorporation in the compound formulation, catalysts that facilitate metathesis ^[12]. Thermoplastic elastomers also represent a step in the direction waste of prevention ^[9].

1.3.5 Rubber recycling processes

Waste rubber recycling basically involves grinding of rubber to ground tyre rubber (GTR) or granules, compression moulding, reclamation and or devulcanisation. A typical scrap tyre contains (by weight) ^[70]:

- 70 % recoverable rubber
- 14 % steel
- 3 % fibre
- 13 % extraneous material (*e.g.* inert fillers)

Tyre recycling is focused mainly on regenerating the rubber component from waste tyres. Recovered steel and fibre have also found value for money in the rubber industry. As for extraneous materials, there are works that have managed to salvage oils used in rubber manufacture.

1.3.5.1 GTR production

The first step in rubber reclamation usually involves grinding the waste rubber to small particle sizes or granules which can then be converted into GTR ^[71-74]. GTR refers to any material derived by size reduction of waste tyres (or other rubber) into uniform granules with the inherent reinforcing materials such as steel, fibre and other inert materials or contaminants removed ^[70]. The main sources of crumb are waste tyres and tyre buffing dust from re-treading of tyres. Comminution of the scrap rubber can be *via*; cryogenic grinding, dry ambient or wet ambient grinding.

i) Cryogenic process

Developed in the 1960s ^[75-77], this process involves freezing vulcanised rubber chips (2 inches or less) using liquid nitrogen and then transferring them to a hammer mill or ball mill for size reduction. The use of cryogenic temperatures, *i.e.* temperatures of around -80 °C or less, ensures embrittlement of most polymers, and it can be applied at any stage of the grinding process. The chips are immersed in or sprayed with liquid nitrogen. Particle size distribution varies depending on time of freezing and sizes of screens used in the grinding process. The

most common sizes are subject to debate, *e.g.* 30-100 mesh has been reported ^[4] while another article reports it to be $\frac{1}{4}$ inch to 30 mesh. Usually, the smaller the size of GTR the more expensive it is. Cryogenic grinding avoids heat generation during grinding, in this way rubber degradation by heat is minimized. The resultant GTR appears shiny, has clean fractured surfaces and very low steel or fibre content ^[4]. The steel is removed by means of magnets while the fibre is aspirated and screened.

Advantages of cryogenic processing include; low equipment and operating costs, high productivity *e.g.* throughput of 4000-6000 pounds of crumb per hour. The GTR improves mould flow and reduces shrinkage. Its surface features allow excellent ventilation of trapped air in uncured rubber sheets and thus minimises cure blistering. Due to its shiny, clean fractured surfaces, it offers low surface area thereby minimising effects of oxidative degradation ^[4].

ii) Dry ambient process

Ambient grinding involves a number of stages of grinding where the rubber feed is passed through a series of machines (granulators or cracker mills) to separate tyre components. The feedstock (of any size including whole tyre) is introduced into the mill at ambient temperature, and ground to small rubber chips. The chips are then passed onto the second stage where they are further ground with removal of fibre and steel components. The ground rubber is then transferred to the final stage where it is ground to the required particle size. At each stage, sifting is done and returns oversized particles, metals are removed magnetically and fabric is removed by means of air separators. Rubber grinding generates heat during processing. With aged rubber, or rubber with high modulus, the amount of heat generated is so high it results in polymer degradation and formation of some pendant groups on polymer main chain ^[4]. Rubber particles produced (generally 10 – 30 mesh size range) usually have rough texture and cut surfaces. Markets for ambient ground rubber include; tyres, mechanical goods, playgrounds, horse arenas, walking/jogging paths, mats for domestic, commercial, recreational, industrial and agricultural use, rubber wheels for carts and lawnmowers, insulation products and other construction products ^[10, 70].

iii) Wet ambient process

This process is also called fine grinding or micro milling. This is due to that coarse GTR (*ca.* 10 – 20 mesh) is mixed with liquid (usually water) forming a slurry, then further ground to very fine sizes (*ca.* 40 mesh or less). 200 – 500 mesh sizes have been reported ^[4]. The process is similar to that of dry ambient grinding except here there is use of water. Aside from production of fine GTR, another advantage of this process is consistency and cleanliness of the GTR produced. In addition, the fine GTR allows for relatively smooth extrudates and calendered sheets.

1.3.5.2 Compression moulding

At high temperatures, di- and poly- sulphidic crosslinks are known to undergo exchange reactions ^[4, 78]. In 1981, it was discovered that GTR could be compression moulded without reclaiming ^[78]. GTR was compression moulded in the presence of curatives to form a rubber product. However, the properties of the compression moulded rubber product were inferior to that of the original rubber. Compression moulding has also been shown to be achievable without addition of curatives ^[2, 6, 79-83].

1.3.5.3 Reclamation processes

i) Reclamation vs. Devulcanisation

Unlike thermoplastics, thermosets cannot be reprocessed simply by heating. This is due to the presence of a crosslink network interconnecting polymer chains. To be able to reprocess thermosets the crosslink network has to be severed, which is the inherent challenge in the field of thermoset recycling. Early reclamation methods sought to break down thermosets to increase plasticity, and then re-use the plasticised vulcanisate in normal processing of new rubber vulcanisates. In 1981, the Rubber Recycling Division of the National Association of Recycling Industries defined reclaimed rubber as the product resulting when waste vulcanised scrap rubber is treated to produce a plastic material which can be easily processed, compounded and vulcanised with or without the addition of either natural or synthetic rubbers ^[4, 6]. Regeneration by early reclamation methods was highly non-selective, *i.e.* would result in both crosslink and

main chain scission. Rubber main chain scission leads to a reduction in the molecular weight (Mw), which is accompanied by a loss in the original rubber properties. Hence the reclaim would be used more like a processing aid. It has been claimed that the use of reclaim in rubber compounding results in; shorter mixing times, lower energy consumption, lower heat development, faster processing on extruders and calenders, lower die swell of the unvulcanised compound, and faster curing of the compounds ^[4]. The amount of reclaim incorporated in formulations is usually based on the application of the product concerned. For many rubber products, about 5-10 % reclaim can be mixed with virgin rubber without serious negative effects on the physical properties ^[11].

A lot of techniques have been employed in an attempt to regenerate original polymer properties from scrap rubber. Unfortunately, none of the existing techniques have been able to regenerate the original polymer properties. This is chiefly due to that chain scission is unavoidable during reclamation. Reclamation results in formation of sol and gel components. The sol is the soluble fraction made up of truncated linear polymer chains that can dissolve in a suitable solvent, while the gel component is the insoluble fraction that still contains crosslinks ^[3]. For recovery of original polymer properties, or at least comparable properties of reclaim, the Mw of reclaimed polymer has to be comparable to the original polymer Mw. It is of the author's belief that devulcanisation is a step towards the goal of achieving original polymer recovery. In ASTM ST P 184A, devulcanisation was defined as a combination of depolymerisation, oxidation, and increased plasticity. This is inaccurate in context of the word. In principle, devulcanisation should be the reverse of vulcanisation. If vulcanisation is crosslink formation then devulcanisation should be breaking of crosslinks, *i.e.* de-crosslinking. Myrhe *et al* ^[84] defined devulcanisation of a sulphur-cured vulcanisate as the process of cleaving, either totally or partially, of the sulphur cross-links formed during the vulcanisation process. So if the reclamation process selectively cleaves crosslinks it can be called devulcanisation. Loads of work has been done and reported on devulcanisation, most of which have not been successful at regenerating original polymer properties and a very few reports claiming to have achieved this goal ^[3, 8].

ii) *Fundamentals of reclamation techniques*

Most, if not all devulcanisation techniques are hinged on the exploitation of certain properties that have been identified to be fundamental weaknesses in the sulphur-crosslink network. These are properties of the chemical bonds involved in the crosslink network, namely; differences in bond energies, differences in shear stiffness, differences in chemical reactivity and susceptibility to biological attack (by bacteria) ^[84].

a) **Differences in bond energies**

The different types of bonds in the crosslink structure have different bond energies. The lower the bond energy is, the lower the amount of energy needed to break it.

Table 1.2: Bond energies of chemical bonds involved in the sulphur crosslink network [84, 85]

Bond type	Bond energy (kJ/mol)	Network location
S-S	270	Di- & polysulphidic crosslinks
C-S	310	Monosulphidic crosslinks
C-C	370	Main chain bonds

When heat (energy) is applied, bonds with the lower bond energies would be cleaved relatively more easily than ones with high bond energies. Microwaves and ultrasounds have been used to exploit differences in bond energies to achieve devulcanisation ^[4, 5, 11, 70].

b) **Differences in shear stiffness**

There is also a difference in the elasticity of the different bonds involved in the crosslink. S–S bonds are relatively stiffer than C–C bonds on the polymer chain, hence when shear forces are applied, S–S bonds would preferentially break first.

Table 1.3: Elastic constants of chemical bonds in the sulphur crosslink network ^[84, 85]

Bond type	Elastic constant	Network location
S-S	~3	Di- & polysulphidic crosslinks
C-S	Intermediate	Monosulphidic crosslinks
C-C	~100	Main chain bonds

c) Differences in reactivity of chemical bonds

The different chemical bonds have different atomic structures and chemical reactivity. This can be exploited by use of chemical agents that specifically attack or react with these bonds to achieve devulcanisation. Chemical probes have been used to selectively cleave different sulphur bonds in the crosslinks e.g. hexanethiol for cleaving di and poly-sulphidic crosslinks, 2-propanethiol for cleaving mono-sulphidic crosslinks, triphenyl phosphine for poly-sulphidic bonds and methyl iodide for mono-sulphidic bonds ^[4, 8].

d) Susceptibility to microbiological attack

Chemolithotrophic bacteria selectively consumes sulphur in crosslinks, thereby causing desulphurisation. The main drawback with this method of recycling is that the bacteria have to be in intimate contact with the sulphur crosslinks. The challenge is that penetration into the rubber matrix is difficult, hence most success is on the rubber surface ^[84]. This can however be improved by increasing the surface area of the rubber.

It is common practice that a combination of different techniques be used to achieve devulcanisation, *e.g.* mechanical methods of reclamation involve shearing, which generates heat during reclamation. This can further be enhanced by incorporating capping agents to prevent recombination of cleaved chains. It is important to note that inasmuch as there are these fundamental differences in the types of crosslink bonds to exploit, the differences so far have not proved to be too great to result in complete devulcanisation without altering the main polymer chain. Processes have mostly been facilitating compatibility of reclaim with the virgin rubber counterpart. These reclamation processes can be classified into four categories, namely ^[4-6, 8, 11, 84],

- Physical techniques,
- Chemical techniques,
- Physicochemical techniques,
- Thermal techniques, and
- Biotechnological techniques

The current study does not seek to explain in full detail the processes involved in rubber reclamation nor confine the number of processes available to those described here, but it briefly describes some commonly used techniques with references to studies that may provide further details on the techniques concerned.

1.3.6 Techniques used in reclamation

1.3.6.1 Physical techniques

These include mechanical, thermo-mechanical, cryo-mechanical (section 1.3.1), microwave and ultrasonic methods. These methods involve application of external energy or force to achieve reclamation ^[4].

i) Mechanical methods.

This technique exploits the differences in the elasticity of S-S bonds in the crosslinks and C-C bonds on the main chain for a sulphur cured rubber. Shear forces are generated within the rubber resulting in preferential degradation of S-S and S-C bonds. For other cure systems, a certain degree of elasticity difference between C-C bonds on the crosslinks and C-C bonds on the main chain exists to allow for preferential crosslink degradation ^[84]. Reclamation by mechanical means can be achieved through various processes such as inside a co-rotating twin-screw extruder ^[8], on an open two roll mixing mill ^[4] and by means of rubber slurry ^[86].

In an extruder, high shear forces generated by the rotating screw are responsible for reduction of crosslink density as well as chain scission ^[87]. Even though the process may be carried out at ambient temperatures, shear forces result in temperature increase. The two roll mill also

operates on the basis of generating shear forces to breakdown the rubber. De *et al* ^[88, 89] reported on mechanical reclamation where they used an open two roll mill at temperatures of 80 °C. They found that the Mooney viscosities of the reclaimed rubber were quite high, *i.e.* above 200 ML which is out of scale, showing existence of crosslinks instead of a more plastic product.

Mechanical reclamation of rubber in slurry is done at ambient temperatures by forcing the rubber slurry through metal screens of decreasing mesh sizes. In this process, various metal alloys act as catalysts to reduce crosslink density. Mechanical reclamation has advantages of not involving the use of chemicals. This implies low costs, low health and safety risks, minimum odours, application in cure systems other than sulphur and is relatively environmentally friendly ^[84].

ii) Thermo-mechanical methods

These techniques are similar to mechanical processes except for the use of high temperature to facilitate reclamation of vulcanisates. Thus they exploit differences in elasticity and energy needed for bond breaking, but usually result in high degree of C-C scission due to intense heat and mechanical working. This is accompanied by significant losses in physical properties of the reclaim produced ^[84]. Most recent reclamation processes make use of this method. In some cases, reclaiming chemicals and oils are used to further aid reclamation ^[6]. There are several methods that are classified under thermo-mechanical reclamation. These include;

- High speed mixing -done at temperatures of around 200 °C at fast mixing speeds of about 500 rpm ^[90],
- Reclaimator process -one of the most successful process involving single extrusion at 200 °C at low extrusion times, which makes it ideal for synthetic rubber which harden with time) ^[91],
- Ficker process – uses a co-rotating extruder and reaches temperatures around 240-280 °C ^[6]
- Milling process –rubber vulcanisate is swollen in suitable solvent and subjected to milling to produce fine rubber powder (*ca.* 20 µm) ^[6].

Other equipment that has been used in this type of reclamation is the counter rotating twin screw extruder at temperature range 100-180 °C ^[92], internal mixer used together with twin screw extruder ^[6].

iii) Microwave method

Developed in the late 1970's by Goodyear Tire and Rubber Company, the use of microwaves is probably the most selective method of devulcanisation ^[5]. This devulcanisation technique exploits differences in the bond energies of S-S, S-C and C-C bonds. Microwave energy causes molecular motion within the rubber resulting in heat generation which gives rise to temperatures of up to 260-350 °C ^[6]. This heat generation occurs at a very fast rate such that if not carefully controlled can result in polymer degradation. This poses an issue for diene based rubbers due to their relatively low thermal stability as compared to the likes of EPDM and butyl rubbers ^[11]. Thus to achieve high degree selective crosslink degradation, the process has to be carefully controlled, which is a huge challenge. For microwave devulcanisation to work the rubber has to be polar enough to absorb the microwave energy at a fast rate (*e.g.* nitrile rubber), or can contain of carbon black. Carbon black containing rubber is susceptible to microwave frequency due to interface or ion polarisation ^[6]. If microwave energy can be set to specifically target crosslinks (*ca.* 915 or 2450 MHz ^[6]), chain scission can be minimised.

iv) Ultrasonic method

This technique makes use of ultrasonic waves to preferentially sever S-S and C-S bonds. However, like many other methods, chain scission is unavoidable, plus it also causes main chain modifications ^[5]. Companies that make use of this technique usually couple it with extruders. So the rubber would be fed into the extruder, heated and or masticated, then subjected to ultrasonic waves to effect devulcanisation. The first work of ultrasonic devulcanisation was reported by Pelofsky ^[93]. In the report, ^[93] rubber vulcanisates immersed in a liquid were effectively disintegrated by subjecting them to ultrasonic radiation of about 20 kHz and at least 60 W power, resulting in dissolution of the rubber. In 1987, Okuda and Hatano claimed to have successfully selectively cleaved an NR vulcanisate using 50 kHz ultrasound within 20 minutes, resulting in reclaim with properties similar to that of the virgin rubber ^[94]. The actual mechanism of devulcanisation by use of ultrasounds is not yet fully understood but extensive work on possible mechanisms and models to explain the process are described by Isayev and Ghose ^[5, 69].

1.3.6.2 Chemical techniques

This technique exploits differences in reactivity of the C-C, S-S and C-S bonds. Usually the rubber is in the form of crumb, to offer a high surface area for chemicals, and swelling solvents are used at high temperatures to facilitate penetration of chemicals into the rubber matrix. Use of chemicals can achieve high selectivity, thereby reducing losses in physical properties of the reclaim produced. However, there is a couple of disadvantages associated with the use of chemicals in reclamation; some are odorous, some may require high temperatures to start working (*i.e.* energy costs)^[5], can be a health and safety hazard, expensive to purchase, may not be totally selective in devulcanisation and may increase factory emissions of volatiles. In addition, the use of organic solvents make it difficult for industries to scale up. Reclamation chemicals can be grouped as;

- *Organic compounds*; these are mostly organic disulphides and mercaptans. Myrhe *et al*^[5] divided the types of reclamation chemicals according to their nature of reaction; (1) chemicals that act as capping agents to prevent recombination *e.g.* disulphides and thiols, (2) chemicals that cleave crosslinks via nucleophilic reactions *e.g.* amines and their derivatives. Examples of chemical reclaiming agents developed and patented since 1910 include diphenyl disulfide, dibenzyl disulfide, diamyl disulphide^[95, 96], bis(alkoxy aryl) disulfides^[97], butyl mercaptan and thiophenols^[97, 98], xylene thiols^[97] and other mercaptans^[97], phenol sulfides and disulfides^[96, 97] have been developed.
- *Inorganic compounds*; *e.g.* nitrous oxide^[8] (causes a lot of chain scission *via* cyclo addition reactions with dienes, thus can be used on diene rubbers that are not Sulphur cured), Grubbs catalyst (is an organometallic complex that causes high degree of chain scission *via* cross metathesis) and lithium aluminum hydride (can be used to convert organic poly- and disulfides into thiols)^[4].
- *Miscellaneous*; *e.g.* phase transfer catalyst (quaternary ammonium salt used to transport hydroxyl group into rubber matrix), and benzoyl peroxide^[99].

1.3.6.3 Physico-chemical techniques

Chemicals and oils are usually used during thermo-mechanical reclamation to further aid the process of rubber plasticisation. These methods can be conducted at ambient temperatures, high temperatures (by deliberately heating) or simply run at ambient and allowed to heat up from frictional forces due to shear. Generally, when conducted at ambient temperature, a reclamation

catalyst, oil, processing oil and reclaiming agent are added to the mixture for reclaiming [4]. There are a lot of mechano-chemical processes in use, some of which have been commercialised. Examples include;

i) Trelleborg cold reclaiming (TCR) process

Small amounts of reclamation chemicals (phenyl hydrazine-methyl halide or diphenyl guanidine) are mixed with cryo-ground rubber powder at room temperature or slightly higher. The chemicals facilitate reclamation [90].

ii) De-Link process

Reclamation is done using vulcanisation accelerators such as mixture of dimethyl dithiocarbamate and mercaptobenzothiazole or tetramethyl thiuram disulphide [6] on a two-roll mill at temperatures of 50 °C for *ca.* 7 minutes [6, 100].

iii) Swelling in benzene with a sulfoxide

Vulcanisates are swollen in benzene containing reclamation chemicals (dimethyl sulfoxide (DMSO), di-n-propyl sulfoxide (DPSO) or a mixture of these with thiophenol, methyl iodide or n-butyl amine) [5]. These are then processed on a mill [101].

1.3.6.4 Thermal techniques

This technique exploits the differences in bond energies of S-S, S-C and C-C bonds. Almost all reclamation processes make use of heat or high temperatures, while a few are carried out at ambient, low or cryogenic temperatures. Use of high temperature conditions dates back to oldest methods of reclamation (*i.e.* thermal, pan/heater and digester processes). The following is a brief description of these methods as well as a description of relatively more recent methods that are based on these early methods;

i) Thermal process

Rubber vulcanisates are heated inside a pan in an autoclave at 260 °C and 60 psi steam exposure for 1 hour, followed by further processing [5].

ii) Heater or Pan process

Rubber vulcanisates are heated inside pans in a single-shell steam autoclave at 100-300 psi in the presence of reclaiming agents, oils, wetting or charring agents. This is done for about 3 hours 15 minutes at 150 lbs steam pressure. Further processing is then done afterwards ^[5].

iii) Digester process

Ground rubber is mixed with fibre dissolving agents, water, plasticisers and reclaiming agents, then heated in a steam autoclave (double jacketed ^[5]) at 180 °C, 15 bar pressure for 8-12 hours. Further processing is then carried out ^[5].

iv) Alkaline process

The fibre in scrap material is digested by use of concentrated (*ca.* 7 %) sodium hydroxide. Further processing then follows. This method is not good for rubbers like SBR as hardening takes place ^[5].

v) Neutral process

This is a modification to overcome hardening that takes place for SBR. The base is replaced by a chloride of calcium or zinc ^[5].

vi) High pressure steam process

Fibre free ground rubber is mixed with reclaiming agents and reclamation done at high pressures and temperatures (280 °C) for *ca.* 1-10 minutes ^[5].

vii) Continuous steam process

High temperatures (260 °C) and pressures (> 15 bar) are used to reclaim ground rubber in a hydraulic column in the presence of reclaiming chemicals. Water is used as transporting medium and helps exclude unnecessary oxygen, otherwise combustion would result from high heat and pressure ^[5].

It is important to note that most of the above mentioned methods are a mixture of thermal and chemical methods, *i.e.* thermochemical methods. For this reason thermochemical methods are not reviewed separately here. A lot of attention has shifted to the use of supercritical fluids (supercritical carbon dioxide ^[7, 10, 102], supercritical water, supercritical alcohol and supercritical ketones ^[103]). in rubber reclamation using autoclaves. The major disadvantage of

using autoclaves is that they are batch processes, therefore not that much of a commercially viable option for industries as compared to large scale continuous processes. However, although their inherent limitations place restrictions on their commercial viability, they can be used to an advantage. Their small scale nature allows them to be used relatively quickly, in a controlled and structured way that makes it possible for analysis of process factors. In this way optimisation of process conditions (*i.e.* temperature, time, amount of agent and pressure) for a particular chemical can be done before scaling up.

1.3.6.5 Biotechnological techniques

These techniques exploit the susceptibility of sulphur to degradation by chemolithotrophic bacteria. The process was developed by Straube *et al* ^[103]. In this process, ground rubber material was desulphurised in a water suspension (aerated) containing the bacteria, thereby releasing elemental sulphur and or sulphuric acid. Bacteria belonging to the genus *Narcadia* was found to cleave 1,4-cis-polyisoprene, and some belonging to the species *Thiobacillus* (*T. ferrooxidans*, *T. thiooxidans*, and *T. thioparus*) were found to oxidise rubber powder in 40 days ^[3, 73, 104]. There are three main factors that affect the effectiveness of biodegradation ^[5];

- *Hydrophobic nature of most rubber*; most rubber surfaces are hydrophobic, meaning that they can only be attacked on the surfaces. Thus for maximum results, finely ground crumb is needed, which also has cost implications.
- *Crosslink structure*; the rubber crosslink network (and or branches) make it impossible for microorganisms to penetrate the rubber matrix. Therefore minimal branching and crosslinking are preferable (which might not be viable for most rubber products based on their applications). Also, size reduction would facilitate efficiency of degradation.
- *Anti-microbial rubber additives*; most rubber formulations include additives that retard growth or action of microorganisms, *e.g.* tetramethylthiuram, mono- and disulfides, and dimethylbutyl-p-phenylenediamine, zinc oxide, mercaptobenzothiazole, dimethyl dithiocarbamate-based accelerators, and paraphenylenediamine antidegradants.

1.4 REVIEW OF LITERATURE

1.4.1 Thermo-chemical devulcanisation

Devulcanisation is essential in the reduction of crosslinks to improve the interaction of devulcanised and raw rubber at a molecular level upon blending of the two. Devulcanisation of rubber by use of chemicals is one of the avenues that are likely to achieve high efficiency devulcanisation. This is due to the selective nature of most chemicals, which allows targeting of crosslinks. Chemical probes have been used to selectively cleave crosslinks [4, 6, 105]. The major disadvantage with the use of probes is that they are uneconomical to use in industries [105].

Kojima *et al* [3] reported on the devulcanisation of unfilled sulphur-cured isoprene rubber (IR) in supercritical carbon dioxide (scCO₂) using a range of chemical devulcanising agents such as; thiophenol (PhSH)/n-butylamine (n-BuNH₂) mixture, triphenyl phosphine (TPP), diphenyl disulphide (DD) and 2-mercaptobenzothiazole (MBT) at 180 °C and 100 kg/cm² pressure [106]. The thiol-amine and DD reagents were found to effectively reclaim the IR vulcanisates, yielding 100 % sol content. Work by Onouchi *et al* [101] using a binary mixture of PhSH/n-BuNH₂ concurred effectiveness of the thiol-amine mixture as a devulcanising agent. However, this was based on styrene butadiene rubber (SBR) in benzene solvent at ambient temperature [101, 107]. Several combinations of thiol and amine have been found to breakdown Sulphur crosslinks [3]. Inasmuch as thiols are efficient in devulcanisation, they have the disadvantage of a pungent foul smell that persists even in the rubber products. This makes them unattractive and unpleasant to work with.

Although 100 % sol was achieved using DD on unfilled IR, the reduced Mw of sol component indicates that there was chain scission during the devulcanisation process [3]. In the absence of DD, Jiang *et al* [7] reported only 15 % sol component yield of butyl rubber, probably due to devulcanisation as a result of thermal degradation in the reactor [108]. Upon introduction of DD in scCO₂, the unfilled butyl rubber vulcanisate was effectively reclaimed, yielding 98.2 % sol. This demonstrates the effectiveness of DD as a reclaiming agent, not only on unfilled rubber vulcanisates, but also CB-filled vulcanisates. Kojima *et al* [3] showed in another study that the presence of carbon black (CB) filler does not prevent any devulcanisation in scCO₂. Allusion to CB filler in vulcanisates is imperative as its presence influences physical (swelling behaviour, diffusivity, tensile strength and elongation) as well as chemical properties (*e.g.* cure

characteristics; cure rate, scorch time and torque changes) of vulcanisates. The scCO₂ acts as an effective medium, penetrating the rubber matrix and in so doing, transporting DD thereby making devulcanisation possible. It is important to note that not preventing devulcanisation does not translate to not hindering devulcanisation. In their work they found that devulcanising NR vulcanisates of different CB content resulted in sol content in the range of 20-40 %, whereas up to 100 % sol content was obtained for unfilled NR vulcanisates. In view of this, it can be said that the CB-filled system does not prevent devulcanisation, but actually hinders or slows down devulcanisation, which is in contradiction to the conclusion by Kojima *et al* that CB does not hinder devulcanisation. Not hindering would imply the presence of CB filler should have no effect whatsoever on the whole devulcanisation process.

MBT and TPP were found to produce low sol contents of 28% and 20% respectively ^[106]. TPP has been used as a probe due to its ability to convert polysulphidic crosslinks to monosulphidic and a small degree of di-sulphidic crosslinks ^[109, 110]. MBT on the other hand, has the advantage that if used as a devulcanising agent, it can aid re-vulcanisation of the devulcanised rubber by acting as an accelerator (*i.e.* it is multifunctional) ^[5]. Mohaved *et al* ^[111] investigated the devulcanisation of EPDM using MBTS (2,2-dithiobis(benzothiazole) disulphide) and TMTD (tetramethyl thiuram disulphide). MBTS was found to be more effective than TMTD, resulting in 20% replacement of original rubber by reclaim rubber in blends ^[111]. Both MBTS and TMTD are multifunctional, making them good choices for devulcanising agents.

1.4.2 Possible devulcanisation mechanism

A lot of work has been done on the devulcanisation of NR and not SBR, as far as the author is aware. As a result the possible mechanisms discussed in this section involve NR only, since the current study does not seek to establish or propose possible mechanisms but simply review mechanisms already suggested as possible devulcanisation routes. Nonetheless, thermal degradation of SBR is alluded to in chapter four.

Adhikari *et al* ^[4] proposed a mechanism initiated by homolytic splitting of the disulphide, accompanied by simultaneous scission of crosslinks or polymer chains by heat and or shear forces (Scheme 1a; steps 1, 2 & 3). Note that this proposed mechanism involves shear and heat components, whereas in the present study shear forces are absent, so only the heat component is considered while the mechanism remains unchanged. Step 4 of Scheme 1a involves coupling

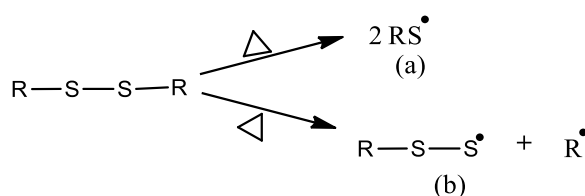
reactions by radical scavenger chemicals (*i.e.* dAs in this case) with the formed fragments, which prevent recombination of polymer chains ^[5]. Chain scission due to heat (step 2) is also a possibility, considering the presence of sol content and its related Mw.

Rajan *et al* ^[6] proposed that for thermochemical devulcanisation, the radical mechanism follows three processes;

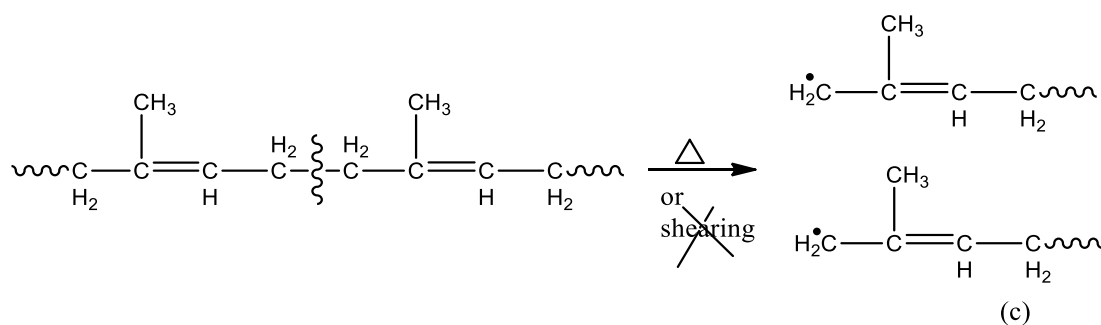
- Activation of dA to initiate radical reactions *via* homolytic splitting of the S-S bond to yield two benzene sulphide radicals.
- Abstraction of the allylic hydrogen resulting in formation of polymer chain radicals,
- Capping of polymer radicals thereby preventing their recombination.

According to Rajan *et al* ^[6] the rate determining step in the reclamation process involves the homolytic splitting of the disulphide bond (S-S) in DD to form benzene sulphide radicals (Scheme 1b). As a result, the time taken for devulcanisation is dependent on the rate of DD decomposition. The efficiency of the overall devulcanisation would then be dependent on the type of radicals formed upon decomposition of DD and of the substrate ^[6]. The same mechanism of action can be applied to MBTS since it is also a disulphide, except in its case the radicals formed are mercaptobenzothiazole (MBT) radicals (Scheme 1b).

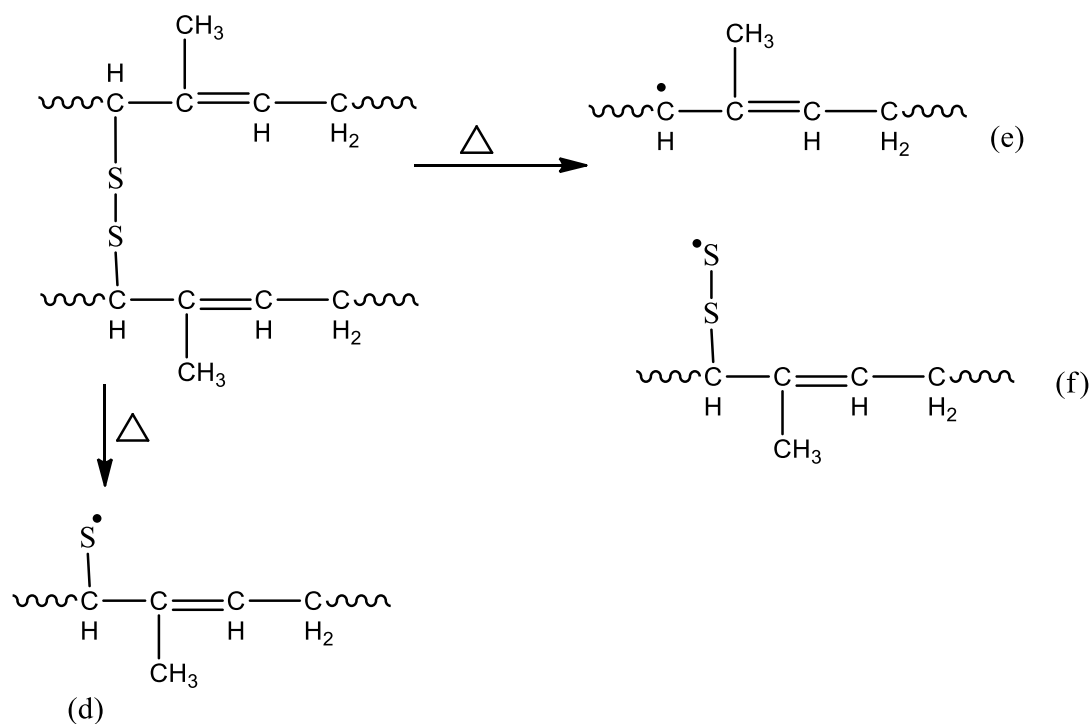
Step1: thermal decomposition of the disulphide devulcanisation agent



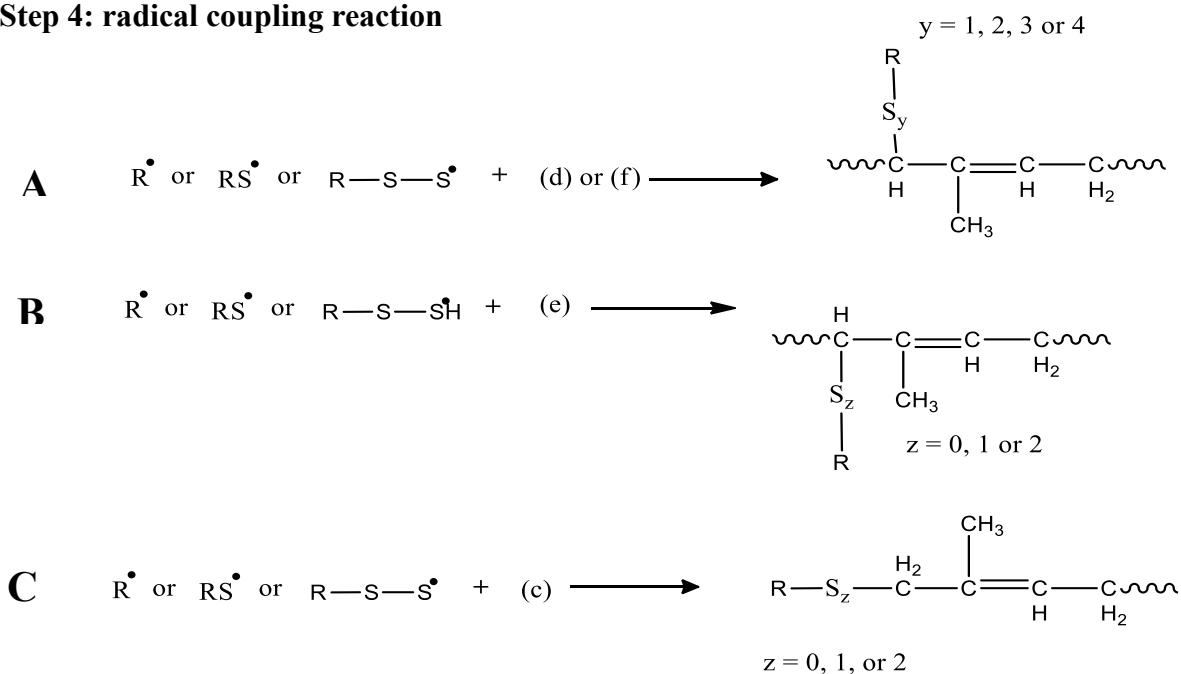
Step2: depolymerisation reactions



Step3: thermal scission of crosslinks



Step 4: radical coupling reaction



Scheme 1a: Proposed mechanism for NR reclamation using disulphides in the presence of heat

[4].

temperature results in change of scCO₂ to gas. Kojima *et al* [3] worked on the devulcanisation of NR and IR in scCO₂ [106, 114, 115]. It was established that scCO₂ swelled the rubber and facilitated the penetration of DD into the rubber matrix. Jiang *et al* achieved complete devulcanisation of butyl rubber in scCO₂, the sol content reaching 100 %. Carbon black tends to reduce swelling of vulcanisates in a manner that is proportional to the filler content (at constant crosslink density) [116, 117]. It also affects the diffusivity of gases for NR vulcanisates [118]. However, Kojima *et al* reported on how different amounts of carbon black filler in NR did not hinder the efficiency of scCO₂ in facilitating devulcanisation using DD [115]. Mangili *et al* and Shi *et al* reported on successfully devulcanising GTR in scCO₂ [119-121]. All the above mentioned reports show the ability of scCO₂ in acting as an effective medium for devulcanisation. Also, the problems faced with the use of reclamation oils or organic solvents are avoided.

This study is focused on the optimisation of devulcanisation conditions for DD and MBTS in scCO₂ medium. A one week aged, conventionally cured blend of NR and SBR is used as the sample for optimisation. Following a 2-level central composite design (CCD), the factors investigated include time, temperature, amount of devulcanising agent and pressure. The degree of devulcanisation was used as the response variable for optimisation. Characterisation of devulcanisation products in terms of sol and gel content was also done. Further analysis into devulcanisation events that occur during the non-isothermal heating range was also studied. Analysis of this region sparked interest, hence single factor optimisation was executed based on findings from the CCD.

1.5 SIGNIFICANCE OF THE RESEARCH

The presence of a three dimensional network of crosslinks in ground tyre rubber (GTR) has been pointed out to be the major cause of incompatibility with raw rubber during blending [7, 10, 102]. The crosslinks result in weak adhesion between the GTR and the raw rubber, and subsequently, poor mechanical properties of the blend [10]. Accordingly, GTR is usually used as a filler, but in small quantities (*e.g.* 10 phr) and reduced sizes (*e.g.* 60 mesh or smaller) [4, 10]. The literature review section briefly described the various methods of devulcanisation that have been used in an attempt to improve the compatibility of GTR with virgin rubber. The major disadvantage of most of these methods is main chain degradation, chiefly due to shear

mechanical forces and thermo-oxidative processes ^[4, 8, 11]. In light of this, this research attempts to minimise the degree of main chain degradation by conducting devulcanisation *via* thermo-chemical means in the absence of oxygen. Also, since the use of oils as swelling agents for devulcanisation has been shown to result in devulcanised rubber of inferior quality, this research makes use of supercritical CO₂ (scCO₂) as the devulcanisation medium ^[4]. The use of scCO₂ has been shown to be effective for conducting devulcanisation reactions due to its advantages over traditional solvents (outlined in the literature review section).

As far as the author is aware, a 2-level central composite design has never been employed in optimisation of devulcanisation conditions. A central composite design has the advantage of a broadened range of scope or analysis by incorporating star points. In addition, statistical approaches of optimisation of devulcanisation conditions have used the sol content as the main response variable to determine optimum conditions ^[122]. This research on the other hand, looks at the use of the degree of devulcanisation (*i.e.* % devulcanisation) as the main response variable for optimisation of devulcanisation. This approach has merit in that, according to the definition of % devulcanisation, its use as the response variable should give a direct indication of how much crosslink scission is taking place at different conditions, thereby enabling ease of optimisation. This system of optimisation would have positive implications on industrial processes, which include; reduction in the amount of energy used in recycling, reduced amount of devulcanisation agents used, improved quality of recycled material, reduced time taken to run devulcanisation processes, no more usage of toxic oils or organic swelling solvents and reduced costs involved in the whole devulcanisation process.

1.6 SCOPE AND LIMITATIONS

The scope of this research covers;

- The use and basic calibration of the supercritical reactor to conduct devulcanisation of typical truck tyre tread vulcanisates. The reactor calibration is important in ascertaining that reaction parameters as expected are what they are in practice, if not, then by how much is the degree of variation between the two. This practice would also expose any confounding variables, *i.e.* unaccounted factors that may influence the devulcanisation reaction.

- Maximising the % devulcanisation using a 2-level central composite design in the optimisation of temperature, time, pressure and amount of devulcanisation agent used in the devulcanisation process. This would achieve good quality devulcanisates.
- Close analysis of changes in the % devulcanisation during the non-isothermal heating stage as well as the isothermal heating stage. The effect of heating rate on % devulcanisation is covered under non-isothermal heating approach.
- The influence of the presence of carbon black filler on % devulcanisation. The effect of the reaction factors (time, temperature, pressure, mass of devulcanising agent used, and heating rate) on % devulcanisation is also looked into. Statistical methods of analysis (t-Test, single factor analysis of variance, and multiple linear regression analysis) are also used to interpret experimental observations.
- Application of optimised devulcanisation conditions on GTR. This establishes if the optimum conditions can work on a commercial waste truck tyre tread. This section includes cryogenically crumbing the tyre tread to simulate comminution of waste rubber in industrial processes. The cryogenic conditions were used to reduce comprising the rubber chain structural integrity.

The limitations of this research include;

- The kinetics aspect of devulcanisation. Although this work would provide a picture and basis for kinetic analysis, the current study is however only limited to the optimisation of devulcanisation conditions to achieve maximum % devulcanisation.
- The state of rubber vulcanisates used as substrates for devulcanisation. Waste tyre vulcanisates are usually recycled when they have reached their end of life use, when they have deteriorated mechanical and physical properties (*i.e.* aged) ^[4, 8]. As such, the vulcanisates used for optimisation of devulcanisation were aged under anaerobic conditions by means of accelerated water ageing. The ageing was restricted to anaerobic thermal ageing so as to rule out chain modifications due to thermo-oxidative degradation and other external factors tyres are exposed to during service ^[30]. This ensures that the observed changes in the % devulcanisation can be directly attributed to the efficiency of the devulcanising agent and optimised conditions. Also, optimisation of devulcanisation was restricted to the use of the laboratory prepared vulcanisates instead of directly using the GTR. This enables ease of analysis and optimisation since the rubber compound formulation is known. However, limitations may arise due to

slight differences in the substrates upon application of the optimised devulcanisation conditions on the GTR, even though they are both truck tyre tread compound formulations.

- Structural analysis of gel and sol. Only qualitative analysis will be conducted to check for any changes in the rubber structure after devulcanisation.
- Mechanical properties of blends. The research does not cover blending of the devulcanised rubber with raw rubber to test their mechanical properties for quality assurance. This is due to the length and time scale of the study.

1.7 OVERVIEW OF CHAPTERS

Chapter One

This chapter introduces vulcanisation and waste rubber recycling. In so doing, portray a clear picture of industrial processes involved in rubber recycling and finally narrow into thermo-chemical devulcanisation, which is the subject of this research work. It covers;

- Vulcanisation; a brief introduction of the whole process, the crosslink network structure, examples of physical and mechanical properties of rubber modified by vulcanisation, as well as its contribution to waste management problems.
- Crosslink network structure; the crosslink distribution and density are introduced and explained, the thermodynamics aspect of polymers in solution, the Flory-Rhener equation and its associated uncertainties in the determination of crosslink densities (using the solvent swelling method) are looked into.
- Waste tyre management; laws and regulations passed, hierarchy of waste tyre management.
- Recycling processes; crumb rubber production, reclamation and devulcanisation

Chapter Two

This chapter looks at the supercritical reactor calibration and use, as well as other instrumentation used in this research study.

Chapter Three

This chapter looks at the optimisation of devulcanisation conditions (time, temperature, pressure and mass of devulcanising agent) following a 2-level central composite design. The optimisation of devulcanisation in this section is focused on the isothermal stage (*i.e.* isothermal devulcanisation). Laboratory prepared vulcanisates from a truck tyre tread formulation were used for optimisation. A comparison of the degree of devulcanisation between the onset of the isothermal region (*i.e.* non-isothermal devulcanisation) and the isothermal region (*i.e.* isothermal devulcanisation) is performed.

Chapter Four

This chapter is based on findings from chapter three; a relatively higher degree of devulcanisation occurs in the non-isothermal region than in the isothermal region. Therefore, focus to maximise percentage devulcanisation was shifted to the non-isothermal region. Multiple linear regression was used to formulate an empirical model to optimise devulcanisation conditions of time, temperature and heating rate (pressure, mass and amount of devulcanising agent were kept constant due to findings from chapter three). Failure to obtain a viable empirical model led to single factor analyses, which was implemented to obtain optimum conditions for devulcanisation. All the devulcanisation conditions were looked into, *i.e.* the effects of temperature, time, pressure, amount (mass) of devulcanising agent, and heating rate, on the degree of devulcanisation. In addition, the effect of the presence of the filler was looked into.

Chapter Five

The final optimum conditions obtained after single factor analysis were then applied onto a ground commercial waste truck tyre tread. This was to ascertain if the optimised devulcanisation conditions were applicable to a typical industrial vulcanisate, of similar formulation (*i.e.* truck tyre tread formulation).

Chapter Six

Conclusions and recommended future work.

1.8 GLOSSARY

Vulcanisation- refers to the formation of a three dimensional network of sulphur crosslinks interconnecting polymer chains ^[14].

Devulcanisation- process of cleaving, either totally or partially, of the sulphur cross-links formed during the vulcanisation process ^[84].

Devulcanising agents- chemicals or biological agents that cleave crosslinks in vulcanised rubber.

Gel component- is the insoluble fraction of rubber material after devulcanisation or reclamation that still contains crosslinks ^[3].

Sol component- is the soluble fraction of rubber material after devulcanisation or reclamation, made up of truncated linear polymer chains that can dissolve in a suitable solvent ^[3].

% Devulcanisation- is a measure of the degree of devulcanisation (ASTM D 6814).

Crosslink distribution- is the relative composition of the different sulphur crosslink types, *i.e.* the distribution of mono, di and poly- sulphide crosslinks ^[15].

Crosslink density (ν)- refers to the molar concentration of sulphur crosslinks per unit volume ^[26].

Co-vulcanisation- is the ability of two elastomers to form a single network structure in which both elastomers, and their interphases, have become crosslinked to similar extents ^[64].

1.9 REFERENCES

1. Lucignano, C., A. Gugliemotti, and F. Quadrini, *Polymer Plastic Technology Engineering*, 2012. **51**: p. 340-344.
2. Kojima, M., et al., *Rubber Chemistry and Technology*, 2003. **76**: p. 957-68.
3. Myrhe, M., et al., *Rubber Chemistry and Technology*, 2012. **85**(3): p. 408-449.
4. Adhikari, B., D. De, and S. Maiti, *Progress in Polymer Science*, 2000. **25**: p. 909-948.
5. Rajan, V.V., et al., *Journal of Applied Polymer Science*, 2007. **104**(6): p. 3562-3580.
6. Jiang, K., et al., *Journal of Applied Polymer Science*, 2013. **127**(4): p. 2397-2406.
7. Imbernon, L. and S. Norvez, *European Polymer Journal*, 2016. **82**: p. 347-376.
8. Mangaraj, D., *Rubber Chemistry and Technology*, 2005. **78**(3): p. 536-547
9. Mangili, I., et al., *Polymer Degradation and Stability*, 2014. **102**: p. 15-24.
10. Forrest, M., *Recycling and Re-use of Waste Rubber*, ed. S.R.T. Ltd. 2014, Shawbury, Shrewsbury, UK: Smithers Rapra Technology Ltd.
11. Smith, R.F., et al., *Green Chemistry*, 2016.
12. Treloar, L.R.G., *The Physics of Rubber Elasticity*. 3 ed. 1975, Oxford: Clarendon Press.
13. Group, A.M and N. limited *Vulcanisation*. 2010. p. 1-31.
14. Group, A.M. and N. limited *Vulcanisation and Accelerators*. 2010. p. 11.
15. Ellis, G., P.J. Hendra, and M.J.R. Loadman, *Kautschuk Gummi Kunststoffe*, 1990. **43**(2): p. 118.
16. Jackson, K.D.O., et al., *Acta*, 1990. **46** (2A): p. 217.
17. McKenna, G.B., K.M. Flynn, and Y.H. Chen, *Polymers*, 1990. **31**: p. 1937-1945.
18. Zaper, A.M. and J.L. Koenig, *Rubber Chemistry and Technology*, 1987. **60**: p. 252-77.
19. Buzare, J.Y., et al., *European Polymer Journal*, 2001. **37**: p. 85-91.
20. Gronski, W., et al., *Rubber Chemistry and Technology*, 1992. **65**: p. 63-77.
21. Hoffmann, U., et al., *Angewandte Makromolekulare Chemie*, 1992. **202/203**: p. 283-93.
22. Akiba, M. and A.S. Hashim, *Progressing Polymer Science*, 1997. **22**: p. 475-521.
23. Tanaka, Y., *Rubber Chemistry and Technology*, 1991. **64**: p. 325-85.
24. Wolfman, G., H. Hasenhidl, and S. Wolf, *Kautschuk Gummi Kunststoffe*, 1991. **22**(2): p. 119.
25. Mok, K.L. and A.H. Eng, *Characterisation of Crosslinks in Vulcanised Rubbers: From Simple to Advanced Techniques*, in *25th POLYCHAR Forum*. 2017, ResearchGate.
26. Quirk, R.P., *Progress in Rubber Plastic and Technology*, 1988. **4**(1): p. 31.

27. Boonkerd, K., C. Deeprasertkul, and K. Boonsomwong, *Rubber Chemistry and Technology*, 2016. **89**(3): p. 450-464.
28. Nielsen, L.E. and R.F. Landel, *Mechanical Properties of Polymers and Composites*. 2 ed. 1994.
29. Cunneen, J.I. and R.M. Russell, *Journal of the Rubber Research Institute of Malaya*, 1969. **22**: p. 300.
30. Choi, S.S., *Journal of Applied Polymer Science*, 2000. **75**: p. 1378-1384.
31. Choi, S.S., *Journal of Applied Polymer Science*, 2002. **83**: p. 2609-2616.
32. Flory, P.J., *Principles of Polymer Chemistry*. Ithaca. 1953, New York: Cornell University Press.
33. Parks, C.R. and R.J. Brown, *Rubber Chemistry and Technology*, 1974. **49**: p. 233-236.
34. Bauer, R.F. and A.H. Crossland, *Rubber Chemistry and Technology*, 1988. **61**: p. 585.
35. Demco, D.E., et al., *Chemical Physics*, 1996. **105**: p. 11285-11296.
36. G.Brereton, M., *Macromolecules*, 1990. **23**: p. 1119-1131.
37. Litvinov, V.M. and P.P. De, *RAPRA technology Ltd*, 2002.
38. Saalwa"chter, K., et al., *Applied Magnetic Resonance*, 2004. **27**: p. 401-417.
39. Simon, G. and H. Schneider, *Makromol. Chem.*, 1991. **52**: p. 233-246.
40. Chapman, A.V. and A.J. Tinker, *Kautschuk Gummi Kunststoffe*, 2003. **56**(10): p. 533-544.
41. Huson, M.G., W.J. McGill, and P.J. Swart, *Journal of Polymer Science*, 1984. **22**: p. 143.
42. Huson, M.G., W.J. McGill, and R.D. Wiggett, *Plastics and Rubber Processing Applications*, 1985. **5**: p. 319.
43. Mareanukroh, M., G.H. Hamed, and R.K. Eby, *Rubber Chemistry and Technology*, 1996. **69**: p. 801.
44. Valentin, J.L., et al., *Macromolecules*, 2008. **41**: p. 4717-4729.
45. Bills, K.W. and F.S. Salcedo, *Journal of Applied Physics*, 1961. **32**: p. 2364.
46. McKenna, G.B., K.M. Flynn, and Y.H. Chen, *Macromolecules*, 1988. **29**: p. 272-275.
47. McKenna, G.B., K.M. Flynn, and Y.H. Chen, *Macromolecules*, 1989. **22**: p. 4507-4512.
48. McKenna, G.B., K.M. Flynn, and Y.H. Chen, *Polymer Chemistry*, 1990. **31**: p. 1937-1945.
49. McKenna, G.B. and F. Horkay, *Polymer*, 1994. **35**: p. 5737-5742.

50. Horkay, F., A.M. Hecht, and E. Geissler, *Journal of Polymer Science*, 1995. **33**: p. 1641-1646.
51. Horkay, F., et al., *Macromolecules*, 1991. **24**: p. 2896-2902.
52. Horkay, F., et al., *Macromolecules*, 2000. **33**: p. 5215-5220.
53. Horkay, F., W.K. Waldron, and G.B. McKenna, *Polymer*, 1995. **36**: p. 4525-4527.
54. Horkay, F., et al., *Polymer*, 1991. **32**: p. 835-839.
55. Mallam, S., et al., *Macromolecules*, 1991. **23**: p. 543-548.
56. Ellis, B. and G.N. Welding, *Rubber Chemistry and Technology*, 1964. **37**: p. 563-570.
57. Ellis, B. and G.N. Welding, *Rubber Chemistry and Technology*, 1964. **37**: p. 571-575.
58. Flory, P.J. and B. Erman, *Macromolecules*, 1984. **15**: p. 800-806.
59. Corish, P.J. and B.D.W. Powell, *Rubber Chemistry and Technology*, 1973. **47**: p. 481.
60. Walters, M.H. and D.N. Keyte, *Rubber Chemistry and Technology*, 1965. **38**: p. 62.
61. Huson, M.G., W.J. McGill, and R.D. Wigget, *Plastics and rubber processing applications*, 1985. **5**(4): p. 319-324.
62. Woods, M.E. and T.R. Mass, *Advanced Chemical Series*, 1975. **192**: p. 386.
63. Schershnev, V.A., *Rubber Chemistry and Technology*, 1982. **55**: p. 537.
64. Zapp, R.L., *Rubber Chemistry and Technology*, 1973. **46**: p. 251.
65. EU, E.E. *Environment waste*. Available from: <http://ec.europa.eu/environment/waste/>.
66. Commission, E., *Landfill of waste directive*. 1999.
67. Waste Regulation. Available from: https://www.environment.gov.za/sites/default/files/gazetted_notices/eca_wastetyreregulations_g30929gen425.pdf.
68. Isayev, A.I., J. Chen, and A. Tukachinsky, *Rubber Chemistry and Technology*, 1995. **68**: p. 267-280.
69. Mark, H.F., et al., *Encyclopedia of polymer science and engineering*, 1988. **14**: p. 787-804.
70. Phadke, A.A. and S.K. De, *Conservation and Recycling*, 1986. 9: p. 271..
71. Rouse, M.W., *Rubber recycling; Manufacturing practices for the development of crumb rubber materials from whole tires*, ed. S.K. De, A.I. Isayev, and K. Khait. 2005: Taylor and Francis Group.
72. Capelle, G. and P. Hunziker, *Rubber World*, 1992. **206**(4): p. 21.
73. Fesus, E.M. and R.W. Eggleton, *Rubber World*, 1991. **203**(6): p. 23.
74. Myrhe, M.J. and D.A. Mackillop, *Rubber World*, 1996. **214**: p. 42.
75. Rouse, M.W., *Rubber World*, 1992. **206**(3): p. 25.

76. Biddulph, M.W., *Conserv. Reyl*, 1977. **1**: p. 169.
77. Leyden, J.J., *Rubber World*, 1991. **203**(6): p. 28.
78. Phadke, A.A. and S.K. De, *Conserv. Reyl*, 1986. **9**: p. 271.
79. U.S. Patents, Editor. 2002.
80. Bilgili, E., et al., *Journal of Elastomers and Plastics*, 2003. **35**: p. 235-256.
81. C, L., G. A, and Q. F, *Polymer Plastics and Technology Engineering*, 2012. **51**: p. 340-344.
82. Gugliemotti, A., C. Lucignano, and Q. F, *Plastics and Rubber Composites.*, 2012. **41**: p. 40-46.
83. Tobolsky, A.V., W.J. MacKnight, and M. Takahashi, *Journal of Physical Chemistry*, 1964. **68**: p. 787-790.
84. Tripathy, A.R., et al., *Macromolecules*, 2002. **35**: p. 4616-4627.
85. Myrhe, M., *Devulcanisation by Chemical and Thermomechanical Means*. Rubber Recycling, ed. S.K. De, A.I. Isayev, and K. Khait. 2005: Taylor and Francis Group.
86. Finazzi, E., A. Gallo, and P. Lucci, *Rubber World*, 2011. **21**: p. 243.
87. Oliveira, L.C., *Process for reclaiming cured or semi-cured rubber*, U.S. Patent, Editor. 1977: U.S. p. 677, 354.
88. Balasubramanian, M., *Journal of Polymer Research*, 2009. **16**(2): p. 133.
89. De, D., B. Adhikari, and S. Maiti, *Journal of Polymer Materials*, 1997. **14**: p. 333.
90. De, D., S. Maiti, and B. Adhikari, *Kautschuk Gummi Kunststoffe*, 2000. **53**(6): p. 346.
91. Yamashita, S., *International Polymer Science and Technology*, 1981. **8**(12): p. 77-93.
92. Singleton, R. and T.L. Davies, *Rubber Technology and Manufacture*, 1982: p. 237-242.
93. Maridass, B. and B. Gupta, *Journal of Elastomers and Plastics*, 2006. **38**: p. 211.
94. Pelofsky, A.H., *Rubber reclamation using ultrasonic energy*. 1973.
95. Okuda, M. and Y. Hatano, *Method of desulfurising rubber by ultrasonic wave*, Japan: Yokohama Rubber Co. Ltd, Editor. 1987: Japan.
96. Elgin, J.C., *Can Patent*. 1949. p. 2, 494, 593.
97. Sverdrup, E.F. and J.C. Elgin, *US Patent*. 1947: p. 2, 415, 449.
98. Sverdrup, E.F. and J.C. Elgin, *Can Patent*. 1948. p. 452.
99. Cotton, F.H. and P.A. Gibbons, *Can Patent*. 1946. p. 2, 408, 296.
100. Rooj, S., et al., *Journal of Polmers and the Environment*, 2011. **19**: p. 382-390.
101. Sekhar, B.C. and A. Subramaniam, *Improvements in and relating to the reclaiming of natural and synthetic rubbers*. 1996.
102. Onouchi, Y., et al., *International Polymer Science and Technology*, 1982. **55**: p. 58-62.

103. Kojima, M., et al., *Journal of Applied Polymer Science*, 2005. **95**: p. 137-143.
104. Straube, G., et al., *Hoelzemann Metallverarbeitung*, 1994.
105. Tsuchii, A., K. Takeda, and Y. Tokiwa, *Applied and Environmental Microbiology*, 1990. **56**: p. 269-74.
106. Nicholas, P.P., US Patent. 1979: Akron, Ohio. p. 4, 161, 464.
107. Kojima, M., et al., *Rubber Chemistry and Technology*, 2002. **76**: p. 957-968.
108. Onouchi, Y., et al., *International Polymer Science and Technology*, 1982: p. 55, 58–62.
109. Moore, C.G. and B.R. Trego, *Journal of Applied Polymer Science*, 1964. **8**: p. 1957.
110. Moore, C.G. and B.R. Trego, *Journal of Applied Polymer Science*, 1961. **5**: p. 299.
111. Mohaved, S.O., et al., *Polymer degradation and stability*, 2014. **111**: p. 114-123.
112. Perrut, M., *Industrial and Engineering Chemistry Research*, 2000. **39**: p. 4531.
113. Kojima, M., S. Kohjiya, and Y. Ikeda, *Journal of Applied Polymer Science*, 2005. **46**: p. 2016-2019.
114. Kojima, M., M. Tosaka, and Y. Ikeda, *Green Chemistry*, 2004. **6**(2): p. 84.
115. Kojima, M., et al., *Journal of Applied Polymer Science*, 2005. **95**(1): p. 137-143.
116. Lorenz, O. and C.R. Parks, *Journal of Polym Science*, 1961. **50**: p. 299.
117. Kraus, G., *Journal of Applied Polymer Science*, 1963. **7**: p. 861.
118. Dawson, T.R. and T.R. Porritt, *Rubber Physical and Chemical Properties*. 1935, Croydon, UK: Research Association of British Rubber Manufacturers.
119. Mangili, I., et al., *The Journal of Supercritical Fluids*, 2014. **92**: p. 249-256.
120. Shi, J., et al., *Polymer Degradation and Stability*, 2014. **99**: p. 166-175.
121. Liu, Z., et al., *Polymer Degradation and Stability*, 2015. **119**: p. 198-207.

CHAPTER 2: REACTOR CALIBRATION AND INSTRUMENTATION USED

2.1 SUPERCRITICAL REACTOR

A stainless steel autoclave was used in this research as a reactor to conduct devulcanisation studies in supercritical carbon dioxide (scCO₂). Figure 2.1 shows the reactor setup.

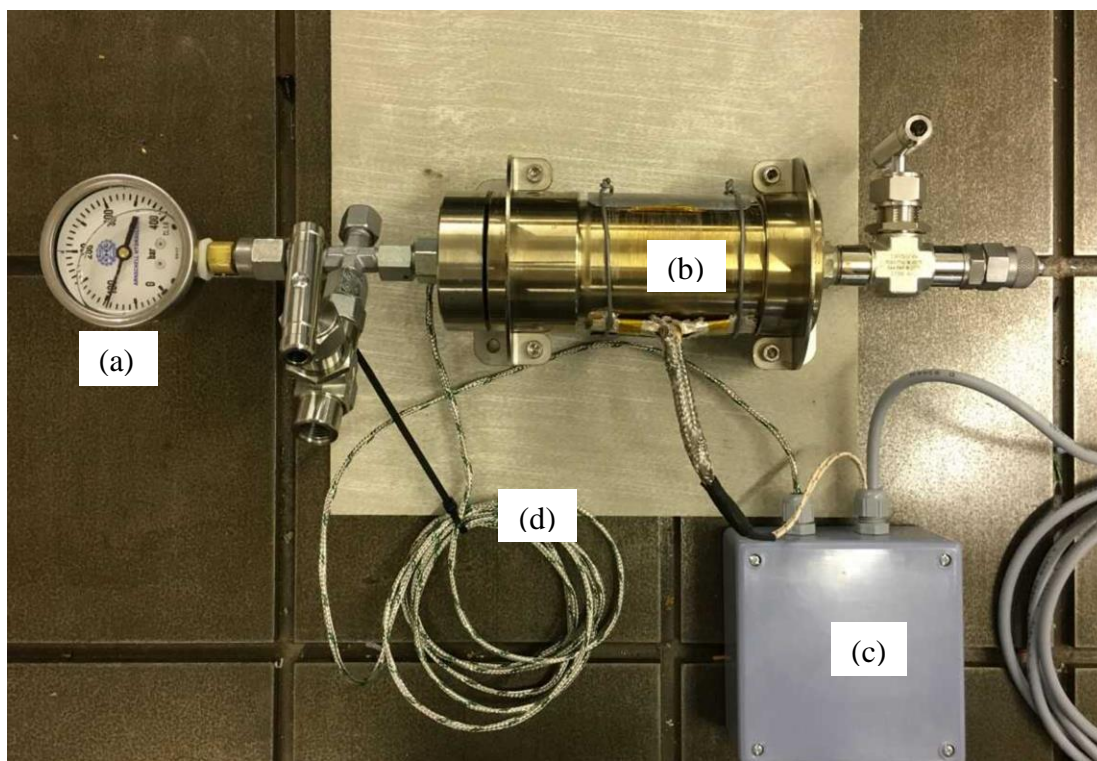


Figure 2.1: Supercritical reactor top view. Labelled in the picture are the major components; (a) pressure gauge, (b) reaction chamber, (c) PID temperature controller and (d) thermocouple connection.

The autoclave was designed by Mr. Stephen Grewar from ENSTA Engineering Solutions. The autoclave is made from a stainless steel 316 body designed to withstand conditions of 25 MPa at 200 °C with a suitable safety factor. The main safety mechanism is a silicon O -ring used to seal tight the reactor lid. The seal will rupture before any other mechanical failure and can be easily replaced (and is affordable at only ZAR 13.00 per O-ring, 2018 price, and easy to mount or dismount on the lid). This seal has Shore A hardness of 70 and offers a broader operating temperature range of -62°C to +260 °C. All fittings on the reactor are rated above 25 MPa and 200 °C. The reactor is equipped with a type-k thermocouple of standard tolerance; $-40\text{ }^{\circ}\text{C} < t^{\circ} < 375\text{ }^{\circ}\text{C}$ $= \pm 1.5\text{ }^{\circ}\text{C}$ (from RS Products) for temperature monitoring as well as a pressure gauge (from Arnschell hydraulics) of 0–400 bar scale. Heating of the autoclave is facilitated by means of a coil heater with insulator jacket (from Thermon S. A). Heating was controlled by means of a PID temperature controller from RS Products.

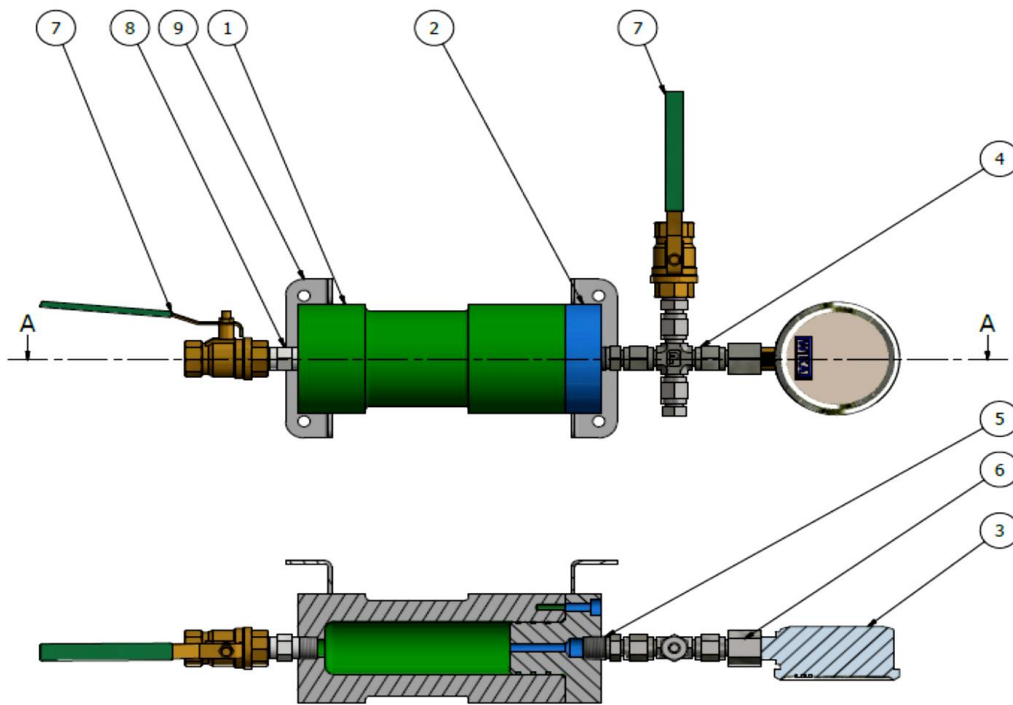


Figure 2.2: Design of supercritical reactor / autoclave. Where (1) body (2) cap/lid (3) pressure gauge (4) parker A-lok – fractional tube $\frac{1}{4}$ (5) parker A-lok Male taper thread- fractional tube $\frac{1}{4} \times \frac{1}{4}$ (7) Parker brass ball valve XV520P (8) DIN EN 10242 hexagon nipple N8 $\frac{1}{4}$ (9) SHT metal stand.

The most important aspect for the proper working of the autoclave is temperature control.

2.1.1 Features of PID Temperature controller

- 35x77mm size.
- Heating or cooling applications
- Thermocouple or PT100 inputs
- Two outputs for control and alarms
- ON/OFF or PID control
- On sensor failure, manual control can be selected.
- Sensor input offset setting
- Two setpoint - selectable from front panel.
- Selectable thermocouple types or PT100 input. (Specify at order).
- PID autotune
- Soft-Start feature.
- Two outputs - Relay (control or alarm) and SSR (control)



Figure 2.3: Temperature controller control panel.

PID controllers are effective at dealing with process disturbances that can have an impact on the quality of the product that is being measured. A PID temperature controller is an on/off process controller that uses mathematical algorithms to determine the difference between the desired temperature (*i.e.* set-point) and current process temperature ^[2]. This ensures the process temperature remains as close as possible to the set-point. To get the best possible control for a particular process, the three elements of the PID algorithm (*i.e.* Proportional, Integral, and the Derivative) have to be tuned. These elements each relate to the variance in the process temperature versus the set-point in a period of time.

- Proportional ^[2] - the variance between the set-point and the current process temperature. The wider the proportional band, the greater the area around the set-point in which the proportional action takes place. This is sometimes referred to as gain, which is the reciprocal of proportional band.
- Integral ^[2]- This function adjusts the proportional bandwidth with respect to the set-point to compensate for offset from set-point; *i.e.* it adjusts the controlled temperature to set-point after the system stabilises.

- Derivative ^[2]- senses the rate of rise or fall of system temperature and automatically adjusts the proportional band to minimise overshoot or undershoot.

A PID temperature controller is capable of excellent temperature control depending on how it is tuned. It can be tuned by trial and error method or set to self-tune where it automatically calculates the best control variables. Figure 2.4 shows graphs that can be obtained at set-point steady state. The desired steady state is when there is minimum deviation from set-point (*e.g.* deviation of $< \pm 1$ °C), not shown on Figure 2.4 but was observed from results (Figure 2.7).

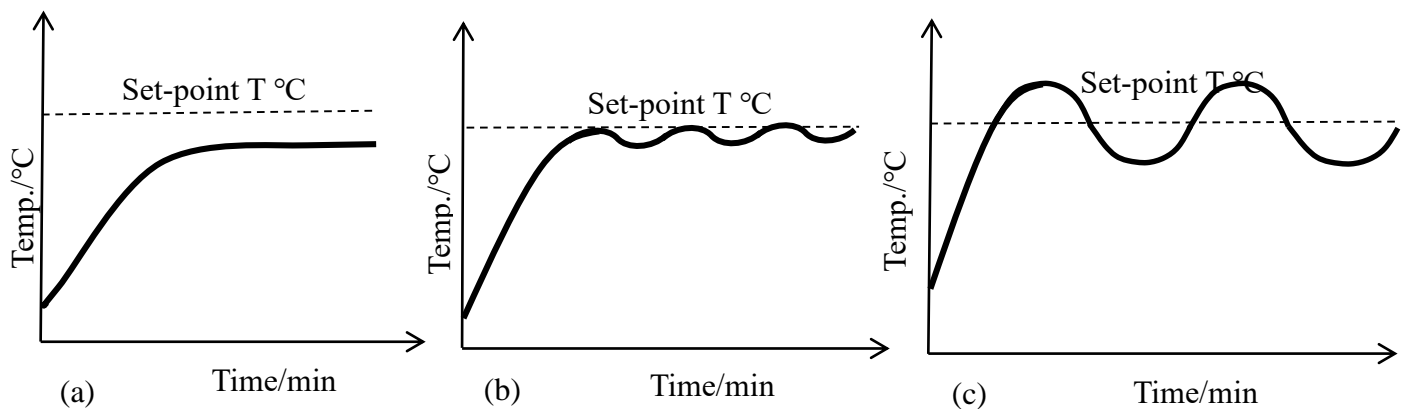


Figure 2.4: Tuning temperature controller; a) set-point not reached, b) closer to set-point c) large deviations at set-point steady state. (*Adapted from OMEGA temperature controller tuning manual* ^[2]).

2.1.2 Reactor calibration

2.1.2.1 Pressure-Temperature relation

Before use, the reactor had to be calibrated or checked if it functions properly since it was its first time use. The main controls of concern were temperature and pressure regulation. As such, the first task was to check if there was flawless communication between temperature, as measured by the thermocouple and the corresponding pressure, as monitored by the pressure gauge. This was done by considering the temperature–pressure relationship according to the ideal gas equation;

$PV = nRT$ where; P = pressure (Pascal, Pa), V = volume (m³), n = number of moles, R = ideal gas constant (8.314 J/mol) and T = temperature (Kelvin, K).

- **1st approach;** mass of CO₂ gas was calculated such that at set-point temperature (*e.g.* 180°C) the pressure would be at 80 bar (*i.e.* the working pressure). The problem faced in this approach was that the rate of sublimation of dry ice, once placed inside the reactor, was so fast by the time the reactor is sealed a significant amount of it would be lost.
- **2nd approach;** an excess amount of dry ice was placed in the reactor initially, calculations based on the ideal gas equation done to determine the pressure at 50 °C, still targeting the same set-point conditions of 180 °C and 80 bar. 50 °C was chosen as the start temperature just to make sure all the dry ice in the reactor was at gaseous state, so as to minimise biased pressure values. At 50 °C the pressure was regulated to match the calculated/theoretical pressure. Figure 2.5 shows an overlay of the theoretically predicted temperature/pressure values vs. experimentally observed values. The 2nd approach worked well and was thus used for running reactions.

Table 2.1a: Reactor parameters

P/Pa	80 000 000
V/m ³	0,0001
m(CO ₂)/g	9,3430
M _w (CO ₂)	44
R/JK ⁻¹ mol ⁻¹	8,314
T/K	453,15

Table 2.1b: Calculated vs. Observed values

T/°C	P _{calculated} /bar	P _{observed} /bar
50	57,0	55
70	60,6	60
90	64,1	63
110	67,6	66
130	71,2	70
150	74,7	73
170	78,2	76
180	80,1	78

Table 2.1a shows the reactor parameters used in predicting pressure of the reactor at the different temperatures as shown on Table 2.1b. Note that all the parameters on Table 2.1a are given in SI – units, for calculation purposes, but for reporting the pressure and temperature were referred to in bar and °C respectively.

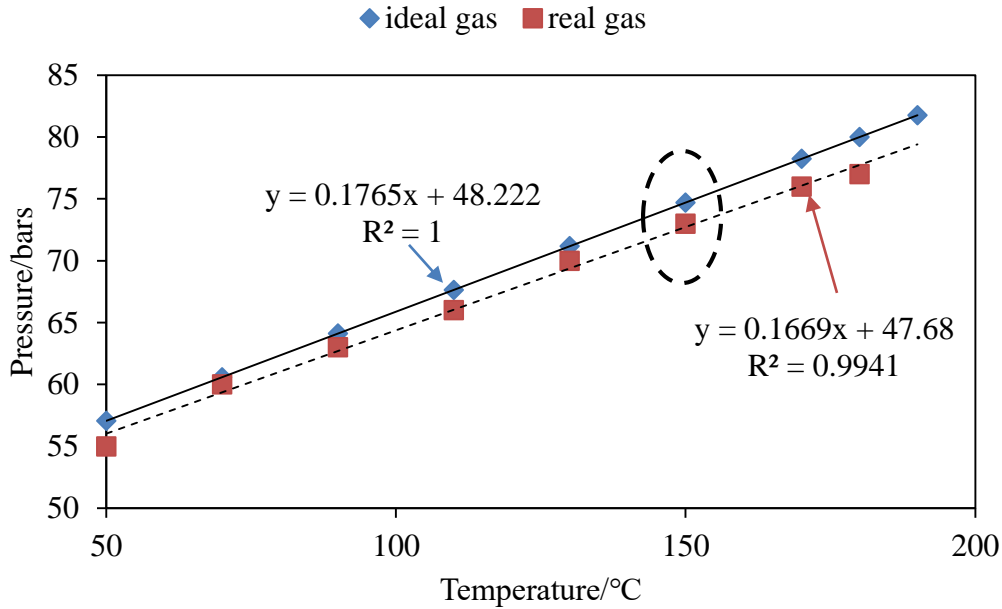


Figure 2.5: Ideal gas behaviour vs. real gas (CO₂) behaviour at 180 °C set-point and 80 bars pressure.

The kinetic theory of gases postulates that ideal gases have a zero molecular volume and no intermolecular interactions (*i.e.* forces of attraction and repulsion between molecules) [3]. This postulation however, fails to fully describe the behaviour of real gases due to their non-zero volume and intermolecular forces. This is evidenced by liquefaction of gases, a behaviour of that is not predicted by the ideal gas theory. Real gases tend to show ideal gas behaviour at low pressures (*i.e.* when pressure approaches zero), but as pressure is increased intermolecular forces and molecular volume become significant, resulting in deviations from ideal gas behaviour [3]. Figure 2.5 shows that at low pressures, the CO₂ gas seems to exhibit ideal gas behaviour, however as pressure is increased with temperature, behaviour shifts to non-ideal behaviour. At the selected initial temperature (*i.e.* at 50 °C) the pressure is below the predicted theoretical pressure. This is probably due to small amounts of dry ice that has not sublimed at that time. This may be a result of thermal lag during the heating of dry ice. Due to the fast heating rate (at 180 °C set-point) the start off temperature was reached before all the dry ice had sublimed. Nonetheless, the pressure difference at the start off point was not that significant. To understand deviation from ideal behaviour as observed, a look into the phase diagram of CO₂ is necessary.

Figure 2.6 shows the phase diagram of CO₂. At the triple point (-56.6 °C and 5.11 bar), CO₂ exists in its three different forms (solid, liquid and gas). Below this point, CO₂ cannot exist as a liquid, but can be solid or gas [4, 5]. As temperature and pressure are increased according to the phase diagram, the critical point is reached (30.98 °C and 72.79 bar) [4, 5]. The critical temperature can be defined as the temperature beyond which the gaseous molecules cannot be liquefied. At the same time, the critical pressure is the minimum pressure required to liquefy the gas at the critical temperature. The combination of the two is the critical point. The combination of the two is the critical point.

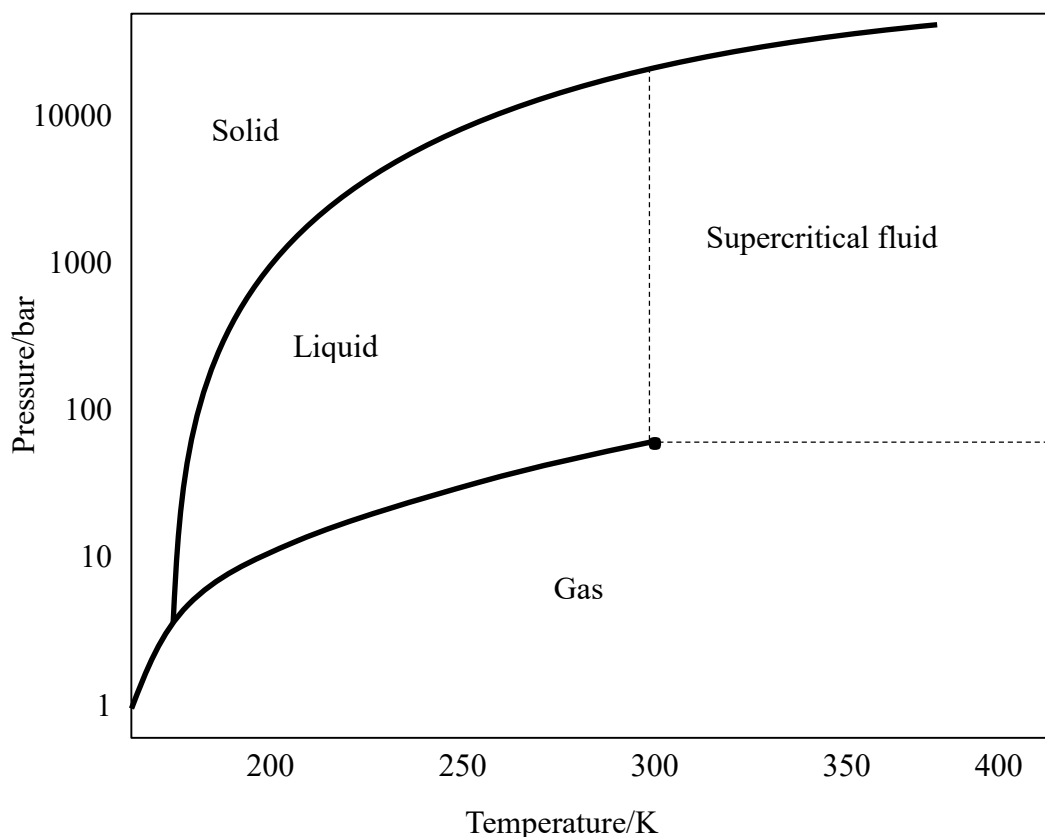


Figure 2.6: CO₂ phase diagram (adapted from Atkins et al [5])

When temperature is increased the density of a liquid decreases, and when pressure is increased the density of a gas increases. At the critical point, the density of the gas becomes equal to that of the liquid phase. The two phases therefore combine to form one continuous phase, the supercritical

fluid. From Figure 2.5, it seems that the onset of distinct deviation from ideal behaviour is at around 73 bar (circled), which marks the onset of supercritical behaviour of CO₂. At this stage, the intermolecular forces and molecular volume are quite significant. Deviation from ideal behaviour can thus be attributed to high pressure, which in the case of CO₂, results in phase change to a supercritical state. Nonetheless, based on the gas behaviour at pressures below the critical pressure, communication between the thermocouple and pressure gauge is shown to be effective. This also implies that the position of the thermocouple (accuracy of ± 0.5 °C) in the reactor is suitable to give a good indication of reaction chamber temperature conditions. Temperature readings obtained would therefore not be far off temperatures reactants are exposed to.

2.1.2.2 Reactor heating profile

The way the autoclave is heated up is important in understanding how the reaction will be influenced. The temperature controller used uses a PID (proportional, integral and differential) on/off switch to regulate temperature. The temperature controller was set to self-tune, where it determines the best PID algorithms to attain the shortest heating time to reach the set-point and maintain temperatures at minimum deviations at set-point.

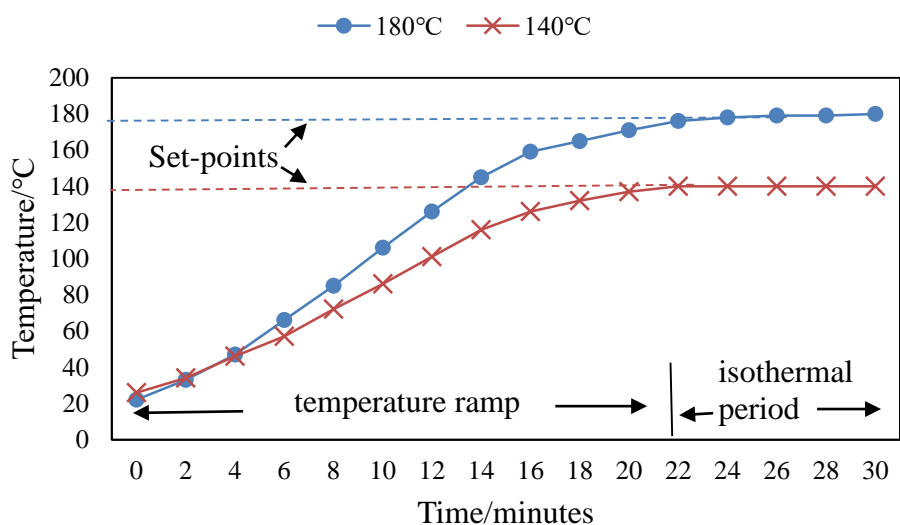


Figure 2.7: Reactor heating profile at 140 °C and 180 °C set-points.

Two set-points were chosen, *i.e.* the extreme temperatures according to the central composite design followed in chapter three, and their heating profiles traced. The maximum deviation from set-point observed during the experimental runs was ± 1 °C, which indicates effective PID temperature control at the set-point temperature. From Figure 2.7, the heating rate at the maximum set-point temperature (180 °C) appears to be faster than that at the lowest set-point temperature (140 °C). The time taken to reach 180 °C set-point is longer (24 minutes) than that for the 140 °C set-point (22 minutes). This is due to the relatively larger temperature range covered to attain the 180 °C set-point than the lower set-point. A comparison of the slopes for the two set-points (Fig. 2.7), shows that the set-point temperature determines the heating rate for the temperature controller. Unfortunately, the temperature controller could not be set to a constant heating rate. So the instantaneous heating rate was determined by curve fitting using Microsoft excel to get the best polynomial function and its first derivative. In this way, the heating rate could be quantified at a specific time.

2.1.2.3 Effect of thermal mass on the heating rate

It was observed that a change in the thermal mass results in subsequent changes in the heating rate (Fig. 2.8). Thermal mass is the ability of a body to store thermal energy, (*i.e.* its heat capacity) [6]. All the mass subject to heating (this includes loaded sample, dry ice, chemicals, and reaction chamber) therefore has an influence or contribution towards the overall thermal mass.

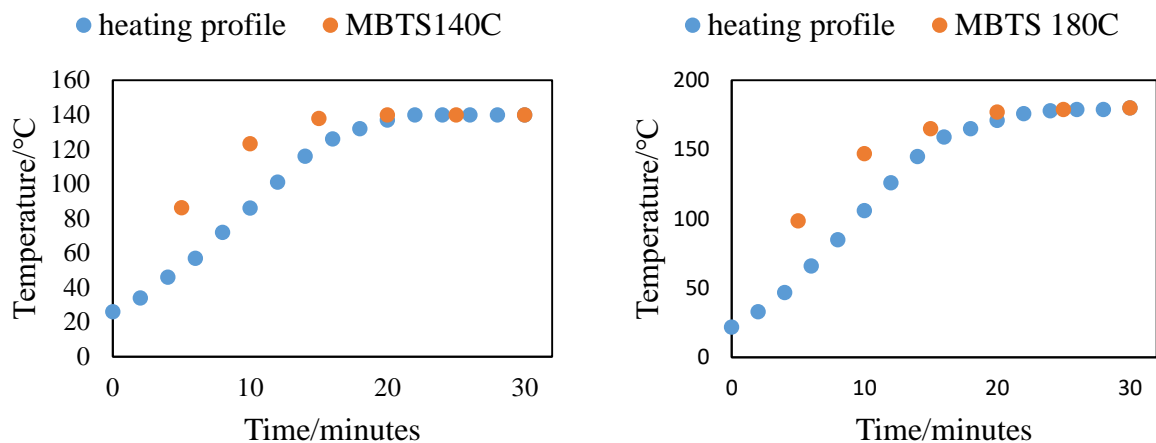


Figure 2.8: Heating profiles showing the effect of thermal mass on the heating rate at 140 and 180 °C set-point. *Note that the control curve (blue dots) was traced from ambient temperature with only CO₂ in the autoclave whereas the curve for MBTS (orange dots) was traced at 5 minutes intervals from 50 °C during a reaction run (i.e. sample and MBTS present).*

Changing the amount of contents inside the reactor affects the overall thermal mass, and consequently, the amount of heat energy absorbed by the total mass. As observed in Fig. 2.8, this in turn affects the rate at which heat is supplied; the heating rate for the MBTS 180 °C curve became greater than that of the control due to increased thermal mass. Changes in the heating rates as thermal mass is changed indicates that the PID control system is able to detect mass changes (or energy demand) in order to achieve pre-set temperature conditions. In other words, the PID control system ensures that enough heat is available for the introduced mass. Due to these findings, care was taken to maintain thermal mass as constant as possible for all reactions.

2.2 OTHER INSTRUMENTATION USED

2.2.1 Weight determination

Weight measurements for devulcanisation agents, vulcanized rubber (treated or untreated) and crumb rubber samples were done using a Mettler Toledo AB204-S analytical balance. These samples were used in cure characterisation, Soxhlet extraction, swelling ratio determinations and devulcanisation procedures.

Instrument specifications:

- Technical data valid at ambient conditions of 10-30 °C, 15-85% humidity.
- Maximum capacity: 220 g (e = 1 mg)
- Minimum capacity: 10 mg (d = 0.1 mg)
- Weighing pan diameter: 80 mm
- Readability: 0.1 mg
- Taring range (by subtraction): 0-51 g

More specifications available at; <https://www.ietltd.com>.



Figure 2.9a: Mettler Toledo weighing balance (AB204-S)

Weight determination of samples for thermal analysis by differential scanning calorimetry (DSC) and thermogravimetric analysis (TGA) was done using a Mettler Toledo MX5 UMT2 microbalance.

Instrument specifications:

- Maximum capacity: 2.1 g (d = 0.1 μ g)
- Weighing pan diameter: 16 mm
- Sensitivity drift at 5-40 $^{\circ}$ C: \pm 0.00015 % with automatic self-calibration
- Readability: 0.1 μ g
- Taring range (by subtraction): 0-2100 mg

More specifications on the instrument available at;
<http://photos.labwrench.com/equipmentManuals>.



Figure 2.9b: Mettler Toledo microbalance (MX5 UMT2)

2.2.2 Rubber compounding

2.2.2.1 Banbury internal mixer

A Banbury internal mixer was used for compounding rubber. The mixer is equipped with tangential steel alloy rotor blades that masticate and mix the rubber with additives in a steel housing enclosed by a pressure lid. A thermocouple is conveniently attached to the mixing chamber for temperature recording observable on a digital meter. The chamber has a water cooling system to assist with temperature regulation, thus preventing scorching due to shear induced heat generation. Ingredients are added at the top of the mixing chamber by means of opening and closing the pressure lid using a control lever.



Figure 2.10a: Banbury internal mixer a) chamber b) open chamber c) tangential mixing blades.

Instrument specifications:

- Capacity: 330 ml
- Fill factor used: 0.75
- Temperature regulation: water cooling system from a low temperature water bath (from Labcon, with temperature range of -30 to 70 °C)
- Rotor speed: 0 – 100 revolutions/minute

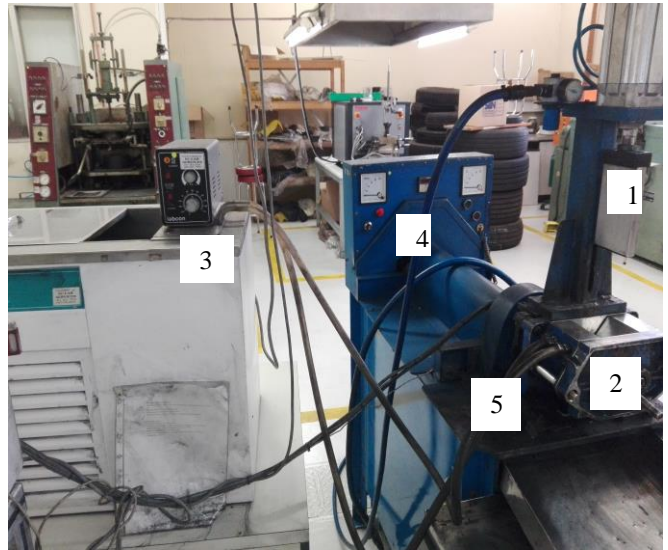


Figure 2:10b: Internal mixer linked with (3) cold water bath through (5) water connection tubes. Indicated Banbury mixer parts include; 1) pressure lid, 2) mixing chamber, and 4) rotor speed monitor.

2.2.2.2 Two roll mill

A two roll mill from Planters Engineering Co. Ltd was used to aid mixing of rubber samples. The instrument consists of two cylindrical, smooth surfaced, stainless steel rolls positioned adjacent to each other. These rotate at different speeds, the rear rotating faster than the front, to aid mixing. The gap between the two rolls, *i.e.* nip gap, can be adjusted depending on requirements. The instrument is equipped with a heating, cooling and rotor speed adjustment control panel for both the rear and front roll. After the first mixing stage in the internal mixer, the sample was taken out and sheeted on the two roll mill. This procedure aids with dispersion and cools down the mixed sample. A roll knife is used to make cuts on the rubber sample as it passes through the two rolls.



Figure 2.11: Two roll mill used for sheeting. Indicated are the 1) two rolls, 2) temperature and rotor speed regulator and 3) safety mechanism (trip switch).

2.2.2.3 Rubber Process Analyser (RPA) ^[7]

Also known as the Dynamic Moving Die Rheometer (D-MDR 3000), the RPA is an advanced dynamic mechanical rheological test instrument, designed to measure the properties of polymers and rubber compounds before, during and after cure ^[7]. The RPA is equipped with a biconical die system; both the lower and upper dies are grooved for maximum efficiency in strain and stress transfer. The upper die is connected to a torque transducer which detects changes in torque. After the sample is loaded onto the die cavity, a sinusoidal strain is applied to the sample by the lower die. This induces stress within the sample. The stress transfers a torque to the upper die, thereby generating a small strain which is detected by the transducer. Characteristics measured by the RPA include; optimum cure time, scorch time, cure rate, tan delta, minimum and maximum torque, viscous and elastic moduli, hysteresis, and correlation of tensile properties.



Figure 2.12: 1) Dynamic moving die rheometer 2) shows upper and lower die systems.

Instrument specifications [7]:

- Calibration: a compliant metal tube or rod with a precisely measured modulus is used to calibrate the RPA. Calibration defines the torque for a defined shear strain at a defined temperature. It also defines internal zero strain. Typical calibration temperature is 177 °C.
- Die cavity volume: 4.5 mm³
- Die closing system: the platen crosshead that contains the upper die and transducer is closed with an air cylinder. The air piston delivers about 10 000 N closing force. This exerts a typical sample pressure of 7 MPa soon after closure, depending on sample properties.

2.2.2.4 Cure press

Compression moulding is a method of moulding that involves pre-heating the mould, then placing the sample in the open heated mould cavity. The mould is then closed using a plug member or force, followed by application of pressure to force the material into contact with the whole mould cavity. Usually, heat and pressure are maintained until the material has cured. Compression moulding of the compounded rubber was done in a cure press from T. H and J. Daniels Ltd, Stroud Engineering firm. The instrument was built following British patents which include; 541377; 550864; 550352; 550351; 542486; 556686; 486716 and others. Figure 2.13 shows the cure press and the mould used in curing rubber. The instrument is equipped with a pressure regulatory system; which is an electronic motor to a hydraulic pump. The pressure exerted on the mould was maintained at 5 bars. It also has two heating plates, *i.e.* lower and upper plates, where the sample mould is placed. The lower plate is adjustable by means of the hydraulic pressure pump. Heating of both plates is by means of a digital temperature controller.



Figure 2.13: Cure press used for compression moulding. Indicated is the 1) motor for the hydraulic system, 2) mould plates, and 3) temperature control unit.

2.2.3 Accelerated ageing

2.2.3.1 Water bath

A water bath from Scientific was used for accelerated ageing of rubber vulcanisates. The water bath is equipped with a water circulator and a digital PID temperature controller for efficient temperature regulation (± 0.3 variation).



Figure 2.14: Water bath used for accelerated ageing.

2.2.4 Soxhlet extraction

For Soxhlet extraction of aged vulcanisates, the setup shown in the experimental section was used. The azeotropic mixture was however tested for quality (*i.e.* consistency in composition) by means of a refractometer.

2.2.5 Refractometer

Refractometers measure the degree at which light changes direction (or is refracted) as it passes a boundary between two media. The refractive index of a material gives an indication of how much

the material bends (or refracts) light, *i.e.* how optically dense the material is. A refractometer takes the refraction angles and correlates them to refractive index (n_D) values that have been established [8]. An ABBE 5 refractometer manufactured by Bellingham and Stanley Ltd was used for determination of refractive index during preparation of azeotropic mixtures. Refractive index is sensitive to temperature changes, so temperatures were maintained constant by running tap water through tubing connected to water nozzles on the refractometer.

Instrument specifications:

- Measurement range (refractive index, n_D): 1.30 - 1.70
- Scale resolution (n_D): 0.0005
- Operating temperature: 5 – 70 °C
- Temperature accuracy: 0.1 °C
- Ambient operating temperature (°C): 5 – 40 °C

More specifications available at;

<https://www.bellinghamandstanley.com>



Figure 2.15: Refractometer for checking consistency in acetone/chloroform composition.

2.2.6 Drying equipment

2.2.6.1 Vacuum desiccator

A vacuum desiccator made from pyrex housing and lid was used in drying rubber samples during analysis. This was done in an attempt to minimise any possible compromise of sample structure due to heat and oxygen. Also, light was excluded by covering the desiccator lid with a sheet of aluminum foil. This was done to prevent any possible photochemical reactions taking place within the rubber samples.

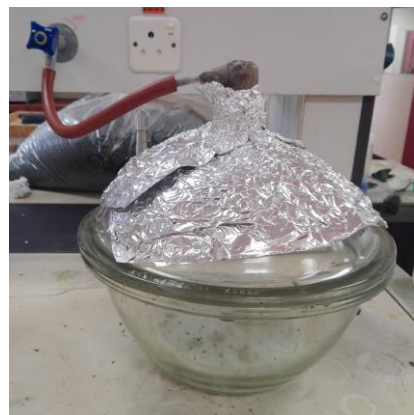


Figure 2.16: Vacuum desiccator.

2.2.6.2 Forced air ventilation oven

A forced air ventilation oven from Labcon was used to dry rubber samples after Soxhlet extraction, during final stage of swelling measurements and during moisture content determination of crumb. Glass ware was also dried using the forced air ventilation oven. The oven temperature range is 0–250 °C, was maintained at 50 °C for drying purposes.

(More specifications available at; <https://vactech.co.za/>)



Figure 2.17: Forced air ventilation oven.

2.2.6.3 Rotary Evaporator

Rotary evaporators are distillation units that incorporate a water condenser with a rotary flask system^[9]. Rotation of the flask containing the sample or solvent, ensures effective heat transfer from the water bath, hence maximising evaporation of the solvent. The rotary evaporator is also connected to a vacuum system, which further increases evaporation by lowering the boiling point of solvent by means of reducing its vapour pressure. Applications of rotary evaporators include; concentration of solutions, degassing liquids, vacuum drying of wet solids, and reclamation of solvents^[9]. An RE300 rotary evaporator from Bibby scientific instruments was used to dry sol fractions. The instrument is equipped with; a simple counterbalanced lift mechanism, PTFE/glass liquid pathway for chemical inertness, sparkles induction motor, long life graphite impregnated PTFE vacuum seal, and efficient flask and vapour tube ejection system^[9].

Instrument specifications ^[9]:

- Speed range: 20-190 rpm
- Lift distance: 150 mm
- Vacuum: < 1mm Hg

More specifications available at;
www.keison.co.uk/bibbyscientific.



Figure 2.18: Rotary evaporator, RE300.

2.2.7 Characterisation and analysis equipment

2.2.7.1 Muffle furnace

A muffle furnace can be described as a furnace in which the subject material is isolated from the fuel and all of the products of combustion, including gases and flying ash ^[10]. The furnace can be used for laboratory or scientific purposes, ashing, sintering, dental, jewelry and heat treatment ^[10]. In this study, a Dionysus Labofurn muffle furnace (manufactured by Kiln Contracts PTY LTD, Cape Town) was used to determine the ash content of crumb rubber.



Figure 2.19: Muffle furnace used for GTR ash content

Instrument specifications ^[11]:

- Heating elements are concealed behind an alumina muffle
- The furnace is equipped with a lift-up door that ensures operator safety
- A chimney is fitted as standard equipment
- Modern ceramic fibre insulation contributes to fast heating cycles, energy savings and low shipping weight.

- Excellent temperature distribution with a maximum of 900 °C.
- The instrument is also equipped with a digital PID temperature controller.
- All elements are isolated when the door is open, by action of door opening a limit switch breaks the circuit to the supply contactor.

More specifications available at; <http://www.kilncontracts.co.za/products>.

2.2.7.2 Fourier transform-infrared spectroscopy, FTIR

The ATR-FTIR operates by directing an infrared (IR) beam onto the optically dense crystal at a specified angle. A short-lived wave is created due to total internal reflectance, which is extended beyond the surface onto the test material held in contact with the crystal. The short-lived waves produced only extend a few microns beyond the crystal surface to make contact with the sample. The short-lived wave is altered or attenuated in the IR regions where the sample absorbs energy. The attenuated energy for each of the short-lived waves is then relayed back to the IR beam, before exiting the reverse end of the crystal into the detector which generates an IR spectrum.

A Tensor 27 FTIR spectrophotometer from Bruker (Billerica, MA. USA) fitted with a Platinum Attenuated Total Reflectance (ATR) accessory was used for sample structural analysis. The Tensor II is fitted with a pure diamond crystal, and can perform measurements in the near, mid and far infrared region. It is important for the refractive index of the crystal to be significantly greater than that of the sample to ensure total internal reflectance.



Figure 2.20: FTIR spectrophotometer, Tensor 27.

2.2.7.3 Gas Chromatograph-Mass Spectrometer (GCMS)

Gas chromatography (GC) is an analytical technique used for quality control as well as to identify and quantify compounds in a mixture. It has the basic requirements like all other chromatographic techniques; *i.e.* a mobile phase (which is an inert carrier gas *e.g.* helium, argon, or nitrogen) and a stationary phase (which may be a packed or capillary column). The separation of the analytes is based on differences in strengths of interaction with the stationary phase. The stronger the interaction of an analyte with the stationary phase implies longer retention time and vice versa. Factors that influence separation of components include; vapour pressure, polarity of components relative to column, column temperature, carrier gas flow rate, column length, and amount of material injected ^[12]. The higher the vapour pressure the lower the retention time, because the component spends more time in the mobile phase (and *vice versa*) ^[12]. Similar polarity of a component relative to stationary phase implies a higher retention time (and *vice versa*). High temperatures and flow rates reduce the retention time but result in poor separation. A longer column usually results in better separation, but this is associated with a higher retention time as well as peak broadening (due to longitudinal diffusion) ^[12]. Most detectors do not need a lot of analyte to produce a detectable signal. Thus a large quantity of analyte may result in poor separation. The GC can be coupled with various types of detectors, these include; a mass spectrometer (GC/MS); flame ionisation detector (FID); thermal conductivity detector (TCD); and an electron capture detector (ECD) ^[13].

GCMS analysis was done using a gas chromatograph (7890A GC system) equipped with a Agilent 7683 Series injector, combined with a mass selective detector (5975C VL MSD, with triple axis detector). The separation column (Phenomenex ZB-5MSi, Torrance, CA, USA) has; a maximum temperature of 360 °C, and dimensions of; 30 m x 250 µm x 0.25 µm of length x internal diameter x film thickness respectively.

More specifications at www.agilent.com on the Agilent 7890 Series GC manual.



Figure 2.21: Agilent GCMS for qualitative analysis of devulcanisation extracts.

2.2.7.4 Differential scanning calorimetry, DSC

Differential scanning calorimetry (DSC) is a technique in which temperature differences between the sample and reference are measured as a function of temperature. The sample and reference are subjected to the same heating programme. The reference material should have a well-defined heat capacity and should not undergo any thermal event over the temperature range of interest ^[14]. The

DSC instrument detects changes in the energy supplied or heat capacity of substances during phase transitions. Applications of DSC include; glass transition (T_g), melting points, crystallisation, desorption, adsorption, decomposition, curing, vaporisation, polymerisation, and polymorphism [15]. The scheme on Figure 2.22a shows a typical setup for a DSC cell. The cell is made up of a material of high thermal conductivity, to achieve symmetrical heating of the cell as well as the sample and reference.

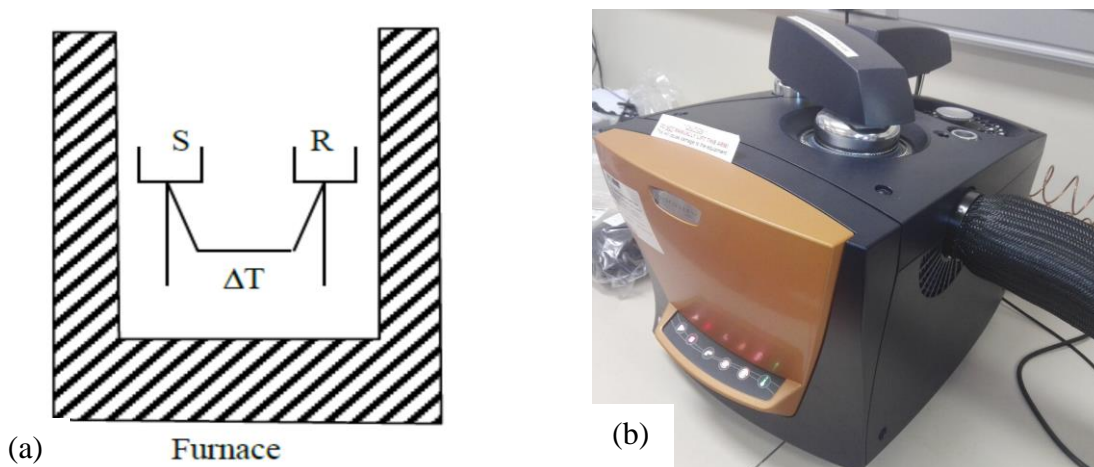


Figure 2.22: a) Scheme for a typical cell of a heat flux DSC [14], b) Discovery DSC instrument.

A Discovery DSC from TA instruments was used to determine the glass transition temperatures of GTR gel components.

2.2.7.5 Thermogravimetric analyser, TGA [16].

Thermogravimetric analysis is a thermal analysis method in which changes in physical properties of a substance are measured as a function of temperature, while temperature is controlled by a heating programme. TGA can provide information such as; vaporisation, sublimation, absorption,

adsorption, desorption, dehydration, decomposition, oxidation and reduction. Composition analysis or characterisation of samples was performed using the Discovery High resolution thermogravimetric analyser (Hi-Res™ TGA) from TA Instruments. The TGA is equipped with a null balance system with weight resolution of 0.01 μg and accuracy of $\leq \pm 0.1\%$ of value or 10 μg (whichever is greater), that can take sample weights up to 900 mg with an 800 mg tare mass. The null balance system consists of the balance meter movement, the balance arm, the balance position sensor, the hang-down wire assembly, and the sample and tare pans. An autosampler loads samples onto and out of the balance. The autosampler platform is equipped with a built in pan punching mechanism used for sealed aluminium pans. A gas delivery module controls the purge gas into the furnace and balance. The heating system is an infrared furnace, which controls the sample temperature by means of a thermocouple assembly positioned under the sample pan. A second independent thermocouple within the assembly protects the furnace from excessive temperature. The Hi-Res™ TGA heating rate of the sample is dynamically and continuously modified in response to changes in the rate of sample decomposition thereby optimising weight change resolution and analysis time.

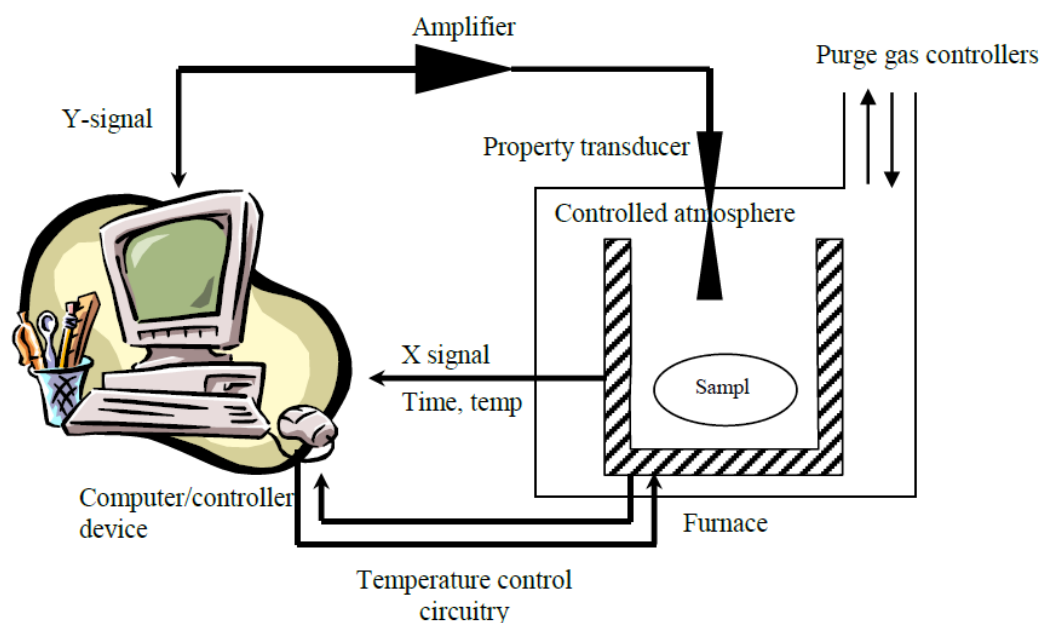


Figure 2.23: Scheme of TGA setup ^[14].

Instrument specifications (some) ^[16]:

- Operating conditions: temperature; 15-35 °C, humidity; 5-80 % (non-condensing), max altitude; 2000 m.
- Temperature range: ambient +5-1200 °C
- Heating rate: linear heating rate from 0.1-500 °C/min (ballistic heating > 1000 °C/min)
- Purge gases: helium, nitrogen, oxygen, air, and argon.
- Purge flow rate: up to 200 mL/min (recommended; 25 mL/min for sample, 10 mL/min for balance)
- Thermocouple: Platinel II (trademark for Engelhard industries)

2.2.7.6 Gel permeation chromatography, GPC ^[1]

Gel permeation chromatography (GPC) is a type of size exclusion chromatography (SEC), but these terms are usually used interchangeably since GPC is the most popular form of SEC used ^[1]. GPC is a technique used to characterise macromolecules, providing data such as; molecular weight, intrinsic viscosity and hydrodynamic radius. GPC is a solution based form of chromatography that separates analytes based on their hydrodynamic size. The stationary phase is made up of gel particles with pores. Separation of analytes is based on their differences in the rates of diffusion into and out of the pores. The bigger analytes spend less time within the pores while the smaller analytes spend more time within pores. Consequently the bigger analytes elute first, and lastly the smallest analytes. A typical GPC system is comprised of a mobile phase reservoir (solvent), vacuum degasser to remove any trapped gases from the mobile phase, a GPC pump to keep mobile phase flowing, an injection loop where the sample is introduced into the mobile phase (has an autosampler option), separation columns in an oven for temperature control, as well as detectors. The detector can be a; refractive index detector (RI), ultra-violet/visible light or photodiode array detector (UV-Vis or PDA), light scattering detector (LS) and or viscometer detector.

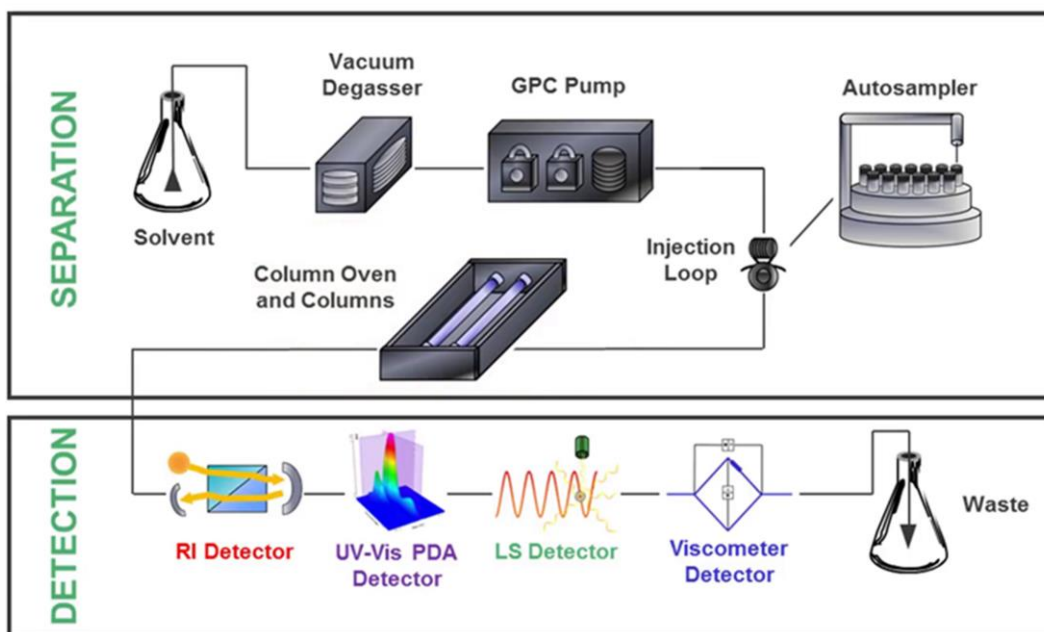


Figure 2.24: General layout of a typical GPC system setup (*adapted from Malvern et al*^[1]).

In this study, a THF-GPC setup was used. It comprised of a Shimadzu LC-10 AT isocratic pump, a Waters 717 injector (with an autosampler), RI detector, a Waters 2487 dual wavelength UV detector, a 50 x 8 mm guard column in series with three 300 x 8 mm, 10 μm particle size, and GRAM columns (2 x 3000 \AA and 100 \AA , PSS). The instrument calibration was done using polystyrene standards of a narrow distribution. 2.5 mg/ml polymer solution concentrations were prepared in THF in the presence of 3 % BHT.

2.2.8 GTR preparation

A 150 W Taurus coffee grinder equipped with burr grinding plates in a stainless steel housing, was used to produce crumb rubber (of size < 2.36 mm) from cryo-frozen rubber.



Figure 2.25: Taurus coffee grinder used to make GTR

2.3 SUMMARY OF FINDINGS

- Communication between changes in temperature as detected by the thermocouple and pressure as monitored by the pressure gauge was found to be effective.
- The rate of heating the reactor was found to depend on the set-point temperature value, *i.e.* the higher the set-point the faster the heating rate.
- The presence of mass in the reactor was found to influence the heating rate. Higher heating rates were observed upon loading samples into the reactor.
- The reactor was found to be conducive to conduct and monitor devulcanisation.

2.4 REFERENCES

1. Williams, K., *An introduction to GPC in 30 minutes*, Malvern, Editor. 2016, Malvern instruments Ltd.
2. OMEGA. *Temperature control: Tuning a PID (three mode) temperature controller*. 2018; Available from: www.omega.com.
3. ChemLibreTexts. *Kinetic Theory of Gases*. 2017; Available from: chem.libretexts.org.
4. ChemLibreTexts. *The Phase diagram of carbon dioxide*. 2017; Available from: <https://chem.libretexts.org>.
5. Atkins, P. and J.D. Paula, *Atkins' Physical Chemistry*. 8 ed. 2006: Oxford University Press.
6. EcoSpecifier Global. *Thermal mass and its role in building comfort and energy efficiency*. 2018; Available from: <https://www.ecospecifier.co.za>.
7. GmbH, M.R.t.i., *D-MDR 3000 Application Manual*. 2008.
8. Ltd, C.-P., *Refractometers*. 2017.
9. products, K. *Bibby scientific RE300 rotary evaporator*. 2018; Available from: www.keison.co.uk/bibbyscientific.
10. CM Furnaces INC. *Production and Laboratory Furnaces. Muffle furnaces*. 2018; Available from: <http://cmfurnaces.com>.
11. Contracts, K. *Laboratory muffle furnace*. 2018; Available from: www.kilncontracts.co.za.
12. Zebtron. *GC selection guide*. Available from: www.phenomenex.com.
13. Agilent. *Agilent 7890 Series GC manual*. 2018; Available from: www.agilent.com.
14. Grooff, D., *Thermal analysis*. 2016, Nelson Mandela University. p. 1-58.
15. incorporated, I.s. *DSC*. 2018; Available from: www.instrument-specialist.com.
16. LLC, T.i.-W., *Discovery TGA Getting Started Guide*. 2013.

CHAPTER 3: ISOTHERMAL PROCESS OPTIMISATION

3.1 INTRODUCTION

The objective of devulcanisation is basically the reversal of vulcanisation ^[1] in an attempt to regenerate original rubber properties. This process can involve total or partial cleavage of crosslinks ^[2]. Horikx *et al* ^[3] showed the relation between the sol and gel fractions of a network that has been degraded. In their report, they theorised that scission can be; random chain scission, crosslink scission or directed scission. Random chain scission involves random depolymerisation while the crosslink density remains unaffected (*i.e.* C-C bond scission). Its relation with the sol content is given by equation 3.1;

$$1 - \frac{v_{e2}}{v_{e1}} = 1 - \frac{\left(1 - s_2^{\frac{1}{2}}\right)^2}{\left(1 - s_1^{\frac{1}{2}}\right)^2} \quad (3.1)$$

Where; v_{e1} and v_{e2} are the effective number of chains before and after degradation, obtained *via* swelling measurements, s_1 and s_2 are the amount of sol before and after degradation.

Mathematically, equation 3.1 implies that a high sol content after degradation is associated with intensive chain degradation. In other words, equation 3.1 shows that degradation of the chains can occur with resultant sol production but without any crosslink scission taking place. Of course this is only theoretical, however, it can be representative of reclamation processes that result in a low degree of decrosslinking but high chain breakdown. So the reclaim rubber produced therein would exhibit poor blending properties due to the presence of crosslinks. The sol component of such inefficient systems is characterised by low Mw of rubber fragments ^[4], which indicate high degree of chain scission. The reclaim thus produced is best used in very small quantities (*ca.* 5-10 phr ^[1]) or as a processing aid.

Crosslink scission involves cleavage of C-S or S-S bonds while chain length is unaffected. The relation between the effective number of chains in gel and sol is given by equation 3.2;

$$1 - \frac{v_{e2}}{v_{e1}} = 1 - \frac{\gamma_2 \left(1 - s_2^{\frac{1}{2}}\right)^2}{\gamma_1 \left(1 - s_1^{\frac{1}{2}}\right)^2} \quad (3.2)$$

Where; γ_1 and γ_2 are the crosslinking indexes before and after degradation.

The crosslink index gives the average number of crosslinks per original chain ^[3]. In the case of this study, the original chain length is given by the masticated uncured rubber (NR/SBR blend). Equation 3.2 is quite sensitive to γ_1 (*i.e.* degree of crosslink of vulcanisate). The expression assumes that no chain scission occurs, so chain distribution and length stay the same while crosslinks are severed. This is also only theoretical as chain scission is practically unavoidable during reclamation or devulcanisation processes. However, this relation can be representative of situations where high crosslink scission is obtained while chain degradation is quite low. Onouchi *et al* ^[5] reported complete degradation of NR using thiols and dimethoxy sulfoxide (DMSO) in benzene. In their report they obtained high degree of swelling but low sol content (2 %), which is indicative of selective crosslink scission.

Directed scission involves chain cleavage at monomeric units bonded to crosslinks (which Horikx *et al* suggests is speculative) ^[3]. The theoretical considerations by Horikx *et al* ^[3] are frequently used to check the relative degrees of chain and crosslink scission of devulcanisation processes ^[6, 7]. Therefore, it can be deduced that for monitoring the degree of devulcanisation, tracking changes in the crosslink densities would make more sense than tracking sol content ^[7, 8]. Changes in crosslink densities would therefore give a direct relation to the degree of devulcanisation according to ASTM D6814 (equation 3.3);

$$\% \text{ Devulcanisation } (\%D) = \frac{\Delta v}{v_o} \times 100\% \quad (3.3)$$

Where; $\Delta v = v_o - v_t$ *i.e.* crosslink density of neat unde vulcanised sample (v_o) and crosslink density at time = t-minutes (v_t).

Using the amount of sol content as a response for optimisation would best fit reclamation processes, where due to random chain and crosslink scissions, more sol is produced. In view of these considerations, % devulcanisation was used as the response for optimisation of devulcanisation conditions. Sol content was also determined, followed by Mw determination to track extent of chain scission.

3.2 EXPERIMENTAL

3.2.1 Materials

3.2.1.1 Compounding materials

All the ingredients used in compound formulation were supplied by S & N Rubbers (unless specified) and were used as obtained. Standard Malaysian rubber (SMR-20) and SBR-1502 were used as elastomers. Polyethylene glycol (PEG) was used as a processing aid. Paraffinic oil was used as a plasticiser. Renacit 7, supplied by Bayer Pty Ltd, was used as a peptiser. High abrasion furnace Carbon black (HAF, CB N330) was used as a reinforcing filler. Zinc oxide (ZnO) and Stearic acid from Frontier chemicals were used as activators. *n*-(1,3-dimethylbutyl)-*n*-phenyl-*p*-phenylenediamine (6-ppd) and *n*-cyclohexylbenzothiazol-2-sulfenamide (CBS) were used as antioxidant and accelerator respectively. Sulphur (Midas sp3) from was used as the vulcanisation agent.

3.2.1.2 Devulcanisation materials

The devulcanising agents (dAs) used to execute devulcanisation reactions were; diphenyl disulphide (DD) and 2,2-dithiobis(benzothiazole) disulphide (MBTS). These were purchased from Sigma Aldrich and were used as received.

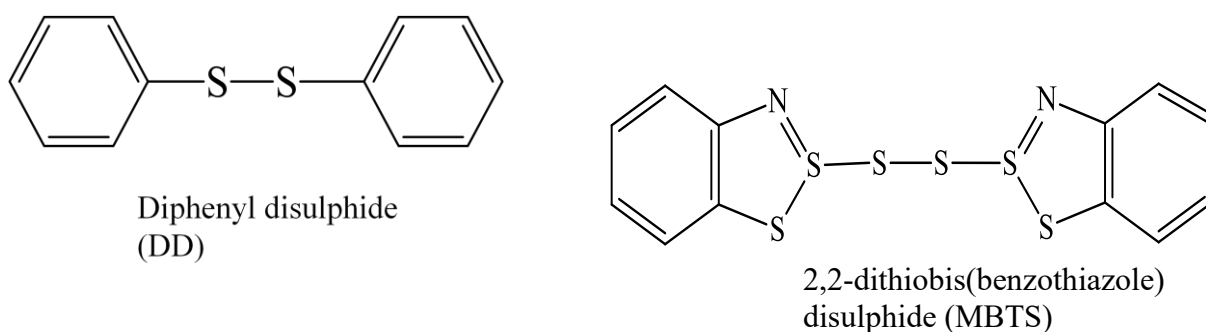
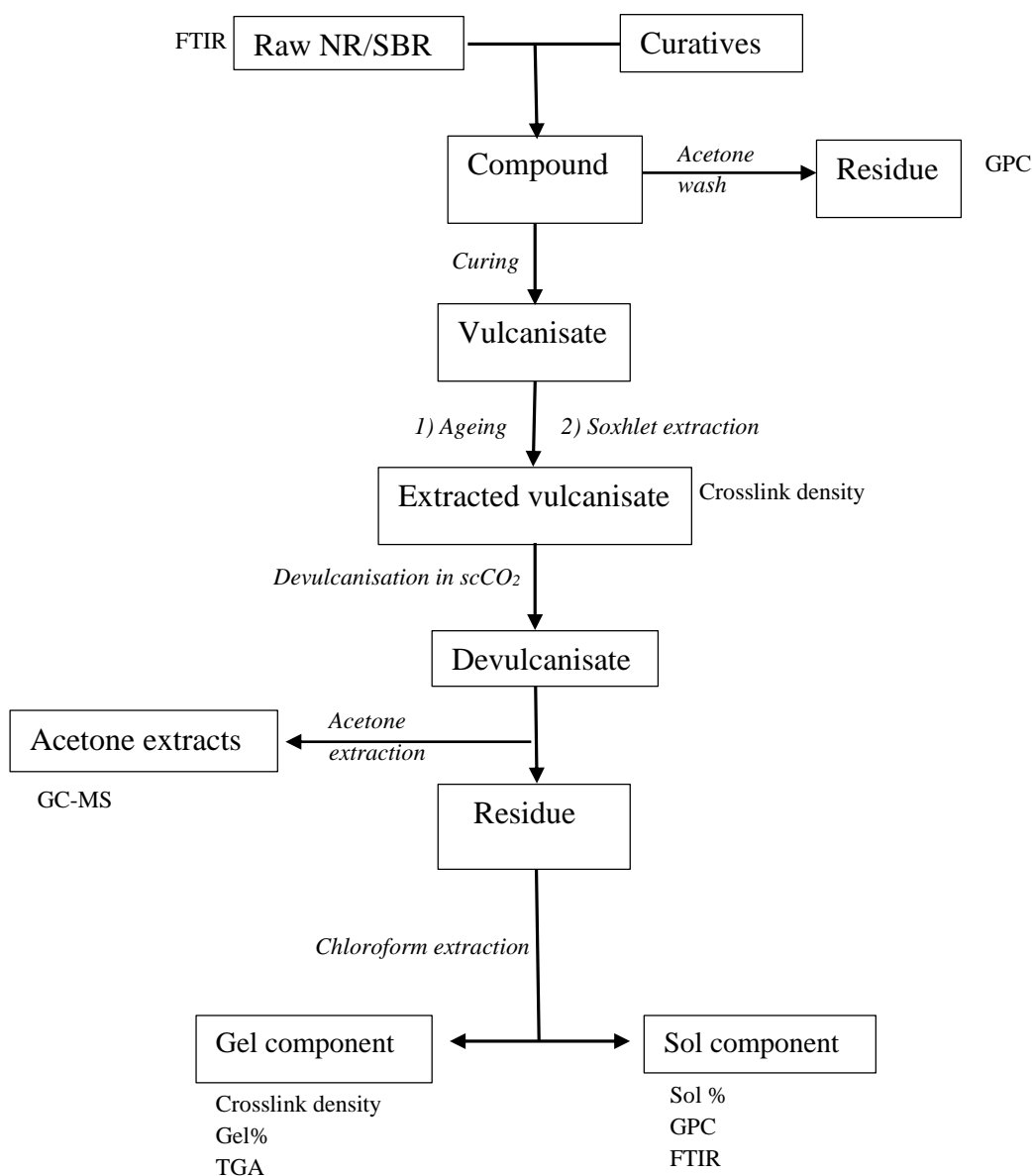


Figure 3.1: Chemical structures of DD and MBTS

3.2.2 General procedure

Experimental procedure was executed according to Scheme 3.1. After mixing of raw rubber with curatives and additives, a small amount of sample was set aside from the mixed batch and washed with acetone to determine its Mw. This is important because upon mixing in an internal mixer, raw rubber undergoes mastication resulting in reduction in Mw. It is this masticated rubber that is vulcanised. Therefore, the sol component Mw was referenced to the masticated rubber Mw to check for any changes in Mw due to devulcanisation reactions. Optimum cure times of the mixed rubber were determined by cure characterisation followed by curing. Vulcanisates were aged in a water bath after at least one week post curing. The idea behind this is that vulcanisates undergo ageing during service. The author understands how varied and uncontrolled conditions of ageing are in practical situations, however in this case accelerated ageing was done in cognisance of the fact that it simulates part of the ageing process (*i.e.* rubber deterioration due to heat). The conditions chosen for the accelerated ageing are not as important as ensuring the sample is deteriorated prior to recycling. Care was taken upon ageing in a water bath to ensure anaerobic conditions for reasons that the investigation aims at probing at efficiency of devulcanisation by chemical agents. As such, influence of oxidative polymer degradation is undesired. Soxhlet extraction of vulcanisates was done to get rid of excess curatives and additives used in compounding and curing. Swelling ratios as determined for the purified vulcanisates serve as reference for any changes that would occur due to devulcanisation reactions.

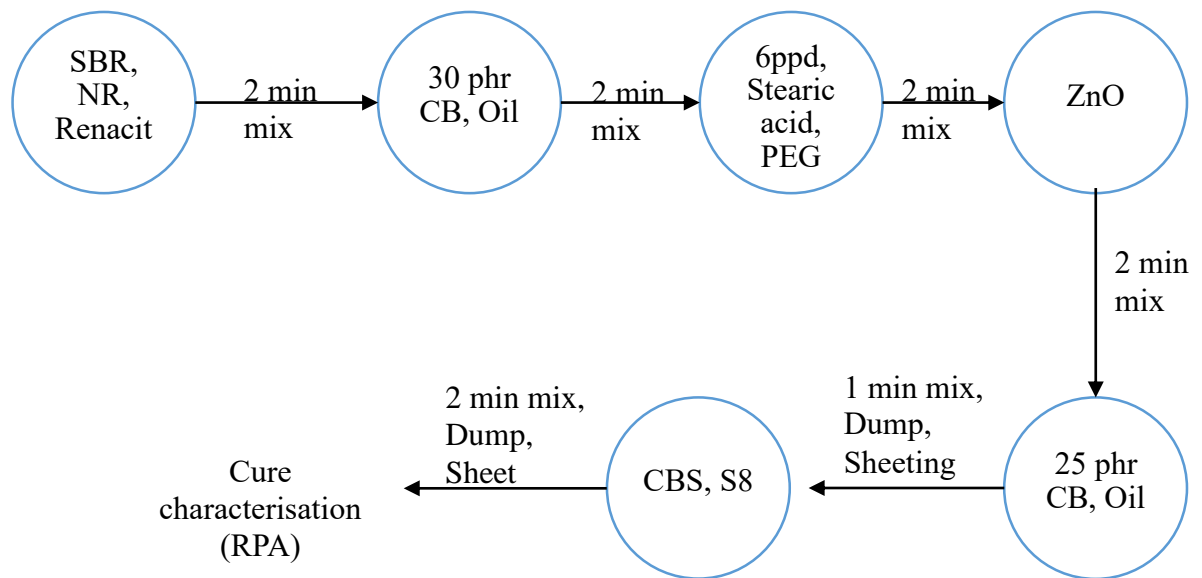


Scheme 3.1: Work flow diagram showing all the stages done in the experimental section.

3.2.2.1 Compounding

The formulation used for compounding represents a typical industrial truck tyre tread formulation (Table 3.1). The latter was chosen so that the findings would be representative of expectations with industrial truck tyre crumb. This eliminates any questions on application of optimum conditions obtained in this study on commercially obtained truck tyre rubber. Compounding was carried out in a 330 mL Banbury internal mixer at 0.75 fill factor, following a two stage conventional mixing procedure. The 1st stage involved sequential addition of all

the ingredients except CBS and sulphur (S_8). Only 30phr CB was added in the 1st stage to avoid overcharging the mixing chamber due to the high amount of CB filler to be added, followed by sheeting in a two roll mill. The sheeted compound was then returned to the internal mixer for 2nd stage mixing. The 2nd stage mixing involved the addition of CBS, S_8 and the remainder of CB filler (*i.e.* 25phr). The mix times and sequence of addition of the ingredients followed the process described in Scheme 3.2;



Scheme 3.2: Compounding sequence followed

Table 3.1: Compound formulation used (*adapted from Nocil Limited*).

Ingredients	CB filled (^aphr)	Unfilled (phr)
<i>SMR20</i>	70	70
<i>SBR1502</i>	30	30
<i>CB</i>	55	0
<i>ZnO</i>	5	5
<i>Stearic Acid</i>	2	2
<i>Renacit7</i>	0.1	0.1
<i>6ppd</i>	5	5
<i>Parafinic oil</i>	10	10
<i>Sulphur</i>	1.5	1.5
<i>PEG</i>	0.5	0.5
<i>CBS</i>	1	1

a = parts per hundred of rubber

Equations 3.4 and 3.5 was used in quantifying ingredients used in the compound formulation. The formula makes use of the assumption that masses and or volumes are additive, thus it does not account for dissolution of substances (which in this case has an insignificant effect on the batch volume) ^[9].

$$M_R = \frac{V_H F_f}{\frac{1}{D_R} + \frac{1}{100} \sum_{i=1}^n \left(\frac{phr_i}{D_i} \right)} \quad (3.4)$$

$$M_i = M_R \frac{phr_i}{100} \quad (3.5)$$

Where; M = mass, V_H = volume of mixing head, F_f = fill factor, D = density, R = rubber, i = ingredient.

Uncured samples were analysed to determine cure properties using the D-MDR 3000. Samples were cured at the determined optimum cure time (defined by t_{90}) as shown on Table 3.1 (Results section), at 150 °C using a compression mould at 5 bar pressure.

3.2.2.2 Ageing

Tyres undergo deterioration in physical properties due to ageing. This ageing process is influenced by several factors that include heat, oxidation, ozone, cyclic flex fatigue, abrasion, exposure to chemicals and many other factors tyres are exposed to during service ^[10]. Bearing this in mind, it is highly improbable for one to recycle a tyre that has been just cured. Recycling is usually done on tyres that have reached their end of life use or simply old tyres that are no longer usable for their intended purpose. For this reason, samples used in this study were cured at the optimum cure time (t_{90}) and then aged. Accelerated thermal ageing (oxidative) is usually done to illustrate real life conditions of tyres ^[10, 11]. However, it is important to note that there may be no correlation between the accelerated ageing tests and natural ageing due to varied conditions of natural ageing. With that in mind, samples that were prepared for devulcanisation were thermally aged in a water bath at 70 °C under anaerobic conditions. Anaerobic conditions were chosen to eliminate the effect of thermo-oxidative degradation of rubber chains ^[12]. To achieve optimum conditions that permit minimum chain degradation, it is pertinent to know if depolymerisation is due to reaction conditions (devulcanising agent and or reaction parameters). Therefore oxidative chain scission would bias findings.

Vulcanisate samples were trimmed into dimensions of 20 x 35 mm. The trimmed samples were packaged in plastic packaging bags, ISO9001 certified. After sealing the bag, air was drawn out of each bag by means of a suction hand pump, thereby creating an anaerobic environment. Ageing was done in a water bath at 70 °C for one week (*i.e.* 168 hours).

3.2.2.3 Soxhlet extraction

After ageing, the samples were extracted by means of Soxhlet extraction method (Fig. 3.3). This technique is used when the extracted vulcanisate is to be analysed and its application is limited to vulcanised NR, SBR, BR, and IR types of rubber products. Substances extracted

include; mineral oils or waxes, bituminous substances, organic accelerators, or antioxidants. The extract amount and contents give valuable information about the quality of the polymer/s present.

Extraction is done using an azeotropic mixture of 32 % acetone and 68 % chloroform composition by volume, boiling point of 64.4 °C, for 16 hours according to ASTM D297. An azeotropic mixture is characterised by a constant boiling temperature and similar ratio of components in the liquid and vapour phase. Azeotropic mixture quality check was done by looking at the boiling point (64.4 °C from ASTM D297) and refractive index from a standard curve (Fig. 3.2). The standard curve was obtained by taking refractive indices (using a refractometer) of acetone/chloroform mixtures varying in composition by volume.

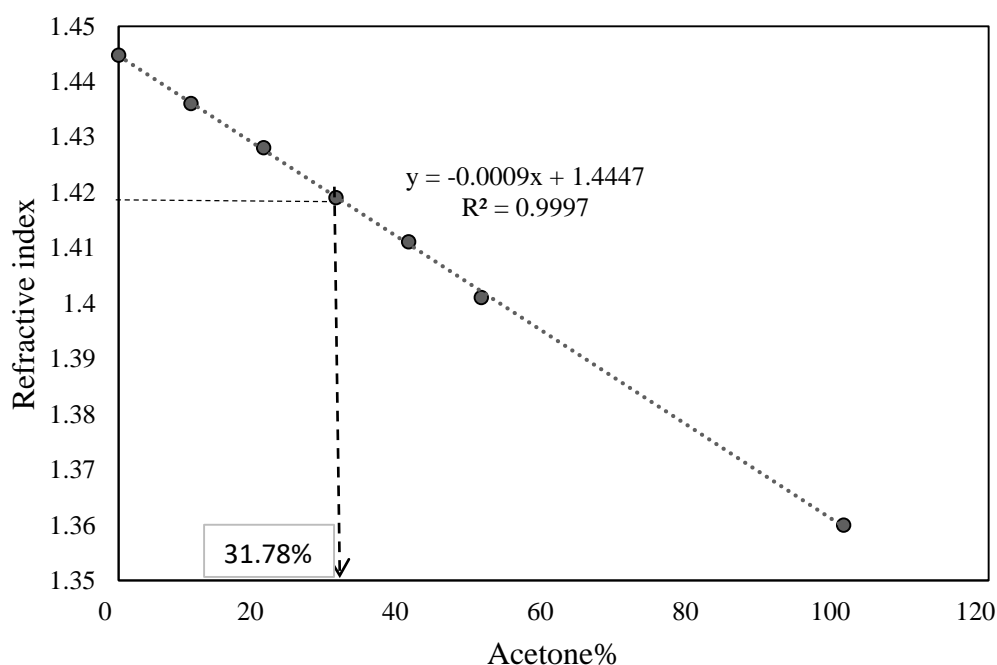


Figure 3.2: Standard curve showing refractive indices of a range of acetone/chloroform mixtures.

The liquid samples were transferred onto the prism surface of the refractometer using a pipette. Care was taken to ensure minimum evaporation of solvent before measurements were done.

The azeotropic mixture was determined to be 31.78% acetone /68.22 % chloroform (at refractive index of 1.4191 and b.p. 64.4 °C), which is similar to the prescribed 32 % acetone/68 % chloroform prescribed by ASTM D297.

Still conforming to ASTM D297, the rate of filling and un-filling of siphon tube was maintained at 3.00 ± 0.50 minutes. Selection of solvent is based on solvent that would not result in degradation of the rubber during the extraction process, yet effective in extraction of residual curatives and additives.

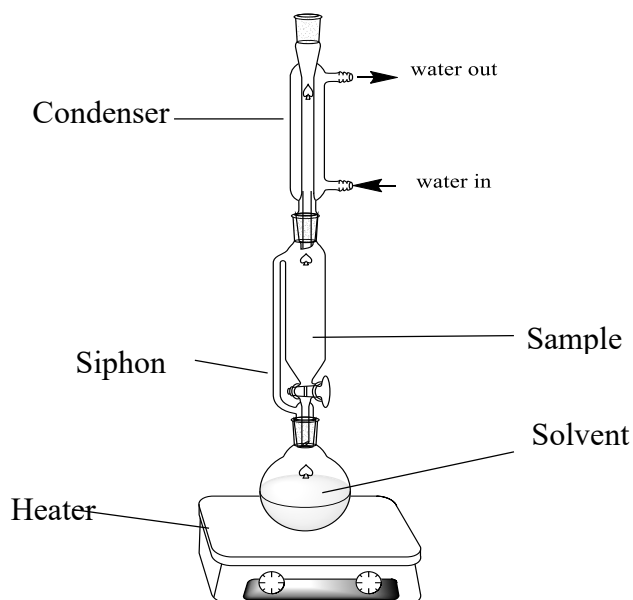
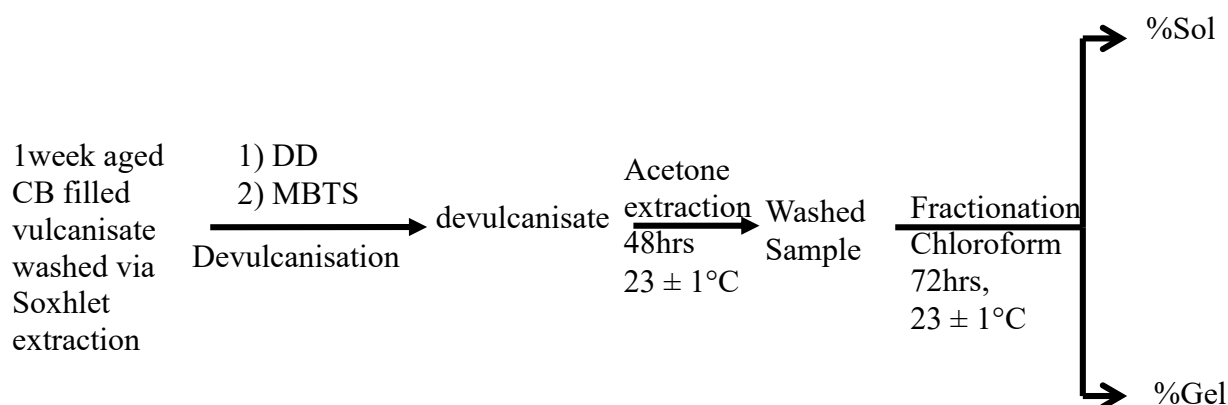


Figure 3.3: Soxhlet extraction setup

Samples were trimmed to dimensions of 20 mm x 30 mm (Length, L x Width, W). These were then weighed and loaded into the thimble for extraction. Extraction was run for 16 hours at 64.4°C. After extraction, samples were dried to constant weight in a forced air ventilation oven at 50 °C. The dried samples were then weighed to determine the amount of extracts.

3.2.2.4 Sol and gel fractionation



Scheme 3.3: Procedures followed to obtain gel and sol fractions.

The devulcanised rubber samples were extracted using 25 mL acetone for 48 hours at room temperature, refreshing the solvent daily, to get rid of excess devulcanising agent and soluble low molecular weights (*i.e.* by-products of devulcanisation). This was followed by drying to constant weight in a vacuum desiccator at ambient temperature. The residue was fractionated to separate sol and gel components using 50 mL chloroform solvent for 72 hours, refreshing the solvent daily at room temperature. The sol fraction is soluble in chloroform (and toluene, dichloromethane) and thus can be easily separated from the gel. Recovery of sol was done by evaporating the chloroform solvent in an RE300 rotary evaporator from Bibby Scientific Instruments.

The sol content could be determined directly because the soluble non-rubber constituents in the vulcanisates were removed by means of soxhlet extraction. In addition, the devulcanisates were washed in acetone to remove residual dAs prior to fractionation. Determination of the amount of sol component produced after devulcanisation was done using the equation 3.6;

$$\%Sol = \frac{m_{sample} - m_{gel}}{m_{sample}} \times 100\% \quad (3.6)$$

Where; m_{sample} is the mass of dried sample before devulcanisation and m_{gel} is the mass of dried gel sample. The gel component was determined according to equation 3.7;

$$\%Gel = \frac{m_{gel}}{m_{sample}} \times 100\% \quad (3.7)$$

3.2.3 Statistical methods

3.2.3.1 Characterisation

A sample is a subset and hence representative of its population ^[13]. Thus by looking at the sample characteristics one can get an idea of the population behaviour. The sample mean is an unbiased estimator of the true mean (population mean), but they are unlikely to be equal ^[13]. As a result, a confidence interval for the true mean can be determined from the standard error of the sample mean. The width of the confidence interval is dependent on; chosen confidence level (CI), size of the standard error (SD), sample size (n) and distribution of the sample mean (t-value). The probability of finding the true mean between the lower (LL) and upper limit (UL) is given by equation 3.8;

$$P(LL < \mu < UL) = 1 - \alpha \quad (3.8)$$

Where, $1 - \alpha$ is the confidence interval. If $1 - \alpha = 0.95$ then $\alpha = 0.05$. This means that for every sample mean (X) calculated, an uncertainty can be defined where there is 95 % confidence that the true average lies between the LL and UL. The two limits are described by equations 3.9 (LL) and 3.10 (UL);

$$\text{Lower limit} \quad X - \frac{SD \times t_{(1-\alpha)/2}^{n-1}}{\sqrt{n}} \quad (3.9)$$

$$\text{Upper limit} \quad X + \frac{SD \times t_{(1-\alpha)/2}^{n-1}}{\sqrt{n}} \quad (3.10)$$

Where; $t_{(1-\alpha)/2}^{n-1}$ is the t-value, determined by the sample size and confidence interval. The uncertainty is given by equation 3.11;

$$\text{uncertainty} = \frac{SD \times t_{(1-\alpha)/2}^{n-1}}{\sqrt{n}} \quad (3.11)$$

3.2.3.2 Isothermal devulcanisation

i) Procedure

Devulcanisation was conducted in a supercritical reactor (Fig. 3.4a) following a central composite design (Appendix, Table 3A.1). Optimisation following a central composite design (CCD) was done according to the experimental domain shown in Table 3.2. A CCD is a full factorial design improved by design points called “star points” at each of the factors in the design as well as at central points. The addition of these star points allows the estimation of curvature in the response surface and the central points allow the estimation of pure experimental error^[14]. Factors involved in the CCD used include; mass of devulcanising agent (dA), temperature and time. Pressure and amount of sample were kept constant at 80 bars and 1.00 g respectively. The pressure was kept constant (at 8 MPa) since increasing pressure to above 10 MPa at high temperatures (above 156 °C) resulted in failure of the silicon O-rings used to seal the reaction chamber lid. Figure 3.4b shows two silicon O-rings after two separate runs; one run was successful (intact O-ring) while the other failed (torn O-ring) due to excessive pressure at higher temperatures. The pressure chosen was a safe pressure at the working temperature range where supercritical conditions of CO₂ are attained. Percentage of devulcanisation was used as the response variable, calculated according to ASTM D6814 (equation 3.3).

Table 3.2: Experimental domain for multiple linear regression of isothermal devulcanisation.

Condition	Temperature/°C	dA/g	^d t _{isothermal} /minutes	^e t _{overall} /minutes
^a Min	140	0,05	30	49
^b Mid	160	0,075	60	80.5
^c Max	180	0,15	90	112

a = minimum, b = midpoint, c = maximum, d = time taken to run reaction from onset of set-point,

e = total reaction time (isothermal + temperature ramp)

The reactor was set up in a fume hood (of temperatures 23 ± 1 °C) for safety reasons. Before sample loading, the reaction chamber was cleaned using acetone, followed by drying using an air dryer. Samples were loaded together with dA and excess dry ice, followed by immediately

closing the reactor lid with the O-ring seal mounted on the lid (Fig. 3.4a). This was done with the reactor valve open, followed by shutting the valve once the lid was secured tightly. Dry ice was loaded in excess to allow for losses in CO₂ as it sublimates fast, and securing the lid would be impossible with the valve closed. So the valve was left open while securing the lid, so as to relieve pressure in the reaction chamber, thus allowing proper lid installation. Mass of CO₂ remaining in the reaction chamber was set to the required pressure by regulating pressure following the ideal gas equation at that temperature (chapter two).

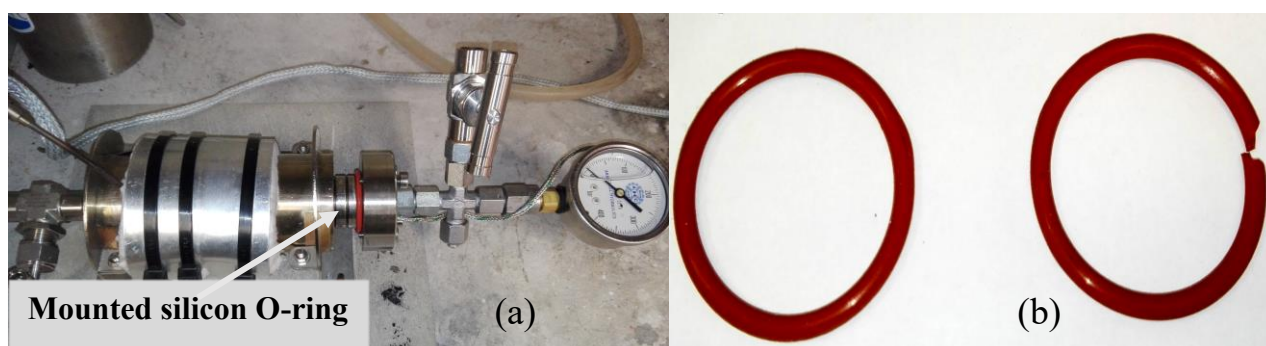


Figure 3.4: (a) Autoclave lid mounted with silicon O-ring (b) comparison between two O-rings after a successful run (intact) and unsuccessful run (torn). *Silicon O-rings were chosen since they seemed to work better than Viton or PTFE (polytetrafluoroethylene) O-rings tested.*

The autoclave was then heated up to the reaction temperature (set-point temperature) and the timer started once set-point was reached. The time taken to heat up the autoclave from room temperature (23 ± 1 °C) to set-point temperature was noted (*i.e.* the non-isothermal heating period), this was for correction samples at each and every set point. During the temperature ramp from 23 ± 1 °C to set-point temperature, devulcanisation events were already occurring and as such, correction samples were done to account for changes occurring prior to set-point temperature. After the reaction time the autoclave was immediately depressurised, lid opened, sample taken out and quenched in cold acetone.

ii) Empirical model formulation

Multiple linear regression was done in an attempt to come up with an empirical model for optimisation. An empirical model allows one to identify and predict statistical effects that process factors have on the response [13]. It enables optimisation of process variables to give highest % devulcanisation. Multiple linear regression analysis was done using the logistic model;

$$\hat{E} = \frac{100}{1 + e^{f(x)}} \quad (3.12)$$

Where; \hat{E} is the predicted devulcanisation efficiency according to the logistic model, $f(x)$ is the empirical model as determined by multiple regression [$f(x) = b_0 + b_1F_1 + b_2F_2 + \dots$] for factors F_i with coefficients b_i , and 100 is the maximum achievable percentage of devulcanisation. The response according to the logistic model then becomes;

$$f(x)' = \text{Ln} \left(\frac{100 - \hat{E}}{\hat{E}} \right) \quad (3.13)$$

Where, $f(x)'$ is the dependent variable according to the logistic model, for % devulcanisation values of \hat{E} . Optimisation using solver function on Microsoft excel was then done by setting values obtained from equation 3.13 as the objective. The null hypothesis (H_0) used for the multiple regression analysis states that, factors that have an insignificant effect on % devulcanisation have a regression coefficient (b_i) equivalent to zero, and is given by;

$H_0: b_i = 0$ (where, $i = 0, 1, 2, \dots$)

Therefore, for factors with p-values greater than 5 %, the null hypothesis is accepted and the concerned factor rejected. P-values give the probability of conditions being true. As an example; for the above null hypothesis, if the p-value for a certain factor is 0.7, then that means there is 70 % probability that the coefficient for that factor is equal to zero. Implying that the factor has no significant effect on the response and therefore can be rejected or removed from the empirical model. If however, the p-value is less than 5 % (considering 95 % confidence interval), then the factor has a significant effect on the response, thus the null hypothesis is rejected and the factor accepted into the empirical model.

3.2.4 Analysis

3.2.4.1 Cure characterisation

Three samples were randomly selected from the uncured rubber compound for shear mode isothermal testing using a dynamic Moving Die Rheometer (D-MDR 3000, otherwise known as the rubber process analyser, RPA 3000) from MonTech Rubber Testing Solutions. This was to determine the sample cure properties of induction, optimum cure time, changes in torque, and cure rate as shown in Table 3.3 (Results section). Sample cure characteristics were determined using the RPA-3000 in rheometer mode under test conditions of 150 °C temperature, 1.67 Hz frequency, 0.5 radians strain and 30 minutes test time. Two types of sample batch were tested, *i.e.* one with carbon black (CB) filler and the other without filler. Test sample weight was maintained between 8-9 g to avoid overflow of rubber test cavity.

3.2.4.2 Thermal decomposition of DD and MBTS

Thermal decomposition of DD and MBTS was analysed using high resolution TGA in an inert N₂ (g) atmosphere. Heating rate was set at 50 °C/min to 400 °C. Sample size was maintained within the range of 2-3 mg. Open platinum pans were also used for loading samples.

3.2.4.3 TGA analysis of vulcanisates and gel

Vulcanisate and gel samples were analysed for composition using high resolution TGA. Temperature was ramped at 50 °C min⁻¹ to 600 °C in N₂ (g) atmosphere. At 600 °C the gas was switched to O₂ (g) and heating done at a rate of 10 °C min⁻¹ to 700 °C. The amount of CB was determined after the O₂ (g) switch at 600 °C, followed by ash content determination after all the CB was burnt. Sample weight was maintained in the range of 2-5 mg. Open platinum pans were used for loading samples.

3.2.4.4 Crosslink density

Vulcanisate samples after soxhlet extraction were dried to constant weight in a forced air ventilation oven at 50 °C while gel samples were dried in a vacuum desiccator. After drying the samples were subjected to crosslink density tests at 23 ± 1 °C in the dark for 72 hours. Toluene was used as swelling solvent according to ASTM D6814. The rest of the dried soxhlet extracted vulcanisate samples were stored in a desiccator, and set aside for devulcanisation. The crosslink density of gel was done at least three times for determination of statistical variations. Procedure for crosslink density determination was done the same way as for vulcanisates.

3.3 RESULTS AND DISCUSSION

3.3.2 Characterisation of uncured rubber, cured rubber and devulcanising agents

3.3.2.1 Cure characteristics of uncured rubber samples

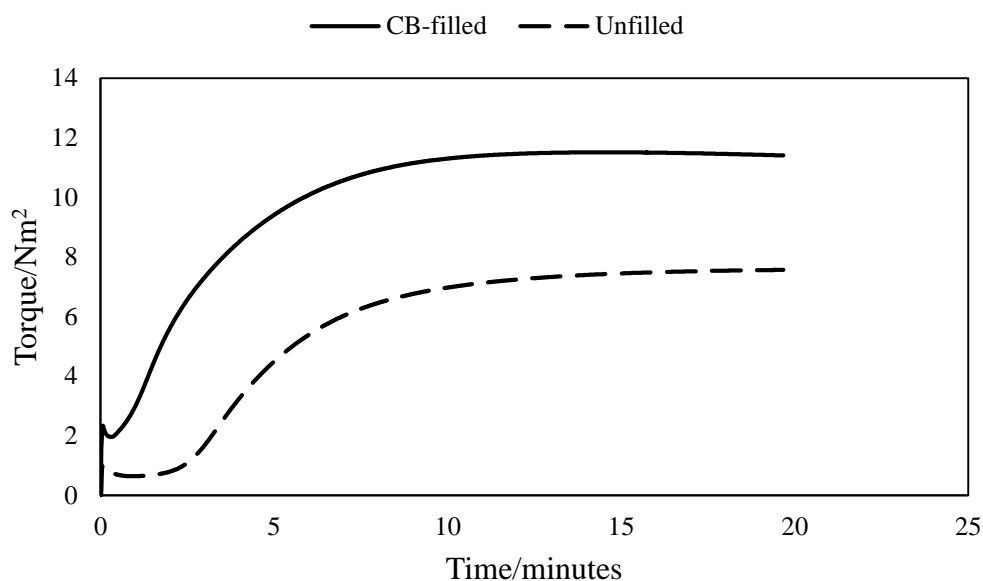


Figure 3.5: Cure curves obtained for carbon black (CB) filled vulcanisates.

The cure characteristics associated with the cure curves in Figure 3.5 are shown in Table 3.1.

Table 3.3: Cure characteristics for CB-filled and unfilled vulcanisates.

Sample	^a t _{induc} /mins	^b t ₉₀ /mins	^c S' _{min} /Nm ⁻²	S' _{max} /Nm ⁻²	ΔS'/Nm ⁻²	Cure rate
CB filled	2.18 ± 0.18	6.93 ± 0.34	2.31 ± 0.06	14.48 ± 0.19	12.17 ± 0.17	12.68 ± 0.19
Unfilled	8.65 ± 0.31	16.37 ± 1.68	1.07 ± 0.08	8.80 ± 0.55	7.73 ± 0.49	7.91 ± 0.55

a = induction time, b = time taken to achieve 90% of maximum cure, c = elastic torque (minimum, maximum and difference between min& max (ΔS'))

Sampling technique (four uncured samples) was used to check the degree of variability in the sample batch. This is important since the compound is a binary blend of two different rubber polymers (*i.e.* NR and SBR), and for accurate analysis the sample has to be uniform throughout. Rubber polymers have been shown to be unable to co-vulcanise^[15,16]. This is due to differences in solubility of curatives in the different rubber phases, which lead to migration of curatives from the rubber in which they are least soluble to the one they are most soluble in, resulting in variations in the degree of vulcanisation of the different phases. In addition, relative rates of vulcanisation of the two polymers would not be the same due to different reaction kinetics of the polymers. In view of this, a comparison of the cure characteristics of a number of samples from one batch should give an indication of variation in the degree of vulcanisation. This indirectly gives an indication of the degree of curative diffusion between different phases or how well distributed the different phases and or interphases are. If for example, the phases are poorly distributed and diffusion to preferred phase occurs, one would expect a marked difference in the cure properties upon sampling. Therefore small variations in the cure characteristics (induction time, t_{90} , $\Delta S'$, and cure rate (Table 3.3) would probably indicate small variations in the degree of vulcanisation throughout the different phases and interphases.

3.3.2.2 Analysis of cured rubber composition.

After curing, the rubber vulcanisates were aged for one week in a water bath at 70 °C. Figure 3.6 shows the changes in the crosslink densities (indicated by means of the reciprocal of the swell ratios^[17-19]) before and after ageing. The CB filled rubber samples appear to have higher crosslink densities than the unfilled vulcanisates due to the presence of CB^[20]. As the samples are aged, there is a general increase in the crosslink density, this is explained in more detail in the section dealing with hardening of vulcanisates (Section 4.3.5.1i). The aged vulcanisates were then subjected to soxhlet extraction prior to analysis. To substantiate this system of using variability in cure properties to check if there is good phase distribution, TGA scans were conducted on three randomly selected samples from the batch. This practice should show how consistent the batch is by looking at the relative composition of the mixed rubbers in the samples. The compound formulation was made up of 70 (NR):30 (SBR), thus the different regions of batch should observe a similar composition.

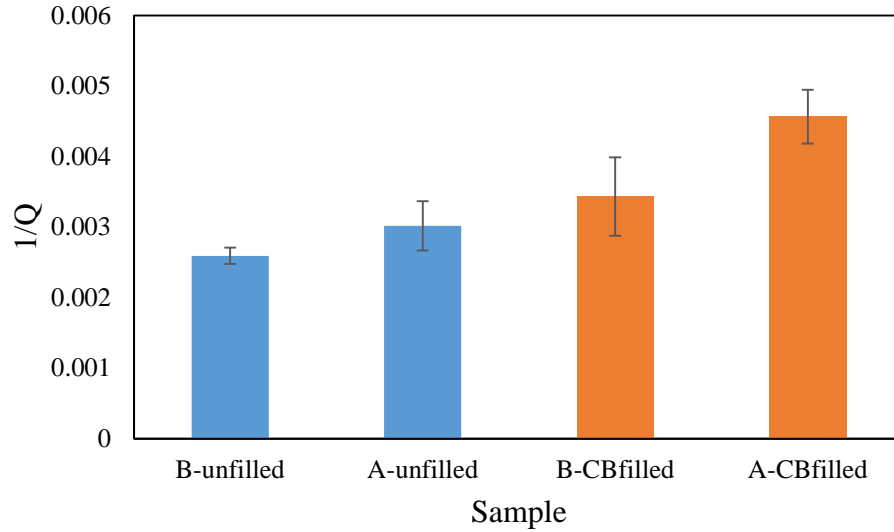


Figure 3.6: Reciprocal of swell ratios of vulcanisates before (B) and after (A) aging of unfilled and filled rubber samples.

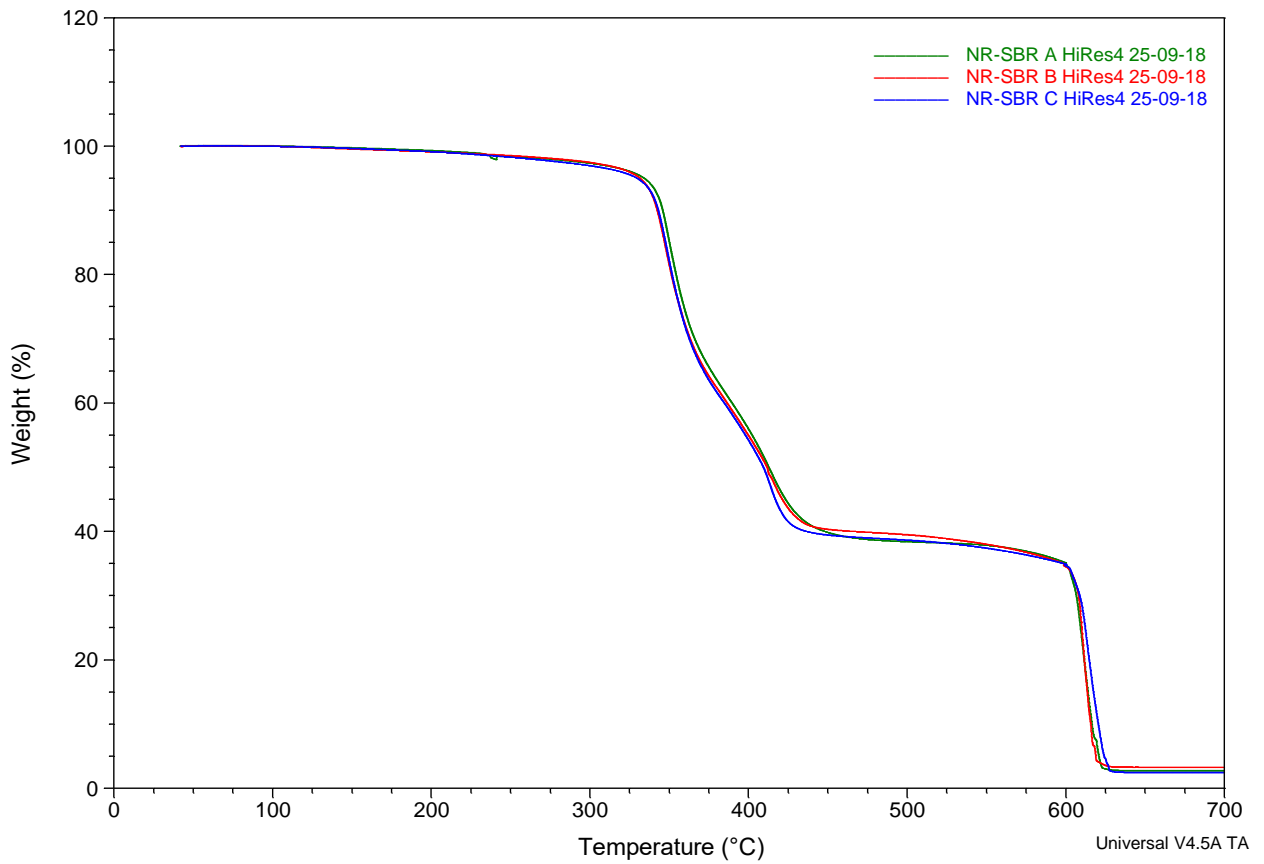


Figure 3.7a: Overlay of TGA curves of three randomly picked samples from cured compound.

The overlay of obtained TGA curves in Figure 3.7a for the three different samples (samples A, B and C) shows a high degree of similarity in the samples. The sample appears to be quite consistent in terms of composition, *i.e.* similar composition of NR:SBR ratio, CB and ash content. The three curves were subjected to the same treatment for quantification of weight changes during decomposition as shown on Figure 3.7b. The degree of uncertainty in composition was then determined.

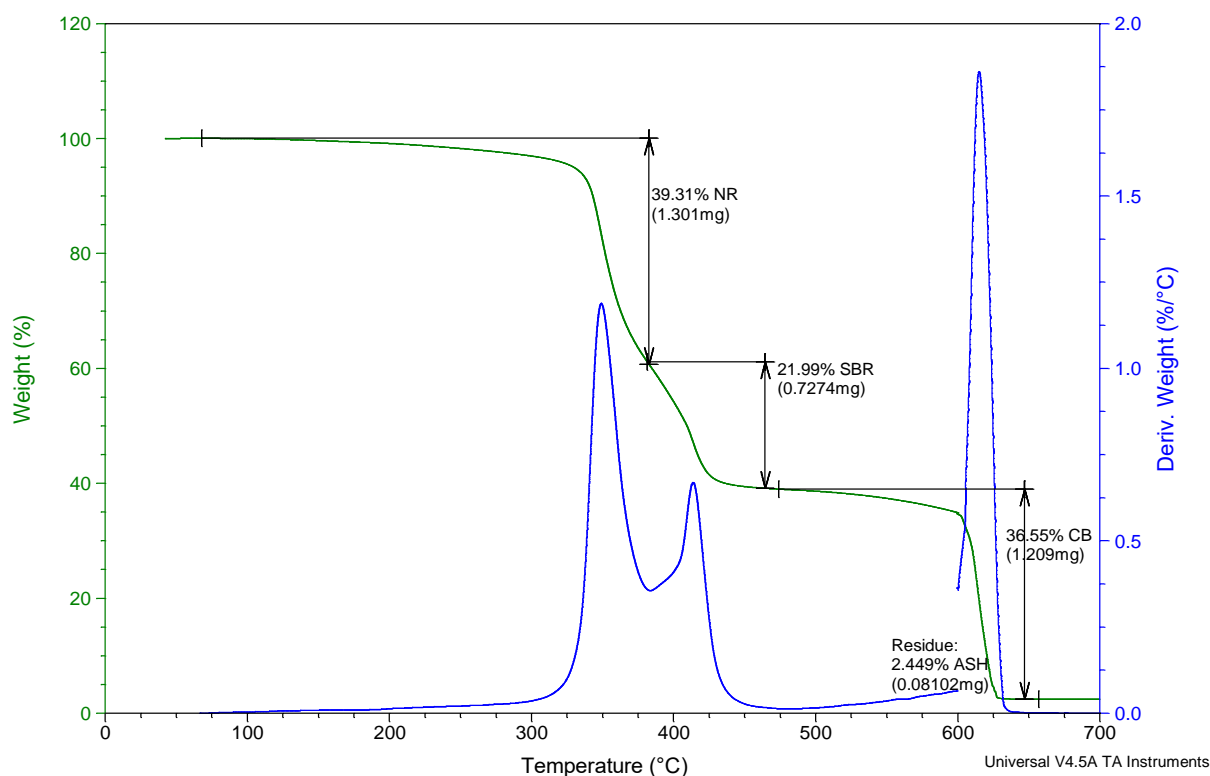


Figure 3.7b: TGA curve quantification of sample composition (sample C). *Note that the same was done for samples A and B, and the results are as shown on Table 3.4.*

Table 3.4: TGA percentage weight changes for identified sample composition.

Component	A	B	C	Average	Uncertainty
NR	38,13	37,36	39,31	38,27	± 2,44
SBR	22,71	22,44	21,99	22,38	± 0,90
CB	35,57	36,55	36,55	36,22	± 1,41
ASH	2,74	3,29	2,45	2,83	± 1,05

The average ratio of NR:SBR observed was 63.1:36.9 which was consistent for the three samples and lies within the acceptable weighing error (*i.e.* according to analytical scale, 10 %

variation in weight measurement is acceptable). The expected 70:30 ratio of NR:SBR was not obtained probably due to overlapping of NR/SBR degradation events. Figs. 3.7a and b show smooth points of inflection at the NR/SBR border around 350 °C.

The results on sample composition show consistency in the sample, both at macro scale (large samples used for testing in the RPA, ~ 9 g) and small-scale (small samples used for TGA, ~ 3 mg). The samples can therefore be used for devulcanisation studies with certainty that, if there are changes in the rubber polymer composition after devulcanisation, it is not due to vulcanised sample inconsistency but due to uneven polymer devulcanisation, *i.e.* if there is any.

It is important to also note that the TGA curves in Figure 3.7a show no signs of volatiles such as oils and other low molecular weights added in the rubber formulation. Volatiles can be defined as organic substances with boiling points of 250 °C or less at atmospheric pressure ^[21]. This is due to rubber treatment using soxhlet extraction (*i.e.* prior to devulcanisation). This procedure facilitates analysis of rubber samples since substances like oils might interfere with the devulcanisation process and cause side reactions that might retard the decrosslinking process. Oils are known to be good radical stabilisers due to their conjugated structures, thus they would likely compete with devulcanisation agents thereby affecting their efficiency ^[1, 22].

3.3.2.3 Thermal analysis of devulcanising agents

TGA analyses of DD and MBTS were conducted to check their decomposition characteristics. It should be noted that the decomposition as executed on the TGA does not in any way attempt to mimic reaction conditions the dAs are subjected to in the reactor, but may guide expectations as to the order of decomposition.

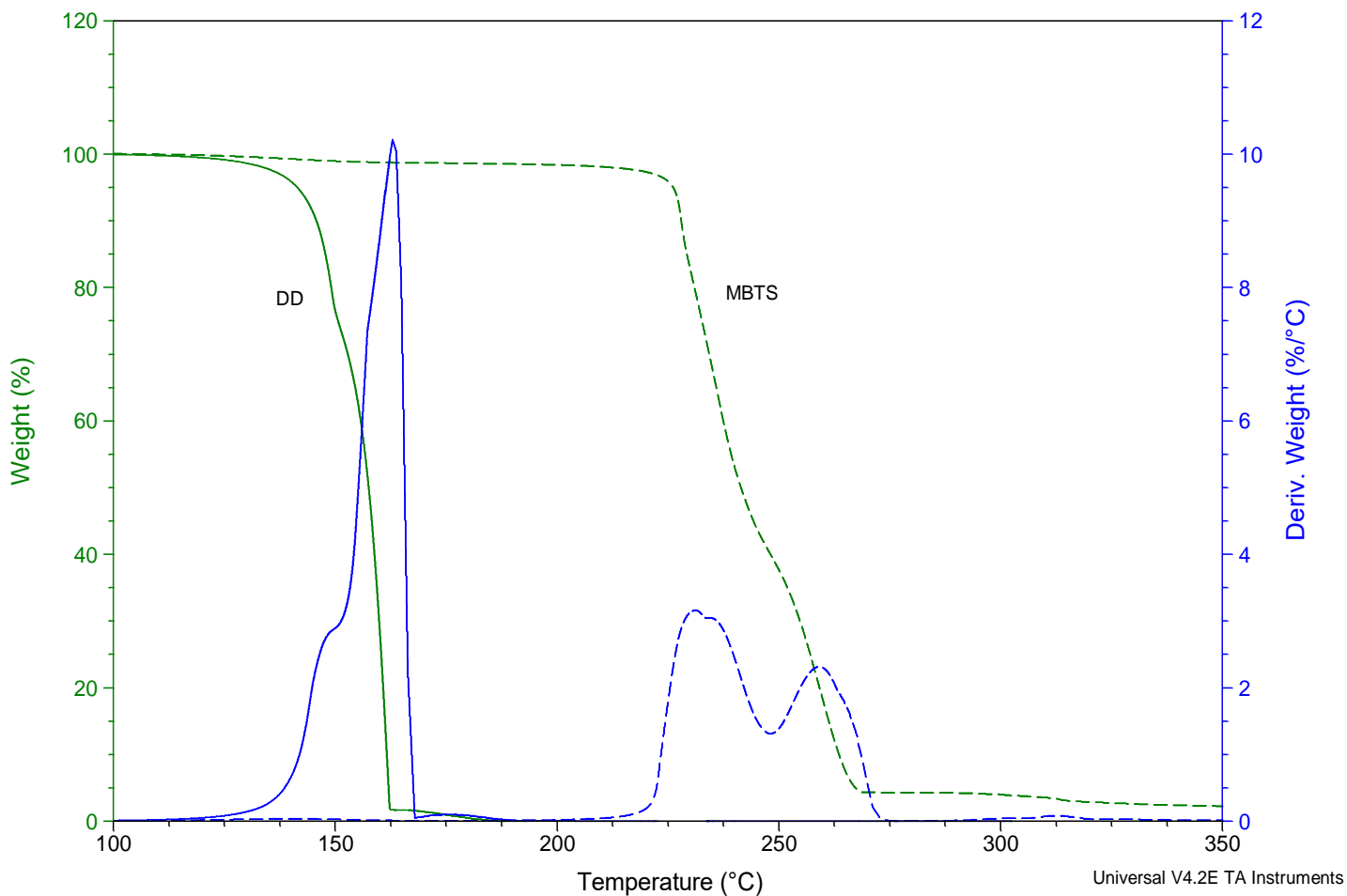
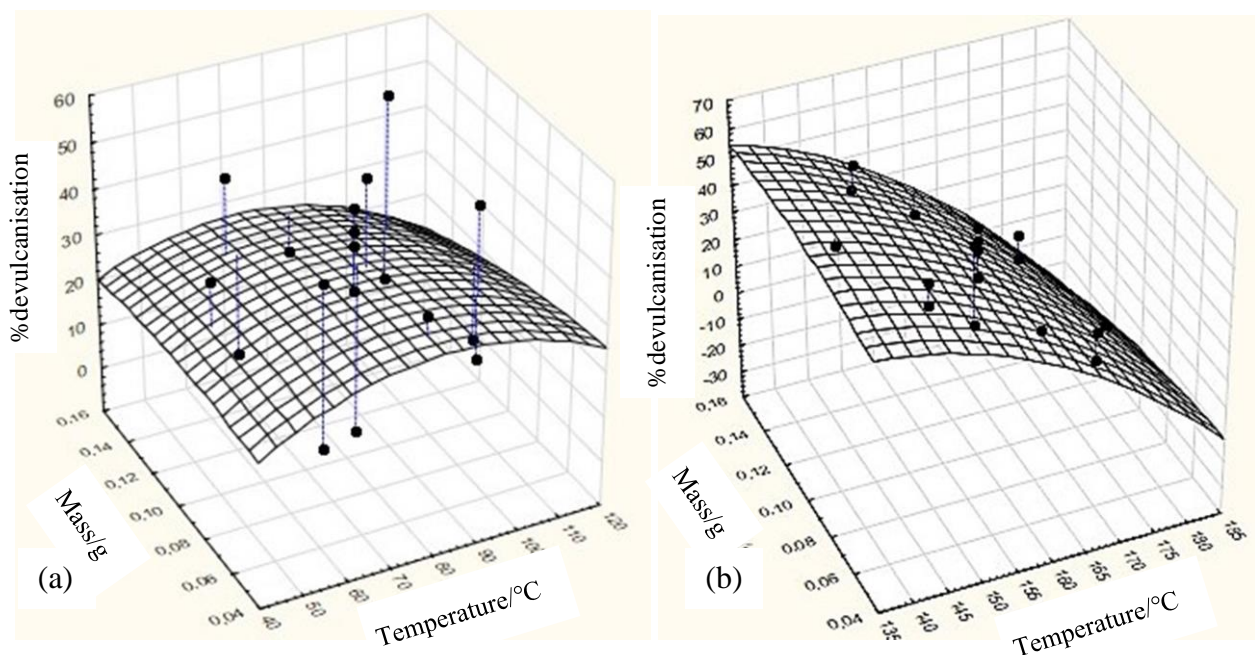


Figure 3.8: Thermal decomposition of DD and MBTS using high resolution TGA at 50 °C min⁻¹ in an inert N₂ (g) atmosphere.

DD is shown to decompose at around 125-162.5 °C, whereas MBTS decomposes at around 225-270 °C. The difference in decomposition temperatures is roughly by a factor of two, which shows the extent of ease of decomposition of DD compared to MBTS (the ease of decomposition becomes important in explaining relative devulcanisation rates in chapter four).

3.3.3 Optimisation of isothermal devulcanisation

Figure 3.9a shows that the amount of dA and time have no significant influence on the % devulcanisation. There is no defined trend that indicates an increase or decrease in the % devulcanisation with either factor. A trend is observed when mass is plotted with temperature against % devulcanisation. Figure 3.9b shows that increases in temperature lower the % devulcanisation. It seems that temperature favours devulcanisation only for a limited period, *i.e.* until further increase results in an antagonistic effect on % devulcanisation. The amount of dA does not seem to show an influence on % devulcanisation. This is observable from the zero gradient curve which shows neither increase nor decrease in % devulcanisation with changes in dA amount. Figure 3.9c emphasizes the antagonistic effect an increase in temperature has on % devulcanisation. A closer look at Figures. 3.9a and c shows that time has a slight degree of influence on % devulcanisation. The % devulcanisation slightly increases mid-way of the time range. This is shown by the slight curvature at the mid-section of the time axis.



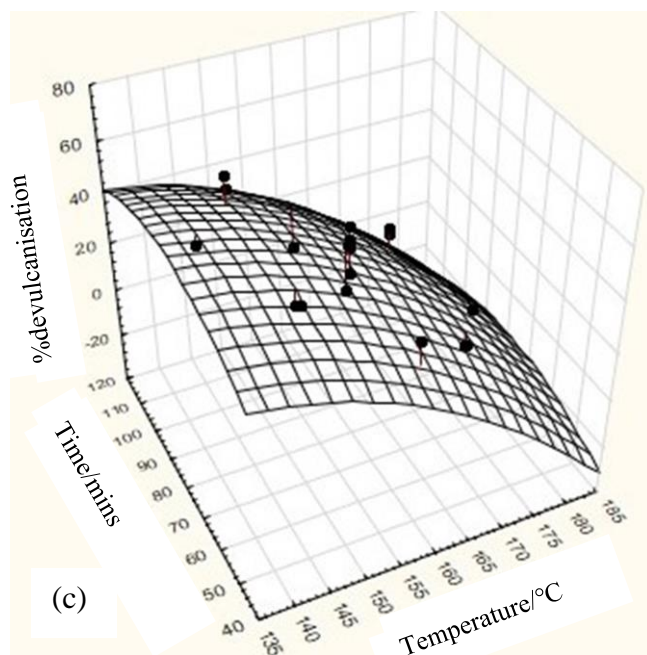


Figure 3.9: Surface plots for (a) dA vs. time (b) dA vs. temperature and (c) time vs. temperature against % devulcanisation.

Inasmuch as surface plots show individual and combined effects of factors on the response variable, multiple regression analysis gives statistical clarity. Tables 3.5a and b show outputs obtained after multiple linear regression of the observed experimental data shown in Figure 3.9. Multiple linear regression was done in an attempt to formulate an empirical model to describe the data.

Table 3.5a: Accepted final regression outputs for DD using logistic model ($H_0: b_i = 0$).

Parameter	Coefficients	Standard Error	t Stat	P-value	R ² -value
Intercept	$b_0 = 53.30$	25.27	2.11	0.05	0.81
^a T	$b_1 = -0.70$	0.32	-2.32	0.03	
T ²	$b_3 = 0.00$	0.00	2.56	0.02	

a = temperature (°C), b = 0.003

Table 3.5b: Rejected regression outputs for DD using logistic model ($H_0: b_i = 0$).

Parameter	Coefficients	Standard Error	t Stat	P-value
tm	0.04	0.29	0.15	0.8852
T ²	0.00	0.00	0.38	0.7171
Tm	0.16	0.39	0.41	0.6888
m ²	145.99	123.73	1.18	0.2654
^a m	3.45	3.51	0.98	0.3465
Tt	-0.00	0.00	-1.07	0.3043
^b t	-0.01	0.01	-1.24	0.2356

a =mass of DD, b = run time (minutes)

Regression yielded a good R-squared value of 0.81 (Appendix; Table A2.2b), meaning the model explains 81% of the data, which is good, but standard residuals values were too high, and all the points are outliers (*i.e.* $\pm 2 <$ residuals, Appendix; Table A2.2a). Continuous regression (Table 3.5a) could not give a good empirical model that explains the observed data. Nonetheless, it can be noted from the above results that temperature seems to play a significant role in the devulcanisation process compared to the other factors (p-value $<$ 0.05).

Table 3.6a: Accepted regression outputs for MBTS using logistic model ($H_0: b_i = 0$).

	Coefficients	Standard Error	t-Stat	P-value	R ² -value
Intercept	-1.99	1.01	-1.98	0.0654	0.27
T	0.01	0.01	2.40	0.0288	

Table 3.6b: Rejected regression outputs for MBTS using logistic model ($H_0: b_i = 0$).

	Coefficients	Standard Error	t Stat	P-value
Tt	0.00	0.00	0.03	0.97
tm	0.03	0.19	0.16	0.88
T ²	0.00	0.00	0.27	0.79
Tm	0.14	0.25	0.57	0.58
t ²	0.00	0.00	1.09	0.30
m ²	120.36	78.40	1.53	0.15
m	2.14	2.39	0.89	0.38
t	0.01	0.00	1.71	0.10

A similar trend was observed for MBTS devulcanisation, *i.e.* temperature seems to be the most significant factor affecting % devulcanisation. Continuous regression also resulted in a model that is unable to explain the obtained data. A very low R-squared value of 0.27 was obtained, meaning only 27 % of the data is explained by the obtained model (Appendix, Table A3.3b). Standard residuals show outliers for all data points except one (Appendix, Table A3.3a). Therefore the two models cannot be used for optimisation.

3.3.3.1 Possible reasons why no model could be found

The main reason why no empirical model could be established is high correlation existing between factors. One of the requirements for an empirical model to be obtained is that the factors should not be correlated [23]. Once there is correlation the model will not work. Correlation factors help in understanding the association of factors or their influence on each other. Correlation factors of time and temperature were determined using the “correl” function on Microsoft excel. A high correlation between temperature and time was observed because the temperature of the autoclave is dependent on the time taken to heat it up. Also, 100 % correlation of T and T² in Table 3.5a would result in the model not working. Another possible

reason is that the amount of devulcanisation agent used is in excess, so any changes in the amount of devulcanisation agent would not result in any observable differences in the % devulcanisation.

It is also important to note that the heating rate could be a confounding variable in the optimisation of isothermal devulcanisation. As such, it would be appropriate to include it as one of the factors for optimisation. The only challenge in this however, is that the heating rate only has an influence on devulcanisation during the non-isothermal stage of heating. Once the onset of the isothermal stage is reached the heating rate would now be zero. Therefore it was not included as one of the factors in the isothermal devulcanisation optimisation, which however, probably plays a significant role in devulcanisation.

3.3.3.2 Isothermal vs. non-isothermal devulcanisation

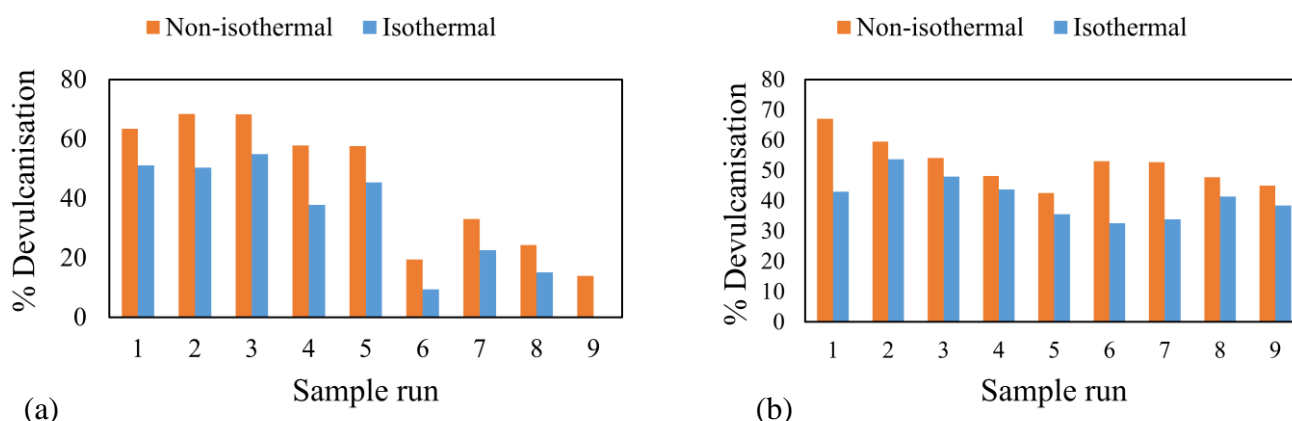


Figure 3.9: % Devulcanisation during temperature ramp (non-isothermal) vs. overall time period (isothermal) for (a) DD and (b) MBTS.

Comparison of % devulcanisation of correction samples and test samples during the non-isothermal and overall heating period (*i.e.* temperature ramp plus isothermal stage) respectively, indicates that during temperature ramp to set-point, a lot of devulcanisation events would have occurred. This is shown by a relatively higher degree of devulcanisation that occurs during the temperature ramp for all sample runs (Fig. 3.9). Since the main objective of this research is to achieve high degree of devulcanisation, focus was therefore shifted to look at processes occurring during the non-isothermal stage.

3.4 SUMMARY OF FINDINGS

- The vulcanisates subjected to devulcanisation were consistent in NR/SBR composition as well as crosslink densities.
- Thermal characterisation of DD and MBTS using TGA showed early decomposition temperature range for DD (125-162.5 °C) compared to MBTS (225-270 °C).
- ScCO₂ was effective as a medium for the devulcanisation of CB filled vulcanisates using DD and MBTS.
- The amount of dA and pressure were found to have no significant effect on the % devulcanisation. However, temperature changes were found to have a huge effect on the % devulcanisation during the isothermal stage.
- No viable empirical model could be established to describe the observed results.
- The % devulcanisation during the non-isothermal period was found to be higher than that of the isothermal period.

3.5 REFERENCES

1. Adhikari, B., D. De, and S. Maiti, *Progress in Polymer Science*, 2000. **25**: p. 909-948.
2. Myrhe, M., *Rubber Recycling; Devulcanisation by Chemical and Thermomechanical Means*. ed. S.K. De, A.I. Isayev, and K. Khait. 2005: Taylor and Francis Group.
3. Horikx, M.M., *Journal of Polymer Science*, 1956. **19**: p. 445-454.
4. Kojima, M., et al., *Rubber Chemistry and Technology*, 2003. **76**: p. 957-68.
5. Onouchi, Y., et al., *International Polymer Science and Technology*, 1982. **55**: p. 58-62.
6. Sripornsawat, B., et al., *European Polymer Journal*, 2016. **85**: p. 279-297.
7. Mangili, I., et al., *Polymer Degradation and Stability*, 2014. **102**: p. 15-24.
8. Liu, Z., et al., *Polymer Degradation and Stability*, 2015. **119**: p. 198-207.
9. Grobler, J.H.A. and W.J. McGill, *Journal of Polymer Science*, 1994. **32**(2).
10. Cunneen, J.I. and R.M. Russell, *Journal of the Rubber Research Institute of Malaya*, 1969. **22**: p. 300.
11. Johnson, B.L. and F.K. Cameron, *Industrial and Engineering Chemistry*, 1933. **25**(10): p. 1151-1152.
12. Bauer, D.R., J.M. Baldwin, and K.R. Ellwood, *Polymer Degradation and Stability*, 2007. **92**: p. 110-117.
13. Bosma, C., *Introduction to data analysis*. 2017, Nelson Mandela University. p. 1-49.
14. Bosma, C., *Experimental design: Central composite designs*. 2017, Nelson Mandela University. p. 1-33.
15. Huson, M.G., W.J. McGill, and R.D. Wigget, *Plastics and Rubber Processing Applications*, 1985. **5**(4): p. 319-324.
16. Huson, M.G., W.J. McGill, and P.J. Swart, *Journal of Polymer Science*, 1984. **22**(3): p. 143-148.
17. Choi, S.S., *Journal of Applied Polymer Science*, 2000. **75**: p. 1378-1384.
18. Choi, S.S., *Journal of Applied Polymer Science*, 2002. **83**: p. 2609-2616.
19. Parks, C.R. and R.J. Brown, *Rubber Chemistry and Technology*, 1974. **49**: p. 233-236.
20. Kojima, M., et al., *Journal of Applied Polymer Science*, 2005. **95**: p. 137-143.
21. Parliament, E., *Directive 2004/42/CE of the European Parliament and of the Council of 21 April 2004 on the limitations of emissions of volatile organic compounds due to*

the use of organic solvents in certain paints, varnishes and vehicle refinishing products and amending Directive 1999/13/EC

2004.

22. Myrhe, M., et al., *Rubber Chemistry and Technology*, 2012. **85**(3): p. 408-449.

23. Marion, G. and D. Lawson, *An introduction to mathematical modelling*, in *Bioinformatics and Statistics Scotland*. 2008. p. 1-31.

3.6 APPENDIX

Experimental design followed for experimental domain shown in Table 3.2;

Table 3A.1: Central composite design followed for optimisation of isothermal devulcanisation.

MBTS				DD				
Run	T/°C	^a t/mins	^b m(dA)	Run	T/°C	t/mins	^c m _R	m(dA)
1	160	60,0	0,10	21	160	60,0	1,0	0,10
2	172	77,8	0,13	22	172	77,8	1,3	0,13
3	172	42,2	0,07	23	172	42,2	0,7	0,07
4	160	90,0	0,10	24	160	90,0	1,0	0,10
5	148	42,2	0,13	25	148	42,2	1,3	0,13
6	160	60,0	0,10	26	160	60,0	1,0	0,10
7	148	77,8	0,07	27	148	77,8	0,7	0,07
8	148	42,2	0,07	28	148	42,2	0,7	0,07
9	160	60,0	0,10	29	160	60,0	1,0	0,10
10	160	60,0	0,10	30	160	60,0	1,0	0,10
11	172	42,2	0,13	31	172	42,2	1,3	0,13
12	180	60,0	0,10	32	180	60,0	1,0	0,10
13	172	77,8	0,07	33	172	77,8	0,7	0,07
14	160	60,0	0,15	34	160	60,0	1,5	0,15
15	140	60,0	0,10	35	140	60,0	1,0	0,10
16	160	30,0	0,10	36	160	30,0	1,0	0,10
17	148	77,8	0,13	37	148	77,8	1,3	0,13
18	160	60,0	0,10	38	160	60,0	1,0	0,10
19	160	60,0	0,05	39	160	60,0	0,5	0,05
20	160	60,0	0,10	40	160	60,0	1,0	0,10

a = time in minutes, b = mass of devulcanising agent, c = mass of rubber sample, d = % devulcanisation

Table 3A.2a: Final parameters after multiple linear regression of DD isothermal devulcanisation ($H_0: b_i = 0$)

Run	T	T²	%Efficiency	Log(\hat{E})	Pred.	Std Residuals
1	140	19600	51.10284	-0.04412	49.62228	3.658363
2	148	21904	45.1825	0.1933	48.93944	-9.28321
3	148	21904	42.10711	0.318378	48.93944	-16.8823
4	148	21904	50.32156	-0.01286	48.93944	3.41513
5	148	21904	54.92101	-0.19748	48.93944	14.78012
6	160	25600	36.25412	0.564352	33.04638	7.92615
7	160	25600	27.62609	0.963085	33.04638	-13.3932
8	160	25600	45.39989	0.184526	33.04638	30.52485
9	160	25600	40.60199	0.380443	33.04638	18.66952
10	160	25600	37.49602	0.510995	33.04638	10.99483
11	160	25600	18.95619	1.452859	33.04638	-34.8161
12	160	25600	27.07594	0.990773	33.04638	-14.7526
13	160	25600	37.83931	0.496374	33.04638	11.84307
14	172	29584	6.980504	2.589688	10.74589	-9.30407
15	172	29584	6.750789	2.625616	10.74589	-9.87168
16	172	29584	15.14399	1.723352	10.74589	10.86747
17	172	29584	17.33448	1.562105	10.74589	16.28005
18	180	32400	-5.75678	#NUM!	3.01	-21.6622

Table 3A.2b: Summary outputs

<i>Regression Statistics</i>	
Multiple R	0.901
R Square	0.811802
Adjusted R Square	0.784916
Standard Error	0.404703
Observations	17

Table 3A.3a: Final parameters after multiple linear regression of MBTS isothermal devulcanisation ($H_0: b_i = 0$)

Run	Temp	%Devulcanisation	Log(\hat{E})	Predicted	Std residuals
1	140	42.90467	0.285742	46.98407	-14.6623
2	148	53.67801	-0.14739	43.98373	34.84344
3	148	47.92114	0.083202	43.98373	14.15196
4	148	42.61452	0.297596	43.98373	-4.92122
5	148	39.45742	0.428125	43.98373	-16.2685
6	160	38.14628	0.483344	39.57081	-5.12007
7	160	32.5036	0.730724	39.57081	-25.4012
8	160	54.72324	-0.18949	39.57081	54.46123
9	160	41.8556	0.328704	39.57081	8.212025
10	160	40.15959	0.39882	39.57081	2.116186
11	160	38.21858	0.480281	39.57081	-4.86022
12	160	35.49	0.597569	39.57081	-14.6673
13	160	36.37267	0.559225	39.57081	-11.4948
14	172	41.37193	0.348611	35.32147	21.74672
15	172	33.84639	0.670147	35.32147	-5.30178
16	172	35.04058	0.617256	35.32147	-1.00958
17	172	23.5656	1.176645	35.32147	-42.2532
18	180	38.42047	0.471739	32.60782	20.89199

Table 3A.3b: Summary outputs for MBTS isothermal devulcanisation

<i>Regression Statistics</i>	
Multiple R	0.514903
R Square	0.265125
Adjusted R Square	0.219196
Standard Error	0.278224
Observations	18

Table 3A.4: Isothermal vs. non-isothermal devulcanisation using DD.

Run	T	t_{ind}	t_{run}	mdA	%E_{ramp}	%E_{overall}	%Sol_{ramp}	%Sol_{iso}
1	140	24,4	84,4	0,1011	63,5	51,1	11,0	35,8
2	148	22,9	100,7	0,0715	68,4	50,3	9,2	24,5
3	148	22,9	100,7	0,1320	68,3	54,9	16,3	46,0
4	160	21,8	81,4	0,0516	57,8	37,8	23,3	31,9
5	160	19,3	81,4	0,1010	57,6	45,4	26,5	31,7
6	160	23,0	83,0	0,1506	19,5	9,4	37,8	45,5
7	172	22,6	100,4	0,0721	33,0	22,5	35,9	34,1
8	172	22,1	99,9	0,1319	24,3	15,1	47,6	40,1
9	180	23,1	83,1	0,1090	13,9	0,0	47,1	37,6

Table 3A.5: Isothermal vs. non-isothermal devulcanisation using MBTS.

Run	T	t_{ind}	t_{run}	mdA	%E_{ramp}	%E_{overall}	%Sol_{ramp}	%Sol_{iso}
1	140	19,65	79,65	0,1009	67,0	42,9	5,5	5,0
2	148	20,47	63,81	0,0728	59,5	53,7	10,8	9,2
3	148	22,75	63,81	0,1326	54,0	47,9	4,4	5,3
4	160	20,62	80,62	0,1042	48,2	43,7	16,0	11,9
5	160	20,62	80,62	0,1500	42,6	35,5	5,1	11,1
6	160	20,62	82	0,0541	53,0	32,5	10,3	16,0
7	172	21,23	63,43	0,1300	52,7	33,8	21,7	24,4
8	172	21,23	63,43	0,0723	47,7	41,4	20,4	18,7
9	180	23,1	83,1	0,1043	45,0	38,4	21,4	15,6

3.3.3.3 Optimisation of non-isothermal devulcanisation

Table 3A.6: Final parameters after multiple regression of DD devulcanisation data ($H_0: b_i = 0$)

Run	t/min	T/°C	R	^a tT	^a TR	%D	f(x)'	\hat{E}	^b Std res
1	10	154	6,66	1540	1026,41	4,84	2,98	4,52	2,39
2	10	156	6,66	1560	1039,74	5,85	2,78	5,25	4,53
3	10	155	6,66	1550	1033,07	4,07	3,16	4,87	-5,77
4	5	98	12,24	490	1199,37	70,63	-0,88	71,19	-4,21
5	5	103	12,24	515	1260,57	74,22	-1,05	75,79	-11,77
6	5	104	12,24	520	1272,80	78,58	-1,30	76,64	14,49
7	3	82	14,92	246	1223,22	35,81	0,58	35,98	-1,30
8	3	83	14,92	249	1238,14	35,69	0,59	37,80	-15,83
9	3	82	14,92	246	1223,22	38,27	0,48	35,98	17,20
10	7	126	9,82	882	1236,88	54,67	-0,19	56,11	-10,77
11	7	126	9,82	882	1236,88	55,07	-0,20	56,11	-7,78
12	7	124	9,82	868	1217,24	56,54	-0,26	54,08	18,52

a = interaction of factors, b = standardised residuals

Table 3A.7: Final parameters after multiple regression of MBTS devulcanisation data ($H_0: b_i = 0$)

t	T/°C	R	T²	tT	tR	%D	Log(\hat{E})	Pred.	Std. residual
5	98	11,728	9604	490	58,64	56,89182	-0,27744	62,8062	-22,2568
5	97	11,728	9409	485	58,64	66,17376	-0,67105	60,39549	21,74455
5	101	11,728	10201	505	58,64	67,51672	-0,73165	68,59224	-4,04733
10	148	6,636	21904	1480	66,36	54,3451	-0,17424	54,32347	0,081397
10	146	6,636	21316	1460	66,36	50,40566	-0,01623	58,96862	-32,2238
10	147	6,636	21609	1470	66,36	51,68455	-0,06741	56,76012	-19,1002
15	162	3,044	26244	2430	45,66	48,57907	0,056853	47,44842	4,254817
15	163	3,044	26569	2445	45,66	49,98485	0,000606	47,05487	11,02597
15	170	3,044	28900	2550	45,66	51,33076	-0,05324	38,80994	47,11787
20	178	0,952	31684	3560	19,04	42,18963	0,314994	49,76597	-28,511
20	177	0,952	31329	3540	19,04	43,55646	0,259183	48,0889	-17,0563
20	177	0,952	31329	3540	19,04	49,34396	0,026243	48,0889	4,722983
25	179	0,36	32041	4475	9	42,81651	0,289341	38,65377	15,66506
25	179	0,36	32041	4475	9	42,80951	0,289627	38,65377	15,63871
25	179	0,36	32041	4475	9	33,96063	0,665049	38,65377	-17,6611
30	180	1,268	32400	5400	38,04	39,88958	0,410068	33,83648	22,77879
30	180	1,268	32400	5400	38,04	29,08802	0,891113	33,83648	-17,8692
30	180	1,268	32400	5400	38,04	32,58058	0,727217	33,83648	-4,72614
3	84	14,1848	7056	252	42,5544	40,21494	0,396517	40,12082	0,354195
3	86	14,1848	7396	258	42,5544	37,26116	0,521029	46,06907	-33,1456
3	84	14,1848	7056	252	42,5544	38,3828	0,473332	40,12082	-6,54045
4	98	12,9264	9604	392	51,7056	72,14074	-0,95145	67,53111	17,34681
4	96	12,9264	9216	384	51,7056	69,04257	-0,80211	64,61357	16,66706
4	97	12,9264	9409	388	51,7056	71,5761	-0,92353	66,17833	20,31266

CHAPTER 4: OPTIMISATION OF NON-ISOTHERMAL DEVULCANISATION

4.1 INTRODUCTION

The results from chapter three showed that there are competing processes during devulcanisation that result in a net decrease in the degree of devulcanisation as the reaction progresses. Devulcanisation reactions left to run for long periods of time *e.g.* + 60 minutes, result in the competing processes gaining prominence compared to decrosslinking processes. This was evidenced by relatively higher % devulcanisation at the end of the non-isothermal stage compared to that of the isothermal stage. Optimisation of devulcanisation conditions during the non-isothermal stage, *i.e.* from 0 to 30 minutes, should therefore yield an optimum characterised by an intense reduction of crosslinks with minimal chain degradation at shorter times. This would therefore translate to reduction in costs involved in devulcanisation through time and energy efficiency, as well as less intense working conditions (*i.e.* lower temperatures and pressures). Consequently, this would result in increased longevity of devulcanisation equipment and most importantly, high quality devulcanised rubber with minimum crosslinks and long chain lengths. Based on findings from chapter three, this chapter seeks to answer a number of questions pertaining to devulcanisation. These include;

- Can % devulcanisation that results in good quality devulcanised rubber be obtained in the non-isothermal region?
- What is the correlation between time, temperature, heating rate, pressure and amount of dA, with % devulcanisation during the non-isothermal period?
- To what extent can time and energy be saved by optimising conditions during the non-isothermal stage?

This chapter attempted to answer these questions by means of multiple linear regression analyses of devulcanisation conditions during the non-isothermal region. This was done in an attempt to formulate an empirical model for optimisation purposes, failure of which would result in single factor analyses of devulcanisation conditions at the non-isothermal stage.

4.2 EXPERIMENTAL

4.2.1 Materials and general procedure

The materials used as well as the general procedure followed in this chapter was the same as that in chapter three.

4.2.1.1 Non-isothermal devulcanisation

Temperature and % devulcanisation were recorded after every 5 minutes interval for 30 minutes at 180 and 140 °C set-point temperatures. The time range was selected by considering the time taken to reach maximum set-point (see chapter two). The onset of reaction monitoring was chosen to be 50 °C. This temperature was chosen to be the start off temperature by considering that the dry ice turns supercritical at minimum conditions of 32 °C and 74 bar. Therefore 50 °C was a safe starting temperature, since not much (or zero) reactions would have taken place and almost all the dry ice would have sublimed. Note that the pressure was kept constant at 80 bar throughout the whole run. Quantitative (% devulcanisation, % sol and % gel) and qualitative (identity of devulcanisation by-product) analyses were done over the time range.

4.2.1.2 Single factor analysis

i) Pressure

During the isothermal studies in chapter three, the pressure was maintained at 80 bar due to failure of silicon O-rings at high pressure (> 80 bar) and temperature (>156 °C). However, after time-temperature optimisation, it was found that the optimum temperatures needed were not too high, hence the silicon O-rings could withstand the higher pressures (> 80 bar). The effect of changes in pressure was investigated by comparing the % devulcanisation at 100 bar and that at 80 bar, under optimum conditions of time and temperature. The amounts of DD and MBTS used were kept the same as those used for optimisation of time and temperature.

ii) Amount of dA used

The amount of dA was varied in the order; 1 %, 5 % and 10 % of the mass of rubber sample (e.g. 1 % of 1.00 g rubber sample = 0.01 g dA). Note that 10 % dA is the amount used for optimisation reactions, and so it serves as a reference here. The mass of rubber sample used maintained at 1.00 g for all runs.

iii) Effect of CB content on % devulcanisation

Compounding of unfilled vulcanisates was done according to the formulation shown in Table 3.1 (chapter three), but in the absence of the CB. Devulcanisation of unfilled samples was conducted at optimum conditions for both dAs, and were compared to CB filled samples under similar conditions. The CB content is inversely proportional to the swell ratio at constant crosslink density ^[1-3]. Therefore, the effect of CB on swell ratio has to be considered when comparing filled and unfilled vulcanisates. The use of % devulcanisation as the response variable allows expression of changes in the crosslink density with reference to the original crosslink density. As a result the effects of CB on swelling are then cancelled out mathematically (chapter three, equation 3.3).

4.2.2 Statistical Methods

4.2.2.1 Empirical model formulation

Multiple linear regression analysis of the non-isothermal heating region was executed by looking into the effects of temperature (T), time (t) and instantaneous heating rate (R) on % devulcanisation (% D). The amount of dA and pressure were kept constant at 0.10 g and 80 bars respectively for 1.00 g rubber samples.

Table 4.1: Experimental domain for multiple linear regression of non-isothermal region

	Time/minutes	Set-point/°C	Temperature/°C	Rate/°C min ⁻¹
Min	5	140	50	0
Max	30	180	180	14.49

The extreme set-points from the CCD (140 °C and 180 °C) were used to analyse the non-isothermal region. These were chosen since they give the lowest and highest heating rates, and also because they cover the whole range of temperatures in the CCD. The empirical model was formulated using the logistic model as in chapter three. The same hypothesis used for multiple linear regression in chapter three was used in this chapter, *i.e.* $H_0: b_i = 0$

4.2.2.2 Statistical analysis

i) Sample t-Tests

- **Selection of optimum set-point temperature for DD.**

Sample t-Test assuming equal variances was executed to determine if there were any differences in the observed % devulcanisation at 140 and 180 °C set-points, hence be able to choose the set-point that gives optimum conditions. The null hypothesis (H_0) for the t-test states that the averages of the maximum % devulcanisation at 180 and 140 °C set-points are equal within measurement error, and is given by;

$$H_0: \mu_{180} = \mu_{140}$$

Where μ_{180} and μ_{140} are the average % devulcanisation at 180 °C and 140 °C set-points respectively.

- **Selection of optimum set-point temperature for MBTS.**

The same t-Test analysis executed on DD was done on MBTS devulcanisation data.

- **Effect of pressure changes on % devulcanisation**

Sample t-test assuming equal variances was done for both dAs at 80 and 100 bar pressure. The null hypothesis used states that the average of the maximum % devulcanisation obtained at 80 bar pressure is equal to the average of the maximum % devulcanisation at 100 bar pressure, and is given by;

$$H_0: \mu_{80} = \mu_{100}$$

Where μ_{80} and μ_{100} are the average maximum % devulcanisation at 80 and 100 bars respectively.

- **Effect of CB on % devulcanisation**

Sample t-tests assuming equal variables were conducted to determine variations in the % devulcanisation due to the presence of CB filler. This would allow conclusive determination of filler effect on % devulcanisation. The null hypothesis used states that the average of maximum % devulcanisation obtained using unfilled sample is equal to that obtained using CB filled sample within measurement error. This is represented by;

$$H_0: \mu_{\text{unfilled}} = \mu_{\text{filled}}$$

Where μ_{unfilled} and μ_{filled} are the average maximum % devulcanisation for unfilled and filled vulcanisates respectively.

ii) Single factor analysis of variance (ANOVA)

- **Amount of dA**

Single factor analysis of variance (ANOVA) was used to compare the averages of the three different samples at different dA loadings. In this way any present variations within and between samples can be identified. Single factor ANOVA is the same as the two sample t-test, except for that in single factor ANOVA, three or more samples are compared at the same time [4]. In place of the t-value, the F-value is used for single factor ANOVA. The F-value follows the F-distribution and is described by the equation [4];

$$F = \frac{\frac{SST - SSE}{2}}{\frac{SSE}{n - 3}} \quad (4.1)$$

Where; (SST-SSE) is the source of variation between groups and SSE is the source of variation within groups. If F-statistic is less than F-critical, then the null hypothesis is accepted, *i.e.* there is no significant difference in the means of the samples. The null hypothesis used states that the average maximum % devulcanisation for 1 % loading of dA is equal to that of the 5 % as well as the 10 %. This is represented by;

$$H_0: \mu_{1\%} = \mu_{5\%} = \mu_{10\%},$$

Where; $\mu_{i\%}$ are the average maximum % devulcanisation observed at 1, 5 and 10 % dA loadings.

4.2.2.3 Instantaneous heating rate determination

The instantaneous heating rate for DD and MBTS devulcanisation was determined by differentiation of the best polynomial fit (based on the R-squared value) of the heating curve. The first derivate function obtained would then give the instantaneous heating rate at any time (x). For example, for DD the heating curve function is given by equation 4.2;

$$y = 0.0099x^3 - 0.7588x^2 + 18.776x + 30.404 \quad (4.2)$$

So the gradient function (*i.e.* instantaneous heating rate function) becomes;

$$\frac{dy}{dx} = 3(0,0099)x^2 - 2(0,7588)x + 18,776 \quad (4.3)$$

Where; x is the time in minutes, recorded from the onset of 50 °C, and dy/dx is the instantaneous heating rate. Figures 4.1a and b illustrate how the instantaneous heating rate functions were obtained for both DD and MBTS.

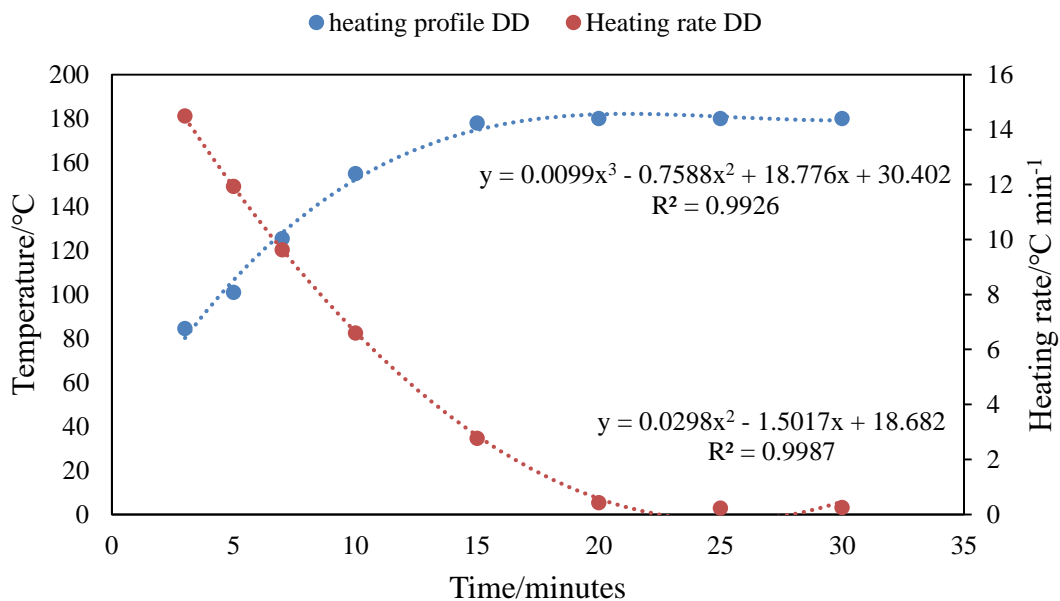


Figure 4.1a: Overlay of heating profile and instantaneous heating rate for DD devulcanisation at 180 °C set-point.

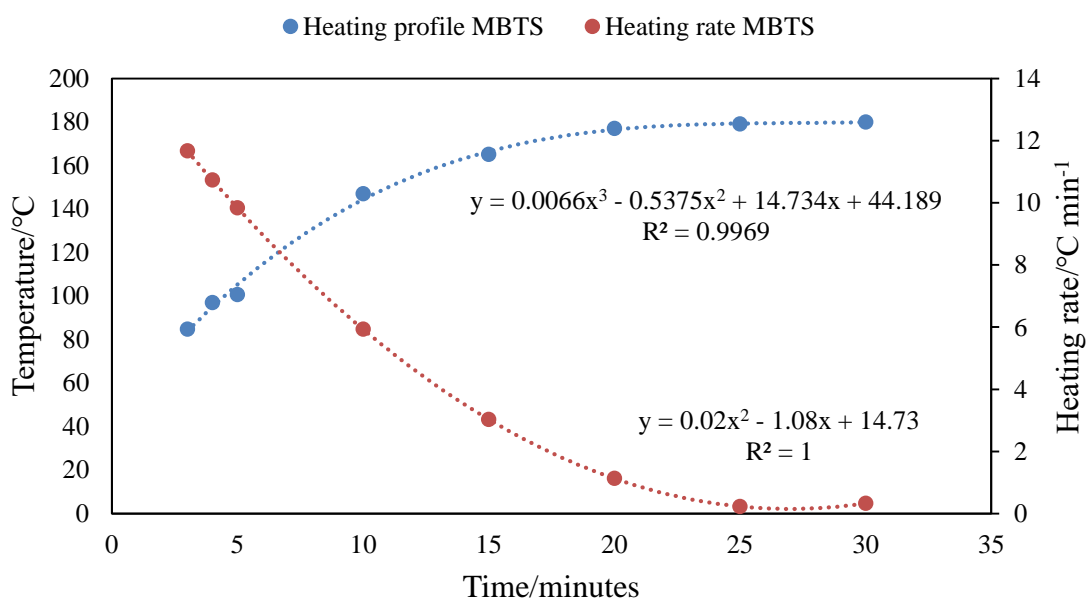


Figure 4.1b: Overlay of heating profile and instantaneous heating rate for MBTS devulcanisation at 180 °C set-point.

4.2.3 Analysis

4.2.3.1 Molecular weight determination

Polymer chain distribution is presented in terms of the average molecular weight which is calculated from the molecular weights of individual chains in the polymer sample ^[5]. The average molecular weight of polymers can be expressed in terms of the; number average molecular weight (M_n), weight average molecular weight (M_w), sedimentation average molecular weight (M_z), and viscosity average molecular weight (M_v) ^[5]. For purposes of this study, only the M_n and M_w will be considered. The M_n represents the total weight of the polymer divided by the total number of polymer molecules present;

$$M_n = \frac{\sum N_i M_i}{\sum N_i} \quad (4.4)$$

Where; N_i , is the number of polymer molecules and M_i , is the molecular weight. The M_w can be expressed according to;

$$M_w = \frac{\sum N_i M_i^2}{\sum N_i M_i} \quad (4.5)$$

From expressions (4.4) and (4.5), it can be deduced that $M_w > M_n$. The ratio of the two, *i.e.* M_w/M_n , known as the polydispersity index (PDI), gives a measure of the broadness of the polymer molecular weight distribution. Mono-disperse polymers have PDI of 1, meaning that $M_w = M_n$ ^[5].

The sol component was analysed for M_w and its distribution using gel permeation chromatography (described in chapter two). The dried sol was suspended in 1 mL chloroform, filtered through a 0.45 μm filter, dried in a rotor-vapour and re-suspended in 1 mL tetrahydrofuran. 2.5 mg/mL polymer solution concentrations were prepared in THF with 3 % BHT (butylated hydroxytoluene). 100 μL volume was injected into the GPC, flow rate of THF set at 1 mL/min at room temperature and the samples ran for 30 minutes. Polystyrene standards were used for calibration (M_w in the range 1.6 x 10⁶ – 468 Da)

4.2.3.2 Structural analysis of sol

FTIR was used for structural analysis of the sol fraction. FT-IR spectra were recorded with OPUS 7.0 software on a Bruker Tensor II spectrometer, using the Attenuated Total Reflection (ATR) mode. Sample scan time of 32 scans was used within the range of 4000-400 cm^{-1} at a resolution of 1 cm^{-1} . The background was measured at background scan time of 16 scans before testing each sample.

4.2.3.3 GCMS analysis

Acetone extracts of devulcanisates were subjected to GCMS analysis to identify products or by-products of devulcanisation. The extracts were dried using a RE300 rotary evaporator from Bibby Scientific Instruments. The dried extracts were then re-suspended in 5 mL of dichloromethane (GC-grade), after which they were filtered using 0.45 μm filters. The GC conditions were as follows: helium column carrier gas, 1 μL injection volume in split-less mode at an injection temperature of 60 $^{\circ}\text{C}$. The oven temperature was ramped at 20 $^{\circ}\text{C min}^{-1}$ from 60 $^{\circ}\text{C}$ (1 min holding time) to 310 $^{\circ}\text{C}$ (at 0 min holding time). The mass spectra detector (MSD) conditions were as follows: full scan mode, m/z 40-550 amu, positive EI mode, ion source temperature, 170 $^{\circ}\text{C}$.

4.3 RESULTS AND DISCUSSIONS

4.3.1 Optimisation of non-isothermal devulcanisation

4.3.1.1 % Devulcanisation obtained using DD

Figures 4.2 and 4.3 show the degree of devulcanisation obtained at the two extreme set-point temperatures of the CCD used in chapter three for DD and MBTS respectively.

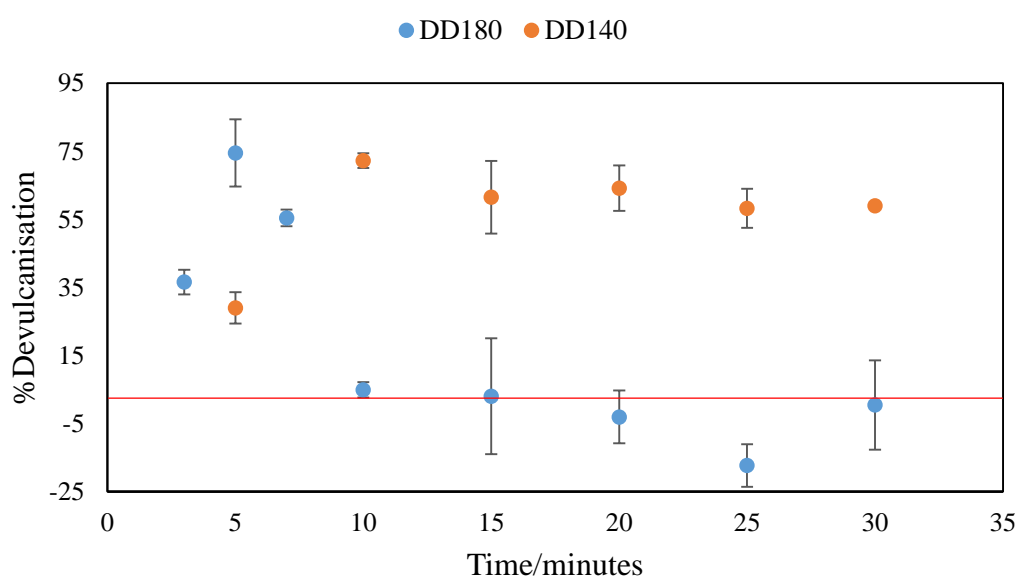


Figure 4.2: % Devulcanisation using DD at 140 °C and 180 °C set-points. *The red line marks the level when zero % devulcanisation was reached.*

Due to differences in the heating rates, 180 °C set-point reaches maximum % devulcanisation of 76.18 ± 5.50 % within 5 minutes whereas 140 °C set-point takes twice the time to reach maximum % devulcanisation of 72.26 ± 2.17 % (Fig. 4.2). The readings at 3 and 7 minutes for 180 °C set-point were done to ascertain what happens on either side of the maximum % devulcanisation at 5 minutes, otherwise the results would be inconclusive. The curve at 140 °C set-point reaches maximum % devulcanisation and then stabilises at roughly the same amount of % devulcanisation within measurement error. On the other hand, the curve at 180 °C set-point rises then drops drastically until it reaches negative % devulcanisation. This behaviour will be explained later on in this chapter under processes involved in devulcanisation.

Table 4.2: t-Test: Two-sample assuming equal variances for DD devulcanisation at 140 °C and 180 °C set-points

	Mean	Variance	t-stat	t-critical	p-value
DD 180 °C	76,18	15.8	0.9	2,78	0.40
DD140 °C	72.30	0.77			

The sample t-test indicates that the average of maximum % devulcanisation at 180 °C set-point is equal to the average of maximum % devulcanisation at 140 °C set-point within measurement error (t-test; $p = 0.40$, 95 % CI). In other words, there is 40 % likelihood within 95 % confidence interval (CI) that the two averages are equal. The null hypothesis is therefore accepted, so either set-point of 140 or 180 °C can be used to achieve the same maximum % devulcanisation. The only difference would be the time taken to achieve maximum % devulcanisation. Now considering time as the discriminant, it would be better to run the reaction at shorter times to achieve good energy efficiency and low production costs yet achieve the same % devulcanisation. Therefore, 180 °C set-point conditions were chosen to give the optimum results for DD non-isothermal devulcanisation.

4.3.1.2 % Devulcanisation obtained using MBTS

Initially, the maximum % devulcanisation was observed at 5 minutes for the 180 °C set-point according to the experimental domain. However, just like for DD optimisation, there was need to analyse the region around the maximum. The reaction gave greater efficiency at 4 minutes, below which (at 3 minutes) the % devulcanisation dropped. Therefore 4 minutes was chosen as the maximum % devulcanisation time for 180 °C set-point. Figure 4.3 shows that curves at the two set-points rise to a maximum and then decline gradually to a minimum as the reaction progresses. MBTS at 180 °C set-point reaches maximum % devulcanisation within 4 minutes, while at 140 °C set-point, it takes 6 minutes longer to reach the maximum. This again can be explained in terms of the heating rate, 180 °C set-point has a relatively faster heating rate than 140 °C set-point.

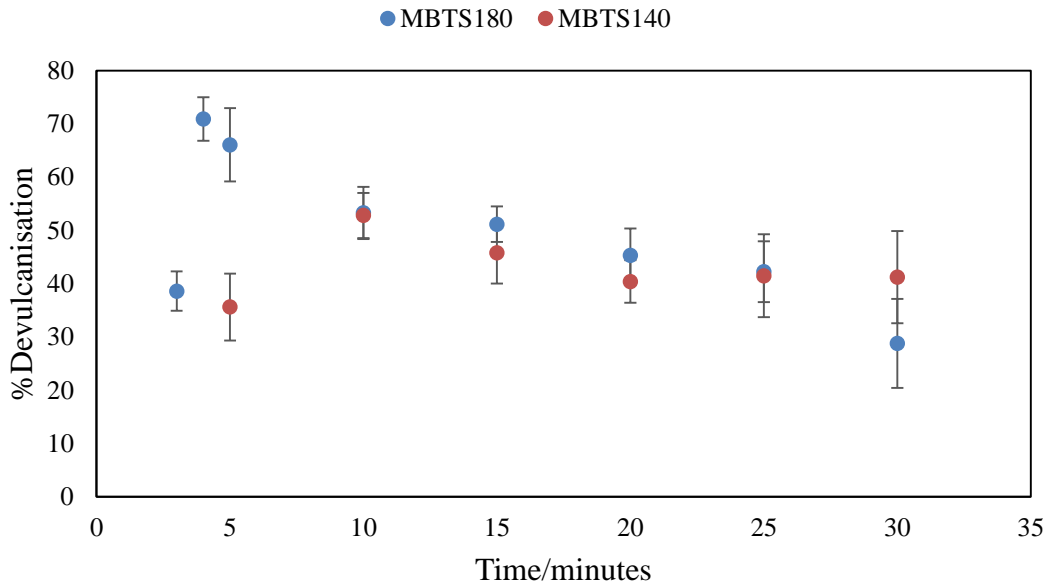


Figure 4.3: % Devulcanisation using MBTS at 140 °C and 180 °C set-points.

Table 4.3: t-Test: Two-sample assuming equal variances for MBTS devulcanisation at 140 and 180 °C set-points

	Mean	Variance	t-stat	t-critical	p-value
MBTS180 °C	70,92	2.72	13.2	2,78	0.00
MBTS140 °C	52.81	2.91			

It can be concluded from the t-test that the averages of maximum % devulcanisation at set-point 140 °C (*i.e.* 52.81 %) and 180 °C (*i.e.* 70.92 %) are not the same within measurement error (t-test; $p = 0.0002$, 95% CI). This is emphasized by the t-statistical value of 13.2, which is way beyond the critical t-value of 2.78. Therefore the null hypothesis is rejected and the optimum conditions are chosen at set-point of 180 °C, where there is relatively higher % devulcanisation for MBTS. Henceforth, attention is shifted to looking at what happens at the optimum set-point (180 °C) only, for both dAs.

4.3.1.3 Thermal contribution towards % devulcanisation

A control experiment was done in the absence of any dA to check the thermal contribution towards % devulcanisation. The run was executed at 180 °C set-point, 0.00 g dA, 80 bars, and 1.00g sample for 5 minutes.

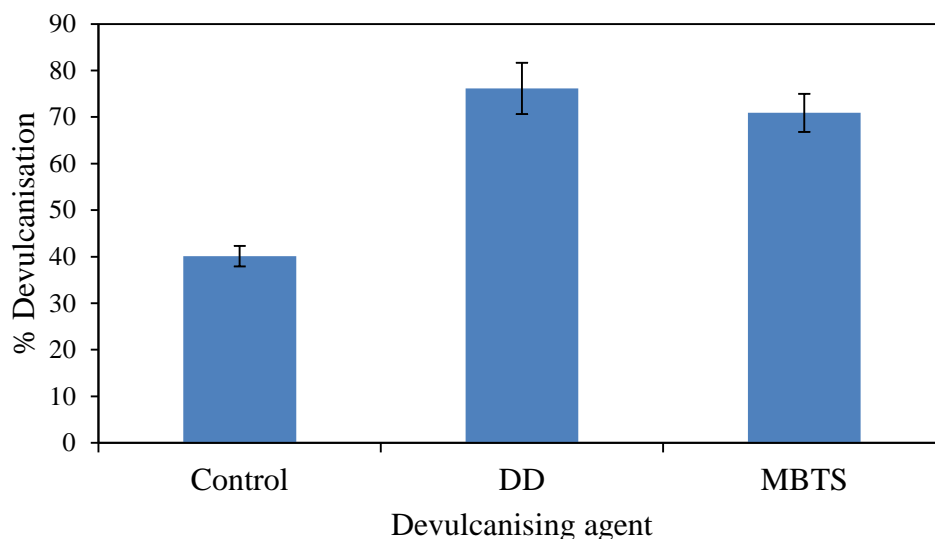


Figure 4.4: Investigation of thermal contribution towards devulcanisation.

The results obtained (Fig. 4.4) show that temperature has a significant contribution towards the degree of devulcanisation. In other words, the amount of heat supplied to the sample within 5 minutes is enough to cause scission of polysulphidic crosslinks (and maybe some di-sulphidic crosslinks). Polysulphidic crosslinks are known to cleave or undergo exchange reactions at temperatures around 80-100 °C [6]. From the bond energy differences highlighted in chapter one (Table 1.2), di- and poly-sulphidic crosslinks are easy to cleave (bond energy 270 kJ/mol.) compared to monosulphidic crosslinks (bond energy 310 kJ/mol.) and C-C bonds in the rubber main chain (bond energy 370 kJ/mol.) The relatively lower bond energy of the di- and poly-sulphidic crosslinks therefore explains why heat (at low temperatures and in the absence of dA) resulted in crosslink density reduction. The thermal contribution towards devulcanisation concurs with the proposed mechanism by Adhikari *et al* [7] that crosslink scission can be induced by heat (chapter one; Scheme 1a; step 3). The effect of heat is probably enhanced by the supercritical conditions and scCO₂, which has good swelling, penetration and diffusion properties.

4.3.1.4 Effect of heating rate on % devulcanisation

Figures 4.1a and b (section 4.2.2.3) show that the heating rate decreases gradually from a maximum as temperature approaches the set-point value. Figures 4.5a and b shows how the heating rate is associated to the degree of devulcanisation. In accordance with the kinetic theory of matter, at the onset of heating there are no active species available to react, *i.e.* a certain amount of energy is needed to activate reactive species. As temperature is increased, more energy is supplied to the reactive species. Eventually this amount of energy supplied becomes enough to activate the reactive species. It is at this juncture that devulcanisation reaction begins. Devulcanisation reaction rate is expected to increase initially as more active species are being formed. After reaching a maximum, devulcanisation declines to a minimum as reactive species get depleted and competing processes (Fig. 4.2 and 4.3) gain importance. Figures.4.2 and 4.3 show a comparison of % devulcanisation at different heating rates determined by set-points of 140 °C and 180 °C. From the graphs (Figs. 4.2 and 4.3), it can be seen that the faster the heating rate the faster the reaction reaches maximum % devulcanisation. Good correlation factors between heating rate and % devulcanisation (62.5 % for DD and 83.9 % for MBTS) emphasize the influence heating rate has on % devulcanisation. DD has a lower correlation factor due to the irregular devulcanisation behaviour observed in Figure 4.2 (*i.e.* negative % devulcanisation).

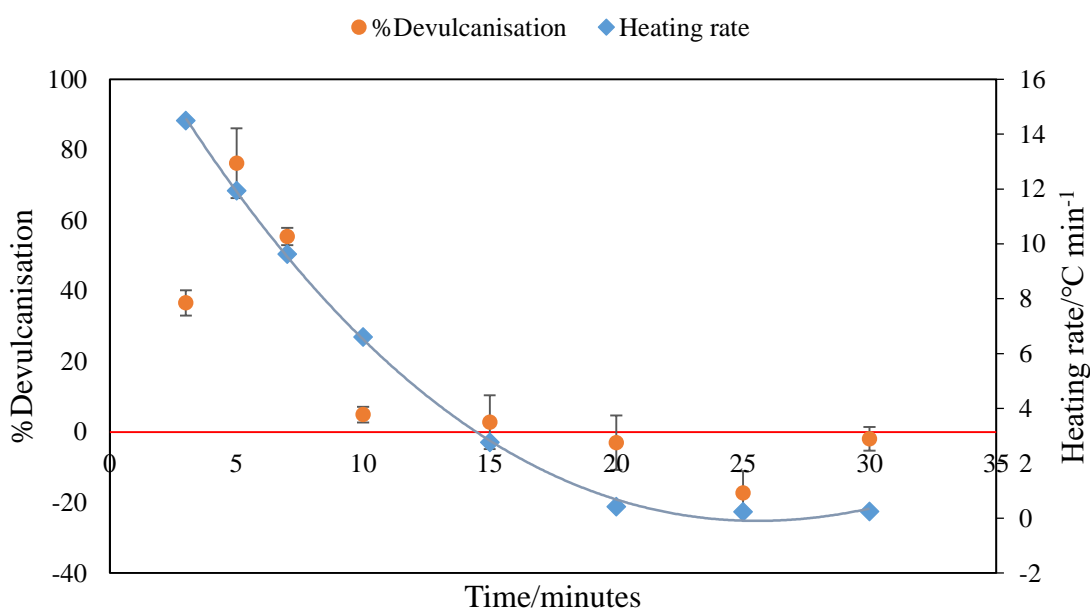


Figure 4.5a: Overlay of % Devulcanisation and heating rate for DD.

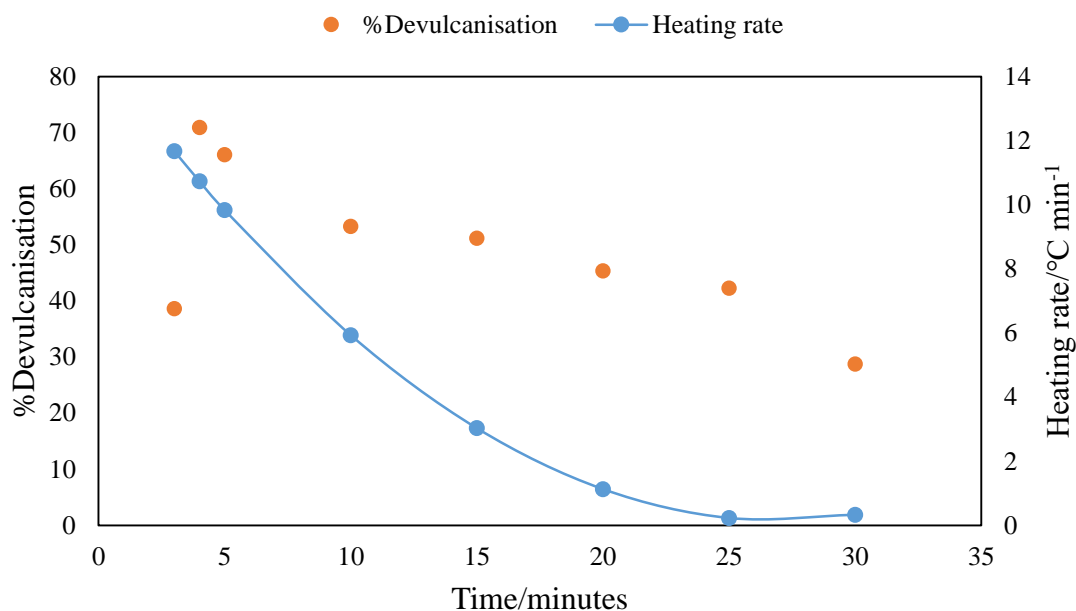


Figure 4.5b: Overlay of % Devulcanisation and heating rate for MBTS.

4.3.1.5 Empirical model formulation

i) Empirical model formulation for DD non-isothermal devulcanisation at 180 °C set-point

Tables 4.4a and b show final regression outputs for DD non-isothermal devulcanisation at 180 °C set-point. Only the reaction times that yielded positive values of % devulcanisation were subjected to regression analysis due to mathematical restrictions of calculating \hat{E} (*i.e.* logarithm of a negative number is mathematically impossible). The final parameters after continuous regression are shown in the appendix section together with associated standardised residuals (Table 4A.3). The accepted parameters represent values where the null hypothesis is not satisfied, *i.e.* $p < 5\%$ for $H_0: b_1 = 0$.

Table 4.4a: Accepted regression outputs for DD devulcanisation; ($H_0: b_i = 0$)

Coefficients			Standard		
			Error	t-Stat	P-value
b0	Intercept	-318,07	125,46	-2,53	0,04
b1	t	21,71	9,63	2,25	0,06
b2	T	1,71	0,35	4,90	0,00
b3	R	17,42	6,27	2,78	0,03
b4	tT	-0,11	0,03	-3,86	0,01
b5	TR	-0,10	0,02	-5,22	0,00

b_i = regression coefficients for; b0 = intercept, b1 = time (t), b2 = temperature (T), b3 = rate (R), b4 = time-temperature interaction (tT) and b5 = temperature-rate interaction (TR).

Table 4.4b: Rejected regression outputs for DD devulcanisation ($H_0: b_i = 0$)

Coefficients		Standard		
Coefficients	value	Error	t-Stat	P-value
t	-1,49	16,62	-0,09	0,93
R ²	0,09	1,60	0,06	0,96
T ²	0,01	0,01	0,65	0,54
t ²	0,44	0,19	2,25	0,06

Model validation was done by means of a validation plot of standardised residuals against predicted % devulcanisation (Fig. 4.6). The random distribution pattern of the residuals implies that the model is a good fit and can be used to explain the experimental data. Also, a high R-squared value (0.996) was obtained for the empirical model, meaning that the model explains about 99.6 % of the experimental data. However, Table 4A.3a in the appendix section shows that the residuals are outliers for all data points. In addition, the variation of outliers is quite big to be ignored (with reference to ± 2 for a Gaussian distribution). As a result the model can still be improved to give better results. The empirical model obtained is represented by the equation 4.6;

$$\hat{Y} = b_0 + b_1t + b_2T + b_3R + b_4tT + b_5TR \quad (4.6)$$

Where; \hat{Y} is the empirical model function for predicted % devulcanisation (*i.e.* $f(x)$), b_i are the regression coefficients for the given factors as described in Table 4.4a. Incorporating equation 4.6 according to equation 3.12 of the logistic model yields equation 4.7, which gives predicted values of % devulcanisation;

$$\hat{E} = \frac{100}{1 + e^{(b_0 + b_1 t + b_2 T + b_3 R + b_4 tT + b_5 TR)}} \quad (4.7)$$

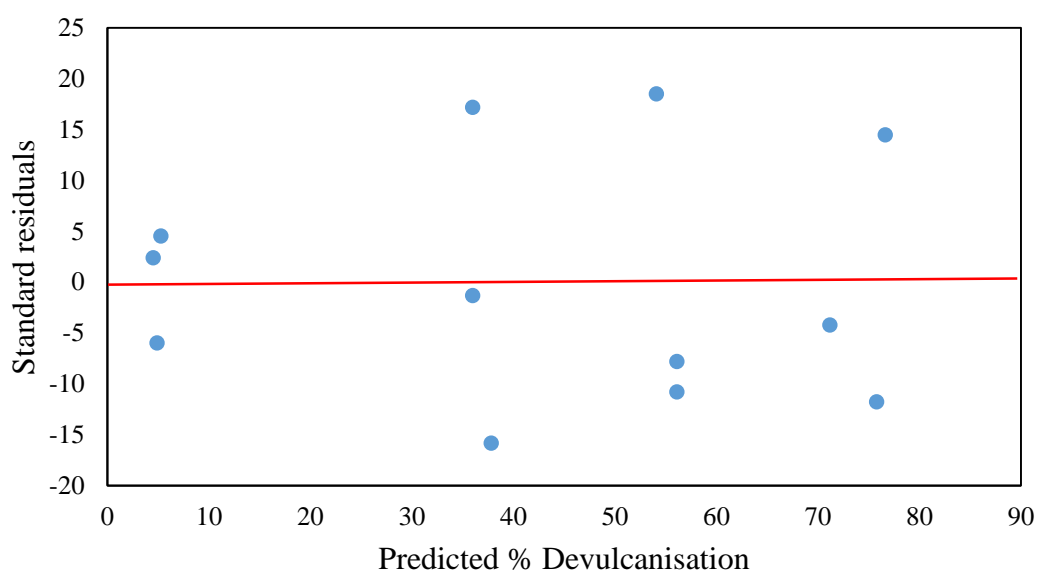


Figure 4.6: Model validation plot for DD non-isothermal devulcanisation at 180 °C set-point.

Optimisation of equation 4.7 using the solver analytical tool in Microsoft excel resulted in the outcome shown in Table 4.5.

Table 4.5: Optimum conditions predicted by solver tool for DD devulcanisation.

t/min	T/°C	R/°C min⁻¹	Predicted
1	50	3,52	100

The conditions predicted to achieve 100 % devulcanisation were not practically possible, *i.e.* the heating rate predicted could not be set directly on the controller and it would not result in 50 °C after 1 minute. Despite the limitation of not being able to set a specific heating rate on the temperature controller, the factors are correlated and thus would likely result in the model not working properly in practice. The temperature is dependent on the heating rate and time, while the heating rate is dependent on the set-point temperature as well as current temperature.

ii) Empirical model formulation for MBTS non-isothermal devulcanisation at 180 °C set-point

The % devulcanisation for MBTS had no negative values, so the whole time range (*i.e.* 5-30 minutes) was analysed. The accepted and rejected regression outputs for MBTS devulcanisation are shown in Tables 4.6a and b respectively. The final parameters after continuous regression are shown in the appendix section together with associated standardised residuals (Table 4A.4) The accepted parameters represent values where the null hypothesis is not satisfied, *i.e.* $p < 5\%$ for $H_0: b_i = 0$.

Table 4.6a: Accepted regression outputs for MBTS non-isothermal devulcanisation ($H_0: b_i = 0$)

Coefficients			Standard		
			Error	t Stat	P-value
b0	Intercept	-11,46	7,17	-1,60	0,13
b1	t	7,52	1,85	4,07	0,00
b2	T	-0,69	0,13	-5,10	0,00
b3	R	2,28	0,57	3,98	0,00
b4	T ²	0,00	0,00	4,91	0,00
b5	tT	-0,04	0,01	-4,08	0,00
b6	tR	-0,08	0,03	-3,16	0,01

b_i = regression coefficients for; b0 = intercept, b1 = time (t), b2 = temperature (T), b3 = rate (R), b4 = time-temperature interaction (tT) and b5 = temperature-rate interaction (TR).

The rejected parameters represent those whose p-values satisfy the null hypothesis; *i.e.* $p > 5\%$ for $H_0: b_i = 0$. This means there is high probability the coefficient is equal to zero, thereby rendering the parameter insignificant.

Table 4.6b: Rejected regression outputs for MBTS non-isothermal devulcanisation; ($H_0: b_i = 0$)

	Coefficients	Standard Error	t Stat	P-value
t^2	0,15	0,04	4,07	0,00
R^2	0,16	0,54	0,30	0,77
TR	0,00	0,01	0,18	0,86

Note that the p-value for t^2 is below 5 % but the parameter was rejected anyways. This is because t^2 affected the p-value of its independent variable (t), hence it was eliminated regardless of its p-value. The empirical model obtained is given by equation 4.8;

$$\hat{Y} = b_0 + b_1t + b_2T + b_3R + b_4T^2 + b_5Tt + b_6Rt \quad (4.8)$$

Incorporating equation 4.8 into the logistic function given by equation 3.12 gives the predicted % devulcanisation for MBTS according to the logistic model as shown on equation 4.9;

$$\hat{E} = \frac{100}{1 + e^{(b_0 + b_1t + b_2T + b_3R + b_4T^2 + b_5Tt + b_6Rt)}} \quad (4.9)$$

Validation was done by means of a validation plot of standardised residuals against predicted %devulcanisation as shown on Figure 4.7. The random distribution of the standardised residuals indicate that the model can be used to explain the data. However, the residuals are all outliers (except for only two points), the degree of which is quite bigger than ± 2 (Appendix, Table 4A.4a). A good R-squared value was also obtained, (0.812) shown in the appendix Table

4A.4b. This implies that the model explains 81.2% of the data. In view of this, the model can still be improved to better explain the data.

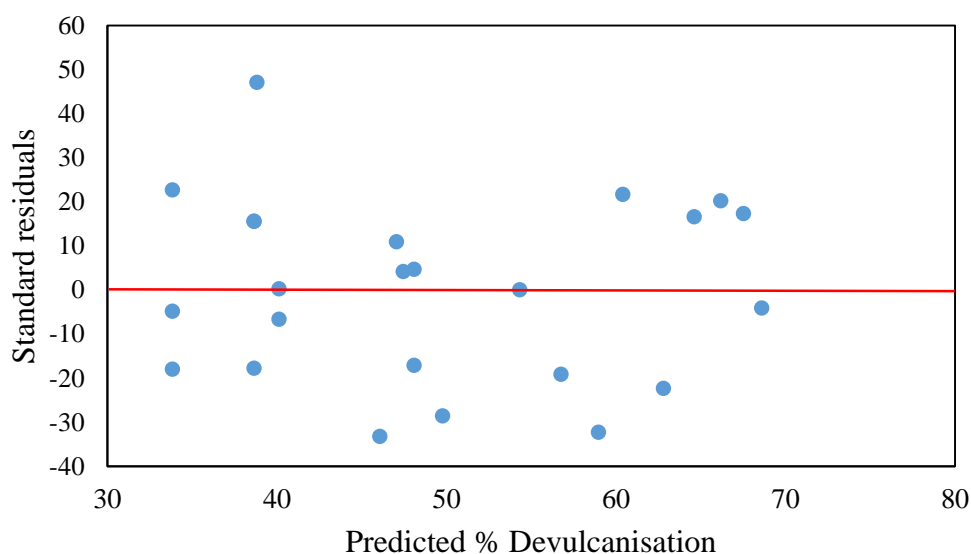


Figure 4.7: Model validation plot for MBTS non-isothermal devulcanisation at 180 °C set-point.

Optimisation using the solver function in Microsoft excel yielded the results as shown in Table 4.7. Equation 4.9 was set as the solver objective to attain maximum % devulcanisation by varying conditions of time, temperature and heating rate.

Table 4.7: Optimum conditions as predicted by the solver tool in Microsoft excel.

t/min	T/°C	R/°C min⁻¹	Predicted
1	99,06	1	100

The conditions predicted by the solver analysis tool were practically impossible to attain using the reactor setup, the heating rate of 1 °C min⁻¹ could not be directly set on the temperature controller, and nonetheless, a heating rate of 1 °C/min would not reach 99.06 °C in 1 minute.

4.3.1.6 Possible reasons why the models were not able to predict feasible optimum

Correlation factors of time, temperature and heating rate are shown in Tables 4.8a and 4.8b, and were determined the same way as in chapter three. Negative factors suggest an antagonistic effect of one variable on the other, *e.g.* in Table 4.8b; time and heating rate have -92.5 % correlation factor, meaning that they are strongly correlated but as the time increases the heating rate decreases. On the other hand, positive correlation indicates a synergistic relation between factors, *e.g.* time and temperature.

Table 4.8 a) Correlation factors for DD devulcanisation process variables at 180 °C set-point

Variable	Correlation factor
Time: Temperature	91.8 %
Time: Heating rate	-100 %
Temperature: Heating rate	-90 %

Table 4.8 b) Correlation factors for MBTS devulcanisation process variables at 180 °C set-point

Variable	Correlation factor
Time: Temperature	86.2 %
Time: Heating rate	-92.5 %
Temperature: Heating rate	-98 %

The empirical models obtained for both dAs could not fully describe the experimental data due to the high correlation between time, temperature and heating rate ^[8]. For an empirical model to work, the factors have to be independent of each other, *i.e.* have no correlation between them ^[8]. As a result, single factor analysis was done on the non-isothermal region.

4.3.1.7 Chosen optimum conditions: time & temperature

Since the obtained models were unable to give predictions that were practically viable in the available experimental setting, the conditions that yielded maximum % devulcanisation were chosen to be the optimum conditions (*i.e.* from Figs. 4.2 and 4.3). The maximum % devulcanisation obtained for DD and MBTS were 76.18 ± 5.50 % and 70.92 ± 4.10 % respectively. The associated conditions are given in Table 4.9.

Table 4.9: Summary of optimum conditions obtained for DD and MBTS.

dA	Set-point/°C	Time/minutes	Temp/°C	^aRate/°C min⁻¹	dA/g	Pressure/bar
DD	180	5	102	11.94	0.10	80
MBTS	180	4	97	10.73	0.10	80

a = instantaneous heating rate

Figure 4.8 shows crosslink densities of the vulcanisate after cure (original), aged vulcanisate (neat or prior to devulcanisation), and vulcanisate devulcanised using DD and MBTS at the chosen optimum conditions. The changes in the crosslink density upon treatment with dAs shows that DD and MBTS were quite effective in the reduction of chemical crosslinks, *i.e.* they are effective devulcanisation agents in scCO₂. The chosen optimum conditions do not show the effect of changes in pressure or amount of dA on non-isothermal devulcanisation, therefore single factor analysis was conducted to look at the effect of pressure and amount of dA used.

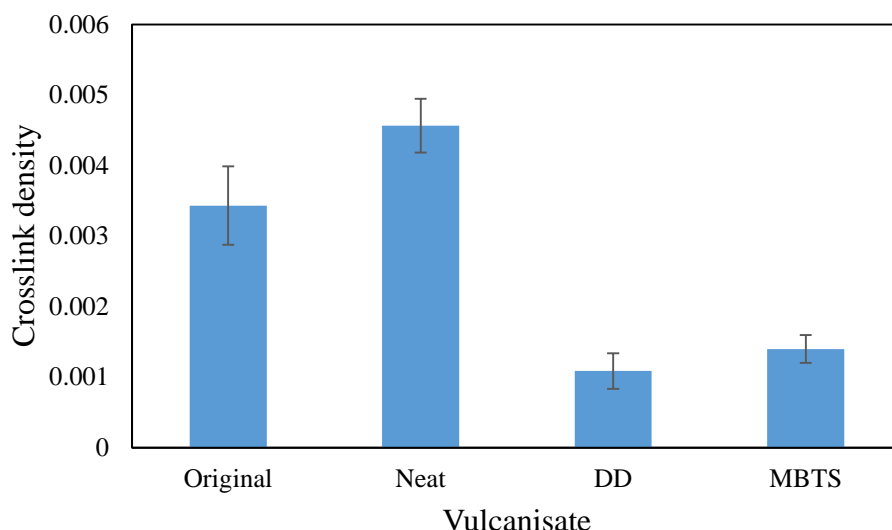


Figure 4.8: Summary of changes in the crosslink densities of vulcanisates during analysis.

4.3.2 Single factor analysis: amount of dA and pressure

Single factor analysis involves analysis of one factor while all the other variables are kept constant. Single factor analyses have the disadvantage of not revealing effects of factor interactions. However, in this study this disadvantage would not have much effect since some interactions were identified to have insignificant effect on the % devulcanisation through multiple linear regression of the CCD (chapter 3; Tables 3.5 and 3.6). The effects of pressure and amount of dA were then studied individually at optimum conditions of time, temperature and heating rate. The effect of CB filler was not done for optimisation purposes, but only to establish if it has an influence on the % devulcanisation.

4.3.2.1 Effect of amount of dA on % devulcanisation

Figure 4.9 shows the % devulcanisation obtained at different amounts of dA (*i.e.* 1, 5 and 10 % of 1.00 g sample). Single factor ANOVA was then performed on the average % devulcanisation obtained at the different dA loadings, to determine variation in the samples.

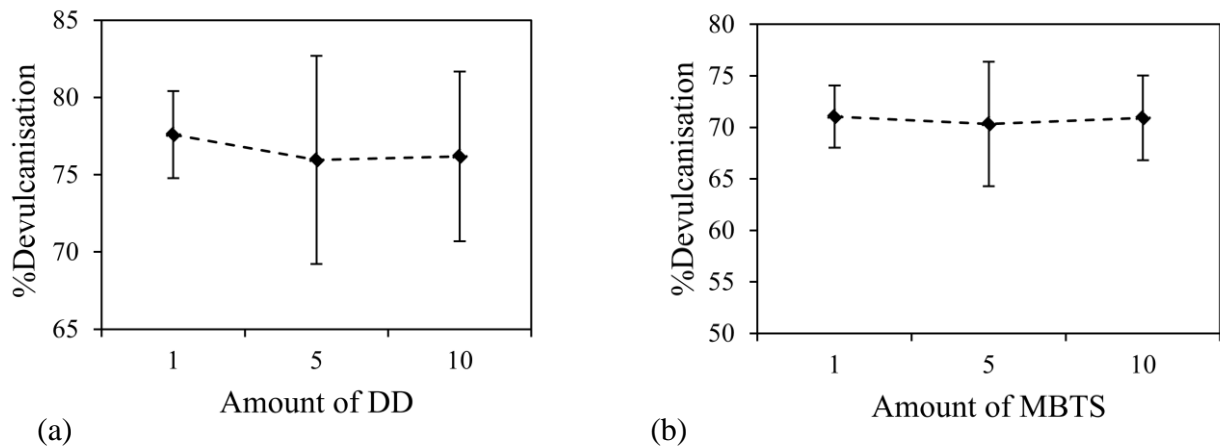


Figure 4.9: Effect of amount of (a) DD and (b) MBTS used on % devulcanisation.

The error bars in Figures 4.9a and b overlap each other's means or central points, indicating a high probability that the samples are similar, within measurement error.

Table 4.10a: Single factor ANOVA outputs for DD % devulcanisation ($H_0: \mu_{1\%} = \mu_{5\%} = \mu_{10\%}$).

SUMMARY

Groups	Count	Sum	Average	Variance
1%DD	3	232.77	77.59	1.29
5%DD	3	227.84	75.95	7.35
10%DD	3	228.54	76.18	4.89

ANOVA: Single factor

Source of						
Variation	^a SS	^b df	^c MS	^d F	P-value	^e F-critical
Between						
Groups	0.89	2	0.45	0.13	0.88	5.14
Within Groups						
Within Groups	20.20	6	3.37			
Total						
Total	21.09	8				

a = sum of squares, b = degrees of freedom, c = mean sum of squares, d = F-statistic

Table 4.10b: Single factor ANOVA outputs for MBTS % devulcanisation ($H_0 : \mu_{1\%} = \mu_{5\%} = \mu_{10\%}$).

SUMMARY

Groups	Count	Sum	Average	Variance
1%MBTS	3	213.14	71.05	1.48
5%MBTS	3	210.97	70.32	5.90
10%MBTS	3	212.76	70.92	2.72

ANOVA: Single factor

Source of Variation	SS	df	MS	F	P-value	F-critical
Between						
Groups	4.75	2	2.37	0.53	0.62	5.14
Within Groups	27.08	6	4.51			
Total	31.83	8				

Tables 4.10a and b show that there is convincing evidence that the average % devulcanisation does not differ significantly for different loadings (1; 5 & 10 %) of DD and MBTS, (ANOVA; $p = 0.88$) and (ANOVA; $p = 0.62$) respectively. Also, the F-statistic for both dAs is less than the F-critical value, 0.13 and 0.53 for DD and MBTS respectively. As a result, 1 % of either DD or MBTS can be used to achieve the same degree of devulcanisation as 10 % of DD or MBTS respectively, thereby saving costs on the amount of dA used. Mangili *et al* [9] also found out using a full factorial experimental design followed by regression analysis, that the amount of DD used (1-25 % DD) for GTR devulcanisation had no significant effect on changes in crosslink density, with p-value of 0.127. One possible reason why no significant differences in % devulcanisation were observed as the amount of dA was reduced is that the amount of dA used was in excess. This was observed on GCMS analysis of acetone extracts for the different amounts of dA (Table 4.11). If the amount of dA was the limiting factor and cleavable crosslinks were in excess, then changing the amount of dA would result in significant differences in % devulcanisation. Therefore, to determine the exact amount of dA to be used, one has to know the exact amount of cleavable crosslinks (and or combined sulphur) present. However, due to uncertainties involved in the determination of crosslink density, combined

sulphur content, crosslink distribution and selectivity of dA, determining the exact amount of cleavable crosslinks might be a problem.

Table 4.11: GCMS analysed of acetone extract for DD and MBTS devulcanisates.

Mass of dA	benzenethiol	DD	^a MBT
1%	8,71	24,52	12,1
5%	9,84	24,84	16,3
10%	25,53	57,97	20,09

a = mercaptobenzothiazole

Acetone extracts shown on Table 4.11 are of a minimum of 95 % quality. Benzenethiol and diphenyl disulphide were detected in DD devulcanizates extracts, whereas mercaptobenzothiazole was observed in MBTS extracts. No MBTS molecules were detected in the acetone extracts. Table 4.11 shows that the masses of dAs used for devulcanisation were in excess. Note that GCMS as used here was for qualitative analysis, not quantitative, to show extract constituents. The presence of thiols in the extracts obtained after devulcanisation proves the mechanism proposed by Rajan *et al* ^[10], where radical fragments of dA abstract the allylic hydrogen thereby forming thiols and inducing crosslink or chain scission (chapter one; Scheme 1b). The GCMS spectra are shown in the appendix section (Figs. A1 and 2).

4.3.2.2 Effect of pressure on % devulcanisation

Figure 4.10 shows the effect of changing pressure, from 80 bar to 100 bar, on the % devulcanisation. Sample t-test assuming equal variances were then performed to ensure statistical differences.

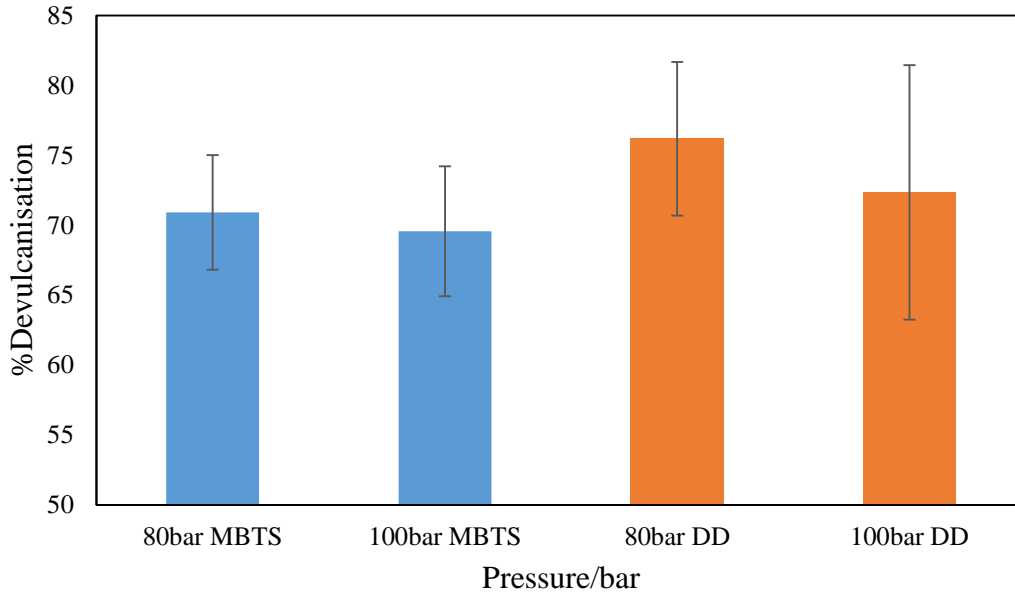


Figure 4.10: Effect of pressure on % devulcanisation using DD and MBTS at optimum conditions.

Table 4.12a: t-Test: two sample assuming equal variance for DD devulcanisation ($H_0: \mu_{80} = \mu_{100}$)

	Mean	Variance	t-stat	t-critical	p-value
80 bar	70,92	2.72	-0,94	2,78	0,40
100 bar	69,57	3.48			

Table 4.12b: t-Test: two sample assuming equal variance for MBTS devulcanisation ($H_0: \mu_{80} = \mu_{100}$)

	Mean	Variance	t-stat	t-critical	p-value
80 bar	76,18	4.90	-1,55	2,78	0,19
100 bar	72,34	13.41			

The average degree of devulcanisation at 80 and 100 bar using DD and MBTS is the same within measurement error (t-test; $p = 0.40$) and (t-test; $p = 0.19$) respectively. This means that increasing pressure by 20 bar (from 80 to 100 bar) had no significant effect on the % devulcanisation. The results observed corroborate findings by Liu *et al* ^[11] and Mangili *et al* ^[9], who showed that pressure has no significant effect on the degree of devulcanisation of waste tyre tread and truck tyre GTR respectively. Liu *et al* ^[11] reported that as long as the pressure is above the supercritical pressure, changing pressure would not affect devulcanisation (p -value = 0.159). On the contrary, Kojima *et al* ^[12] reported that pressure changes have an effect on devulcanisation by tracing the amount of sol generated at different pressures for optimisation of devulcanisation. The findings by Kojima *et al* ^[12] were different probably due to the use of sol content as the response variable, which does not directly indicate changes in the degree of devulcanisation. Nevertheless, the ability to use lower pressures to achieve the same level of devulcanisation as with high pressures (*i.e.* as long as the supercritical state is established) translate to energy savings, increased reactor life span and low cost of materials (CO₂, gas compressor and replacement of reactor components worn out by higher pressures) for analysis or devulcanisation processes.

4.3.3 Final optimum conditions

Combining results obtained upon selection of optimum set-point conditions (of time, temperature and instantaneous heating rate based on maximum % devulcanisation) and those obtained upon single factor analysis (of pressure and amount of dA), yields optimum conditions shown in Table 4.13;

Table 4.13: Final optimum conditions obtained for DD and MBTS.

dA	Set-point/°C	Time/minutes	Temp/°C	Rate/°C min ⁻¹	dA/g	Pressure/bar
DD	180	5	102	11.94	0.01	80
MBTS	180	4	97	10.73	0.01	80

4.3.4 Effect of CB filler on % devulcanisation

The results in Figure 4.11 show that the degree of devulcanisation for unfilled rubber is relatively higher than that of filled rubber for both dAs. DD still shows superior devulcanising abilities in unfilled rubber than MBTS, but by a slight difference.

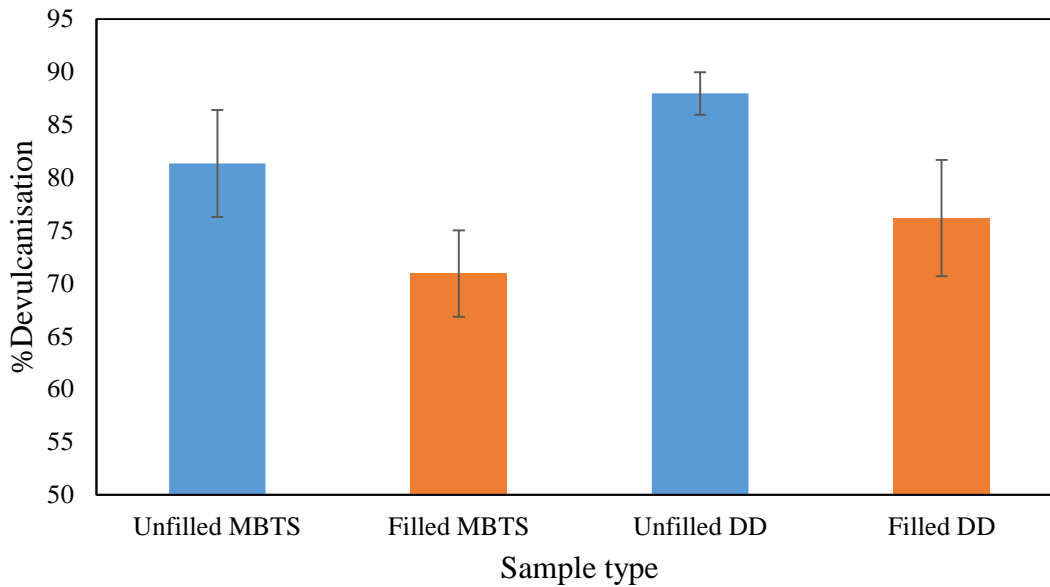


Figure 4.11: Effect of filler on degree of devulcanisation using DD and MBTS.

Table 4.14a: t-Test: Two-sample assuming equal variations for DD devulcanisation.

	Mean	Variance	t-stat	t-critical	p-value
DD unfilled	87.95	0.65	8.66	2,78	0,00
DD filled	76.18	4.89			

Table 4.14b: t-Test: Two-sample assuming equal variations for MBTS devulcanisation

	Mean	Variance	t-stat	t-critical	p-value
MBTS unfilled	81,33	4.13	6.89	2,78	0,00
MBTS filled	70.92	2.72			

The t-tests show that there is convincing evidence that CB filler has an effect on the average % devulcanisation using DD and MBTS (t-test: $p = 0.0010$) and (t-test: $p = 0.0023$) respectively. The null hypothesis is therefore rejected, meaning the % devulcanisation for filled vs. unfilled are different within measurement error. Therefore CB filler has a significant effect on the degree of devulcanisation using DD and MBTS in $scCO_2$. The presence of CB filler did not prevent devulcanisation from occurring (which agrees with findings by Kojima *et al* ^[13]) but it retarded devulcanisation efficiency (which disagrees with Kojima *et al* ^[13]). In their work, Kojima *et al* ^[13] concluded that CB does not disturb devulcanisation by DD in $scCO_2$ based on observation that sol content for various CB contents varied in the range 20-40%. This is however inconclusive as the crosslink densities of their test vulcanisates was not the same, also, no statistical method (*e.g.* t-test) of analysis was conducted to determine the degree of variation in the results obtained.

4.3.5 Processes involved during devulcanisation

4.3.5.1 % Devulcanisation vs. % sol

The degree of devulcanisation should give a direct indication of the efficiency of crosslink scission, while the sol content can be a result of both crosslink and chain scission. A high sol content has been shown to be associated with reduction in Mw due to chain scission ^[7, 12, 14-16]. %Devulcanisation and % sol were overlaid with changes in the crosslink density (given by the reciprocal of the swell factor, $1/Q$ ^[17-19]) to establish which of the two strongly correlates with the degree of crosslink scission (Fig.4.12).

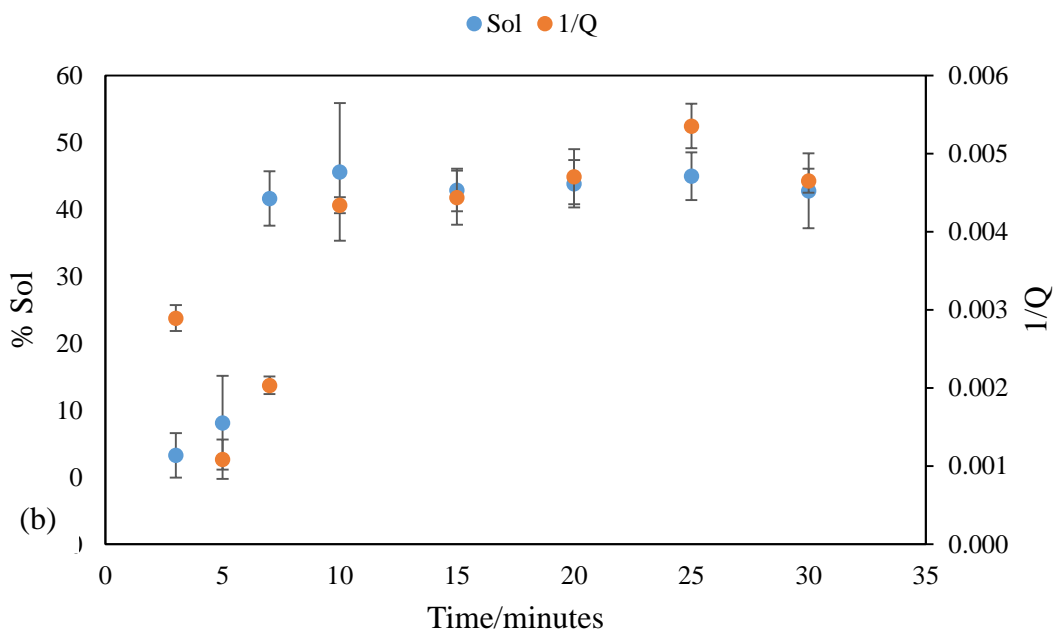
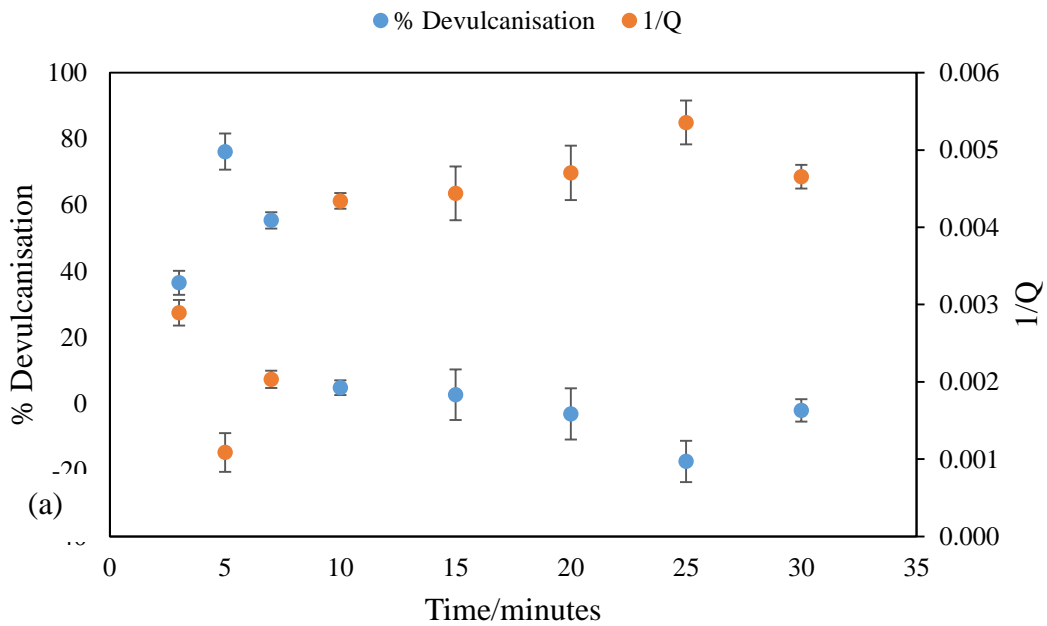


Figure 4.12: Relation between the (a) degree of devulcanisation and (b) amount of sol produced with changes in the crosslink density over time using DD.

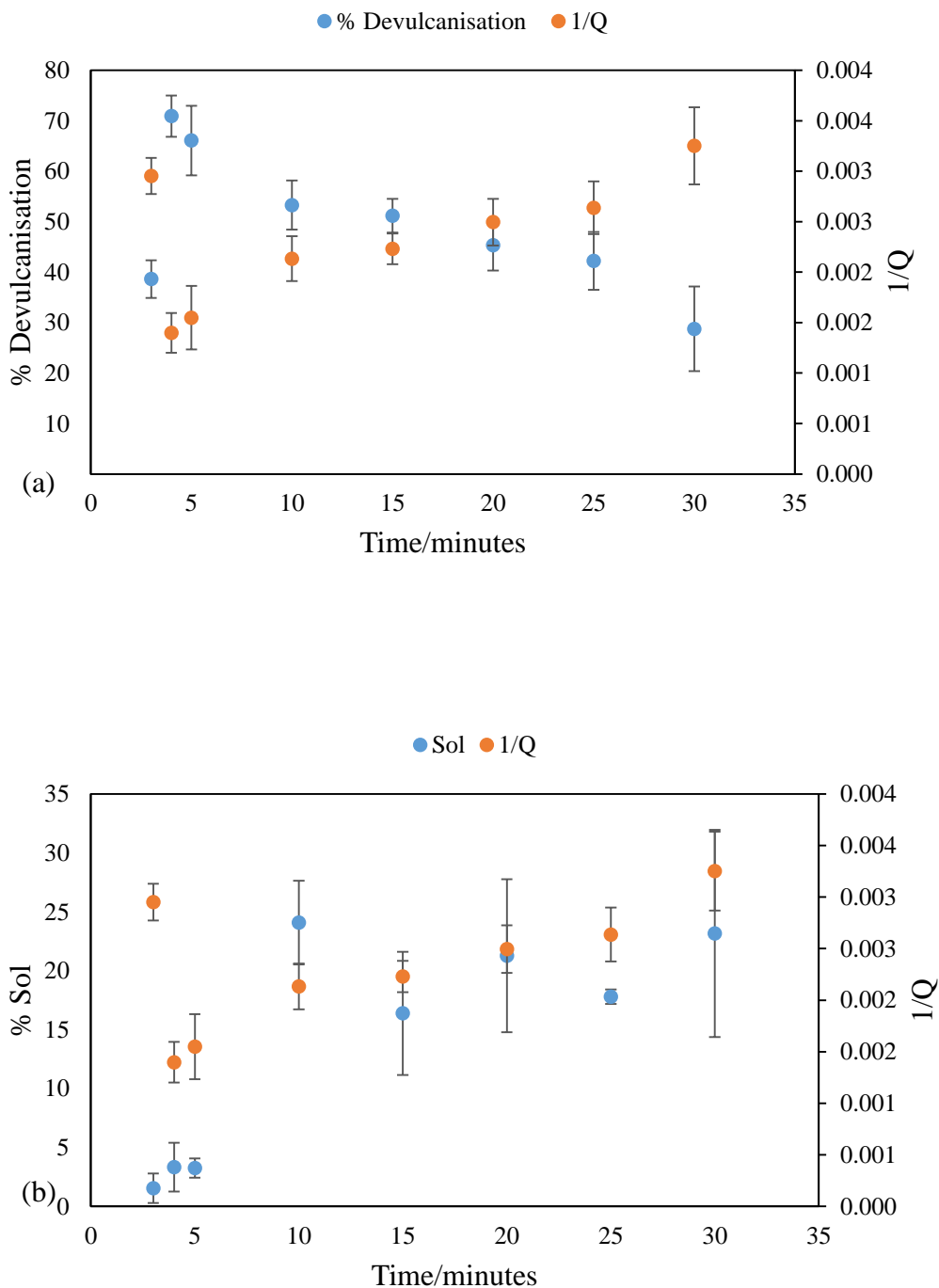


Figure 4.13: Relation between the (a) degree of devulcanisation and (b) amount of sol produced with changes in the crosslink density over time using MBTS.

The graphs indicate that increases in the % devulcanisation are accompanied by corresponding decreases in the crosslink density and *vice versa*. The maximum % devulcanisation coincides with the lowest crosslink density, and *vice versa*. The correlation between % devulcanisation

and crosslink density is further emphasized by a correlation factor of -100 % for both DD and MBTS. The negative correlation is due to the fact that an increase in devulcanisation reduces the number of crosslinks. On the other hand, % sol shows a general increase with time, regardless of changes in the crosslink density for both dAs. The highest sol content does not coincide with the lowest crosslink density, and neither does the lowest % sol coincide with the lowest crosslink density. The correlation of % sol and crosslink density is clarified by correlation factors of 70 and 44 % for DD and MBTS respectively. The positive correlation is due to the fact that the amount of sol produced is directly dependent on the number of liberated chains, which result from a combination of crosslink and chain scission. It can therefore be concluded based on the observations that % devulcanisation gives a better indication of crosslink density changes occurring during devulcanisation. It should also be noted that at the highest degree of devulcanisation the sol amount produced is minimal and *vice versa* (Appendix, Figs. A3 and A4. This inverse correlation between % sol and % devulcanisation is in agreement with the theory of selective crosslink scission [10, 20]. According to Horikx *et al* [20], for a situation where only crosslink scission takes place, the number of effective chains remains the same while only reduction in crosslink density is observed. This idea is not practically possible as devulcanisation is usually accompanied by a certain degree of chain scission. The molecular weights of the sol content produced is evidence of chain scissions taking place during devulcanisation.

4.3.5.1 Devulcanisation vs. competing processes

According to Rajan *et al* [10], the rate of decomposition of the disulphide is the rate determining step for devulcanisation. With this in mind, it can be deduced from Figures 4.2 and 4.3, that the rate of decomposition of DD is relatively faster than that of MBTS. This would explain why DD devulcanisation reaches completion earlier than MBTS (Figs. 4.2 and 4.3). Thermal analysis of DD and MBTS using TGA affirms the early decomposition of DD compared to MBTS (chapter three, Fig. 3.8). It can be deduced from the thermogram in Figure 3.8 that not much temperature is needed to cause decomposition of DD and MBTS under supercritical conditions. It appears decomposition of both dAs is accelerated in scCO₂ as it occurs at relatively lower temperatures (*ca.* 80 °C). This is evidenced by the presence of thiols (~30 % peak area) in the GCMS extract analysis (Table 4.11) at low temperatures (80-105 °C). Accelerated decomposition of DD and MBTS in this system may be due to supercritical

conditions or induction by polysulphidic crosslink scission due to heat. Polysulphidic crosslinks are known to undergo degradation at temperatures around 80-100 °C. The formation of radical ends due to polysulphidic crosslink degradation is most likely to induce decomposition of the dAs.

From Figure 4.2, it seems that at zero % devulcanisation, decrosslinking reactions would have reached a minimum and competing processes gained prominence due to continued heat supply as time progresses. Competing processes become increasingly important until they result in the crosslink density (ν) of the gel (ν_i) being greater than that of the undevulcanised sample (ν_o), resulting in negative % devulcanisation ($\%D = \frac{\nu_o - \nu_i}{\nu_o}$) for DD (Fig. 4.2). In other words, crosslink formation has become dominant. On the other hand, MBTS devulcanisation reaches a steady state within measurement error after 15 minutes (Fig. 4.3). At this point the % devulcanisation is fairly constant, which implies a balance in decrosslinking and crosslink formation. Longer times, *i.e.* around 30 minutes, tilt the balance in favour of competing processes, resulting in a further decrease in % devulcanisation.

i) Hardening

SBR is known to undergo hardening at high temperature conditions [21]. An increase in temperature assists gel formation (or crosslinking) in SBR due to unsaturation [22]. According to Sarkhar *et al* [22], thermal degradation starts on the butadiene units where hydrogen transfer reactions [23] as well as the formation of cyclic [23] and crosslink structures occur [22] (Appendix; Figs. A6-8). DD and MBTS devulcanisates, shown in Figure 4.16, show formation of gel structures in the devulcanisates as indicated by peaks at the region around 1325 cm^{-1} [22, 24]. Note that peaks indicating the gel structures are absent in the vulcanisate as well as the SBR standard. This supports the suggested reaction mechanisms of degradation of SBR. SBR degrades by means of a crosslink formation mechanism [22], which results in hardening. This explains the negative % devulcanisation values observed for DD (since $\nu_o < \nu_i$). Completion of devulcanisation within 10 minutes using DD implies that there is relatively more time for competing processes to dominate, compared to when there is a gradual decrease in % devulcanisation as observed for MBTS (Fig. 4.3). The increase in the ν of SBR containing gel under supercritical conditions was also observed by Liu *et al* [11]. They attributed this increase

to unsaturated butadiene units forming crosslink structures ^[11] as well as to concentration of DD lower than 10 g/L. However, in their report Liu *et al* ^[11] did not check for any excess dA. In this study, the amount of dA is in excess as shown by GCMS analysis, therefore hardening due to SBR crosslinking is the most probable reason for ν increase.

In a binary polymer blend, the dA might be more selective to one component polymer than the other. As a result, major devulcanisation would likely occur in the most preferred polymer phase. This should show by a reduction in the relative composition of the preferred phase. TGA analysis was executed to track the relative composition of NR/SBR in the devulcanisates with time. This should give an indication of whether there is preferential devulcanisation taking place or not.

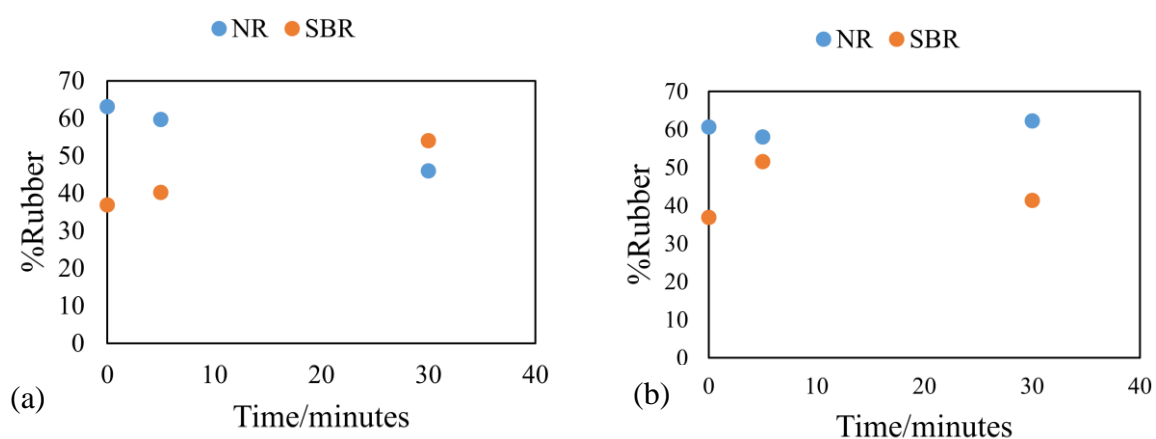


Figure: 4.14: Change in NR/SBR relative composition due to preferential devulcanisation by (a) DD and (b) MBTS

TGA analysis was conducted on vulcanisates prior to devulcanisation at $t = 0$ minutes, followed by analysis of devulcanisates at 5 and 30 minutes respectively (*i.e.* the two extremes). It can be seen in Figure 4.14 that DD seems to exhibit high preference for NR devulcanisation. This is shown by the linear decrease in the relative composition of NR with a corresponding linear increase in the relative composition of SBR. Preferential devulcanisation of NR over SBR by DD corroborates why negative % devulcanisation was observed for DD and not MBTS. Uneven devulcanisation by DD would result in more SBR content in the gel, which subsequently enhances competing processes as relatively more SBR is available for crosslink formation. On the other hand, MBTS showed no observable trend to indicate the presence of preferential devulcanisation, which supports the gradual decrease in % devulcanisation.

According to the FTIR spectra in Figure 4.16, SBR degradation occurs in both DD and MBTS samples, as shown by the presence of gel structures. However, the increase in the relative composition of SBR in DD devulcanisates implies an increased negative effect on the % devulcanisation. This phenomenon of preferential devulcanisation presents problems in the reclamation industry. It results in uneven reclamation of the polymer phases with subsequent processing problems and most likely negative effects on reclaim properties.

Shore A hardness tests were conducted on devulcanisates to show changes in hardness over time. Samples at 5, 15 and 30 minutes were tested to see if there was any observable trend in shore-A hardness over time. The shore-A hardness instrument used has an uncertainty of ± 4 units, therefore only hardness tests for large time gaps were done to determine the trend of changes in hardness. ASTM D2240, DIN 53505 was followed for shore-A hardness tests. A general increase in hardness with time was observed, which is confirmatory to the explanation given for the observed negative % devulcanisation results.

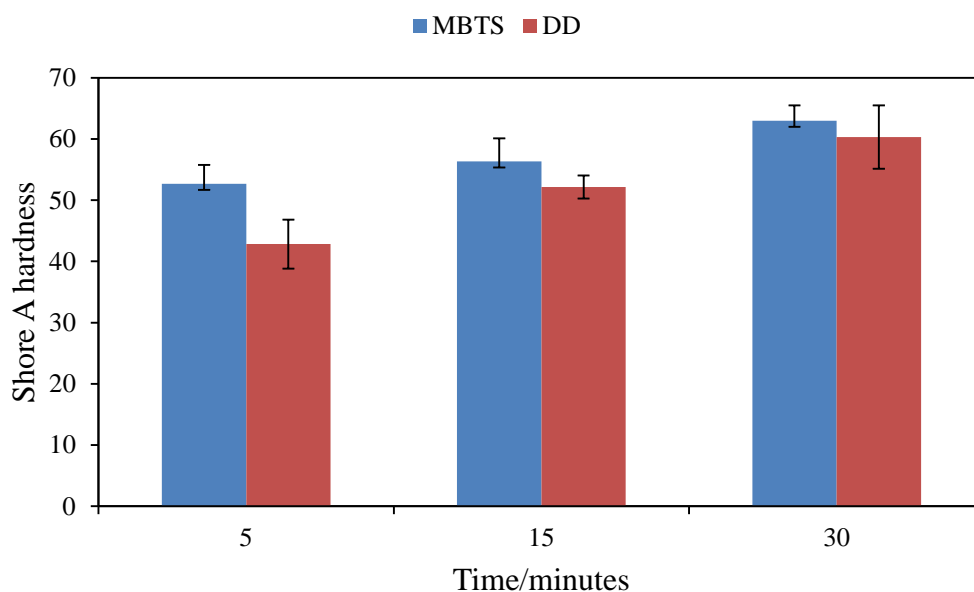


Figure 4.15: Shore-A hardness of gels taken at 5, 15 and 30 minutes.

ii) Chain scission

Degradation of polymer molecular chains is inevitable during devulcanisation, and the best that can be done is to minimise the extent of chain scission. Figure A7 in the Appendix shows how

chain scission on the SBR main chain can occur (prior to crosslink formation). However, due to SBR chemistry, it seems that crosslink formation predominates, especially where DD is concerned (as shown in Fig. 4.14). As a result, most chain scission would likely occur on the NR main chain.

4.3.6 Product analysis

4.3.6.1 GPC analyses

The level of chain scission can be monitored by looking into the molecular weights of sol component at the various devulcanisation times. Molecular weights of the sol component were determined using GPC. A conventional calibration curve using polystyrene standards was used (Appendix, Fig. A5) to determine molecular weights of the sol components. Table 4.15a and b show the average molecular weights and distribution for the sol fractions obtained from devulcanisation using DD and MBTS.

Table 4.15a: Sol component molecular weights from DD devulcanisation

Sample (DD)	^a Mn/Da	^b Mw/Da	^c PDI
Control	14 311	57 612	4.02
5 mins	26 163	90 557	3.46
10 mins	11 276	46 242	4.10
30 mins	12 297	58 874	4.79

a = number average molecular weight, b = weight average molecular weight, c = polydispersity index

Table 4.15b: Sol component molecular weights from MBTS devulcanisation

Sample (MBTS)	Mn/Da	Mw/Da	PDI
Control	14 311	57 612	4.02
4 mins	13 392	37 186	2.78
10 mins	16 063	57 200	3.56
30 mins	11 736	36 724	3.13

The control rubber sample represents the uncured masticated NR/SBR blend. This was used as a point of reference for changes on molecular weights. The PDI for the control sample is quite high (4.02), which shows that there is a wide distribution of chain lengths upon mastication in the internal mixer. Shear mechanical forces in the internal mixer are mainly responsible for chain degradation during mastication, while the peptiser (renacit 7) used in the formulation acts as a capping agent. Tables 4.15a and b show that as time progresses, changes in the Mw are minimal. However, a general slight increase in the PDI with time (which is more pronounced for DD) is observed. The broad molecular weight distribution observed as time progresses is likely due to an interplay between chain degradation and recombination processes. Chain degradation results in shorter chains whereas recombination results in longer chains, thereby broadening the molecular weight distribution. DD was found to preferentially cleave NR more than SBR, while MBTS showed no preference. This may be the reason why PDIs for DD are higher than for MBTS. In addition, this may also be caused by the fact that DD reaches 0 % devulcanisation in 10 minutes whereas MBTS does not reach 0 % devulcanisation. Consequently, after devulcanisation has completed for DD, competing processes immediately gain importance, thereby resulting in the broadening of chain distribution due to more chain scission and recombination occurring. At 5 minutes devulcanisation activity is at its peak, thus there is minimal chain scission. The Mw obtained (90 557 Da) is about twice the size of the control sample. This may imply persistence of few crosslinks linking two polymer chains or simply minimal chain scission.

4.3.6.2 FTIR analyses

The full spectra for the devulcanisates is shown on the appendix section as well as a brief description of the region above 2000cm^{-1} for NR (Fig. A.9). Figure 4.16 only shows the fingerprint region to identify modifications due to devulcanisation. The SBR FTIR spectrum shows bands at; 699 cm^{-1} due to the polystyrene units; 760 cm^{-1} due to 1,4-cis; 910 cm^{-1} due to 1,2-vinyl; and 964 cm^{-1} due to 1,4-trans-butadiene units [22]. These bands are a signature for SBR, and their presence suggests the presence of SBR. At 841 cm^{-1} is the C–H out of plane bending of the cis–1,4 addition characteristic of NR, which is present in the vulcanisate and both devulcanisates but is absent in SBR. This band can only be attributed to the presence of the cis–1,4 isoprene monomer in NR [25].

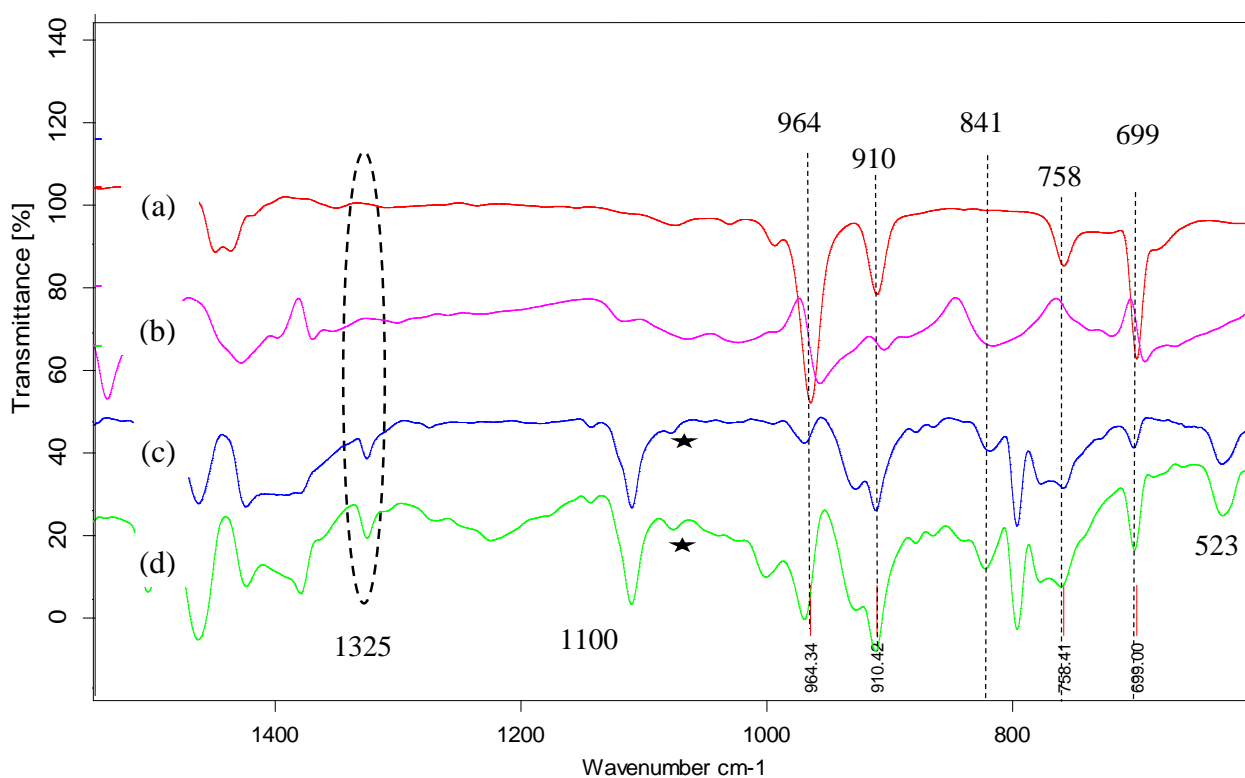


Figure 4.16: FTIR analyses of DD and MBTS devulcanisates. The spectra shows; a) standard SBR, *i.e.* uncured starting material, b) neat vulcanisate c) MBTS devulcanisate and d) DD devulcanisate.

A decrease in intensity is observed for the 1,4-trans-butadiene units (at 964 cm^{-1}), which implies modifications in the backbone structure due to devulcanisation^[11]. At 910 cm^{-1} there is peak crowning indicating modification of the 1,2-vinyl units. Peak distortions at 758 cm^{-1} indicate modifications due to attachment of DD and MBTS pendant groups to the polymer chains, as shown by dA phenyls groups around 738 cm^{-1} for both dAs^[11]. The FTIR spectra of the dAs are shown in the appendix section (Figs. A11 and A12). Spectra (c) and (d) show a C-S-C band at 1076 cm^{-1} in the gel component for both DD and MBTS (star marked). This band is however absent in the sol component of DD (Appendix, Fig. A10, star marked). The presence of the peak at 1076 cm^{-1} can be explained by the attachment of the benzenesulphide (from DD) or MBT (from MBTS) radicals onto the polymer chain thereby forming pendant groups, according to the mechanisms proposed by Adhikari *et al*^[7] and Rajan *et al*^[10]. The peak at 1076 cm^{-1} on the MBTS spectrum (Appendix, Fig. A12) affirms the C-S-C band, which is present in the MBTS chemical structure. The C-S-C band can also be simply due to monosulphidic crosslinks being accentuated by their relative increase in composition during the devulcanisation process. At 523 cm^{-1} , are S-S vibration bands, which can be due to di- or polysulphide crosslinks, S-S links formed upon attachment by dA pendant group, or a combination of both. However, the increased intensity of the S-S stretch vibration, which is known to exhibit a weak vibration band, emphasizes attachment of dAs. The presence of the band at 1100 cm^{-1} is representative of a thiocarbonyl group (C=S), which corroborates the proposed decrosslinking mechanism by Rajan *et al*^[10]. The absence of the C=O peak at 1715 cm^{-1} as well as the C-O peak at $1270\text{-}1255\text{ cm}^{-1}$ indicates absence of thermo-oxidative degradation^[24]. The sol components showed similar peaks and the FTIR spectra are shown in the appendix (Fig. A10).

Table 4.16: Summary outputs of optimum conditions

Parameter	^bUntreated	DD	MBTS
^a 1/Q (x 10 ⁻³)	4.57	1.09	1.40
% Devulcanisation	0.00	76.18 ± 5.50	70.92 ± 4.10
% Sol	0.48 ± 0.08	8.13 ± 7.00	3.33 ± 2.07
% Gel	99.52 ± 0.08	91.87 ± 7.00	96.67 ± 2.07
Mw/ Da	57 612	90 557	37 186
PDI	4.02	3.46	2.78
^c Cost/ ZAR	–	R608 per 50 g	R554 per 100 g
Preferential devulcanisation	–	yes	no

$a = \frac{1}{Q} \propto \nu$, b = masticated sample, c = costs obtained from Sigma Aldrich

4.4 SUMMARY OF FINDINGS

- The degree of devulcanisation (or % devulcanisation) was found to be a good and direct indicator of crosslink density changes as compared to sol content.
- A relatively higher degree of devulcanisation was observed at 180 °C compared to 140 °C set-point temperature for both DD and MBTS.
- High degree of devulcanisation was observed for both DD and MBTS (76.18 ± 5.50 % and 70.92 ± 4.10 % respectively) within 5 minutes (DD) and 4 minutes (MBTS) at 180 °C set-point temperature.
- Temperature was found to have a significant contribution towards devulcanisation even in the absence of DD or MBTS.
- A higher heating rate resulted in a relatively faster devulcanisation for both DD and MBTS. Since the heating rate was dependent on the set-point temperature, the higher set-point temperature (180 °C) resulted in higher % devulcanisation in a short amount of time compared to the lower set-point temperature (140 °C).
- The empirical models formulated for both DD and MBTS could not be applied in practice.
- Single factor analysis showed that the amount of dA used and pressure above supercritical conditions had no significant influence on the % devulcanisation.
- The presence of CB in the vulcanisates has an influence on the degree of devulcanisation for both DD and MBTS.
- During devulcanisation, there are competing processes that lower the % devulcanisation for both DD and MBTS in scCO₂ medium under the executed reaction conditions (180 °C set-point, 80 bars, and 30 minutes maximum run time).
- DD was found to result in uneven devulcanisation, resulting in more NR being devulcanised than SBR. On the other hand, MBTS showed no preference in devulcanisation.
- The quality of the devulcanised rubber did not show much variation from the raw rubber except for indications of dA attachment onto the polymer chains according to FTIR analyses. Chain degradation for both DD (PDI = 3.46) and MBTS (PDI = 2.78) was kept minimal in comparison to the PDI obtained for the masticated sample (PDI = 4.02).

4.5 REFERENCES

1. Parks, C.R. and O. Lorenz, *Journal of Polymer Science*, 1961. **50**(154): p. 299.
2. Parks, C.R. and O. Lorenz, *Journal of Polymer Science*, 1961. **50**(154): p. 253-556.
3. Kraus, G.J., *Journal of Applied Polymer Science*, 1963. **7**(3): p. 861.
4. Bosma, C., *Introduction to data analysis*. 2017, Nelson Mandela University. p. 1-49.
5. Umoren, S.A. and M.M. Solomon, *Polymer Science: Research Advances, Practical Applications and Educational Aspects*, 2016: p. 412-419.
6. Group, A.M. and N. limited *Vulcanisation and Accelerators*. 2010. 11.
7. Adhikari, B., D. De, and S. Maiti, *Progress in Polymer Science*, 2000. **25**: p. 909-948.
8. Marion, G. and D. Lawson, *An introduction to mathematical modelling*, in *Bioinformatics and Statistics Scotland*. 2008. p. 1-31.
9. Mangili, I., et al., *Polymer Degradation and Stability*, 2014. **102**: p. 15-24.
10. Rajan, V.V., et al., *Journal of Applied Polymer Science*, 2007. **104**(6): p. 3562-3580.
11. Liu, Z., et al., *Polymer Degradation and Stability*, 2015. **119**: p. 198-207.
12. Kojima, M., et al., *Rubber Chemistry and Technology*, 2003. **76**: p. 957-68.
13. Kojima, M., et al., *Journal of Applied Polymer Science*, 2005. **95**: p. 137-143.
14. Forrest, M., *Recycling and Re-use of Waste Rubber*, ed. S.R.T. Ltd. 2014, Shawbury, Shrewsbury, UK: Smithers Rapra Technology Ltd.
15. Jiang, K., et al., *Journal of Applied Polymer Science*, 2013. **127**(4): p. 2397-2406.
16. Myrhe, M., et al., *Rubber Chemistry and Technology*, 2012. **85**(3): p. 408-449.
17. Choi, S.S., *Journal of Applied Polymer Science*, 2000. **75**: p. 1378-1384.
18. Choi, S.S., *Journal of Applied Polymer Science*, 2002. **83**: p. 2609-2616.
19. Parks, C.R. and R.J. Brown, *Rubber Chemistry and Technology*, 1974. **49**: p. 233-236.
20. Horikx, M.M., *Journal of Polymer Science*, 1956. **19**: p. 445-454.
21. Myrhe, M., *Devulcanisation by Chemical and Thermomechanical Means*. *Rubber Recycling*, ed. S.K. De, A.I. Isayev, and K. Khait. 2005: Taylor and Francis Group.
22. Sarkar, M.D., P.P. Mukunda, and A.K. Bhowmick, *Rubber Chemistry and Technology*, 1997. **70**(5): p. 855-870.
23. Golub, M.A. and R.J. Gargiulo, *Polymer Letters*, 1972. **10**: p. 41-49.
24. Wang, S.M., J.R. Chang, and R.C.C. Tsiang, *Polymer Degradation and Stability*, 1996. **52**: p. 51-57.

25. Arroyo, M., M.A. Lopez-Manchado, and B. Herrero, *Polymer*, 2003. **44**(8): p. 2447-2453.

4.6 APPENDIX

4.3.1 Optimisation of non-isothermal devulcanisation.

Table 4A.1: t-Test: assuming equal variances for DD devulcanisation

	DD180 °C	DD140 °C
Mean	76,2	72,3
Variance	15,8	0,77
Observations	3	3
Pooled Variance	8,3	
Hypothesized Mean Difference	0	
df	4	
t Stat	0,9	
P(T<=t) one-tail	0,2	
t Critical one-tail	2,1	
P(T<=t) two-tail	0,4	
t Critical two-tail	2,8	

Table 4A.2: t-Test: assuming equal variances for MBTS devulcanisation

	MBTS180 °C	MBTS140 °C
Mean	70.9	52.8
Variance	2.7	2.9
Observations	3	3
Pooled Variance	2.8	
Hypothesized Mean Difference	0	
df	4	
t Stat	13.2	
P(T<=t) one-tail	9.5E-05	
t Critical one-tail	2.1	
P(T<=t) two-tail	0.0002	
t Critical two-tail	2.8	

4.3.1.5 Optimisation of devulcanisation conditions

Table 4A.3a: Final regression outputs for DD following CCD

Run	T	T ²	%D	Log(\hat{E})	Pred.	Std Residuals
1	140	19600	51.10284	-0.04412	49.62228	3.658363
2	148	21904	45.1825	0.1933	48.93944	-9.28321
3	148	21904	42.10711	0.318378	48.93944	-16.8823
4	148	21904	50.32156	-0.01286	48.93944	3.41513
5	148	21904	54.92101	-0.19748	48.93944	14.78012
6	160	25600	36.25412	0.564352	33.04638	7.92615
7	160	25600	27.62609	0.963085	33.04638	-13.3932
8	160	25600	45.39989	0.184526	33.04638	30.52485
9	160	25600	40.60199	0.380443	33.04638	18.66952
10	160	25600	37.49602	0.510995	33.04638	10.99483
11	160	25600	18.95619	1.452859	33.04638	-34.8161
12	160	25600	27.07594	0.990773	33.04638	-14.7526
13	160	25600	37.83931	0.496374	33.04638	11.84307
14	172	29584	6.980504	2.589688	10.74589	-9.30407
15	172	29584	6.750789	2.625616	10.74589	-9.87168
16	172	29584	15.14399	1.723352	10.74589	10.86747
17	172	29584	17.33448	1.562105	10.74589	16.28005
18	180	32400	-5.75678	#NUM!	3.01	-21.6622

Table 4A.3b: Summary output

<i>Regression Statistics</i>	
Multiple R	0.901
R Square	0.811802
Adjusted R Square	0.784916
Standard Error	0.404703
Observations	17

Table 4A.4a: Final regression outputs for MBTS following CCD

Run	T	%D	Log(\hat{E})	Predicted	Std residuals
1	140	42.90467	0.285742	46.98407	-14.6623
2	148	53.67801	-0.14739	43.98373	34.84344
3	148	47.92114	0.083202	43.98373	14.15196
4	148	42.61452	0.297596	43.98373	-4.92122
5	148	39.45742	0.428125	43.98373	-16.2685
6	160	38.14628	0.483344	39.57081	-5.12007
7	160	32.5036	0.730724	39.57081	-25.4012
8	160	54.72324	-0.18949	39.57081	54.46123
9	160	41.8556	0.328704	39.57081	8.212025
10	160	40.15959	0.39882	39.57081	2.116186
11	160	38.21858	0.480281	39.57081	-4.86022
12	160	35.49	0.597569	39.57081	-14.6673
13	160	36.37267	0.559225	39.57081	-11.4948
14	172	41.37193	0.348611	35.32147	21.74672
15	172	33.84639	0.670147	35.32147	-5.30178
16	172	35.04058	0.617256	35.32147	-1.00958
17	172	23.5656	1.176645	35.32147	-42.2532
18	180	38.42047	0.471739	32.60782	20.89199

Table 4A.4a: Summary output

<i>Regression Statistics</i>	
Multiple R	0.514903
R Square	0.265125
Adjusted R Square	0.219196
Standard Error	0.278224
Observations	18

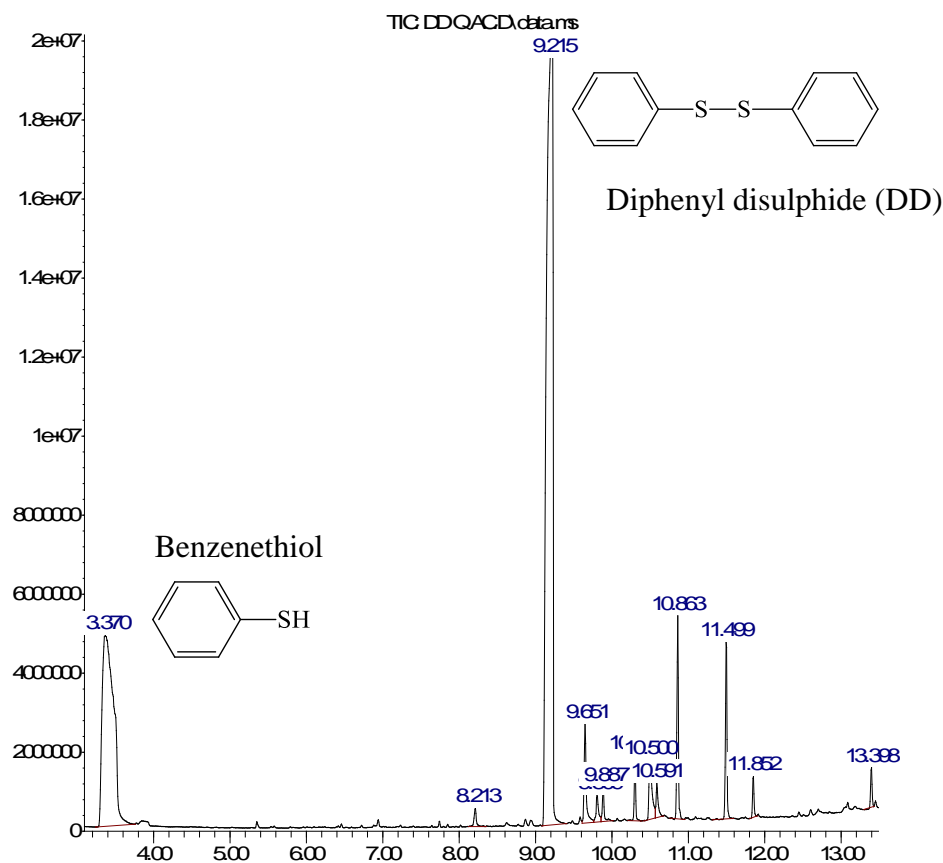
4.3.2.1 Effect of amount of dA on % devulcanisation

Table 4A.5a: Anova: Single Factor for DD

Table 4A.5b: Anova: Single Factor for MBTS

SUMMARY					SUMMARY				
Groups	Count	Sum	Average	Variance	Groups	Count	Sum	Average	Variance
1%DD	3	232.77	77.59	1.29	1%MBTS	3	213.14	71.05	1.48
5%DD	3	227.84	75.95	7.35	5%MBTS	3	210.97	70.32	5.90
10%DD	3	228.54	76.18	4.89	10%MBTS	3	212.76	70.92	2.72

Abundance



Time->

Figure A1: GCMS spectra for DD extracts after devulcanisation at optimum conditions.

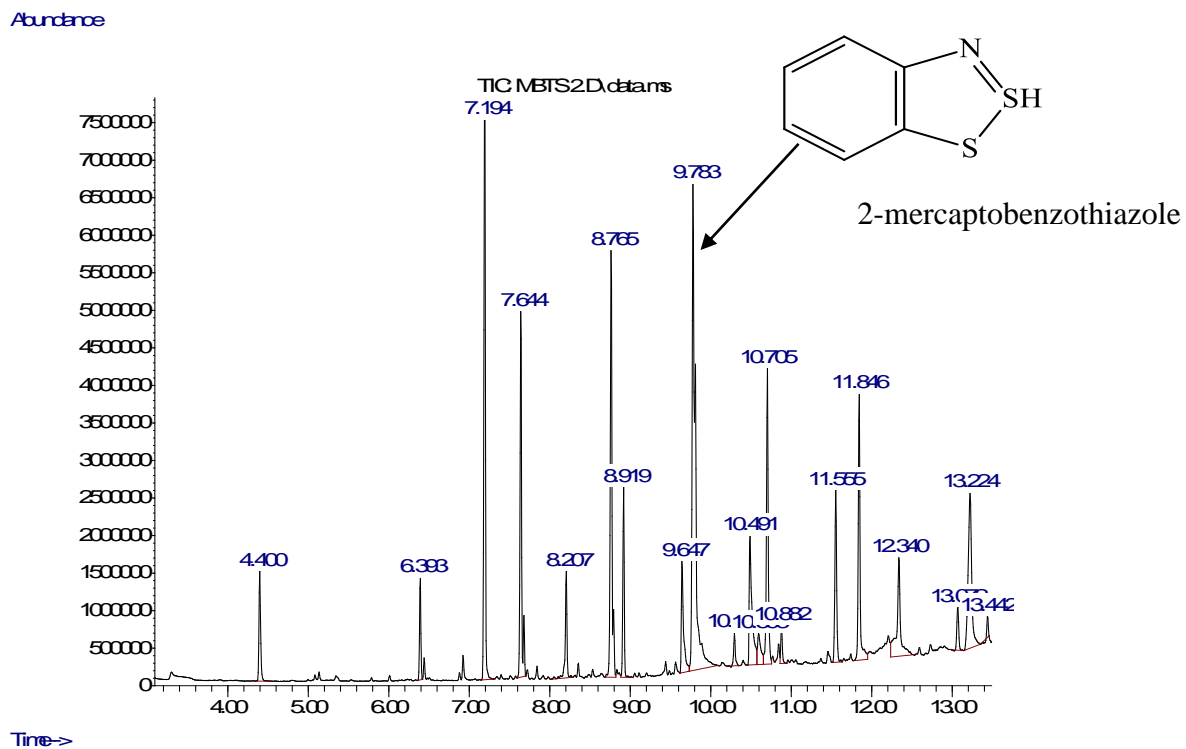


Figure A2: GCMS spectra for MBTS extracts after devulcanisation at optimum conditions.

4.3.2.2 Effect of pressure on % devulcanisation

Table 4A.6a: t-Test: Two-Sample Assuming Equal Variances

Table 4A.6b: t-Test: Two-Sample Assuming Equal Variances

	100bar MBTS	80bar MBTS		100bar DD	80bar DD
Mean	69,56964	70,9198	Mean	72,34253	76,18005
Variance	3,483578	2,722705	Variance	13,41042	4,895734
Observations	3	3	Observations	3	3
Pooled Variance	3,103141		Pooled Variance	9,153077	
Hypothesized Mean Difference	0		Hypothesized Mean Difference	0	
df	4		df	4	
t Stat	-0,93871		t Stat	-1,55351	
P(T<=t) one-tail	0,200513		P(T<=t) one-tail	0,097632	
t Critical one-tail	2,131847		t Critical one-tail	2,131847	
P(T<=t) two-tail	0,401026		P(T<=t) two-tail	0,195265	
t Critical two-tail	2,776445		t Critical two-tail	2,776445	

4.3.3 Effect of filler on %devulcanisation

Table 4A.7a:t-Test: Two-Sample Assuming Equal Variances

Table 4A.7b:t-Test: Two-Sample Assuming Equal Variances

	MBTS	Filled MBTS		DD	Filled DD
Mean	81,3313	70,9198	Mean	87,9536	76,1800
Variance	4,13206	2,72270	Variance	0,65039	4,89573
Observations	3	5	Observations	2	4
Pooled Variance	3,42738		Pooled Variance	3	
Hypothesized Mean Difference	0		Hypothesized Mean Difference	0	
df	4	3	df	4	3
t Stat	6,88776		t Stat	8,65916	
P(T<=t) one-tail	0,00116		P(T<=t) one-tail	0,00048	
t Critical one-tail	2,13184		t Critical one-tail	2,13184	
P(T<=t) two-tail	0,00232		P(T<=t) two-tail	0,00097	
t Critical two-tail	2,77644		t Critical two-tail	2,77644	
	5			5	

4.3.4 % Devulcanisation vs. % Sol

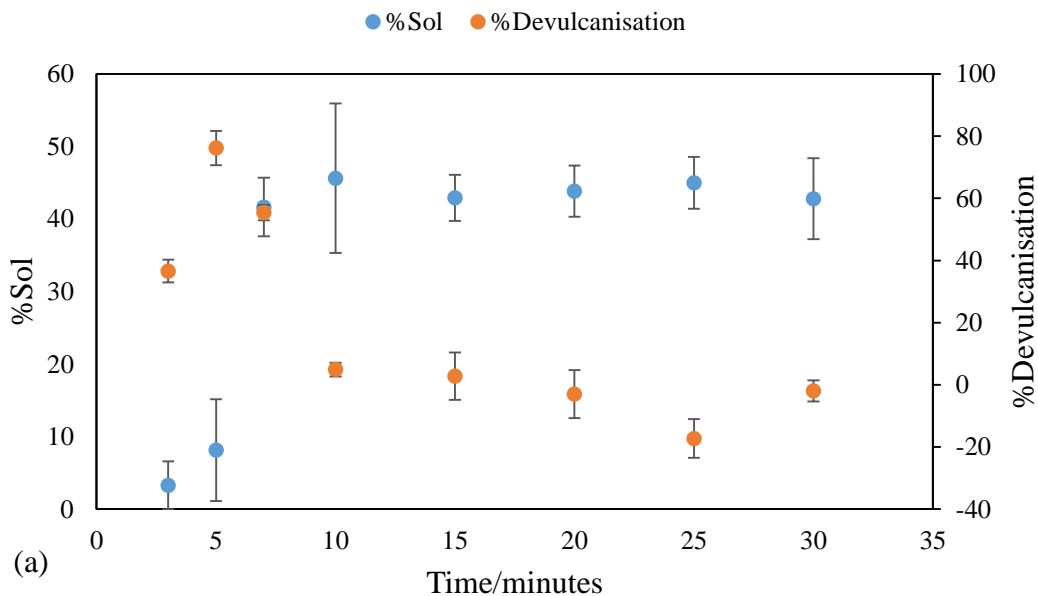


Figure A3: Relation between the % devulcanisation and % sol over time (DD).

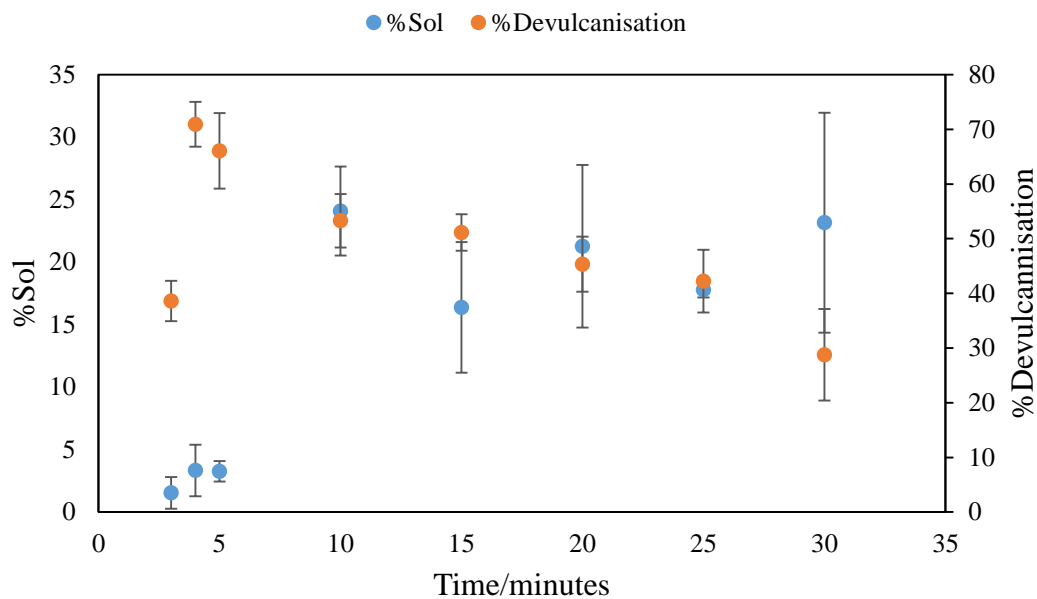
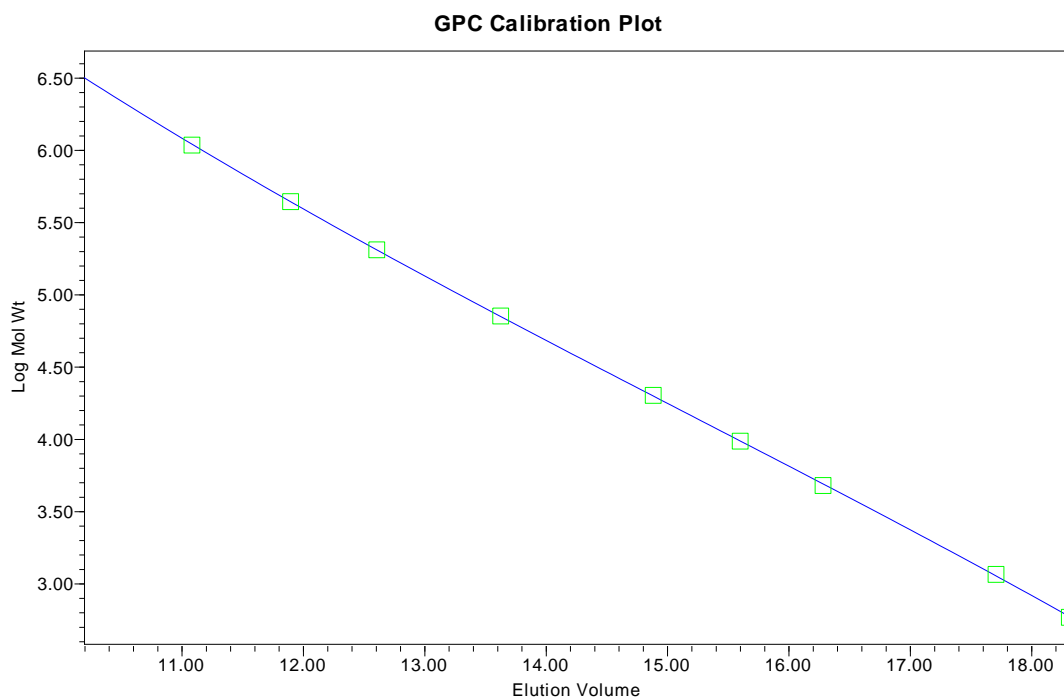


Figure A4: Relation between the % devulcanisation and % sol over time (MBTS).

Table 4A.8: Correlation factors for %sol and % devulcanisation with crosslink density (1/Q)

dA	%Sol:(1/Q)	%D:(1/Q)
DD	0.70	-1.00
MBTS	0.44	-1.00



GPC Relative Calibration Table

	Elution Volume (ml)	Mol Wt (Daltons)	Log Mol Wt	Calculated Weight (Daltons)	% Residual	Ignore [n]	Manual Point	Standard Type
1	9.964	6035000	6.780677			No	No	Narrow
2	11.901	436200	5.639686	435450	0.172	No	No	Narrow
3	14.889	19920	4.299289	19671	1.264	No	No	Narrow
4	17.712	1150	3.060698	1121	2.560	No	No	Narrow
5	10.196	3187000	6.503382	3162352	0.779	No	No	Narrow
6	12.611	202100	5.305566	202301	-0.099	No	No	Narrow
7	15.605	9590	3.981819	9630	-0.417	No	No	Narrow
8	18.317	580	2.763428	587	-1.120	No	No	Narrow
9	11.088	1074000	6.031004	1089963	-1.465	No	No	Narrow
10	13.632	70500	4.848189	69867	0.906	No	No	Narrow
11	16.288	4730	3.674861	4851	-2.485	No	No	Narrow
12	18.250	162	2.209515			No	No	Narrow

Figure A5: Standard curve for polystyrene standards used for Mw determination.

4.3.5 Thermal degradation of SBR

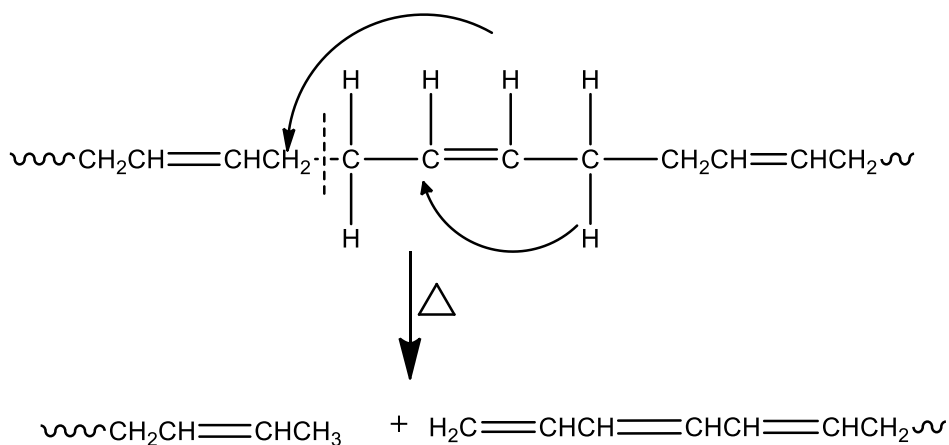


Figure A6: Hydrogen transfer reaction.

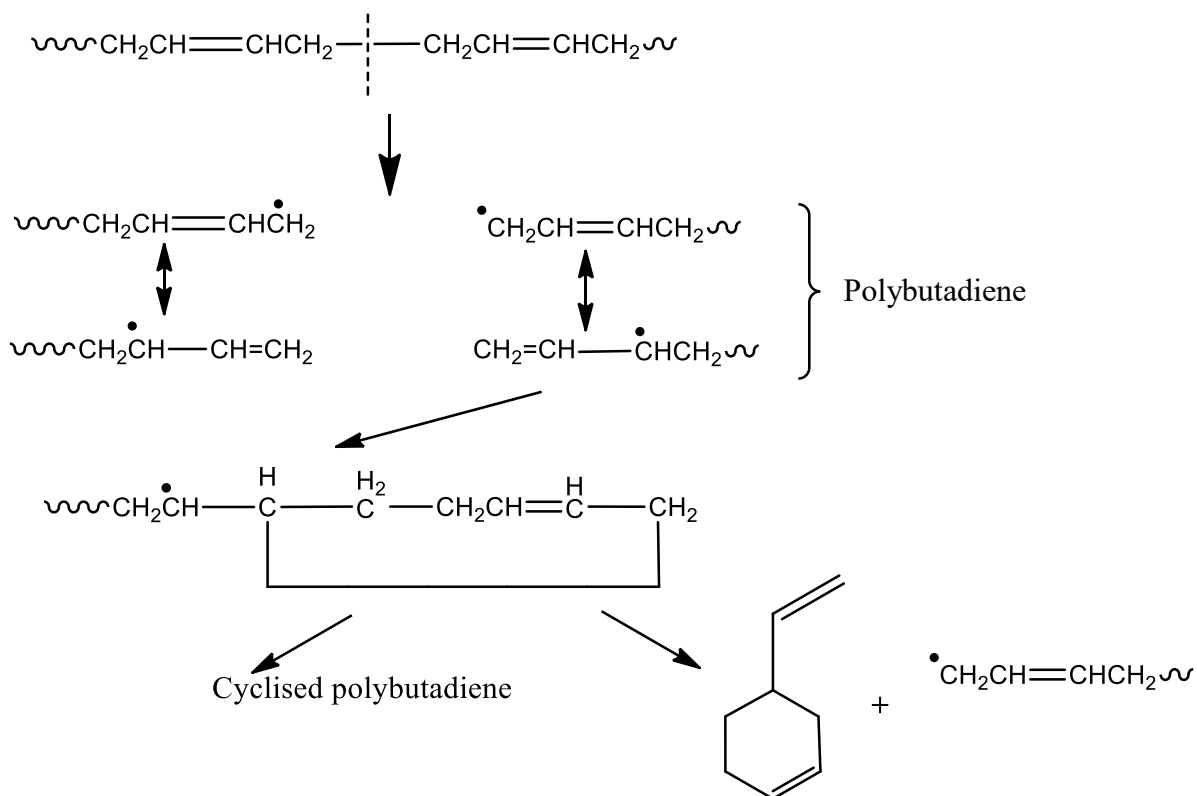


Figure A7: Mechanism of thermal degradation of butadiene units of SBR.

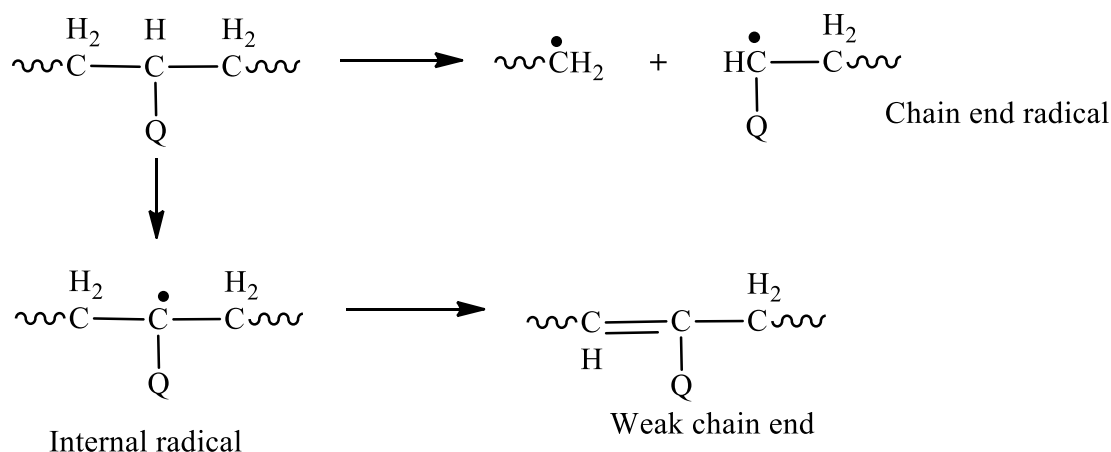


Figure A8: Mechanism of degradation of segments containing styrene units. Where *Q* is a pendant group.

The reaction schemes on Figures A6-A8 shows possible reaction mechanisms used to explain reactions associated with the degradation of styrene and butadiene units in SBR. A lot of reactions are likely to take place upon formation of radicals. These include; crosslinking or hardening (S-S and C-C bond formation), chain scission (C-C scission) and decrosslinking (S-S scission).

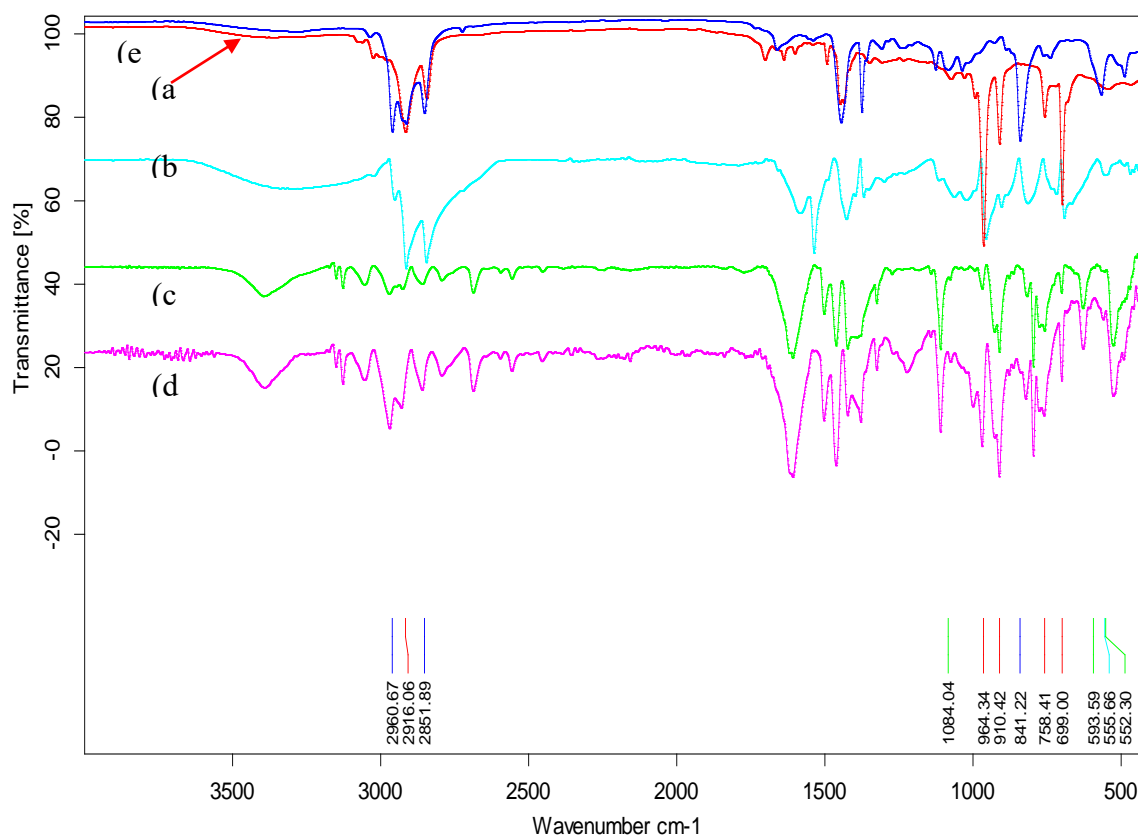


Figure A9: FTIR spectra of gel component.

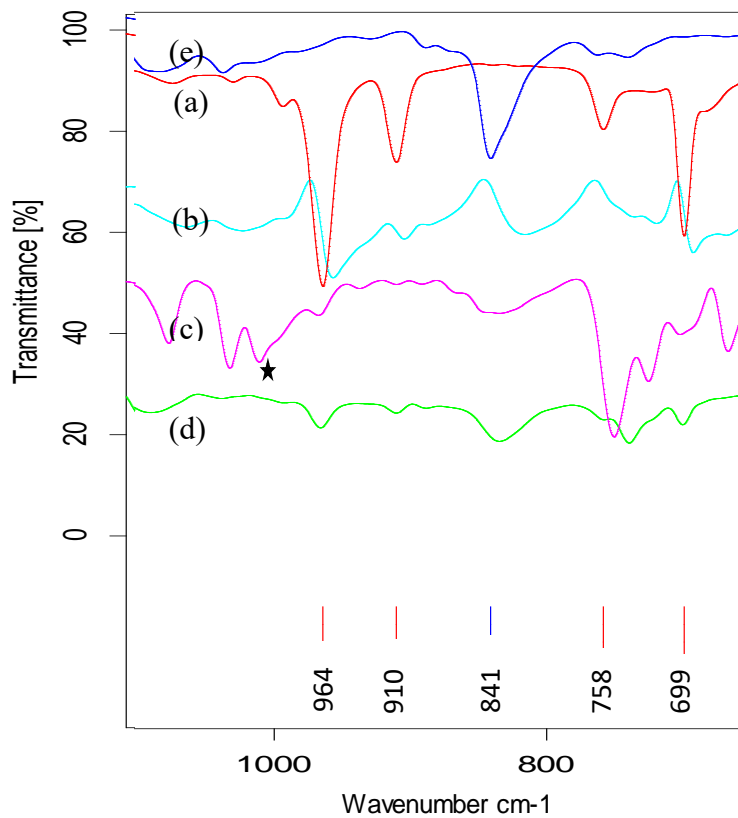


Figure A10: FTIR analysis of DD and MBTS sol component. The spectra shows; a) standard SBR and (e) NR, *i.e.* uncured starting material, b) neat vulcanisate, c) MBTS and d) DD sol components.

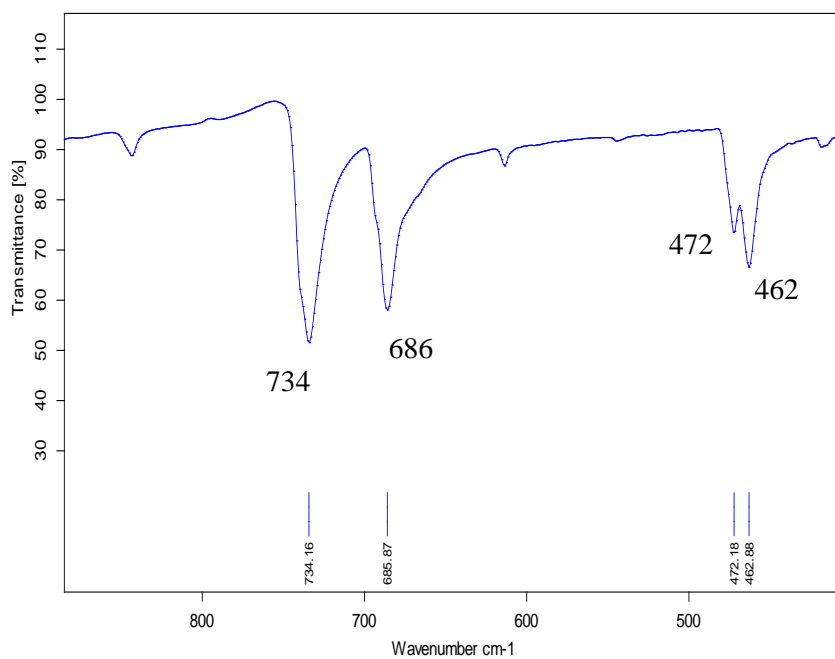


Figure A11: FTIR spectrum of DD.

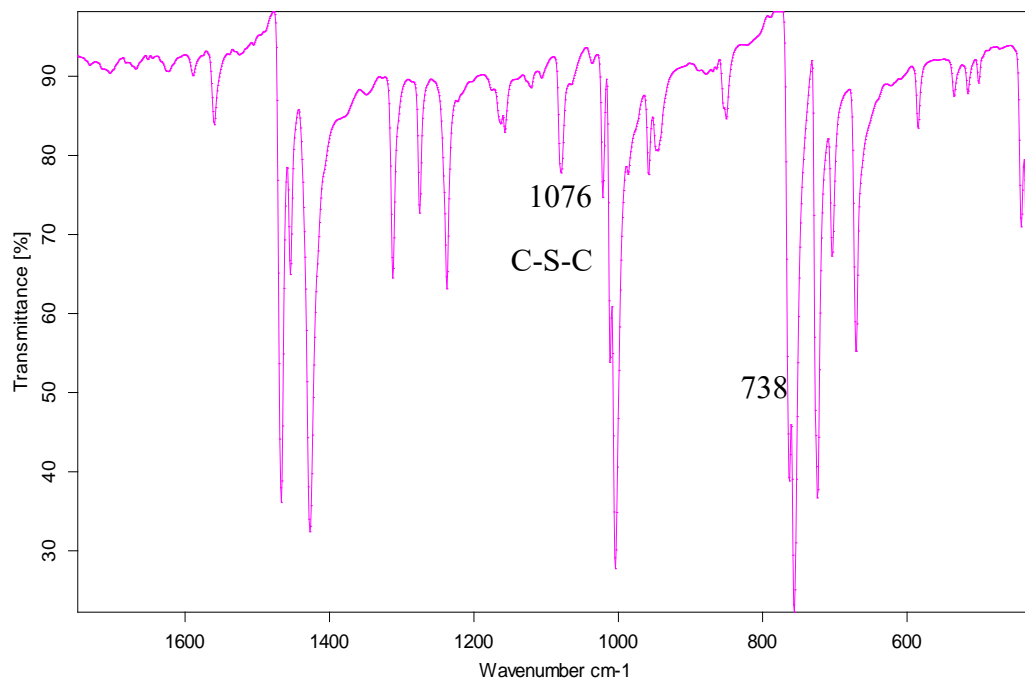


Figure A12: FTIR spectrum of MBTS.

DEVULCANISATION OF CRUMB RUBBER USING OPTIMISED CONDITIONS

5.1 INTRODUCTION

Chapter one of this study highlighted several methods that have been developed to regenerate rubber from waste, while chapter three narrowed these methods to thermo-chemical devulcanisation in supercritical CO₂ medium. The key objective of thermo-chemical devulcanisation in this study is to improve the quality of devulcanised rubber by ensuring scission of crosslink network with minimal chain scission. In chapters three and four, the optimisation focused on manipulating reaction conditions to achieve maximum % devulcanisation instead of % sol. The monitoring of % devulcanisation gives a direct indication of the efficiency of crosslink scission. In this way, incompatibility problems faced due to existence of crosslinks in GTR would be minimised, if not eliminated.

To overcome incompatibility issues of GTR, the crosslink network has to be severed selectively to improve adhesion at a molecular level. Mangili *et al* ^[1] reported that devulcanising GTR up to 50 % devulcanisation could result in an increase in compatibility with virgin NR. This was evidenced by improved mechanical properties of tensile strength and elongation at break. In a report by Zhang *et al* ^[2], 69 % devulcanisation of GTR resulted in an increase in the tensile strength from 13.7 to 23.2 MPa for NR matrix containing 10% GTR. In addition, strain at break was increased by 47% ^[2].

In this chapter, optimised conditions from Chapter two were applied to GTR from a truck tyre tread. Devulcanisation was executed in scCO₂, which has been shown to be an effective and greener medium for devulcanisation ^[1, 3-6]. The quality of the devulcanised GTR was checked by looking into changes in the crosslink density, polymer structure, sol molecular weights and the glass transition temperature.

5.2 METHODS AND MATERIALS

5.2.1 Materials and reagents

The devulcanising agents, DD and MBTS, propane-2-thiol, hexanethiol, and piperidine were purchased from Sigma Aldrich and used as obtained. Also purchased from Sigma Aldrich, the solvents used include; toluene from sigma, acetone, chloroform, heptane and dichloromethane. Liquefied CO₂ was purchased from AFROX chemicals. Cryo-GTR from a truck tyre tread was used in this study. The tyre description (Fig. A5.1 for description key) for the truck tread used for this study was; Firestone T-494 (brand name and design), 7.50-16 (cross-ply construction, 7 inch section width, 50 aspect ratio, 16 inch rim diameter), 118/116 L (load and speed index, L = light truck tyre with 120 km/hour max speed), 76 PSI, made in South Africa, 1916 (19th week of 2016).

5.2.2 GTR preparation

GTR was prepared by size reduction of waste truck tyre tread to small (*ca.* 1-2inch sizes) chips by cutting using a stainless steel knife. These small chips were then downsized to even smaller sizes by cryo-freezing in liquid nitrogen and splintering using a stainless steel hammer. The rubber fragments obtained were cryo-frozen again and further ground to even, smaller sizes using a 150 W Taurus coffee grinder equipped with burr grinding plates in stainless steel housing. Care was taken to minimise heat generation during the size reduction process as presence of heat would compromise rubber integrity.

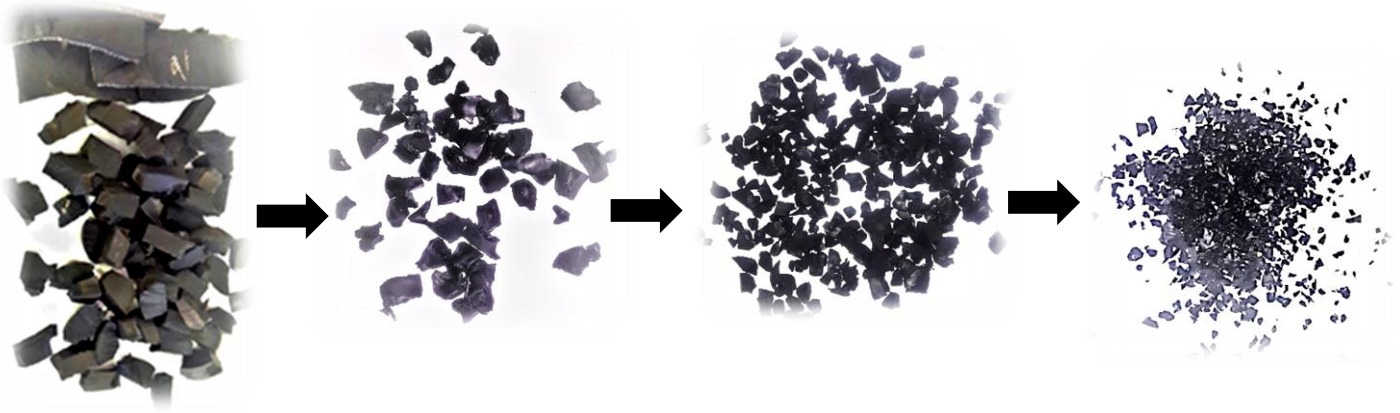


Figure 5.1: Size reduction to achieve coarse grade crumb; $1 < x \leq 2.36$ mm (*i.e.* 8 – 18 mesh) size range. Where x is the rubber particle size used for the study.

5.2.3 Characterisation

5.2.3.1 Size determination

The standard for measuring crumb sizes is the U. S Standard Tyler screen. Mesh is defined as the number of linear openings per inch ^[7]. Therefore more number of openings across the screen surface give a fine mesh. The GTR was sieved by placing it on a 2.36 mm sieve mounted on a 1.00 mm sieve, followed by shaking over a tray for *ca.* 2 minutes (according to ASTM D5603). Rubber particles of size range 1.00 - 2.36 mm (as determined by the ASTM E11 sieves) were chosen for the study.

5.2.3.2 Surface features

Particle surface morphology was mapped using an optical light microscope (Leica S6D).

5.2.3.3 GTR composition

i) Amount of extractables

Low molecular weight compounds were extracted from the GTR by means of soxhlet extraction. The extraction was conducted the same way as in Chapter three. The mass of dry sample before and after soxhlet extraction of GTR was recorded to obtain the amount of extracted material. Drying of samples was done in a forced air ventilation oven overnight at 50 °C.

ii) Moisture content

Moisture content of the sample was determined by drying pre-weighed samples overnight in a forced air ventilation oven. The oven temperature was kept at 50 °C. Samples were allowed to cool to ambient temperature in a desiccator before weighing. Moisture content was then determined by taking mass of sample before and after drying.

iii) Ash content

Muffle calcination was used to determine ash content at 750 °C for 5 hours. Weight of dry samples was determined before and after calcination to obtain ash content. TGA was also applied in the determination of ash content at 600 °C in oxygen atmosphere.

iv) Polymer composition

TGA was used in the determination of polymer composition of extracted GTR samples. This was done at a heating rate of 50 °C min⁻¹ in N₂ (g) atmosphere, which was later switched to O₂ gas at 600 °C for ash content determination. Standard platinum pans were used in the analysis of GTR of sample size 11.7742 mg. The rubber contents were calculated following equation 5.1;

$$\% \text{ Rubber} = \frac{x}{P_{\text{Total}}} \times 100 \% \quad (5.1)$$

Where; % rubber is the percentage of the type of rubber constituent in 100 % of polymer (*e.g.* % NR or % SBR component in the sample), P_{Total} is the total polymer composition of the sample, and x is the % weight change of the respective polymer as shown on the TGA. An example of the calculation is shown on the appendix.

5.2.4 GTR devulcanisation

The GTR samples were stored in a desiccator so as to avoid accumulation of moisture on the samples. The devulcanisation of the GTR was conducted in the supercritical reactor described in Chapter two. The devulcanised GTR (dGTR) was then washed with acetone solvent to get rid of excess dA and acetone-soluble by-products of devulcanisation. This was followed by fractionation to separate the sol and gel components using chloroform solvent. Both the acetone wash and chloroform fractionation were done according to the procedures described in chapter three.

5.2.5 Analysis of GTR and dGTR

The GTR and dGTR were subjected to structural, crosslink density, sol and gel content determination and or analysis. The sol component was analysed using FTIR, for composition and any structural changes, and GPC for molecular weights. The analysis procedures followed for the respective methods mentioned were done the same way as in chapter three.

5.2.6 Determination of crosslink distribution

5.2.6.1 Polysulphidic crosslink determination

Samples were left to stand in 50 mL of n-heptane for 16 hours at room temperature ($23 \pm 1^\circ\text{C}$) in the dark. The heptane was then discarded prior to addition of probe (*i.e.* propane-2-thiol). A

mixture of propane-2-thiol/piperidine in heptane was added until a concentration of 0.4 M with respect to the thiol and amine was attained. The treatment was left to stand for 2 hours at 23 ± 1 °C under nitrogen gas. Treated rubber samples were then washed with 100 mL of n-heptane (4 times each with fresh heptane) and subsequently dried overnight in a vacuum desiccator. The difference in crosslink density (ν) between the neat and treated samples gives the polysulphidic crosslink density.

5.2.6.2 Mono & di-sulphidic crosslink determination

A mixture of n-hexanethiol/piperidine (7 mL and 43 mL respectively) was added to the extracted rubber samples to cleave both polysulphidic and disulphidic crosslinks. The samples were sealed in vacuo and treatment done at 23 ± 1 °C for 48 hours. Monosulphidic crosslink density (ν) was then determined from the treated sample. The di-sulphidic ν would be the difference between the neat and sum of poly and mono sulphidic crosslinks (equation 5.2).

Piperidine was added to both propane-2-thiol and n-hexanethiol to enhance the nucleophilic properties of Sulphur atoms in the piperidium thiolate ion pair. After treatment, samples were extracted with acetone for 12 hours and then dried to constant weight at 50 °C in a vacuum oven.

The crosslink distribution is based on the relative crosslink densities of the mono, di and polysulphidic crosslinks (ν_i) of the treated samples according to equations 5.1-5.3;

$$\nu_{mono} = \nu_{neat} - \nu_{di\&poly} \quad (5.1)$$

$$\nu_{di} = \nu_{neat} - \nu_{poly+mono} \quad (5.2)$$

$$\nu_{poly} = \nu_{neat} - \nu_{mono\&di} \quad (5.3)$$

Where; ν_{neat} is the crosslink density of untreated sample. The distribution would then be given by the relative composition of the type of crosslink;

$$\% \text{ Crosslink type} = \frac{\nu_i}{\nu_{neat}} \times 100\% \quad (5.4)$$

5.3 RESULTS AND DISCUSSION

5.3.1 Characterisation of GTR

5.3.1.1 GTR surface morphology

Cryogenic processing of crumb rubber produces crumb characterised by clean, fractured and shiny surfaces. Under cryogenic conditions most elastomeric materials become brittle, *i.e.* are below their glass transition temperatures (T_g). The T_g is the temperature at which there is a transition from a glassy to rubbery state due to a change in the free volume of a polymer. Truck tyre tread mainly constitutes of NR and synthetic rubbers (*e.g.* SBR and polybutadiene, BR) whose T_g values are above cryogenic temperatures [6, 8]. As such, the tread becomes frozen and brittle under cryogenic temperatures. Hammering and grinding would result in shattering to small particles characterised by smooth, fractured surfaces.

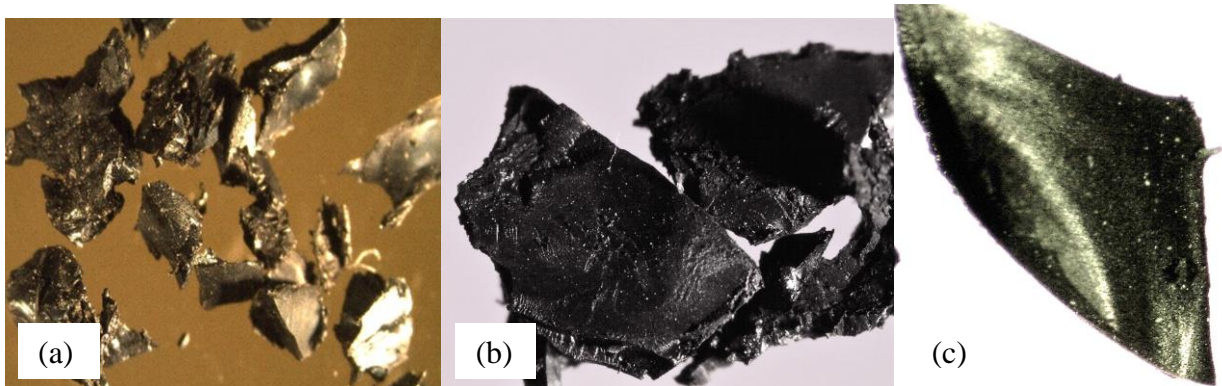


Figure 5.2: Cryogenically ground truck tyre tread produced (a, b and c). *Images taken using a Leica S6D optical light microscope at (a) 10 × and (b & c) 40 × magnification.*

From the surface morphology in Figure 5.2, it can be deduced that the cryogenic crumb processing was effective but some heat was generated, probably due to shear heat generation during the grinding process. The rough surfaces of the cryogenically produced GTR shows evidence of heat generation during grinding of the rubber. Burning of the GTR compromises the

structural integrity of the rubber and subsequently the devulcanised product obtained from it. Figure 5.2 shows that the GTR in (b) and (c) largely have smooth and fractured surfaces. Close inspection of the rubber edges shows some degree of roughness, which is indicative of burning^[8]. Some edges are sharp (from fracturing), as observed on (c), whereas other GTR edges are rough (from burning), as in (b).

5.3.1.2 Determination of GTR composition using TGA

It was shown in chapter three that the type of polymer(s) present and CB content have an influence on the devulcanisation efficiency using DD or MBTS. Also, due to the radical nature of the devulcanisation reaction mechanism, the presence of oils might interfere with the process. Therefore determination of the GTR composition, *i.e.* polymers present, CB content, presence of low molecular weight compounds as well as the ash content is important.

Figure 5.3 shows determination of GTR composition before devulcanisation. The TGA thermogram shows that the GTR contains NR (degrading between 300-400 °C) and synthetic rubbers. The synthetic rubbers can either be SBR or BR or both, considering that their degradation temperatures overlap (in the range 380-500 °C)^[9]. The polymer composition of the GTR was found to be 55.04 % NR and 44.95 % synthetic rubbers.

The CB content for the GTR (34.72 %) was found to be similar to that of the compounded vulcanisates used in chapter three (36.22 ± 1.44 %), implying that the influence of CB on dAs would be comparable. The ash content obtained using the TGA was found to be the same as that obtained using muffle calcination, within measurement error. High ash content can interfere with tyre compounding and be a negative influence^[7].

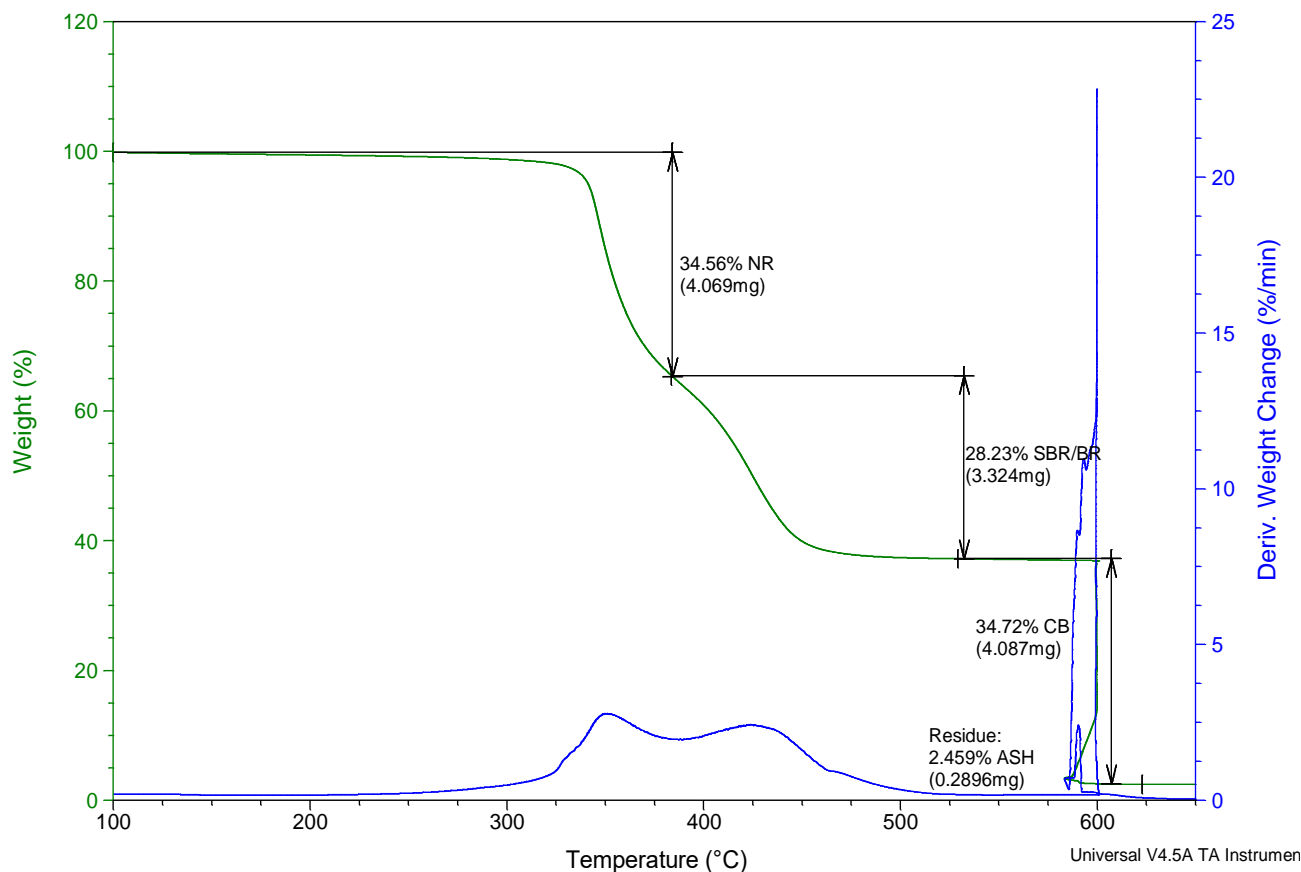


Figure 5.3: Determination of GTR composition using high resolution TGA.

It can be noticed from Fig. 5.3 that the TGA curve does not show the presence of any volatiles, *i.e.* materials with relatively low degradation temperatures (< 250 °C). This is due to soxhlet extraction of the GTR before analysis. The extractable content represents low molecular weight compounds and oils extracted from the crumb *via* soxhlet extraction using the azeotropic acetone/chloroform mixture (ASTM D297).

Table 5.1 shows a summary of GTR composition before it was subjected to devulcanisation. The TGA run was done on one sample, as a result the uncertainty for the respective constituents could not be calculated. Uncertainty could however be determined for runs done on more than three samples, *i.e.* for; the ash content (from muffle calcination), moisture content (from oven drying) and amount of extractable (from soxhlet extraction).

Table 5.1: Summary of GTR composition.

Content	Amount (%)	Uncertainty (95%, CI)
Extractable	7.93	±0.58
Ash (muffle)	2.63	±0.32
Ash (TGA)	2.425	
Moisture	0.0020	±0.0006
CB	34.72	
NR	55.04	
Synthetic rubber	44.95	

*CI = confidence interval

Considering the GTR composition shown in Table 5.1, the optimised conditions and dAs obtained in chapter four can be expected to work when employed in the devulcanisation of the GTR.

5.3.2 Devulcanisation of GTR under optimised conditions

The optimum conditions obtained in chapter four were applied to devulcanise GTR. Table 5.2 shows the optimised reaction parameters followed, note that the amount of rubber devulcanised was kept the same, *i.e.* 1.00 g mass. Also, the set-point temperature dictates the heating profile of the reactor, hence the manner or rate at which the sample will be heated up in the reactor (as shown in chapter two).

Table 5.2: Final optimum conditions obtained for DD and MBTS.

dA	Set-point/°C	Time/minutes	Temp/°C	Rate/°C min⁻¹	dA/g	Pressure/bar
DD	180	5	102	11.94	0.01	80
MBTS	180	4	97	10.73	0.01	80

Figure 5.4 shows the graph obtained after devulcanisation of GTR using optimum conditions. To verify if the optimised conditions were applicable to GTR, *i.e.* gave maximum or comparable %devulcanisation, points on either side of the optimum (*i.e.* ± 1 minute) were run as well.

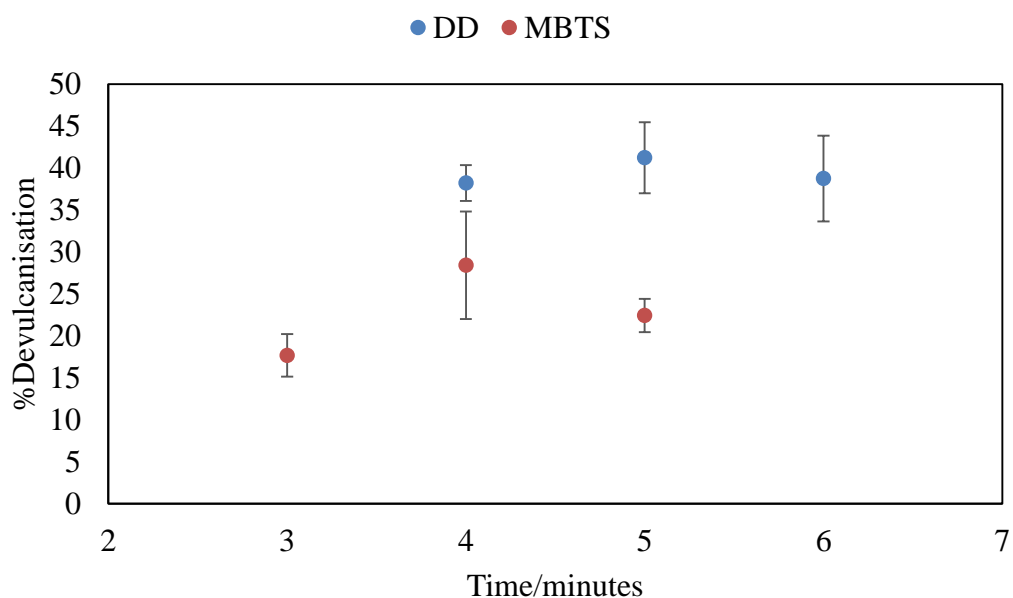


Figure 5.4: Degree of devulcanisation of GTR obtained at optimised conditions. *The optimum times for DD and MBTS are 5 and 4 minutes respectively. The adjacent times were executed to check if there is a decline on either side of the optimum.*

The maximum degree of devulcanisation of GTR is not expected to be exactly the same as that of optimisation experiments due to differences in the substrates (*i.e.* rubber samples) used. Nevertheless, the differences should at least be minimal, considering that the compound formulation used to make vulcanisates for optimisation was for a typical truck tread. On the contrary, the overall % devulcanisation of GTR obtained using optimised conditions was found to be significantly lower than that obtained from optimisation experiments for both dAs. For DD, a maximum of 41.22 ± 4.22 % devulcanisation was obtained, which is about $\frac{1}{2}$ times the amount obtained upon optimisation using the laboratory prepared vulcanisate (LPV), *i.e.* 76.18 ± 5.50 %. For MBTS, a maximum of 28.41 ± 1.97 % devulcanisation was obtained compared to $70.92 \pm$

4.10 % for the LPV. The possible reasons for the different maximum % devulcanisation observed are; different synthetic rubber(s) in the vulcanisates, different network structures (*i.e.* crosslink density and distribution) ^[4, 10], different substrate sizes, and different amounts of CB in the vulcanisates ^[5].

In chapter three it was determined that different dAs behave differently to different types of rubber polymers. For example, DD was seen to result in relatively more NR than SBR devulcanisation. Therefore the presence of BR might have a negative influence on % devulcanisation. It seems that, although the formulation used to make the compounded rubber in chapter three is for a typical truck tyre tread vulcanisate, the minor differences in the formulation might have consequences on the % devulcanisation. The GTR showed presence of BR rubber instead of just SBR as used in the compound formulation in chapter three.

It seems that, although the crosslink density would likely influence the % devulcanisation, since according to its expression, % devulcanisation is sensitive to changes in initial crosslink density (chapter three, equation 3.3), its influence is overshadowed by the other mentioned factors. This is deduced from comparison of the crosslink densities of the GTR (0.004100 ± 0.000052) and the LPV (0.00460 ± 0.00038). From the crosslink density values it would be expected that the higher crosslink density result in lower % devulcanisation, however, lower % devulcanisation was observed for GTR. In view of this, it is likely that the GTR vulcanisate has more of monosulphidic crosslinks than polysulphidic crosslinks. Knowledge of the GTR crosslink distribution would therefore aid in understanding its contribution towards % devulcanisation.

Different cure systems as well as heat ageing result in different network structures ^[4, 10, 11]. Therefore the types and density of crosslinks would not be the same. The compounded vulcanisates followed a CV cure system, which results in a high degree of polysulphidic crosslinks. Even after a week of accelerated aging at 70 °C, the composition of polysulphidic crosslinks would still be quite significant. Kojima *et al* ^[4] reported on the influence of varying the sulphur to accelerator ratio on devulcanisation. In their report, they found that for an EV cure system (*i.e.* more monosulphidic crosslinks formed) the degree of devulcanisation is reduced compared to that of a CV system (*i.e.* with more polysulphidic crosslinks). Cuneen *et al* ^[10] reported that as the tyre ages due to thermal degradation during service, the amount of monosulphidic and disulphidic crosslinks increase at the expense of polysulphidic crosslinks. DD

is known to be more effective in polysulphidic crosslink cleavage [4, 8], whereas not much is known or reported about MBTS (as far as the author is aware). Thus a change in the distribution of crosslinks would definitely affect the efficiency of devulcanisation. Fig. 4.5 shows the crosslink distribution of the one week aged LPV and GTR before they were subjected to devulcanisation.

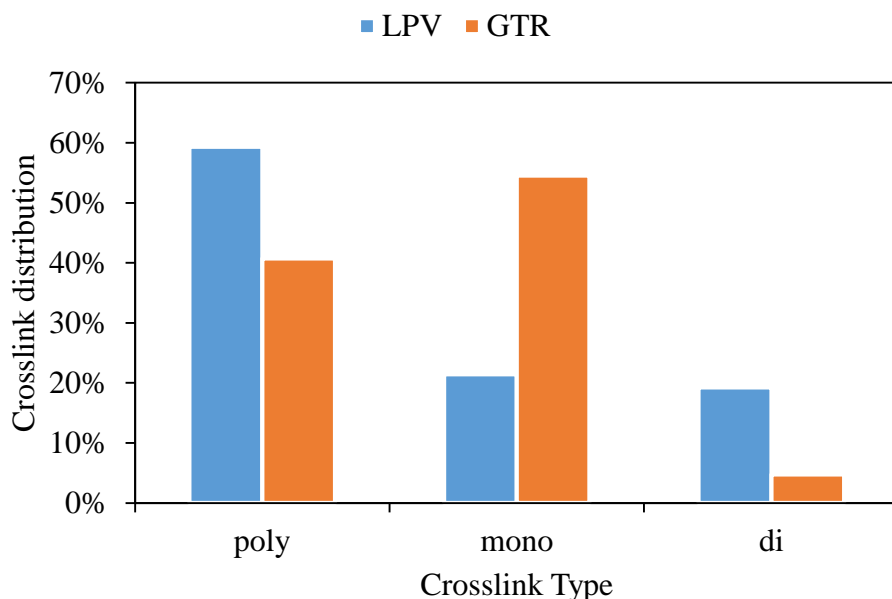


Figure 5.5: Crosslink distribution of LPV and GTR.

From Figure 5.5, it is evident that the relatively high degree of mono-sulphidic and low polysulphidic crosslinks present in the GTR are the main cause of the relatively low degree of devulcanisation of GTR observed. On the other hand, the LPV had a relatively high amount of polysulphidic and low mono-sulphidic crosslinks, which would explain why a relatively high degree of devulcanisation was observed for the LPV. A lot of dAs have been reported to be incapable of cleaving monosulphidic crosslinks [8]. As a result, a crosslink network with a high degree of mono-sulphidic crosslinks would be hard to cleave, thereby resulting in a low degree of devulcanisation.

Differences in the content of CB is expected to influence the degree of devulcanisation. However, the CB content is relatively similar for GTR and compounded vulcanisate (*i.e.* 34.72

% vs. 36.22 ± 1.41 % respectively), thus it cannot result in any significant differences in % devulcanisation.

The differences in the % devulcanisation could also be due to differences in vulcanisate sample sizes and morphology (*i.e.* 1.00 – 2.36 mm GTR vs. (*ca.* 20 x 35 mm) sheets of rubber). This effect would likely be due to the differences in the surface areas of the samples. Surface area is known to have an influence on the rate of chemical reactions ^[8, 12]. The higher the surface area the faster the reaction and vice versa. Contrary to this expectation, the high surface area provided by the small particle sized GTR did not result in any increase in the degree of devulcanisation. Instead, high % devulcanisation was observed for the LPV. This observation leads to the deduction that surface area only influences the reaction rate and not the yield of a reaction. (Note that this is opposed to the effect of heating rate or temperature, which was found to influence both the rate as well as the degree of devulcanisation in chapter three).

Single factor ANOVA was executed to compare the sample averages. This would assist in drawing conclusions as to whether the observed % devulcanisation at the optimised time can be improved or not. The null hypothesis used was;

$$H_0 : \mu_{t1} = \mu_{t2} = \mu_{t3},$$

Where; μ_{ti} is the sample average % devulcanisation at time *i* –minutes.

Table 5.3: Single factor ANOVA for DD devulcanisation of GTR

Summary						
Groups	Count	Sum	Average	Variance		
4	3	114,63	38,21	0,74		
5	3	123,68	41,23	2,89		
6	3	116,26	38,75	4,24		

ANOVA						
Source of Variation	SS	df	MS	F	P-value	F crit
Between Groups	15,52	2	7,76	2,96	0,13	5,14
Within Groups	15,74	6	2,62			
Total	31,26	8				

Table 5.3 shows that there are no significant differences in the averages of % devulcanisation using DD between the optimum time and the adjacent times (ANOVA, $p = 0.13$). The null hypothesis is therefore accepted. This implies that there is no defined or absolute maximum degree of devulcanisation obtained, the % devulcanisation at the optimum (5 mins) is similar to that of adjacent times (4 and 6 mins). Therefore there may be need to determine what happens at more different devulcanisation times (*i.e.* time optimisation using the GTR sample and not the compounded vulcanisate).

Table 5.4: Single factor ANOVA for MBTS devulcanisation of GTR

Summary						
Groups	Count	Sum	Average	Variance		
3	3	53.00	17.67	1.05		
4	3	85.24	28.41	6.63		
5	3	67.24	22.41	0.63		

ANOVA						
Source of Variation	SS	df	MS	F	P-value	F crit
Between						
Groups	173.92	2	86.96	31.38	0.00066	5.14
Within Groups	16.62	6	2.77			
Total	190.54	8				

Table 5.4 shows that at least one pair of the samples differs significantly with respect to the average % devulcanisation (ANOVA, $p = 0.00066$). Therefore the null hypothesis is rejected, since the average % devulcanisation at the different times are not the same within measurement error. Figure 5.4 shows an increased % devulcanisation using MBTS at the optimum time (4 mins) compared to surrounding times (3 and 5 mins), implying that a maximum % devulcanisation value was reached. However, this value is also relatively lower (about $\frac{1}{2}$ times) than that obtained from devulcanisation of compounded vulcanisates using MBTS. Sample t-tests to identify which of the sample pair results in differences of the average % devulcanisation are not necessary in this case since the primary concern is to determine if the % devulcanisation at the different times (*i.e.* 3, 4 and 5 mins) are the same or not; hence establish if a maximum % devulcanisation value is reached at optimum conditions.

5.3.4 Analysis of devulcanisation products

5.3.4.1 Determination of molecular weights and distribution.

GPC was used in the determination of molecular weights of the sol components produced during devulcanisation using DD and MBTS. A conventional calibration method using polystyrene standards was used to determine molecular weights. The calibration curve is shown in the appendix section of chapter three.

Table 5.5: Molecular weights as determined by GPC

Sample (DD)	Mn/Da	Mw/Da	PDI
^a Masticated	14 311	57 612	4.02
DD	16 168	48 986	3.03
MBTS	15 600	43 557	2.79

a = the masticated NR/SBR rubber during compounding of LPV

The range of molecular weights shown in Table 5.5 are quite close to that of the masticated rubber for both dA. This may imply a lower degree of chain scission occurring during the devulcanisation process at the optimised conditions. However, it is important to note that the degree of mastication may differ depending on the mixing procedure, so the degree of mastication used in compounding the GTR samples could be different to that obtained in the case of the LPV. As such, the masticated sample in this case does not serve as a standard of reference, but serves to just give an approximate idea of Mw likely to be obtained upon mastication. As observed in chapter 3 on molecular weights obtained, the PDI for MBTS is still lower than for DD. The preferential devulcanisation observed with DD might be the reason for its relatively broader PDI compared to MBTS.

5.3.4.2 FTIR analysis of the GTR and sol components

Fractionation of sol and gel results in separation of liberated linear polymer chains that are soluble in suitable solvent, *e.g.* chloroform in this case, from the insoluble gel. Gel component represents the part of vulcanisate that still has crosslinks. Figure 4.6 shows the presence of NR and SBR/BR polymer chains in the sol component as evidenced by the overlay of peaks from the two polymers with those of the sol component. Vibration bands in the $3100 - 2000 \text{ cm}^{-1}$ and $1500 - 400 \text{ cm}^{-1}$ regions are attributed to C–C and C–H bonds of the macromolecules. At 841 cm^{-1} is the C – H out of plane bending of the cis–1, 4 addition characteristic of NR, which is also present in the sol but not on SBR/BR. This band can only be attributed to presence of cis – 1, 4 isoprene monomer.

Strong asymmetrical $-\text{CH}_2$ and symmetrical $-\text{CH}_2$ stretching of methylene group vibrations present in NR are observed around 2960 and 2851 cm^{-1} respectively ^[13]. Bands occurring at around 2960 cm^{-1} are characteristic of polymers containing the methyl group, and have two distinct vibrations. According to Chaudhry *et al* ^[14], the first band results from asymmetrical stretching where two $-\text{C}-\text{H}$ bonds of the methyl group extend while the third one contracts. The second band arises from symmetrical stretching in which all three of the $-\text{C}-\text{H}$ bonds extend and contract in phase.

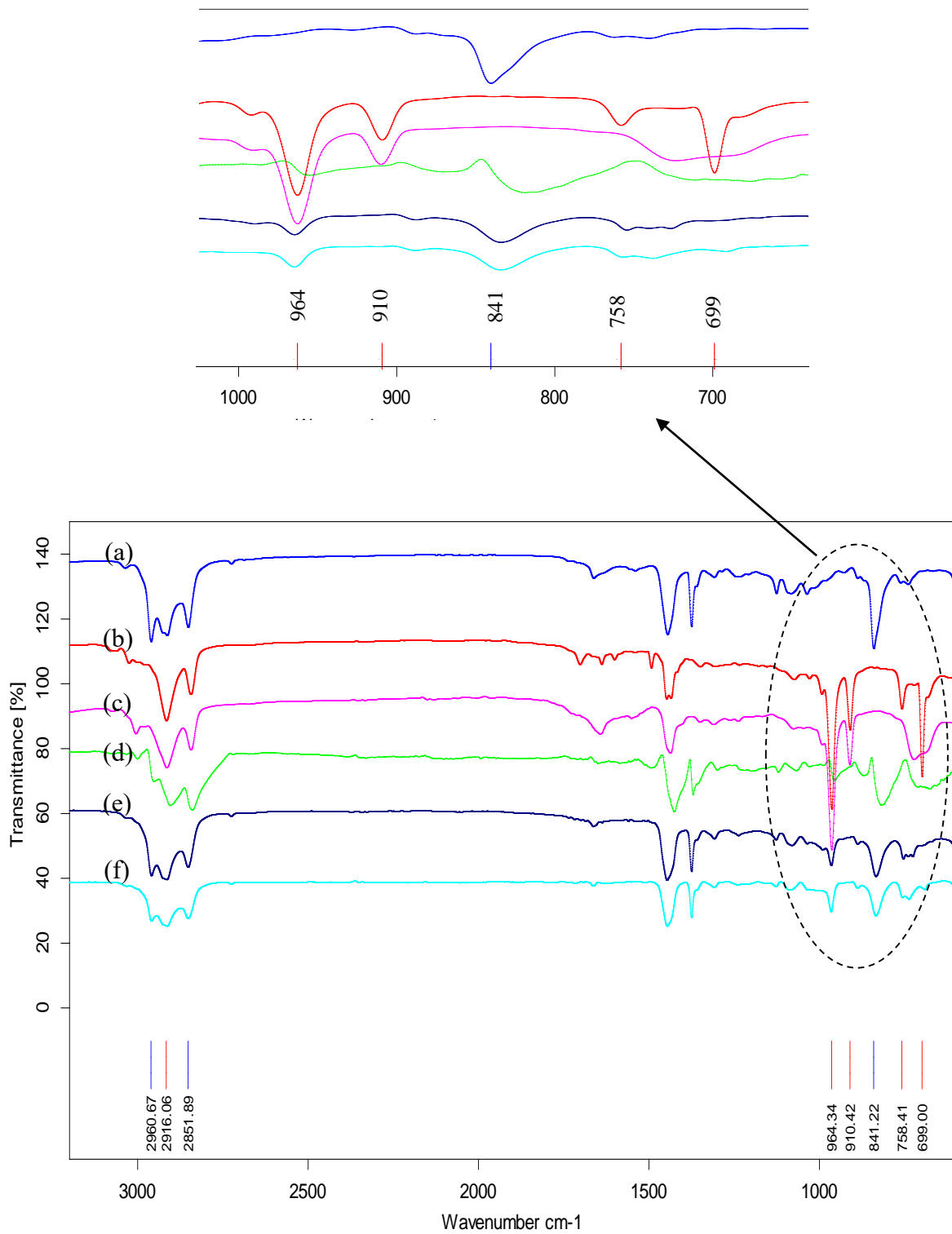


Figure 5.6: FTIR analysis of d) neat GTR and sol components obtained from devulcanisation using (e) DD and (f) MBTS. (a), (b) and (c) represent raw NR, SBR and BR respectively.

The FTIR spectrum for the synthetic component of the sol shows bands at; 758 cm^{-1} due to 1,4-cis; 910 cm^{-1} due to 1,2-vinyl; and 964 cm^{-1} due to 1,4-trans-butadiene units ^[15]. The differences in peak shapes and intensities are an indication of modifications of the structural integrity of the polymer chains. A decrease in intensity is observed for the 1,4-trans-butadiene units (at 964 cm^{-1}), which implies modifications in the backbone structure due to devulcanisation ^[6]. The same observation was made for the 1,2-vinyl peaks. The bands around the regions; 699 and 758 cm^{-1} , indicate modifications due to the presence (*i.e.* attachment to the polymer chain) of dA pendant groups; *i.e.* phenyls at 686 and 738 cm^{-1} respectively ^[6] (FTIR spectrum of dAs shown in appendix). In the observed spectra, the peaks at 758 cm^{-1} are probably a combination or overlap of the 1,4-cis-butadiene units and the phenyl component of dA at 738 cm^{-1} , which would explain the observed broad peaks with slight crowning. The bands at 699 cm^{-1} have become so broad it is impossible to ascertain if there is a polystyrene or butadiene component. The neat GTR however shows a peak similar in shape to the BR spectrum (*i.e.* at 699 cm^{-1}), which may indicate the presence of BR and not SBR. However, the same peak can be as a result of modification of the polystyrene peak due to vulcanisation. The spectrum for the neat GTR shows that modifications of chains also occurs upon vulcanisation. This is observed from changes or distortions in intensity and shapes of basically all the peaks shown (*i.e.* at 964, 910, 758, and 841 cm^{-1}).

The FTIR spectra obtained for the gel component in Figure 5.7 shows the presence of similar peaks observed in the sol component. Observable differences are marked on the spectra; new peaks (starred) at 523 cm^{-1} due to S-S bonds (can be crosslinks or sulphide links formed upon attachment by dA pendant group); at 910 cm^{-1} there is peak crowning indicating modification of the 1,2-vinyl units, and at 1100 cm^{-1} there is a thiocarbonyl group (C=S). The absence of the C=O peak at 1715 cm^{-1} and the C-O peak at 1270-1255 cm^{-1} indicates the absence of thermo-oxidative degradation ^[16]. These observed modifications can be explained by the possible mechanisms of devulcanisation proposed by Adhikari *et al* ^[8] and Rajan *et al* ^[17] (in chapter one). The structures derived from the possible mechanisms are shown in the Appendix section Scheme A1. Interestingly, the peak at 699 cm^{-1} in Figure 5.7 is sharper than that observed in Figure 7.6. This peak's shape was quite similar to that of BR in Figure 5.6, however, in Figure 5.7 the spectrum is similar to that of the polystyrene unit of SBR. This may be due to dA attachments in the sol component and not on the gel at that region, or simply the presence of SBR and BR in the GTR.

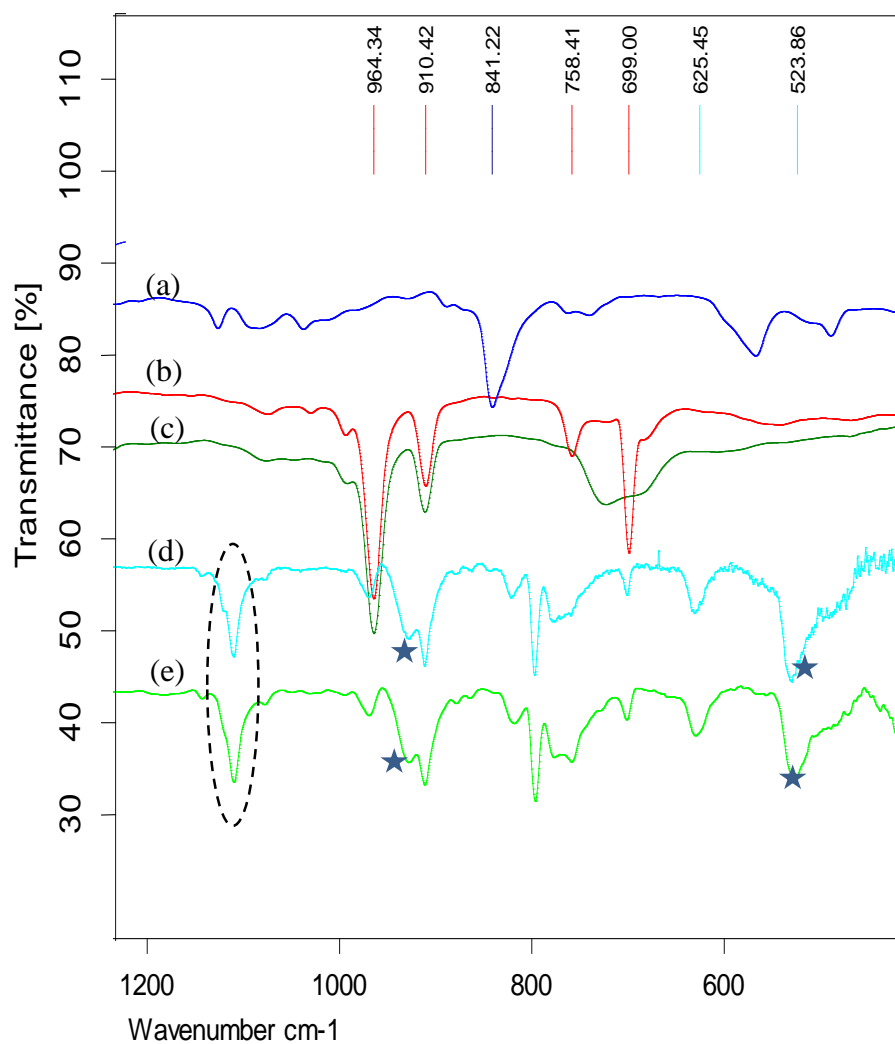


Figure 5.7: FTIR spectra of GTR devulcanisates showing (a) raw NR, (b) raw SBR, (c) raw BR, and GTR devulcanisates obtained from using (d) DD and (e) MBTS. *Only the peaks of interest are shown, the full spectrum is shown on the Appendix.*

5.3.4.3 Glass transition determination, T_g.

The glass transition temperature (T_g) of the gel components was determined to check if there were any significant changes in the structure of the constituent polymers. The T_g graph obtained shows only NR and no synthetic components. This might be due to that during T_g determination, the DSC instrument detects changes in the heat capacities of constituent polymers. And since the relative composition of the synthetic part was small, changes in the heat capacities detected were insignificant. As a result, only the T_g for the major component polymer (*i.e.* NR) was detected. Nonetheless, the graphs show that the T_g of NR (-60.75 °C in the neat GTR) did not change much after devulcanisation. The observed slight shifts towards higher temperatures can be explained by attachment of dA forming pendant groups (which restrict mobility of chains). However, this shift is too small to be considered as a change in the T_g. This might imply low degree of compromise in the structural integrity or rubber quality due to devulcanisation.

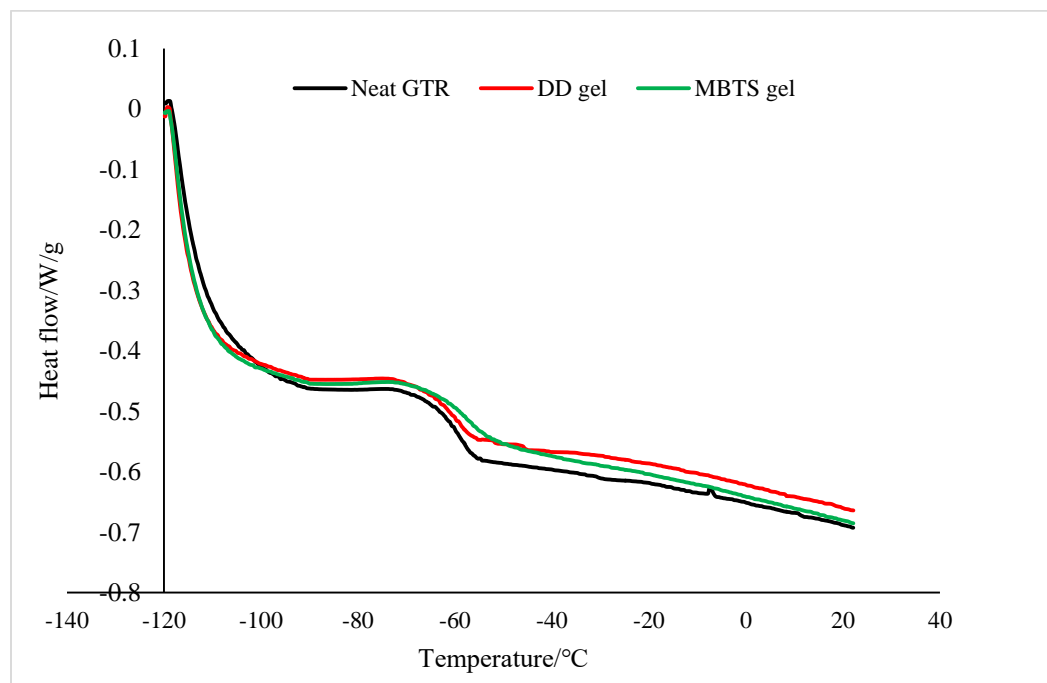


Figure 5.8: T_g of GTR gel samples for neat GTR, devulcanisates of DD and MBTS. *The T_g was found to be -60.75 °C, in the range -64.70 to -56.36 °C as shown on Figure 5A.3*

Table 5.6: Summary of GTR devulcanisation outputs

	GTR	^a GTR _{DD}	^b GTR _{MBTS}
1/Q	0.0041 ± 0.000053	0.0024 ± 0,000170	0.0032 ± 0.000082
% Devulcanisation	–	41.22 ± 4.22	22.41 ± 1.97
% Sol	7.16 ± 1.46	32.21 ± 9.80	20.83 ± 4.89
% Gel	92.83 ± 1.46	67.78 ± 9.80	79.17 ± 4.89

a & b = GTR devulcanised by DD and MBTS respectively

Table 5.6 shows that the sol content obtained with the GTR was relatively higher compared to the one obtained for the devulcanisates in chapter four, Table 4.16 (32.21 ± 9.80 vs. 8.13 ± 7.00 and 20.83 ± 4.89 vs. 3.33 ± 2.07 , for DD and MBTS respectively). Despite differences in the crosslink networks, differences in morphology certainly played a significant role in the production of the relatively high sol content observed for the GTR. In chapter three, the samples used were rectangular sheets of dimensions 20×35 mm, whereas, the GTR used was crumbs of dimensions in the range 1.00-2.36 mm thus having a relatively high surface area based on particle size. The relatively small sized GTR provided more surface area for heat distribution and subsequently more sol production than crosslink scission. Also, the morphological study of GTR revealed evidence of scorching, especially on the GTR edges (Figure 5.2). This most likely contributed to the high sol contents, which can even be observed for the control (untreated) GTR sample, which has an exacerbated % sol of 7.16 ± 1.46 .

5.4 SUMMARY OF FINDINGS

- The cryo-ground GTR was characterised by a general smooth surface with fractured edges. Some degree of roughness was also observed especially on the edges.
- The sol content obtained for both dAs was quite higher than expected from optimisation experiments (32.21 ± 9.80 vs. 8.13 ± 7.00 and 20.83 ± 4.89 vs. 3.33 ± 2.07 , for DD and MBTS respectively). On the other hand, the degree of devulcanisation obtained using the optimised results on the GTR was found to be significantly lower than that obtained on the LPV for both DD and MBTS (41.22 ± 4.22 % vs. 76.18 ± 5.50 % and 28.41 ± 1.97 % vs. 70.92 ± 4.10 % respectively).
- The degree of chain scission in the GTR, as shown by Mw of sol and the associated PDI, was relatively lower than that of the masticated LPV sample for both DD and MBTS (PDI= 3.03 and 2.79, respectively, compared to PDI = 4.02 for LPV).
- FTIR analysis showed slight modifications of the polymer structure due to devulcanisation. The absence of carbonyl groups in the sol and gel components were proof that thermo-oxidative degradation was successfully avoided. The FTIR showed presence of both SBR and BR in the GTR, from sol and gel analysis.

5.5 REFERENCES

1. Mangili, I., et al., *Polymer Degradation and Stability*, 2014. **102**: p. 15-24.
2. Zhang, X., C. Lu, and M. Liang, *Journal of Polymer Research*, 2009. **16**(4): p. 411-419.
3. Jiang, K., et al., *Journal of Applied Polymer Science*, 2013. **127**(4): p. 2397-2406.
4. Kojima, M., et al., *Rubber Chemistry and Technology*, 2003. **76**: p. 957-68.
5. Kojima, M., et al., *Journal of Applied Polymer Science*, 2005. **95**: p. 137-143.
6. Liu, Z., et al., *Polymer Degradation and Stability*, 2015. **119**: p. 198-207.
7. Rouse, M.W., *Rubber recycling; Manufacturing practices for the development of crumb rubber materials from whole tires*, ed. S.K. De, A.I. Isayev, and K. Khait. 2005: Taylor and Francis Group.
8. Adhikari, B., D. De, and S. Maiti, *Progress in Polymer Science*, 2000. **25**: p. 909-948.
9. Rybinski, P., A. Kucharska-Jastrzabek, and G. Janowska, *Modification of Polymers*, 2014. **56**(4): p. 477-486.
10. Cunneen, J.I. and R.M. Russell, *Journal of the Rubber Research Institute of Malaya*, 1969. **22**: p. 300.
11. Fan, R.L., et al., *Polymer Testing*, 2001. **20**: p. 925-936.
12. Oey, T., et al., *Journal of the American Ceramic Society*, 2013. **96**(6): p. 1978-1990.
13. Arroyo, M., M.A. Lopez-Manchado, and B. Herrero, *Polymer*, 2003. **44**(8): p. 2447-2453.
14. Chaudhry, A.N. and N.C. Billingham, *Polymer Degradation and Stability*, 2001. **73**(3): p. 505-510.
15. Sarkar, M.D., P.P. Mukunda, and A.K. Bhowmick, *Rubber Chemistry and Technology*, 1997. **70**(5): p. 855-870.
16. Wang, S.M., J.R. Chang, and R.C.C. Tsiang, *Polymer Degradation and Stability*, 1996. **52**: p. 51-57.
17. Rajan, V.V., et al., *Journal of Applied Polymer Science*, 2007. **104**(6): p. 3562-3580.

5.6 APPENDIX



Figure 5A.1: Description of typical tyre nomenclature (taken from Wikipedia).

1) TGA composition calculation

$$\% \text{ Rubber} = \frac{x}{P_{\text{Total}}} \times 100 \% \quad (4.1)$$

As an example, % NR content;

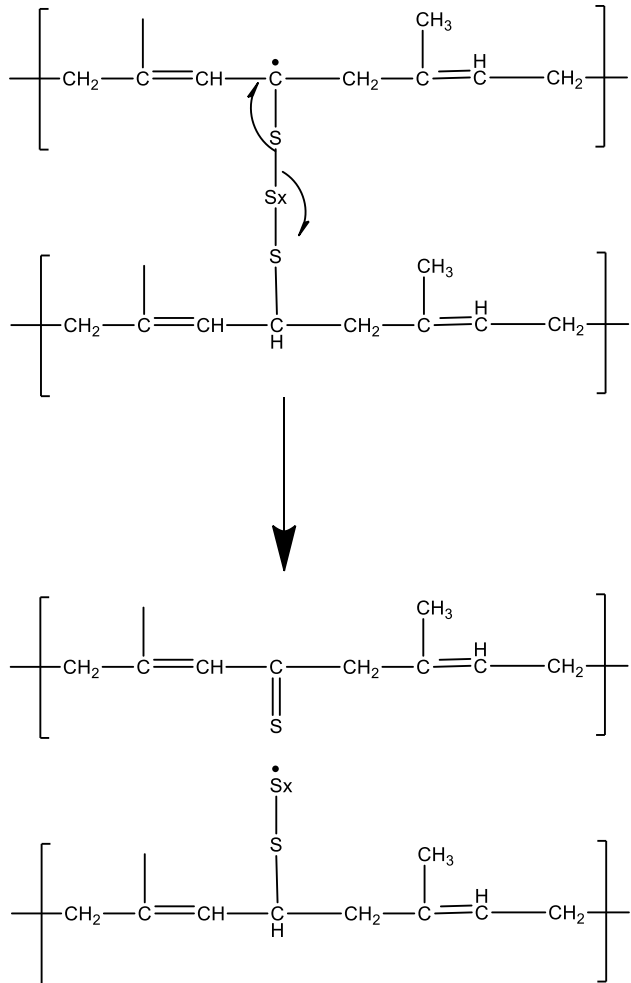
$$\begin{aligned} \% \text{ NR} &= \frac{34.56}{62.79} \times 100 \% \\ &= 55.04 \% \end{aligned}$$

2)

$$1 - \frac{v_{e2}}{v_{e1}} = 1 - \frac{\gamma_2 \left(1 - s_2^{\frac{1}{2}}\right)^2}{\gamma_1 \left(1 - s_2^{\frac{1}{2}}\right)^2} \quad (3.2)$$

Where; γ_1 and γ_2 are the crosslinking indexes before and after degradation.

3) Formation of pendant groups and thiocarbonyls during crosslink scission.



- *The radical on the allylic carbon is a result of allylic hydrogen abstraction as proposed.*
- *This induces crosslink cleavage.*

- *Thiocarbonyls are formed*

- *Pendant groups would then form by attachment of dA (capping) onto the free sulphide radical formed.*

Scheme1: Possible reaction mechanism for the formation of thiocarbonyls and dA pendant groups (*adapted from Rajan et al* ^[17]).

4) Full FTIR spectra for the GTR gel component

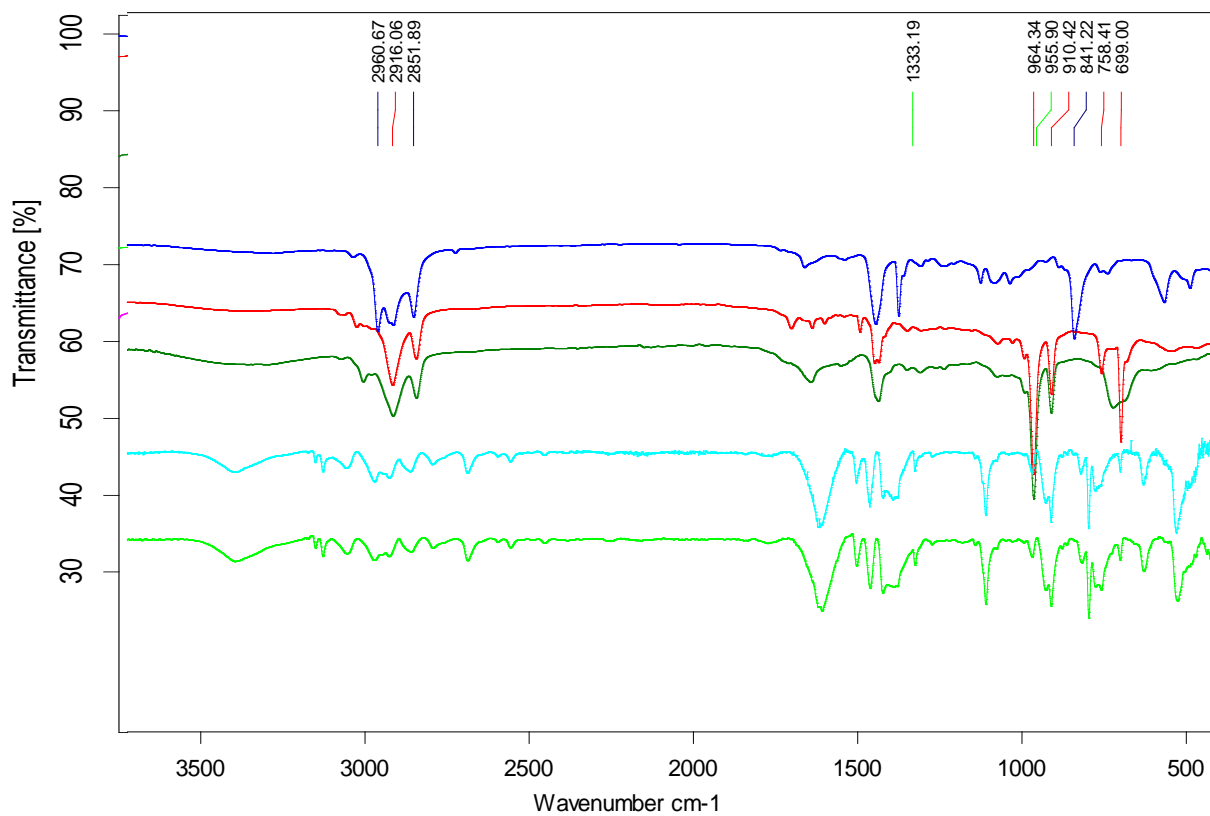


Figure 5A.2: FTIR spectra for the gel component.

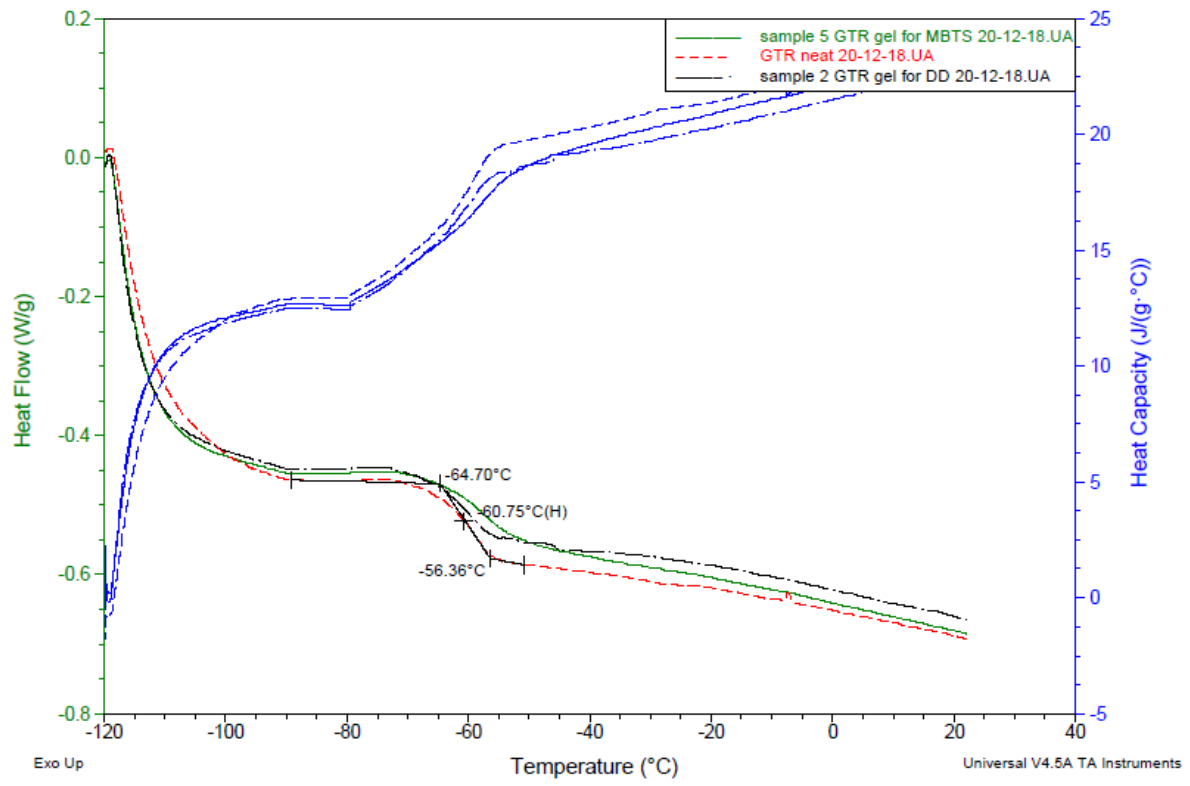


Figure 5A.3: Tg of GTR gel samples for neat GTR, devulcanisates of DD and MBTS.

CHAPTER 6: CONCLUSIONS AND RECOMMENDATIONS FOR FUTURE WORK

6.1 CONCLUSIONS

The study showed that in achieving isothermal conditions to conduct devulcanisation reactions, a lot of chemical events would have occurred during the temperature ramp or non-isothermal stage. This was shown by a relatively higher degree of devulcanisation during the non-isothermal period compared to the overall or isothermal run. This realisation has positive implications of cutting down on time spent in running reactions, resulting in lower production costs due to time and energy savings. As an example, instead of running a reaction for 1 hour, optimisation has shown that the reaction can be run in 5 minutes, resulting in a high degree of crosslink scission. However, due to the scope of this research, the quality of the devulcanisates were not tested by means of blending with virgin rubber material to check for changes in mechanical properties.

In practice, chain scission is unavoidable, but the study showed that it can be minimised. It has shown that high degree of crosslink scission at low sol production is achievable upon optimisation using the degree of devulcanisation as the response variable. The study established that the % devulcanisation is a good and direct indicator of crosslink density changes *via* determination of the correlation factors of % devulcanisation and % sol with changes in crosslink densities. The high degree of swelling accompanied by a low sol content corroborates Horikx theory of selective crosslink scission. As such, the findings from this work are relevant to the devulcanisation industry as most devulcanisation processes optimise processes by tracking the sol content, which makes it challenging in directly determining the degree of crosslink scission during the process. The use of sol content as a response variable to optimise devulcanisation processes is likely to work best on condition it is accompanied by molecular weight determinations to monitor the extent of chain degradation. Therefore the best approach in maximising crosslink scission while maintaining minimal chain scission is by tracking the % devulcanisation as was done in this study. This way, reclaim with a relatively higher degree of broken crosslinks than the main chains can be obtained.

DD and MBTS proved to be effective devulcanising agents in scCO₂; which proved to be an efficient medium for devulcanisation. Relatively higher extent of devulcanisation was achieved using DD (76.8 ± 5.50 %) as compared to MBTS (70.92 ± 4.10 %) in a period of 5 and 4 minutes respectively. The choice of devulcanisation agent to use industrially would be partly influenced by the attributes determined from experimental findings as listed in Table 4.16. Unsatisfactory attributes of DD involve relatively high cost and uneven devulcanisation of the NR/SBR polymer blend, which has been shown to impart negative effects on final properties of rubber. Its advantage is relatively high degree of devulcanisation, in both filled and unfilled vulcanisates. Therefore DD would be best suited for NR products. Unsatisfactory properties for MBTS involve relatively low degree of devulcanisation (but still a fair amount) and that it has been reported to cause allergic contact dermatitis. Its advantages involve not showing preference of polymer to devulcanise in the NR/SBR blend, its multifunctionality (*i.e.* can devulcanise and as well as accelerate vulcanisation), and it is relatively cheap.

The degree of devulcanisation obtained using the optimised results on the GTR was found to be significantly lower than that obtained on the LPV for both DD and MBTS; 41.22 ± 4.22 % vs. 76.18 ± 5.50 % and 28.41 ± 1.97 % vs. 70.92 ± 4.10 % respectively. Nonetheless, it can be deduced from the findings that the optimum conditions gave a distinct maximum for MBTS whilst the maximum was not apparent for DD. Perhaps optimisation using the GTR for applications of optimised conditions on the GTR would have clarified findings (instead of optimisation using LPV), considering differences in the substrates. The most probable cause for the significant differences in % devulcanisation was however identified to be the different crosslink distributions of the GTR and LPV. Based on literature findings, a high degree of polysulphidic crosslinks is easier to devulcanise compared to a high degree of monosulphidic crosslinks. Literature has also shown that DD is efficient in the devulcanisation of high polysulphidic crosslink composition. Not much is known about MBTS. However, considering the results obtained, the high degree of monosulphidic (and low polysulphidic) crosslinks in the GTR resulted in a significantly low % devulcanisation for both DD and MBTS. On the other hand, for the high degree of polysulphidic than monosulphidic crosslinks in the LPV, both dAs produced quite high % devulcanisation.

Cognisant of the fact that the degree of mastication of the GTR and LPV could never be exactly the same, the molecular weights of the GTR sol component were however quite comparable to the LPV control sample (*i.e.* uncured masticated rubber sample). This, to a certain extent, implies a low degree of chain scission during the devulcanisation process. FTIR analysis showed slight modifications of the polymer structure due to devulcanisation. Features of radical capping by dA forming pendant groups on the polymer chains as well as the formation of thiocarbonyl groups were observed. These features are a confirmation of the proposed possible devulcanisation mechanisms. The absence of C=O and C-O groups in the sol and gel components were proof that thermo-oxidative degradation was successfully avoided.

6.2 RECOMMENDATIONS FOR FUTURE WORK

The optimisation processes as conducted in the current research can still be improved by means of a better temperature regulatory system. Due to limitations of the reactor system, factors that could otherwise have been made constant to avoid interdependency or high correlation between factors could not be fixed. For example; upon reactor calibration it was found that the thermal mass has an influence on the heating rate, and also the heating rate is affected by the reactor temperature (*vice-versa*). The only true independent variable optimised for in the study was time. Consequently, this affected the viability of the empirical models determined for the non-isothermal region, hence single factor analysis was conducted.

Due to the scope of this research, the quality of the devulcanisates were not tested by means of blending with virgin rubber material to check for changes in the mechanical properties. Therefore it would suffice to determine the physical and mechanical properties of blends of the produced devulcanisates with original rubbers. In that way, the quality of the devulcanisates would be assured.

The research focused at a temperature range below 180 °C, and the highest heating rates (determined by the set-points) were at 180 °C set-point. Also, from the study, an increase in the heating rate resulted in high % devulcanisation, but the question would be what happens at even higher heating rates. Looking into the effects of even higher heating rates (*i.e.* higher set-points) would therefore help in showing the direction of devulcanisation.

The study showed that devulcanisation can be effectively monitored using the experimental setup in this study. Therefore it would be beneficial to perform extra studies on the kinetics aspects of devulcanisation.